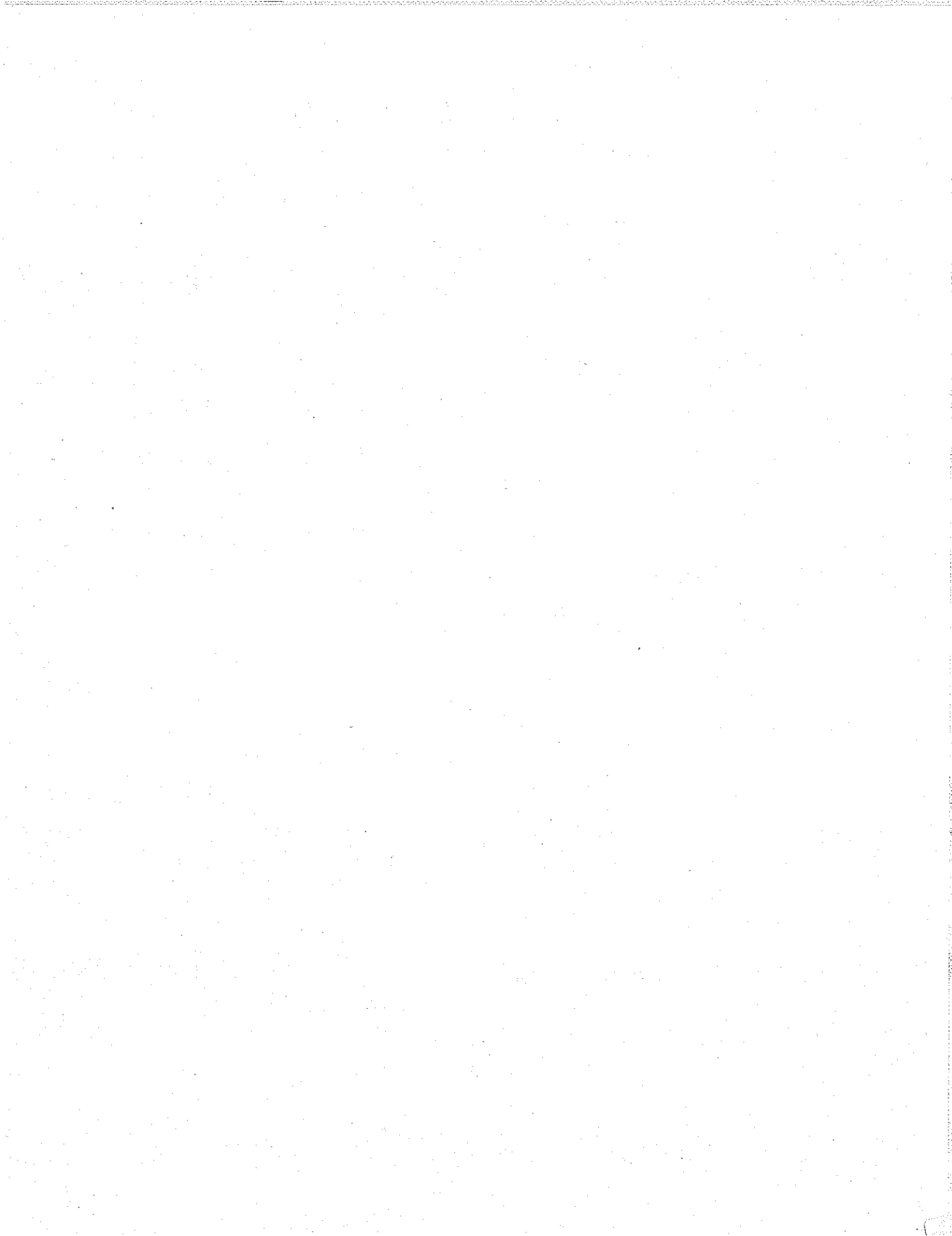


AIRCRAFT AEROELASTIC DESIGN AND ANALYSIS

**Terrence A. Weisshaar
School of Aeronautics and Astronautics
Purdue University**



Preface - Aeroelasticity and Design

Theodore von Karman described flight vehicles as being an answer to the challenge to "move swiftly and transport loads through the air." Because this transport process must be done at competitive prices, heavy emphasis is placed upon efficiency and different measures of "performance". Some measures of efficiency, such as cost per passenger mile or cost per ton-mile, are relatively easy to quantify. Other measures of cost may not be so easy to quantify; an example is life-cycle cost for an uncertain usage.

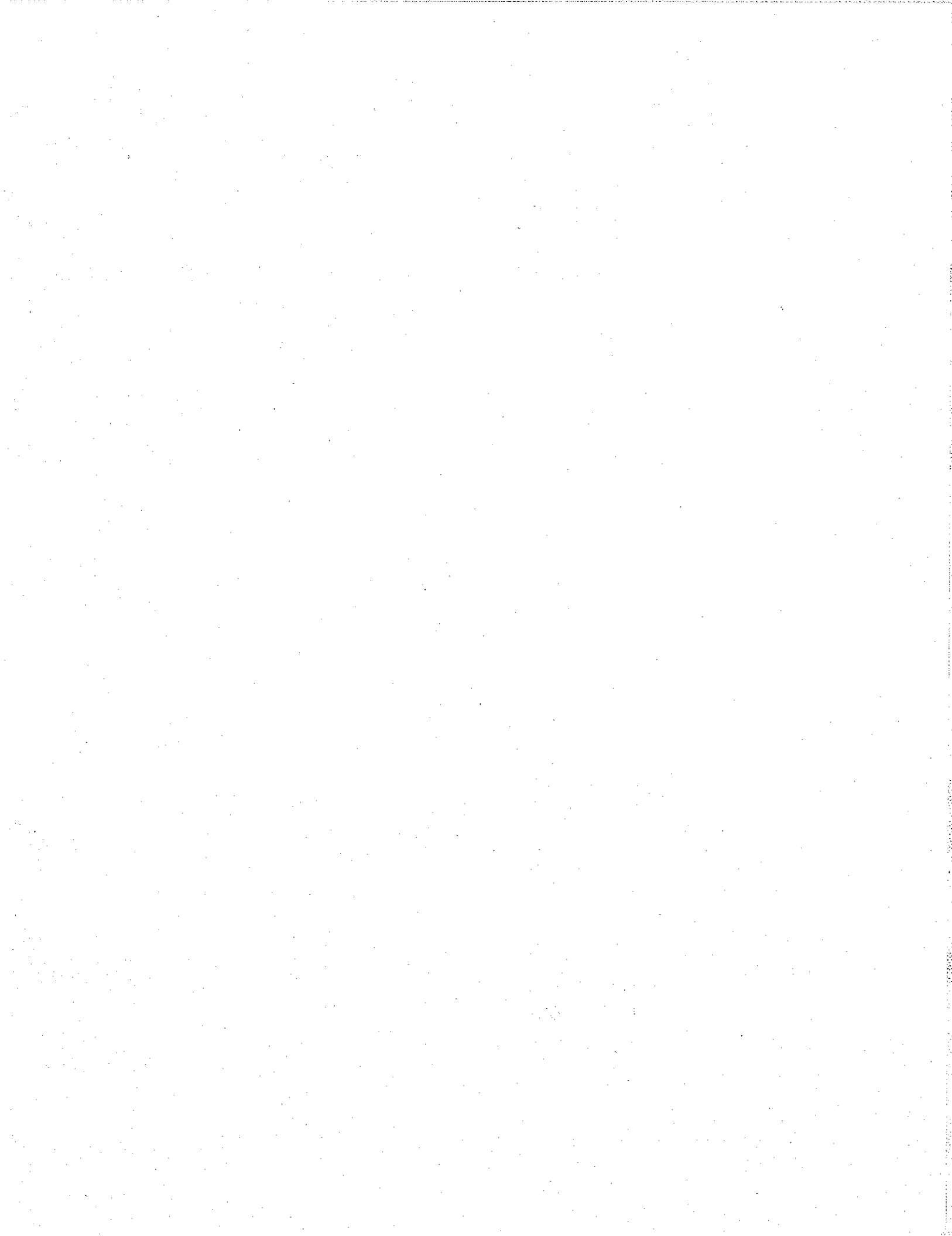
Technological advancements tend to improve aircraft performance but also increase performance expectations. New materials, more powerful engines and better avionics increase the effectiveness of aircraft designs and make previous aircraft designs obsolete. To aid in choosing the best from an ever widening range of possibilities, the design process continues to become more scientific as opposed to empirical. High-speed, large memory computers reduce the risk of failure and increase confidence in a particular design choice. The high reliability of many useful mathematical models makes it possible to choose quickly from among several possibilities that exist only in a computer memory and then "test" them to identify relative strengths and weaknesses.

A design team today has a vastly increased computational capability for peering into the future and considering the myriad of "what ifs". As a result, today they may be more inclined to consider innovative concepts than have been considered in the past. Aircraft structural flexibility is a case in point. When aircraft flew slowly and designers had few refined mathematical models, prudence dictated very strong structures. Only a small fraction of the parts comprising the structure were ever analyzed. This conservatism lead to high strength and low stresses.

These structures were relatively stiff or inflexible at the speeds at which they were flown. Significant flexibility usually made itself known by way of disaster, such as destructive flutter - a self-excited dynamic instability possible only if the structure has significant flexibility. Thus, considerations of flexibility were an add-on feature of a design synthesis. Inadequacy of descriptive mathematical theories and elaborate computation further slowed the process. Cures for adverse effects of flexibility usually involved added structural stiffening. This, in turn, resulted in a structure over designed for strength. The term "stiffness penalty" was used to describe the added structural weight.

One way to eliminate problems caused by structural flexibility is to design a "rigid" airframe and eliminate offending deformations. Certainly, if one eliminates the effects of one group of forces, in this case deformation induced aerodynamic forces, a number of problems can be made to disappear. However, one might well ask whether or not this approach is the most effective. The answers to those questions can be found only if the problem itself and its underlying causes are studied.

Computational procedures have reached the point where such answers are readily obtained. Given the state of computational capabilities, deflection induced problems can be detected and corrected early in the design process. The means of detection for serious problems in aircraft design has improved dramatically in recent years. To find a cure, one must understand the problem. That is what this text is all about - understanding the problems of aeroelasticity so that we can understand the fundamental causes and cures for these phenomena and enable the aircraft to fulfill von Karman's objective to "move swiftly and transport loads through the air".



"The development of aviation is a struggle against limitations imposed by nature upon man, created to live on the ground, but nevertheless endeavoring to move in unlimited space surrounding our globe." - Theodore von Karman

CHAPTER ONE

Introduction to Aeroelasticity

Aeroelasticity is a design activity concerned with the consequences and trade-offs created by interactions between aerodynamic forces and structural deformation. The most important consequence of this activity is that structural weight and stiffness is often redistributed or added to change the pressure distributions on aerodynamic surfaces created by bending and twisting motion. The term aeroelasticity was first used by Cox and Pugsley in Britain during the early 1930's to call attention to these design problems. Aeroelasticity is not just fluid mechanics or solid mechanics, but instead is concerned with the problems created by fluid/solid interaction.

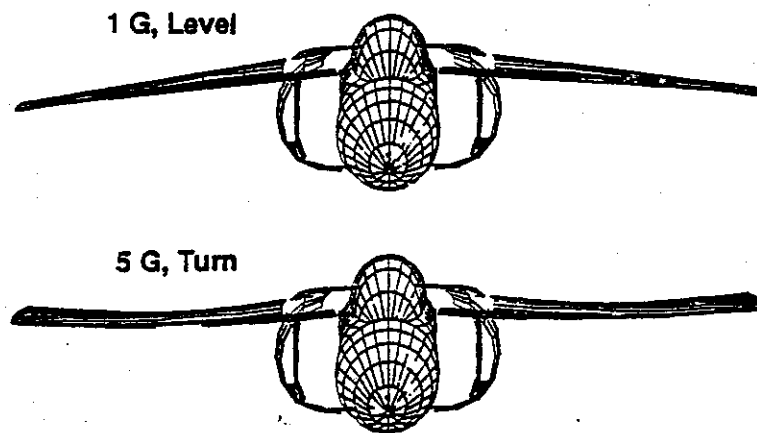


**Figure 1.1 - Aircraft wing deflection in level flight and during a 5g turn
(McDonnell-Douglas Corp.)**

Figure 1.1 shows the results of the analysis of the deflection of a modern fighter aircraft during 1g level flight and during a sustained 5g turn. In each case the wing is distorted by the pressures acting to keep the airplane aloft. In the case of the 5g turn, these distortions are so extreme that it takes little encouragement to believe that the pressure distribution over the wing is different from one case to the next.

Figure 1.2 shows the wing of a B-52 aircraft for a negative 1g and positive 2.5g load condition. Normal operational conditions lie somewhere in between these two extremes. Again, there is little doubt that the airloads are changed in either case.

For nearly all everyday structures such as cars and buildings, structural deformations are thought of as being objectionable. On the other hand, aircraft wing deflections are both

permitted and considered normal. These deflections are the result of efficient, light-weight structural design that encourages efficient, minimal weight design with stresses as near to the yield stress as permitted.

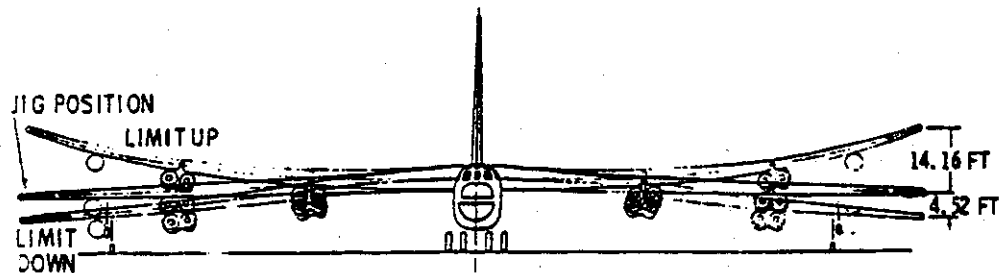


Figure 1.2 - B-52 wing deflections under limit loads
(drawing courtesy of McDonnell-Douglas Corp.)

Structural distortion and its interaction with wing lift is part of a feedback loop between aerodynamic loads and wing and fuselage deflections. This feedback process may cause instabilities, such as flutter, or changes in aircraft handling qualities. Thus, aeroelasticity is the study of the static and dynamic response of the flexible airplane.

To understand why wing deformations produce local changes in lifting surface incidence look at Figure 1.3. Bending deformation creates a local angle of attack with respect to the airstream. This angle is computed to be $-\phi \sin \Lambda$ where ϕ is the local bending slope measured along the swept wing axis indicated in Figure 1.3 and Λ is the wing sweep shown positive in the figure. Bending of a swept wing redistributes aerodynamic lift on the wing. This redistribution may require added trim loads or may cause the airplane to accelerate upward or downward.

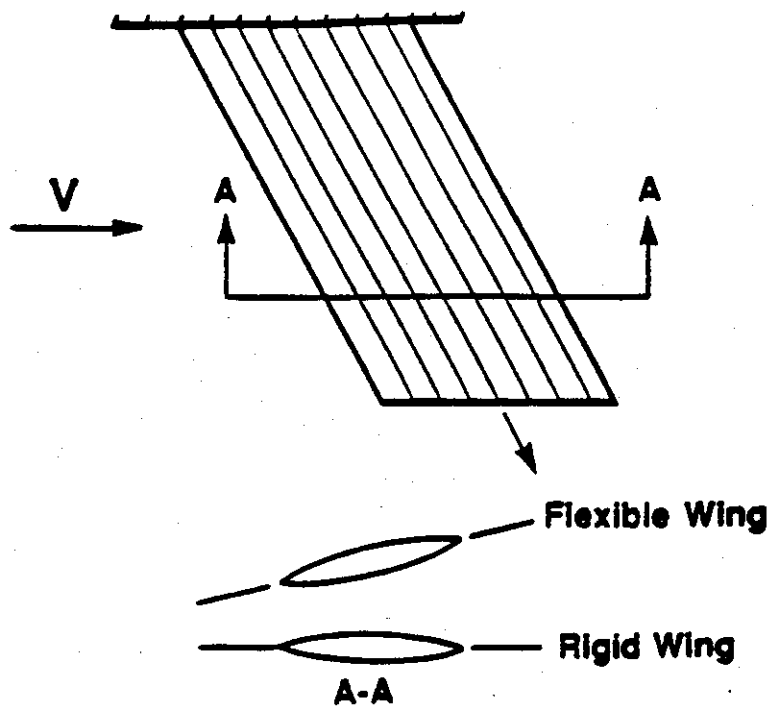


Figure 1.3 - Change in wing section incidence due to swept wing bending

The forces acting upon and within a flight vehicle structure are divided into three groups:

- Aerodynamic and propulsive forces
- Mass or inertia forces
- Elastic or structural forces

The interaction among these force categories is described by the three-ring diagram shown in Figure 1.4 in which each ring represents one of the three above categories. Intersections and overlaps of these rings represent types of phenomena that are of interest to aircraft designers.

Figure 1.4 shows that aircraft dynamic stability phenomena and analysis require considering aerodynamic forces (perhaps "corrected" for static aeroelastic effects) and mass or inertia forces. Mechanical vibration involves interacting inertia forces and internal structural (elastic) forces. These phenomena are not aeroelastic because there is no aerodynamic force change with changes in the other forces.

Aeroelastic effects are either static or dynamic. Computing the steady-state loads on flexible aircraft, computing control effectiveness and aeroelastic divergence includes interaction between structural flexibility and aerodynamic forces that are independent of time. These are referred to as static aeroelastic problems and indicated in the upper right side of the three ring diagram.

The center region of the three-ring diagram shows an area where all three types of forces interact. This region, referred to as dynamic aeroelasticity, includes problems such as flutter, buffet, and dynamic response to atmospheric turbulence.

Aeroelasticity interaction

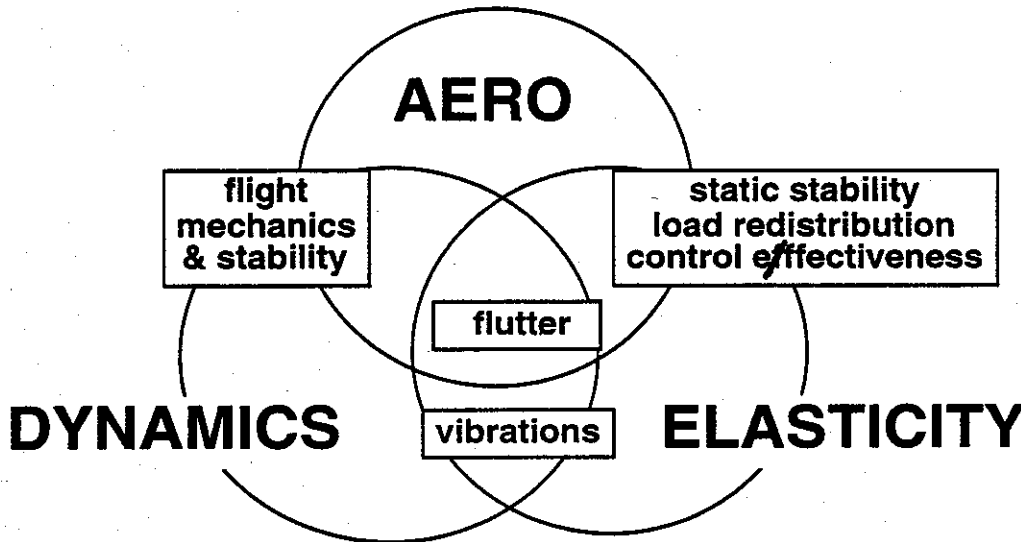


Figure 1.4 - Three-ring aeroelastic interaction diagram[1]

Changes in aerodynamic loads because of lifting surface distortion have been an important part of aeronautical engineering from the very beginning of controlled, powered flight. In fact, the failure of Samuel P. Langley's Aerodrome (NASA Langley Research

Center and Langley AFB were named for this distinguished aviation pioneer), seven days before the initial success of Orville and Wilbur Wright, had its origin in a load/deformation problem related to the Aerodrome's highly cambered wings.

Professor Langley launched his airplane, the Aerodrome (shown in Figure 1.5), from a houseboat in the Potomac River down river from Washington, D.C. and failed on each of two attempts. The first failure was most likely due to the front-wing guy post becoming caught on the catapult launch mechanism[6]. The failure of the second and last Aerodrome flight was for a number of years attributed to insufficient wing-torsional stiffness that led to structural static divergence, an instability that leads to excessive torsional deformation of the wing. Professor Collar, a noted British aeroelastician, wrote, "It seems that but for aeroelasticity Langley might have displaced the Wright brothers from their place in history" [7].

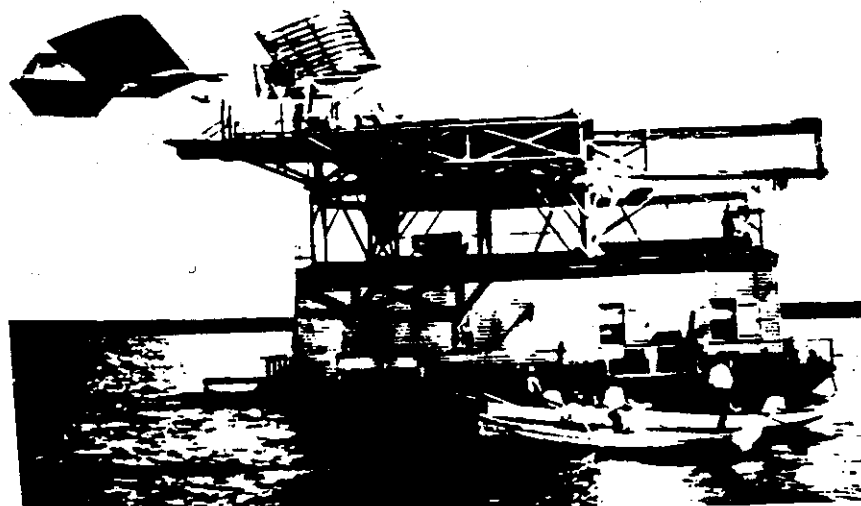


Figure 1.5 - The Langley Aerodrome mounted on its launcher in the Potomac [6]

The wing of the Aerodrome was subjected to nose down twist because of wing camber. The twist increased as airspeed on the catapult increased allowing the torsionally weak wing to twist downward and break off. Modern tests performed on the original Langley Aerodrome refute speculation that an interactive aeroelastic instability caused the Aerodrome crash [8]. These tests found the front wing shear center to be very close to the wing aerodynamic center. As we will discuss in Chapter 2, this lack of a measurable offset between the shear center and wing aerodynamic center excludes aeroelastic interaction, but not wing twist.

The Wright Brothers, used controlled airload/wing twist interaction in the design of their Wright Flyer. The structural truss arrangement of the original Wright Flyer biplane, and a early model kite shown in Figure 1.6 [2], produced a deep structural cross-section that was extremely stiff in bending. However, torsional flexibility was intentionally designed into the outer wing bays to allow a control cradle, operated by the prone pilot's hip movements, to transmit loads to move cables attached to the wings. Movement of these cables created differential wing twist or "warping" of the biplane wings to create an aircraft rolling moment.

The wing warping concept that provided lateral control was part of the Wright Brothers' provision for three-axis control of their aircraft, the Wright Flyer [3]. The wing warping idea on other early airplanes is illustrated in Figure 1.7.

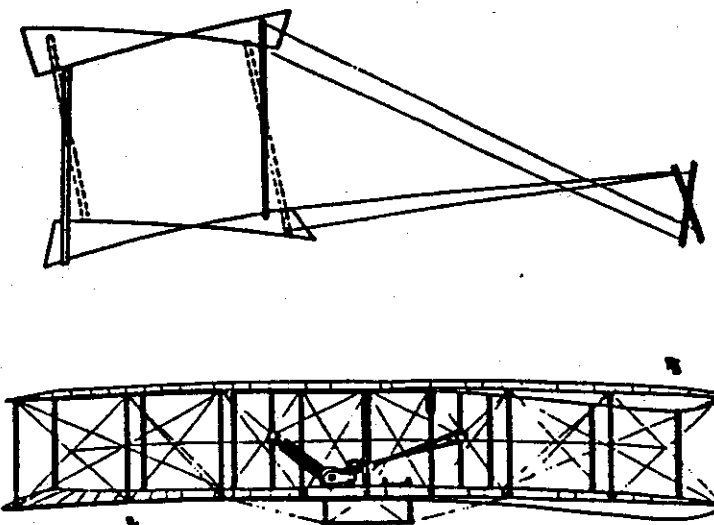


Figure 1.6 - Wright Flyer prototype with wing warping [2]

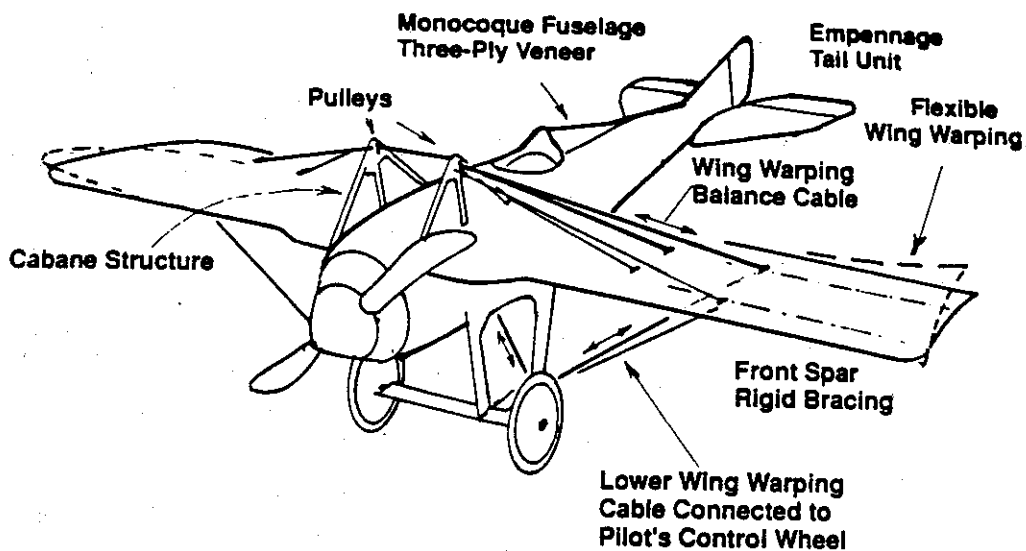


Figure 1.7 - Early monoplane design with wing warping [3]

Early aeroelastic design problems

Until a few years before World War I, airplane speeds were slow enough and structural stiffness large enough that loads due to aeroelastic deformation were inconsequential for most airplanes. There were spectacular exceptions. In 1909, only six years after the Wright's first flight, Bleriot flew across the English Channel from France at a speed of about 40 mph. The Bleriot XI was an externally braced monoplane with wing warping control[3]. This design was immediately popular (see Figure 1.8).

The effectiveness of the wing warping concept required keeping the wing torsional stiffness relatively low so the wing could be twisted by the pilot. As engine power and airspeeds increased this low stiffness created aeroelastic problems that led to wing failures.

As late as 1915, the Fokker Eindecker, a German monoplane fighter aircraft flown by the German ace Max Immelmann, used wing warping [9].

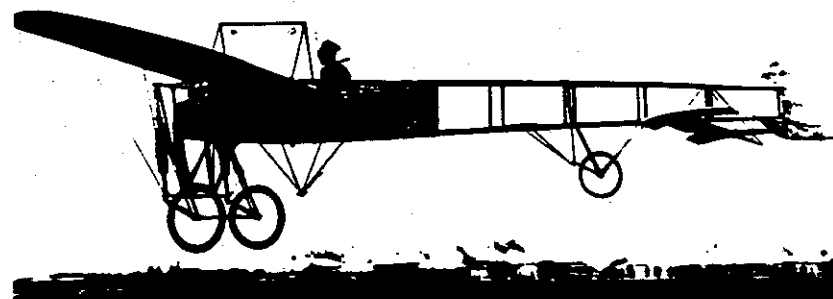


Figure 1.8 - Early Bleriot monoplane

New engines on the Bleriot XI soon pushed the airspeed up to nearly 80 mph. Wing collapse of these airplanes began to occur for no apparent reason. At first, these structural failures were thought to be the result of insufficient wire bracing strength. Bleriot strengthened the guy wires on his airplane and increased the size of the main wing spar, but the failures still occurred.

This set of events caused the British in 1912 to ban monoplanes from Britain until the approach of World War I required rescinding this ban. The problem with the thin wing monoplane designs was that the twisting caused by loads during maneuvering. The torsionally flexible wings allowed the load to twist the wing tips easily at high speeds and overload the wing before the pilot could recover.

Bleriot's design influenced airplane designers all over Europe even though he had also inadvertently discovered a new aeroelastic effect, later to be associated with wing divergence. At the time there was not enough known about analysis of such problems so that the basic mechanism could be understood. We will discuss these interactions in Chapter 2 so that Bleriot, if he had been aware of this interaction, would immediately have been able to make design changes and perhaps have been able to develop monoplane design more quickly.

The first documented aeroelastic wing failure of a fighter aircraft during World War I. occurred on the German Fokker D-VIII monoplane. This high performance aircraft had numerous failures began to occur during high-speed pull-out maneuvers. As a result of static strength and deflection measurements, it became apparent that the failure was due to wing-torsional deformation that caused increased airloads on the wing, just like the Bleriot airplane. Increasing the torsional stiffness of the wing by repositioning a wing strut eliminated the problem.

During World War I, a self-excited, vibratory aeroelastic instability called flutter occurred on the horizontal tail of the British Handley Page 0-400 bi-plane bomber[10]. Investigations in 1916 revealed that tail flutter failure was the result of a coupling or interaction between the fuselage twisting motion and the anti-symmetrical pitch rotations of the independently actuated right and left elevators. They also found that this coupling could be eliminated by connecting the elevators to a common torque tube to eliminate anti-symmetrical motion. Later tail flutter difficulties toward the end of World War I were overcome by the same redesign. As a result, the attachment of both elevators to the same torque tube became standard design practice.

Following World War I, engines continued to become lighter and more powerful. speeds increased and monoplane designs again reappeared, this time as low drag, semi-monocoque designs. A new type of aeroelastic instability, called wing-aileron flutter plagued the aircraft design effort. Just as the wing warping type of control had led to wing divergence, the new aileron control led to dynamic aeroelastic failures.

Wing-aileron flutter occurs when the lift generated by the oscillation of an aileron or tab drives the wing bending or torsion deformation. The oscillation frequency depends on the airspeed because the aileron acts as a weathervane whose rotational stiffness increases as airspeed increases. The accelerations of the aileron, as well as the airloads transmitted to the wing will force the oscillations of the wing and create a mutual coupled vibration.

As indicated in Figure 1.9, the relative phase between the aileron rotational motion and the wing bending motion is important and is a function of the airspeed and where the center of gravity of the aileron is with respect to the hinge. If a disturbance in the moving airstream creates an oscillation where the aileron lift acts upward when the wing moves upward and acts downward when the wing moves downward, then the airloads do positive work on the wing and energy is input into the wing itself. This energy will cause a large oscillation of the wing that will eventually tear it off.

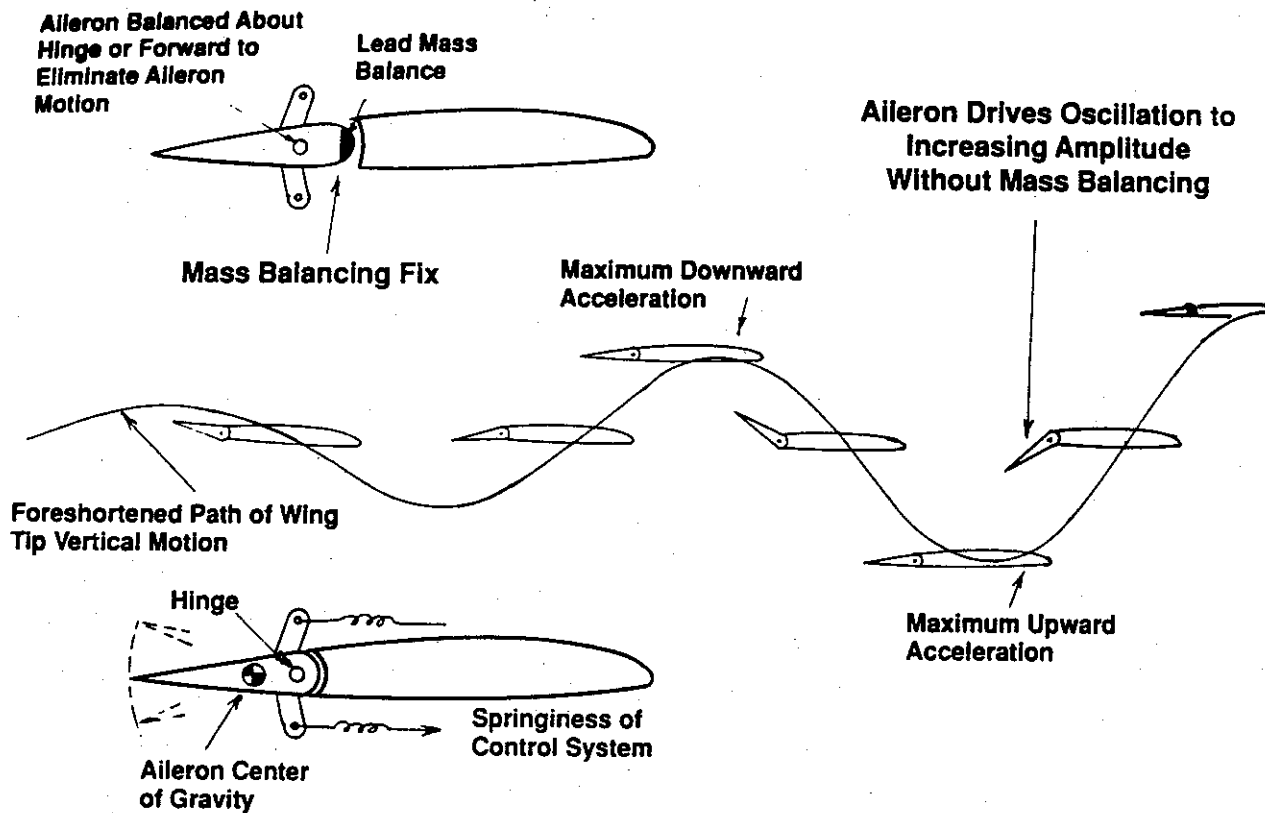


Figure 1.9 - Wing aileron dynamic coupling to create flutter [3]

The unstable oscillation occurs because the steady airstream contains an enormous amount of energy that can impart unsteady motion to the wing-aileron combination because of an effect called dynamic coupling. We will examine in Chapter 3 the necessary conditions for this coupling and how to uncouple the oscillations and make them stop. In Germany, Bambauer and König conducted experimental and theoretical investigations of wing bending motion and motion of the ailerons. They emphasized the concept of decoupling

modes of motion to prevent flutter. Decoupling of the wing and aileron motion was done by attaching weights to the aileron ahead of the hinge line; this "mass balancing" principle is still used to this day.

Wing flutter

Flutter is a self-excited dynamic instability. Theodore von Karman once remarked that "some men fear flutter because they do not understand it, while others fear it because they do" [8]. A classic work "The Flutter of Aircraft Wings," British A.R.C. R.&M. 1155, known ever since as the "Flutter Bible," was published in 1928. In this monograph, Frazer and Duncan outlined principles on which flutter investigations have been based ever since. The origins of flutter and methods of analysis are also discussed and reviewed in a number of excellent reference texts [10-14].

Flutter depends on coupling together two or more modes of motion whose oscillations create aerodynamic forces that allow energy to be transferred from the airstream to the structure so that the amplitude of the motion will grow in time. Even early aircraft structures texts discuss flutter as a mode of failure and illustrate vibration modes. Figure 1.10 shows a figure from one of the more well-known texts used in the 1940's [15]. This figure indicates that it is important to know or estimate the vibration modes of the aircraft in flight.

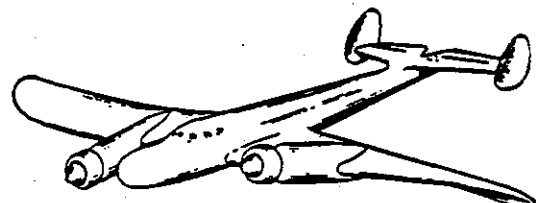


FIG. 20:4.

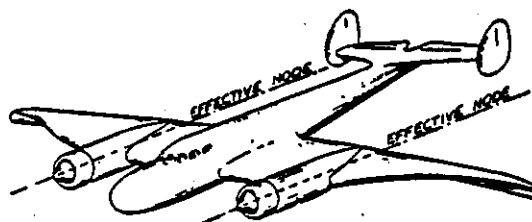


FIG. 20:5.

Figure 1.10 - Airplane vibration mode shapes on early transports [15]

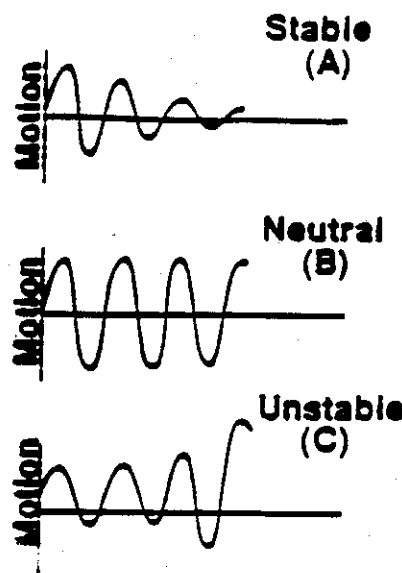
Figure 1.11 shows the time histories of three possible types of dynamic displacement behavior at a point located on a wing responding to a disturbance occurring during flight. At an airspeed corresponding to point A, the response is damped and any initial disturbing motion decays with increasing time.

As airspeed is increased to point B, an initial disturbance produces (after some transient motion) harmonic oscillatory motion at a fixed amplitude. An attempt to operate at the airspeed associated with point C will lead to disaster, since the amplitude of the response to the initial disturbance grows rapidly with time. The motions associated with airspeeds at A, B, C are classified as stable, neutrally stable and unstable, respectively.

To understand what is taking place, we focus attention on two characteristic types (or modes) of possible flexible wing motion. If a sinusoidal force with fixed maximum/minimum values and a specified frequency were applied to the wing operating at dynamic pressure A,

then resonant or natural frequencies would be observed as indicated in Figure 1.11. One mode of resonant motion has an instantaneous deformed shape, or mode shape, that resembles bending of the wing with respect to its cantilever support. The other type of

Time Histories



Modal Coupling

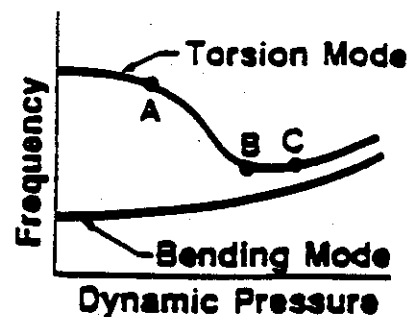


Figure 1.11 - Wing frequency and dynamic response at different airspeeds.

resonant motion has a predominantly torsional or twisting form. The wing motion at any airspeed is neither purely bending nor torsional in nature, but instead is a linear combination of both types.

As airspeed and dynamic pressure increase, the values of the first two wing resonant frequencies will change or shift due to deformation-induced aerodynamic forces acting upon the wing as it deflects. These frequency shifts lead to changes in motion such as those seen for wing-aileron motion discussed previously.

At point B, if the sinusoidal forcing is removed, one of these modes will be aerodynamically damped and decay with time. However, one mode will have no damping, as indicated in the central portion of Figure 1.11. In this example, this undamped mode is the so-called "torsion mode," an aerodynamically coupled bending/torsion oscillation, but with wing torsional motion predominant. At point C, the flow conditions create a situation that allows the wing to gather energy from the airstream and transform it to kinetic energy in the wing. As a result the wing oscillation amplitude builds rapidly with time.

Figure 1.11 indicates that warning of impending flutter caused by coupled motion shows up as the tendency of two or more resonant frequencies to coalesce or merge. At a special airspeed, at point B, one of the aeroelastic vibration modes becomes self-sustaining or auto-oscillatory when excited. Above this airspeed, the phenomenon referred to as flutter occurs. The amplitude of the oscillatory motion grows exponentially with time unless it is limited by nonlinearities, or structural failure.

The effect of flutter on modern aircraft design and operation

Survey articles (cf. Collar [7]; Garrick and Reed[8]) cover a wide spectrum of historical data related to flutter. Because flutter is caused by what may be regarded as an excessive amount of time-dependent structural, aerodynamic, inertial interaction, it may be cured by some combination of inertia change, structural flexibility change or aerodynamic change. Let's consider some of these possible changes and their likely consequences. First let's consider the inertia or weight distribution.

The inertia distribution of the aircraft is determined by fuel placement, cargo or payload placement (including underwing stores such as bombs and missiles) and by engine size and placement, as well as structural weight. Because the wing structure is sized initially for load carrying ability (strength), redistributing wing structure to cure a flutter problem is not likely to be an available option. Similarly, wing internal fuel storage volume requirements that lead to "wet wings" are crucial to the aircraft's mission. Fuel cannot be eliminated even if its removal would lead to an increased flutter airspeed.

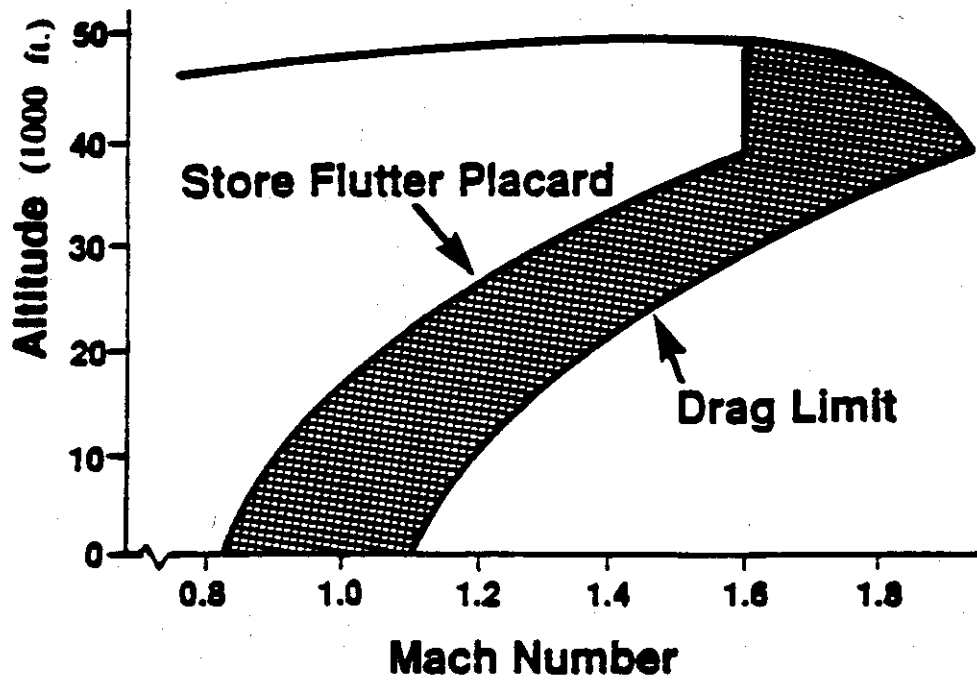


Figure 1.12 - Placard speed limitation caused by underwing store attachment.

Fighter aircraft carry a wide variety of underwing armaments or "stores." Underwing store locations significantly change the aircraft wing inertia distribution. Their positions are determined by a combination of structural, aerodynamic and flutter constraints. However, operational requirements create a large number of possible store carriage combinations. This, in turn, may result in a mission where flutter at some airspeed cannot be avoided. When this occurs, a placard airspeed, above which the aircraft must not fly, is placed on the aircraft. This degraded performance, depicted in Figure 1.12, contracts the operational envelope (flight must be inside this region) and is often the only alternative to an expensive redesign effort.

Transport aircraft often have large engines attached to their wings. Re-positioning under-the-wing engines, attached to flexible pylons, can be used to increase flutter speed. In

some designs, ballast (lead weights) has been placed in engine nacelles to decouple critical vibration modes and delay modal coalescence.

More often than not, the inertia distribution required for aircraft mission performance is the cause rather than the cure for flutter problems. Added mass, such as lead in engine nacelles or small balance weights attached to control surfaces, is the weight penalty paid for decoupling flutter critical motions that arise because other design criteria have taken precedence over structural flexibility.

Changing the lifting surface planform shape or wing thickness to cure flutter problems are not unlikely to occur. Extreme examples of aerodynamic planform changes to increase flutter speed have included the intentional removal of wing tips of early monoplane air racers. The removal of lifting surface area decreases some aspects of aircraft performance for a multi-mission aircraft so that it is not viable as an aeroelastic design alternative. That brings us back to the consideration of structural changes to modify flutter speed.

Changing the stiffness distribution usually means increased wing skin thickness or increased size of structural elements. Such changes will affect both the lifting surface mass and stiffness distribution so that the natural frequencies and their mode shapes will be changed. As a result, structural size and weight will increase, over and above that necessary to resist stresses from flight critical loads. The stresses in the material decrease to inefficient levels.

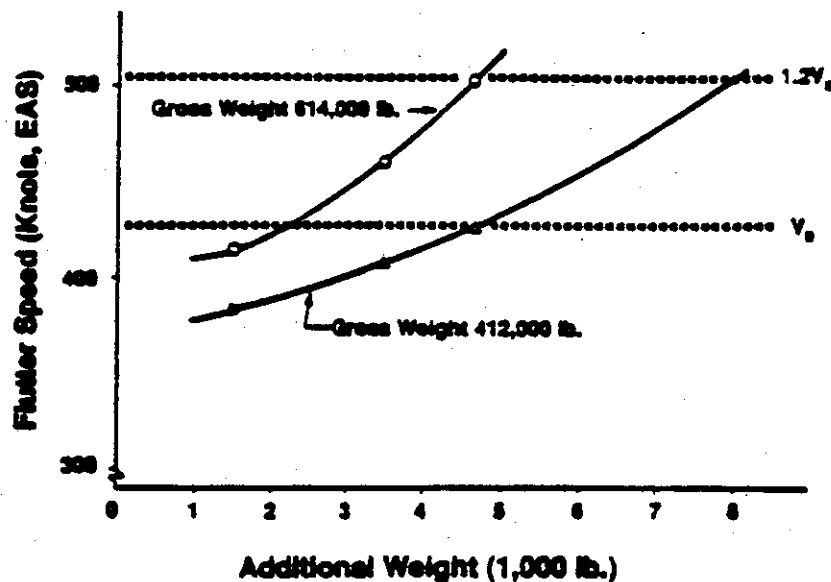


Figure 1.13 - Transport weight increases to meet flutter speed requirements [4].

Although the added weight required for flutter prevention is not usually very large, as a percentage of take-off gross weight, adding this weight may be expensive and irritating if done late in a design development. An example of the magnitude of the weight increase required to increase the flutter speeds of two transport category aircraft is shown in Figure 1.13 [4].

Static aeroelasticity-lift effectiveness and load redistribution

When time-dependent aerodynamic and inertial loads are excluded, inertia effects are restricted to gravitational effects or constant acceleration scenarios such as steady turns and

pull-outs. In contrast to flutter, which limits operational airspeeds and determines the shape and size of an operational envelope, static aeroelasticity determines mission performance and aircraft operation inside the operational envelope.

The shape of the aircraft determines the aerodynamic pressures that translate into the lift, drag and pitching moments that counteract weight and thrust. Flexibility, which leads to slight changes in geometry during flight, is the direct result of the high structural efficiency (allowing the development of high stress and low weight) of airframe components, especially the wing.

The bending deflection of a wing tip is expressed as a combination of geometrical, aerodynamic and structural parameters, as

$$\frac{w_{tip}}{L_{wing}} = K \frac{\sigma_{allowable}}{E} \left(\frac{\text{wing aspect ratio}}{\text{wing thickness to chord ratio}} \right)$$

where K is a constant depending upon geometrical factors such as planform shape, $\sigma_{allowable}$ is the allowable stress in the material used for the wing, E is the effective Young's modulus for the wing material, and aspect ratio is computed as the square of the wing span divided by the wing planform area. Note that L_{wing} is measured from the wing/fuselage junction out the swept span and is larger than the semi-span of the wing itself when the wing is swept.

We see from this formula that the larger the allowable stress, the larger the wing tip deflection will be. In addition, for high speed wings, the thickness-to-chord ratio is small (of the order of 0.04-0.12). Subsonic jet transports have slender, high aspect ratio wings. These wings also will have large wing tip deflections, all other factors considered.

Figure 1.14 shows an ultimate load test of a commercial airliner. Note the large deflection permitted by efficient structural design and the tendency of the wing tip to twist nose downward as seen from this perspective. Notice also the fuselage skin buckling produced by the stresses in the wing feeding into the fuselage through wing attachments and the center torsion box.

Among the static aeroelastic effects important to the design of flexible swept wings is lift effectiveness, which, for a swept wing, primarily involves the effect of in-flight bending deformation on spanwise lift distribution. As shown previously in Figure 1.3, a torsionally rigid, but bending flexible, swept wing will deform upward along the swept reference lines indicated. Although no rotation or twist of the wing surface occurs perpendicular to these spanwise reference lines, the sections rotate downward with respect to the streamwise axis (view A-A the Figure 1.3).

This nose-down incidence with respect to the airflow produces an angle-of-attack reduction of each wing section, referred to as wash-out, that redistributes the load along the wing span and reduces the total lift on the wing. As a result, the effectiveness of the airfoil in generating lift at a particular angle of attack is reduced. To attain lift comparable to a similar rigid wing, the overall incidence of the wing at the root must be increased to generate the lift required for any maneuver (including 1-g flight).

Concern for lift effectiveness is not confined only to wings. The purpose of a vertical stabilizer is to stabilize the yawing motion of an airplane. Often times these stabilizers are swept back to move the center of pressure as far back from the airplane c.g. as possible.

Designers want the vertical stabilizer to be as small as possible. Because of vertical stabilizer bending the effectiveness of the surface is reduced. This reduction may be corrected either by increasing surface area or by adding material to stiffen the stabilizer. Both solutions involve placing additional structural weight in the tail of the aircraft. As a result, the aircraft c.g. moves aft and creates an adverse longitudinal stability change that must be overcome by other re-design efforts. Neither option is desirable.

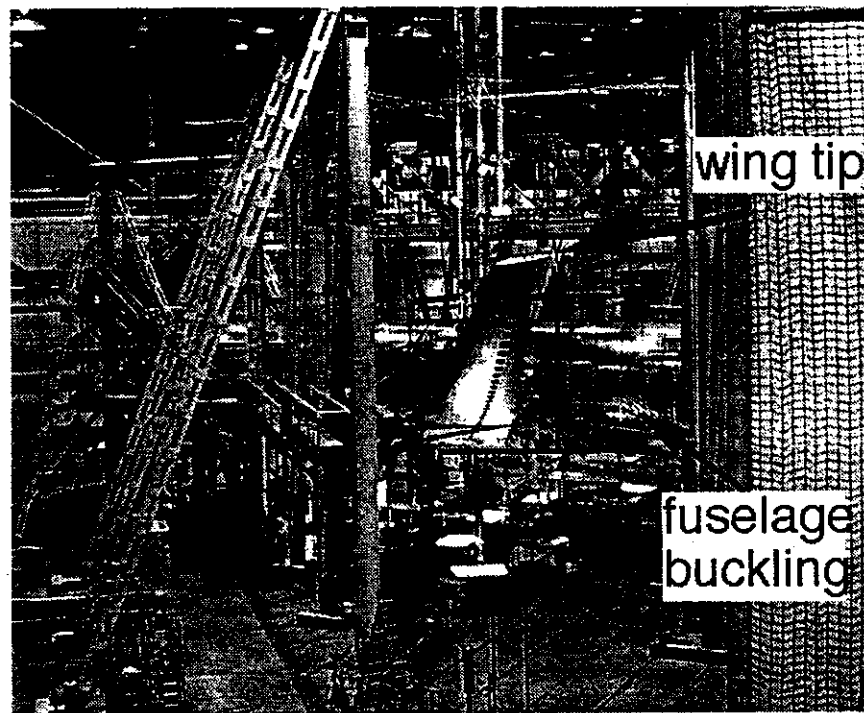


Figure 1.14 - Boeing 767 static ultimate load test

Figure 1.15 illustrates the effect of flexibility on the airload distribution of a high-aspect ratio sweptback wing. The areas under the two curves shown are identical, because the two

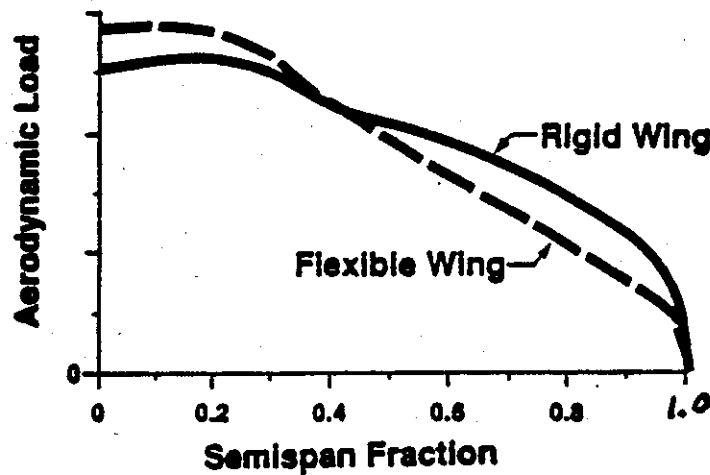


Figure 1.15 - Spanwise distribution of aerodynamic load due to swept wing bending/torsion deformation.

configurations, one rigid the other flexible, develop the same total lift. Note, however, that the outboard region of the flexible wing is "unloaded" in comparison to the rigid wing. Although the spanwise twist of the rigid wing is constant, the streamwise angle-of-attack of the flexible wing begins as a positive angle at the wing root and declines toward the tip.

The change in spanwise load distribution influences other measures of wing aerodynamic efficiency. Figure 1.16 shows how forces and moments may change due to swept wing bending deformation [1.15]. In general, because of the wash-out feature of sweptback wing bending deformation, the lift-curve slope will be reduced when the wing bends, as indicated in Figure 1.16a.

On the other hand, the drag-polar which plots lift versus drag, Figure 1.16b, may be favorably affected by flexible wash-out. However, the static longitudinal stability of the aircraft may be affected adversely, as indicated by the change in slope of the C_L versus C_M relationship shown in Figure 1.16c. Bending deformation modifies the airloads to create a longitudinally unstable aircraft at this particular airspeed.

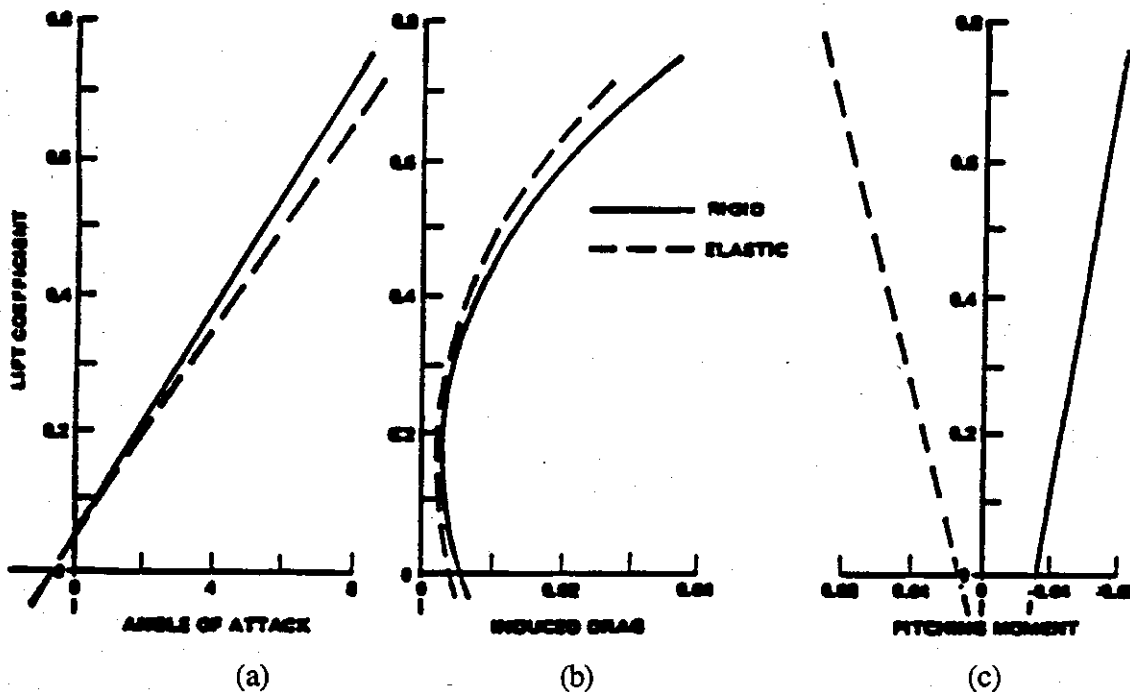


Figure 1.16 - Changes in forces and moments due to swept wing deformation
 (a) lift-curve slope; b) drag polar; (c) static longitudinal stability .

Static aeroelastic and flutter criteria are particularly important to performance of high speed, high performance aircraft. High speed aircraft tend to have thin wings. The wing thickness-to-chord ratios at both the wing root and the tip are low so that very little material cross-sectional area and moment of inertia is available to resist wing bending and twisting. This leads to a wing that is flexible in bending and torsion.

Figure 1.17 provides an example of the weight penalty required when the thickness of a wing of constant area is reduced [5]. In the design of a tapered wing with thickness-to-chord ratios above 6%, strength criteria are likely to provide acceptable aeroelastic stiffness.

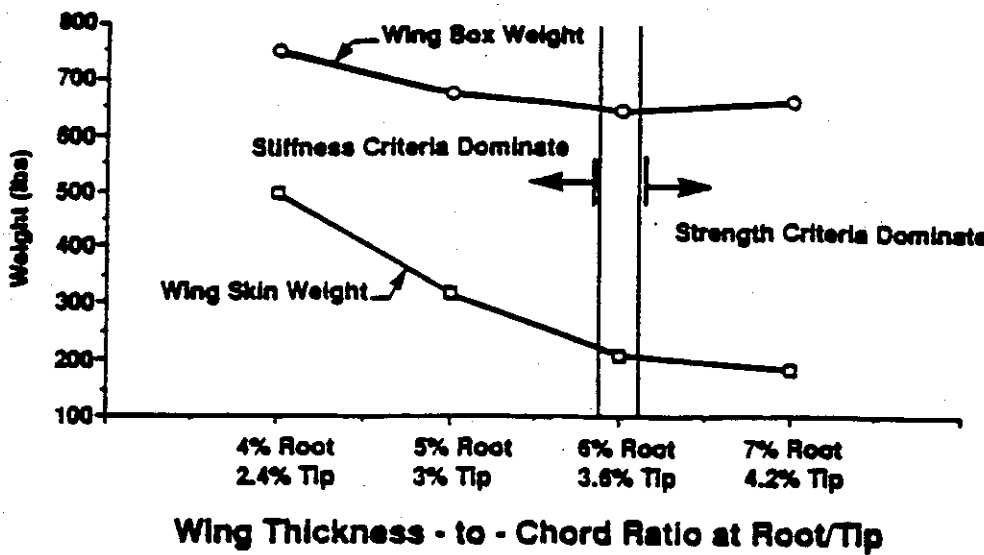


Figure 1.17 - Wing weight penalties as a function of wing root/tip thickness to chord ratio [5].

Below 6% additional structural material is necessary to satisfy aeroelastic requirements. Modern fighter aircraft have wing thickness less than 6%.

Static aeroelasticity-control effectiveness

Control effectiveness is the ability of a control surface, usually an aileron, to produce aerodynamic forces and moments to control and maneuver the aircraft. The ability to create a high steady-state roll rate is one measure of aileron effectiveness. Wing flexibility usually reduces control effectiveness. Figure 1.18 shows how the aileron roll-rate generation changes with airspeed.

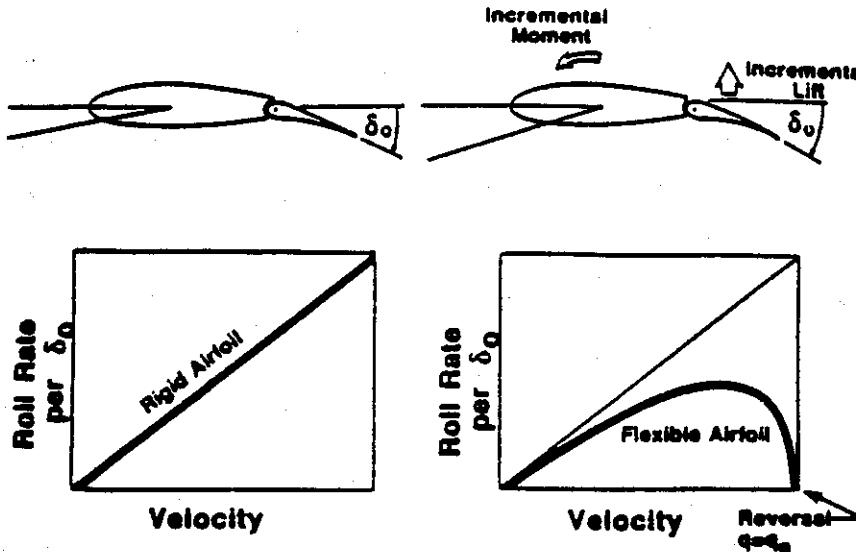


Figure 1.18 - Control effectiveness as a function of airspeed for a 2-D airfoil with a trailing edge flap: without aeroelastic effects; with torsional flexibility.

Deflection of the aileron produces an incremental lift proportional to dynamic pressure that, in turn, produces an incremental rolling moment and acceleration that builds a rolling velocity or rate, denoted as the symbol p (rad/sec). Rolling velocity, p , also creates a damping-in-roll moment, proportional to airspeed, V , that opposes roll motion. When the aileron rolling moment and the opposing damping-in-roll moment become equal, the terminal steady-state roll rate, p , is established. This steady-state roll rate is proportional to airspeed (rolling moment divided by damping-in-roll).

Without flexibility, the terminal roll rate is a linear function of airspeed, as indicated in Figure 1.18. The slope of this curve depends on wing planform geometry and the aileron spanwise location on the wing.

When flexibility is taken into account, the terminal roll-rate is different. In addition to rolling moments, the incremental lift of the aileron also creates a nose-down twisting moment on the wing structure. The size of this twisting moment depends upon: the size of the control surface; the amount of aileron deflection; structural stiffness; and, the dynamic pressure. Twisting of the airfoil reduces the airfoil sectional angle of attack, thus reducing the size of the net roll moment or what is referred to as aileron rolling power.

Figure 1.18 indicates that at some airspeed the aileron roll effectiveness increases to a maximum and then decreases. Because of this reduction in effectiveness at higher airspeeds, large aileron deflections may be required to maneuver the aircraft, a situation that may lead to increased drag and servomechanism problems.

At a special airspeed called the reversal speed, the net roll moment generated by aileron deflection is zero. At the reversal speed, a force couple is created that produces surface distortion, but unfortunately, no additional net rolling moment. An increase in airspeed above the reversal speed will produce a reversed control, a situation in which incremental control surface lift induces excessive structural twist that causes the net lift to act downward, not upward.

Sweepback makes the control reversal tendency worse. The incremental lift created by a downward aileron deflection not only causes detrimental nose-down twist of an aft swept surface, but also bends the surface upward. As we have seen, upward bending of a sweepback wing produces an effective nose-down streamwise incidence that exacerbates the aileron effectiveness problem. As a result, the spanwise location and sizing of control surfaces on sweepback wings is crucial to the success of the design. In some cases, the use of ailerons at high speeds has been abandoned altogether and lift spoiler devices used in their place.

Static aeroelastic stability-aeroelastic divergence

Structural deformation creates internal stresses that attempt to restore the system to its original, undeformed position. This characteristic is referred to as structural stiffness. If small deflections arise in response to large forces, the structure is categorized as stiff. Structural stiffness depends on: material stiffness such as Young's Modulus; and, geometric details such as thickness, slenderness. Since wing structural distortion creates aerodynamic loads, the relationship between aerodynamic stiffness depends on airstream dynamic pressure, planform details and flow conditions such as Mach number. The sum of aerodynamic and structural stiffness is called aeroelastic stiffness.

If aerodynamic and internal structural forces reinforce each other, then the aeroelastic stiffness at a certain flight speed will be greater than the structural stiffness. This is the case for bending induced aerodynamic loads on sweepback wings. When a sweepback wing is

bent upward, the deformation induced angle of attack leads to a reduction in load. This incremental reduction of aerodynamic load makes it easier to restore the wing to its original equilibrium position, reinforcing the effects of the structural restoring forces.

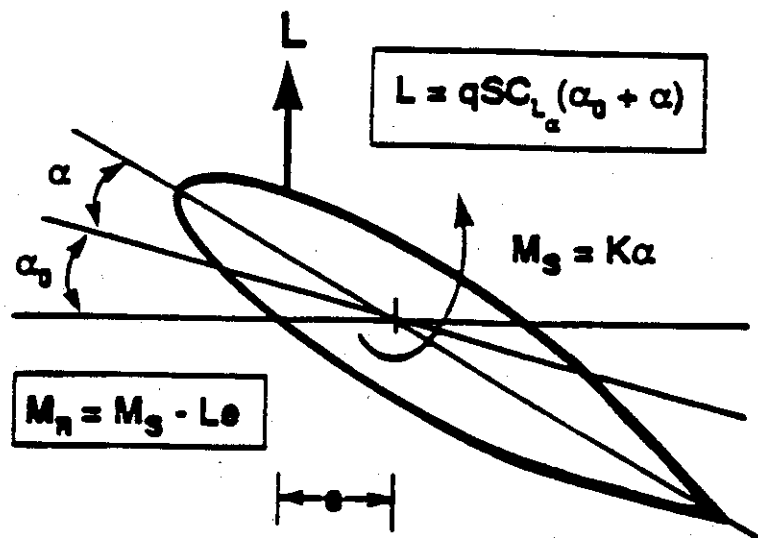


Figure 1.19 - Unswept wing section showing external aerodynamic and internal structural moments.

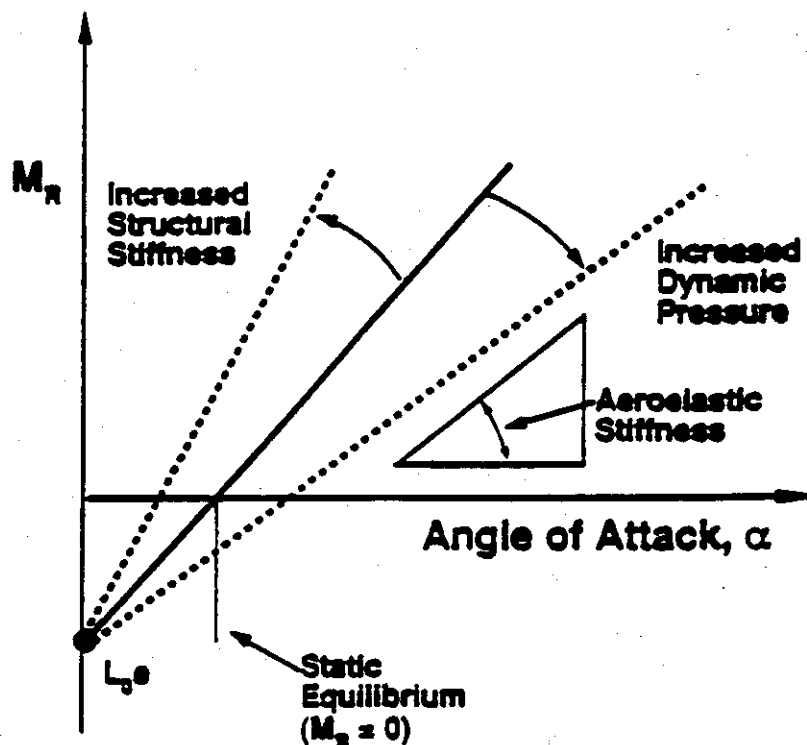


Figure 1.20 - Applied external moment on an unswept wing section vs. twist angle α (L_0 is due to the initial angle of attack).

Torsional deformation of a wing section such as that shown in Figure 1.19 (with α being the elastic twist angle and α_0 the initial angle of attack), creates a restoring structural twist moment; the aerodynamic force due to twist can create an overturning moment. This moment is proportional to an offset distance, e , that measures the distance between the airfoil aerodynamic center and the structural shear center, or center of twist. If the aerodynamic moment is an overturning moment, as is the usual case in subsonic flow, the aerodynamic stiffness is classified as negative stiffness.

The aeroelastic stiffness is proportional to the slope of the line that relates restoring moment to twist angle, α , shown in Figure 1.20. Since aeroelastic stiffness is the sum of two terms (one depends upon structural stiffness while the other is proportional to flight dynamic pressure) at some specific dynamic pressure, the sum of the two stiffness terms may be zero. This special or critical value of dynamic pressure is known as the divergence dynamic pressure. Divergence is classified as a static instability; at this hypothetical dynamic pressure, the structure is overpowered by the applied aerodynamic load. The plot of the total aeroelastic restoring moment versus twist angle is a horizontal line.

Wing design

In the United States, the Federal Aviation Administration regulations govern certification of commercial aircraft [16]. In particular, FAR 23.369 and FAR 25.369 require definition of the transport aircraft flutter speed and assurances that it is 20% above the limit dive speed while FAR 23.301(c) and FAR 25.301(c) require that the aircraft loads properly account for deflection of the structure.

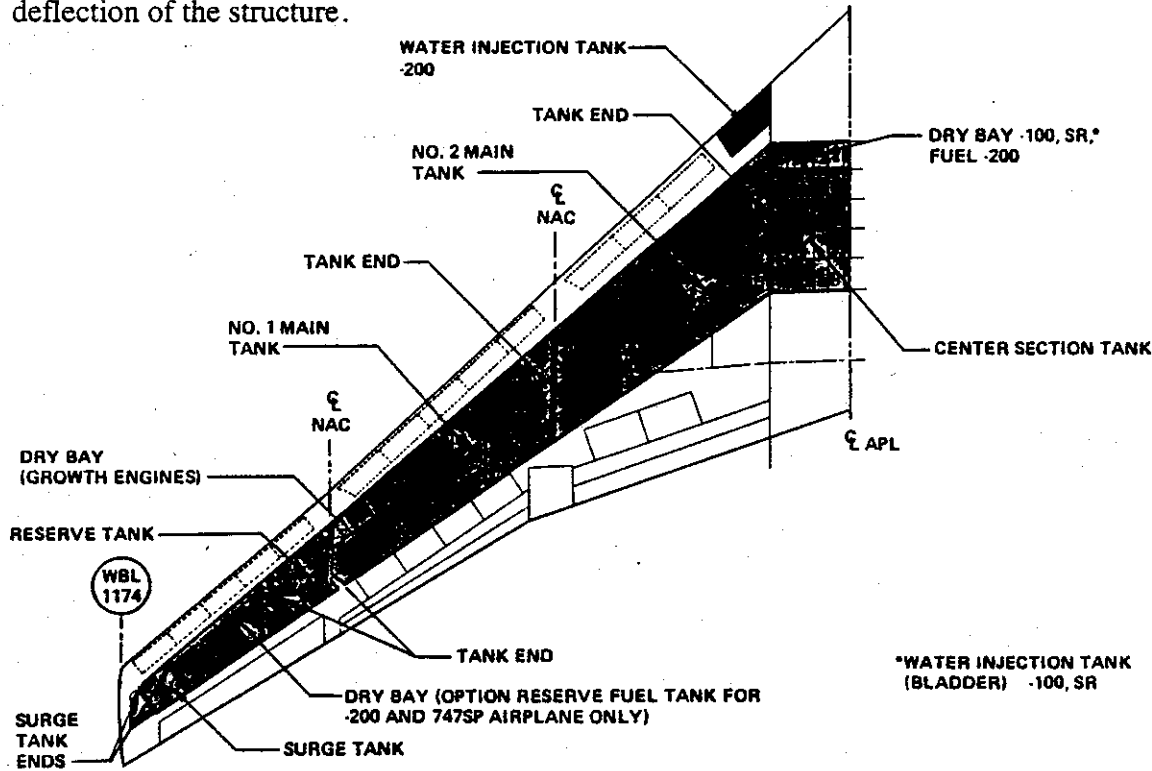


Figure 1.21 - Boeing 747 wing planform

Commercial transport wings are complicated multi-functional designs. Induced drag is reduced by increasing the wing span, while weight will increase if span is increased due to the outward movement of the wing spanwise center of pressure. Wing design involves a

trade between aerodynamic performance and wing weight, the result being that the wing weighs about 10% of the aircraft take-off gross weight.

Figure 1.21 shows the planform of the Boeing 747 wing. The fuel tanks lie between the front and rear spars in the shaded area. Numerous fittings and attachments must be provided for the trailing edge flaps and ailerons indicated in the figure. The main bending load carrying structure is between the spars and is seen to be a relatively high aspect ratio beam-like structure.

The internal complexity of a lifting surface structure is seen in Figure 1.22 which shows details of the horizontal stabilizer. Note the numerous cutouts for access holes and inspection. Additional details such as attachments and the mass balance on the elevator are also apparent.

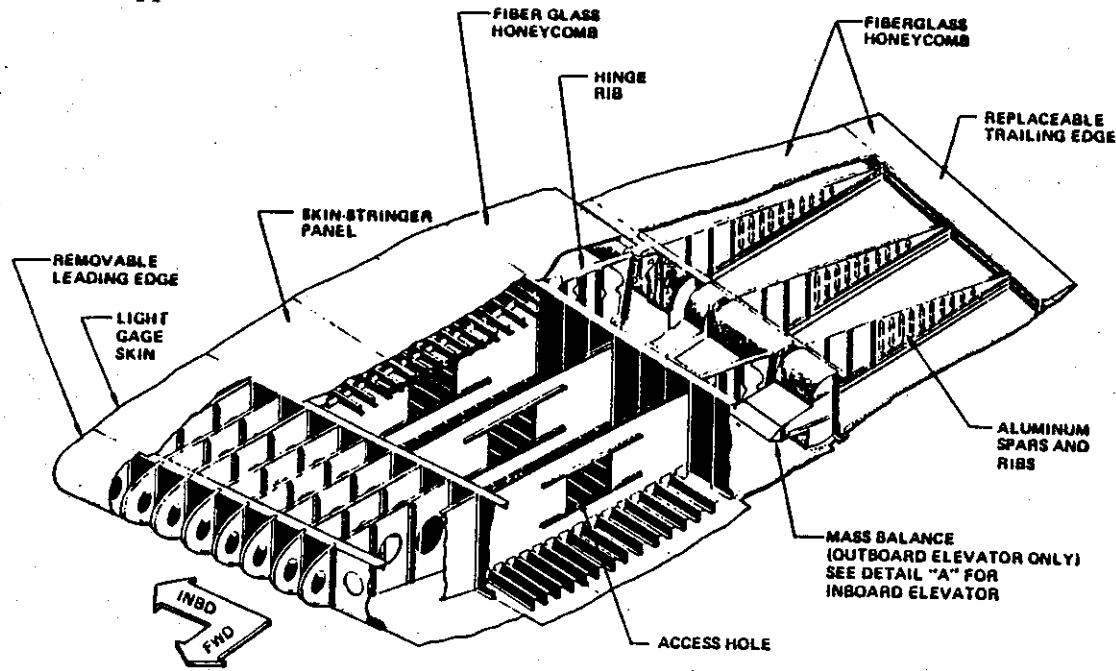


Figure 1.22 - Boeing 747 horizontal stabilizer structure

Mathematical modeling of the wings and tails of aircraft is a complicated art. We can use a variety of models depending upon the purpose of the analysis. If the intent is to estimate stresses, it is important to model the attachments and include precise detail of the internal structure. On the other hand, this detail is not usually needed for aeroelastic analysis since the estimates of external deformation are more important than internal details.

Summary

Aeroelastic phenomena are created by interactions between aerodynamic loads and external airframe deflection. Phenomena such as divergence, control ineffectiveness and flutter occurred early in aircraft flight history and continue to be important flight vehicle design considerations. Substantial portions of aircraft development budgets are set aside for analysis and scaled aeroelastic models for wind tunnel testing to certify that aeroelastic phenomena do not interfere with flight performance or mission goals. Additional time is appropriated for full-scale flight testing and certification.

An aeroelastician is a specialist who is expected to have extensive knowledge, analytical skill and understanding of aerodynamics, structures and dynamics. His (or her) duties require intensive study of such problems and their resolution. On the other hand, the best resolution for some aeroelastic problems is to avoid them in the first place. This text is dedicated to helping the reader understand the origins of aeroelastic problems and, as a result, to avoid undesirable interactions at the outset, or to take advantage of favorable interactions.

Chapter Two introduces basic terminology of aerodynamics and structures. This initial discussion will be unnecessary to those who are well versed in either subject. A simple analytical model is then introduced to understand the scope of the static aeroelastic interaction. The scope is then expanded to swept wings and the important influence of sweep on static aeroelastic behavior. Also included in Chapter Two is a discussion of the effects of advanced composite materials on structural stiffness and aeroelastic effectiveness.

Chapter Three examines dynamic aeroelastic phenomena, particularly flutter. This chapter begins by defining terminology and analyzing the effects of aerodynamic forces on free vibration of wings and other lifting surfaces. The features of unsteady lift produced by oscillating surfaces are then explained and examined. The various methods of solving for flutter are then reviewed.

REFERENCES - CHAPTER ONE

1. Yates, E.C., Jr., *Flutter and Unsteady-Lift Theory*, in NASA SP-258, pp. 289-374.
2. Culick, F.E.C. and Jen, H.R., *Aerodynamics, Stability and Control of the 1903 Wright Flyer*, in *The Wright Flyer - An Engineering Perspective*, 1970, Smithsonian Institution Press: Washington, D.C. pp. 19-44.
3. Cook, W.H., *The Road to the 707*, TYC Publishing Company, Bellevue, Wash., 1991.
4. Grande, D.L., *Flutter Suppression System*, in *Education in Creative Engineering Seminar - Massachusetts Institute of Technology*, 1970, Halliday Lithograph Corp.: Boston. pp. 184-185.
5. Love, M.H., "Aeroelastic Tailoring of Fighter Aircraft," *Proceedings of the ASME Winter Annual Meeting*, Boston, Mass., Dec. 1987, pp.
6. Gibbs-Smith, C.H., *Aviation: An Historical Survey from Its Origins to the End of World War II*, Her Majesty's Stationery Office, London, 1970.
7. Collar, A.R., "The First Fifty Years of Aeroelasticity," *Aerospace*, Vol. 5, No. 2, 1978, pp. 12-20.
8. Garrick, I.E. and Reed, W.H.I., "Historical Development of Aircraft Flutter," *Journal of Aircraft*, Vol. 18, No. 11, 1981, November, pp. .
9. Loftin, L.K., Jr., *Quest for Performance - The Evolution of Modern Aircraft*, NASA SP-468, NASA, Washington, D.C., 1985.
10. Bisplinghoff, R.L., Ashley, H., and Halfman, R.L., *Aeroelasticity*, Addison-Wesley, Reading, Mass., 1955.
11. Bisplinghoff, R.L. and Ashley, H., *Principles of Aeroelasticity*, Dover Publications, New York, 1975.

12. Dowell, E.H., et al., *A Modern Course in Aeroelasticity*, Sijthoff and Noordhoff, The Netherlands, 1980.
13. Fung, Y.C., *An Introduction to the Theory of Aeroelasticity*, Dover Publications, Inc., New York, 1969.
14. Scanlan, R.H. and Rosenbaum, R., *Aircraft Vibration and Flutter*, Dover Publications, Inc., New York, 1968.
15. Younger, J.E., *Mechanics of Aircraft Structures*, McGraw-Hill Book Company, Inc., New York, 1942.
16. *Subchapter C - Aircraft, Parts 21-35*, in *Code of Federal Regulations, Title 14, Aeronautics and Space (14 CFR. 1,1)*, 1987, U.S. Government Printing Office: Washington, D.C.

"Sweep wing backwards - data to follow"
telegram from George Schairer to Boeing XB-47
team, May 1945

CHAPTER TWO STATIC AEROELASTIC PROBLEMS

Background

In April 1945 Theodore von Karman, at the request of U.S. Army Air Forces Chief of Staff General Henry A. (Hap) Arnold, led a team of eminent American scientists and engineers to Germany to examine captured aeronautical data and interview German aeronautical engineers and scientists. The impressive secret work of the Germans during the war astounded the American engineers.

One the many valuable items captured by the American team was data on high speed swept wings that led to George Schairer's telegram. This data spread throughout the aircraft industry in America and the Soviet Union and revolutionized aircraft design.



Figure 2.1 - B-47 jet bomber [2.1]

The B-47 project was the first to use high aspect ratio, thin swept wings in its design. The commitment to use this geometrical feature triggered new structural problems and caused new static aeroelastic problems. The pronounced deflection of thin, high aspect ratio wings within their design envelope is seen in Figures 1.1 and 1.3.

Two effects of bending of these wings are important to design. The streamwise angle of attack is reduced by upward bending. This shows up as a perceived elastic streamwise

twist, even though the effect is due to bending. The effective streamwise twist is written as $\alpha_{bending} = -\phi \sin \Lambda$ where ϕ is the local bending slope and Λ is the sweep angle (positive for sweepback). The negative sign indicates that bending of a sweepback wing will reduce the angle of attack, particularly at the wing tips where the bending slope is the greatest.

Reduced angle of attack due to bending reduces the airloads along the wing so that the flexible wing must be given a larger overall incidence or angle of attack than would be the case if the wing were rigid in bending. The second result of the reduced angle of attack along the wing is that the center of pressure is shifted inboard and forward along the wing. This was illustrated in Chapter One.

The shift in the spanwise center of pressure forward creates a potential longitudinal stability problem. Early tests on the XB-47 found that this shift in the center of pressure due to wing bending was equivalent to an unfavorable, destabilizing rearward shift in the c.g. of 15% of the mean aerodynamic chord. This is the equivalent of a 15% reduction in the static margin of the aircraft.

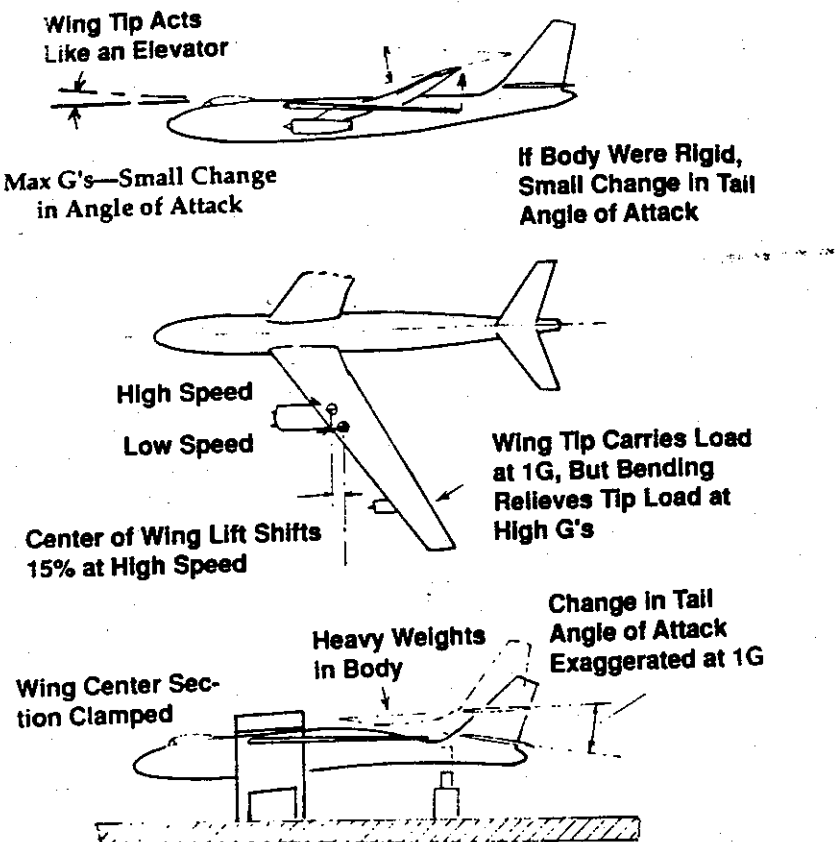


Figure 2.2 - Deformed XB-47 showing wing and tail deflections [2.2]

When the aircraft maneuvers the load factor, defined as the total lift divided by the aircraft weight, changes. An increased load factor is created by loading the wing which in turn bends the wing more. This bending then further shifts the aerodynamic spanwise center of pressure forward and will cause the aircraft to pitch up. This pitch up is countered by an elevator deflection commanded by the pilot to provide a counteracting pitching moment. The combination 15% change in the static margin due to bending and the requirements for maneuvering require a larger tail and elevator than normally would be necessary if the swept wing were rigid in bending.

Fortunately the XB-47 had one more static aeroelastic effect to consider. The slender fuselage bends downward under its own weight, an effect that increases as the structure is subjected to maneuvering g loads. As shown in Figure 2.2, downward bending creates a change in the tail surface incidence that in turn produces a moment to counteract the pitch up of the wing bending. The Boeing designers "lucked out."

This example illustrates the importance of static aeroelastic phenomena with moderate to strong interaction between internal structural forces and external deformation dependent airloads. In addition to the problems described, flight mechanics and controls engineers (not to mention the pilots) are vitally concerned with static aeroelastic effects such as lift effectiveness, wing divergence, and control surface effectiveness and reversal so that they can provide satisfactory maneuvering performance and stability characteristics. The structural engineer must design a structure that combines optimum strength with adequate stiffness characteristics.

Our goals in this chapter include introducing the aeroelastic analysis process to obtain insight and an interdisciplinary analysis perspective. The formulas obtained from the idealized models used in this chapter will illustrate how disciplines fit together in aeroelastic analysis process.

Matrix structural analysis

Mathematical models help to explain and anticipate aeroelastic interactions. An essential component of these models is a structural component. In the early days of aviation, construction was done by "cut and try" methods based loosely on methods adapted from civil engineering, in particular bridge building. Test pilots decided whether or not they liked the flying qualities. The airplane either stayed together or fell apart. Analysis and testing were mostly nonexistent or, at best, primitive.

Even as computational techniques improved, engineers fifty or sixty years ago still designed aircraft using computational tools requiring no more than a slide rule and a mechanical desk calculator. The demands for performance, efficiency and high speed for modern aircraft would be unreasonable today were it not for high-speed computers and modern automated analysis procedures such as finite element (FEM) structural methods

and aerodynamic paneling methods and computational fluid dynamics (CFD) efforts. These advanced analysis methods provide complex analytical models to aid design decision-making and shorten the time required to make decisions.

The field of finite element development owes its beginnings to the aircraft industry and in particular flutter and vibration clearance efforts. About 40 years ago, the need to accurately represent aeroelastic and vibratory interactions of geometrically complex flexible airplane structural elements at the earliest stages of design led to the development of the finite element method of structural analysis.

A 1956 paper by Turner, Clough, Martin and Topp at the Boeing Airplane Company ("Stiffness and deflection analysis of complex structures," *Journal of the Aeronautical Sciences*) was the result of the quest for accurate analytical procedures for vibration and stress analysis on transport airframes. Within a few years, this idea had exploded onto the analytical scene and became the mainstay of modern structural analysis.

For finite element analysis purposes, a flexible aircraft structure is assumed to be a mathematical assemblage of many different types of load bearing elements. The result is an analytical model that looks like that shown in Figure 2.3. The relationship between the structural forces and displacements on each of these elements is expressed as a set of linear (or nonlinear) algebraic equations whose coefficients are referred to as the stiffness matrix.

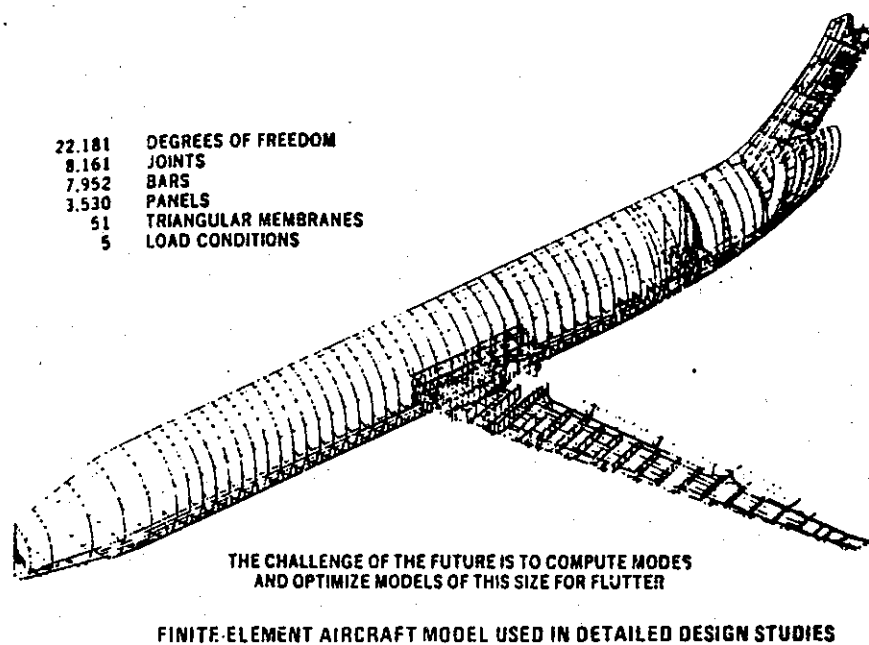


Figure 2.3 - Finite element gridwork for aircraft structural analysis

The finite element method that has evolved rapidly over the past thirty years has led to accurate elements and many large scale computer codes such as NASTRAN and ANSYS. These codes are used widely by both aerospace and non-aerospace companies.

The structural idealization of an aircraft structure and the definition of the loads on the structure require selecting degrees of freedom of motion. These degrees of freedom may be actual displacements (including rotation) of the structure or they may be amplitudes of assumed continuous displacement functions (shapes) or vectors used to describe the structural deformation. The final result is that the actual structure, with infinitely many degrees of freedom, is replaced by an idealized model with a manageable number of unknown displacement quantities or degrees of freedom such as shown in Figure 2.3.

Aircraft loads are combinations of distributed pressures and inertia or relatively concentrated forces or inertia (such as engines) and moments. For matrix analysis, both the distributed and concentrated loads must be converted to a set of equivalent discrete forces and moments associated with each of the degrees of freedom. The result is a set of generalized forces (the term generalized force can refer to *either* a force or a moment) denoted as $\{F_i\}$. Each element F_i is associated with a corresponding deflection vector element u_i (these generalized displacements can also be *either* a deflection or a rotation).

The generalized forces applied to the aircraft and displacements of the aircraft structure are related to each other. If the structure behaves as a linear elastic system, this relationship may be written as follows.

$$\{F_i\} = [K_{ij}][u_j] \quad (2.1)$$

Equation 2.1 is called the stiffness equation, and $[K_{ij}]$ is the system stiffness matrix. The elements, K_{ij} , of this matrix are called stiffness influence coefficients. The column K_{ij} represents the set of forces that must be applied to a structure to achieve a unit value (one inch, one foot, etc.) of u_i while keeping all other displacements, u_j ($j \neq i$) equal to zero.

In a system without dissipative outlets such as friction, total energy must be conserved. Therefore, all of the work done by the external forces must be stored within the structure. If the structure is restrained against rigid body motion (such as sliding) and the forces are applied slowly, the work done is stored as strain energy or potential energy, since it can be recovered when the loads are removed.

Consider the simple spring element shown in Figure 2.4. If the external force applied very slowly so that the acceleration is so small that static equilibrium is maintained approximately throughout the loading process, then the work done, W , by the force F in moving through displacement u is

$$W = \frac{1}{2} F u = \frac{1}{2} K u^2 \quad (2.2)$$

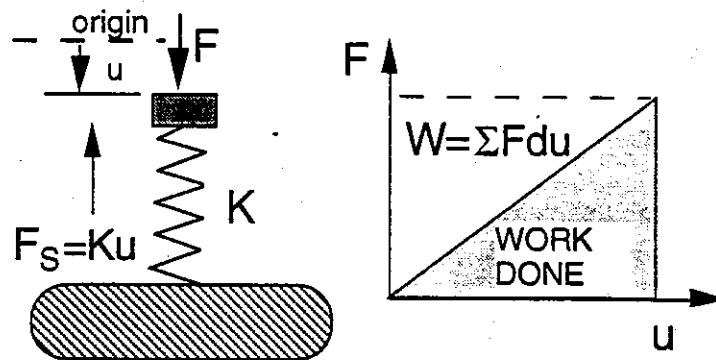


Figure 2.4 - Spring-mass-force system

In the more general case where there are many displacements and many forces located at the same points as displacements are measured, the work done by the forces is

$$W = \frac{1}{2} [F_i] \{u_i\} = \frac{1}{2} \{u_i\}^T \{F_i\} \quad (2.3)$$

The factor of 1/2 appears in Eqns. 2.2 and 2.3 because the relationship between the loads and deflections is assumed to be linear and the loads build slowly from zero to their final values, F_i and u_i . Substitution of Eqn. 2.1 into 2.3 provides an expression for work done in terms of the structural displacements and the stiffness matrix in Eqn. 2.1.

$$W = \frac{1}{2} \{u_i\}^T [K_{ij}] \{u_j\} \quad (2.4)$$

The deformation energy stored within the structure is called strain energy and is denoted as U . Because of energy conservation, W is equal to U so that

$$U = \frac{1}{2} \{u_i\}^T [K_{ij}] \{u_j\} \quad (2.5)$$

If we differentiate U with respect to u_i we obtain a force equilibrium equation for that degree of freedom, written as

$$\frac{\partial U}{\partial u_i} = \sum K_{ij} u_j = F_i \quad (2.6)$$

Differentiating Eqn. 2.6 with respect to u_j we recover the stiffness matrix elements for the rows and columns representing the equations of motion.

$$\frac{\partial^2 U}{\partial u_i \partial u_j} = K_{ij} = \frac{\partial^2 U}{\partial u_j \partial u_i} = K_{ji} \quad (2.7)$$

since the order of differentiation in Eqn. 2.7 may be interchanged. The stiffness matrix is symmetric.

The stiffness matrix elements may be positive, negative or zero when $i \neq j$, but the main diagonal elements must be positive (or zero if the structure is unrestrained in some way). If this were not so, we could withdraw energy from the structure by applying a load.

Example - Construction of a stiffness matrix

The idealized two-dimensional "structure" shown in Figure 2.5 has two linear elastic springs with stiffness K_1 and K_2 (lb/in or N/m). The deformation state of this model is defined by a downward deflection, h , at the reference point, and a pitch rotation, θ , about this point, positive counterclockwise. The external force is the resultant of all forces and pressures acting on the structure, while M is the resultant of the moments about the reference point of all the forces and pressures acting on the structure. We will compute the stiffness matrix to relate P and M to h and θ .

We use force and moment equilibrium equations to derive matrix equations. Consider the free-body diagram of the deformed system (shown in Figure 2.6), including the forces internal to the springs. When θ is small ($\sin \theta \approx \theta$), the compression of the right hand spring K_1 is $h - a\theta$, while the compression of the left spring K_2 is $h + b\theta$. Note that the dimensions a and b measure the spring positions relative to the reference point (or origin) for h .

The spring restoring forces are proportional to K_1, K_2 , $h - a\theta$ and $h + b\theta$. Summing forces and moments about the reference point we have two equations.

$$\sum F = P - K_1(h - a\theta) - K_2(h + b\theta) = 0$$

$$\sum M = M - K_2b(h + b\theta) + K_1a(h - a\theta) = 0$$

We can write these two equations in matrix form as:

$$\begin{Bmatrix} P \\ M \end{Bmatrix} = \begin{bmatrix} (K_1 + K_2) & (K_2 b - K_1 a) \\ (K_2 b - K_1 a) & (K_2 b^2 + K_1 a^2) \end{bmatrix} \begin{Bmatrix} h \\ \theta \end{Bmatrix} \quad (2.8)$$

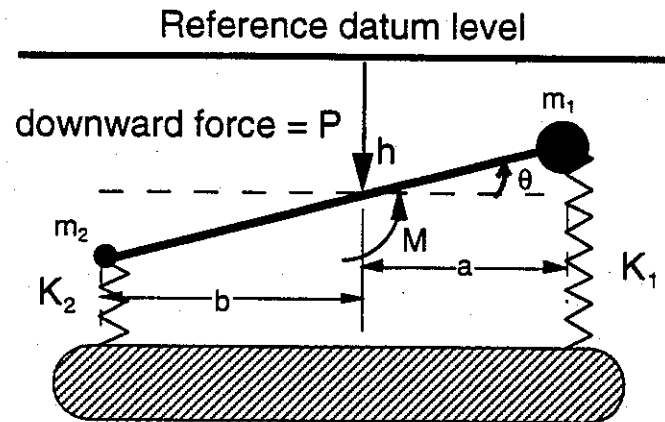


Figure 2.5 - Two dimensional bar and spring system

Equation 2.8 relates the applied external loads (a force P and moment M) at the reference point to the deflection and rotation at this point. Elastic or static coupling is indicated by the off-diagonal terms ($K_2 b - K_1 a$); in Eqn. 2.8 a θ rotation by a force, P , while an h displacement is accompanied by a moment, M .

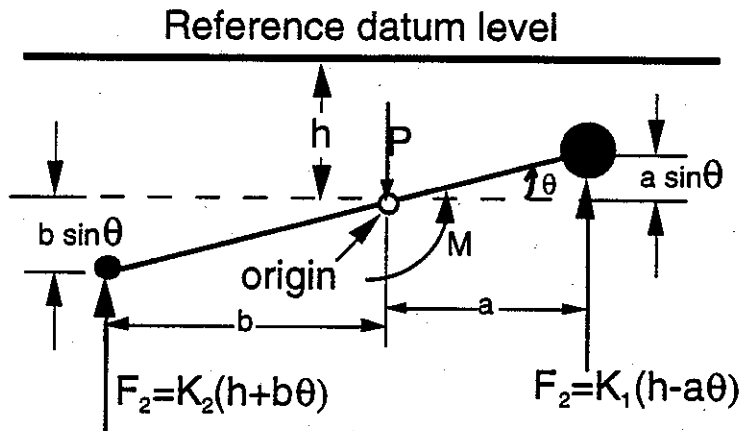


Figure 2.6 - Two dimensional bar free body diagram

The structural stiffness elements are functions of the two spring stiffnesses and location of the reference point (geometry). Elastic or static coupling depends on the coordinate system chosen. Because the force created by each spring is proportional to deflection, the spring with the highest load will deflect more, allowing the bar to tilt in its direction.

If we change the location of the reference point, the dimensions a and b must be changed. The size of the resultant force P (it is the sum of all the vertical forces acting on the structure) remains the same, but the size and perhaps the sign of M will change, since it represents the net external moment of a combination of external forces about the reference point. From Equation 2.8 we can see that, if K_1a is equal to K_2b , the elastic coupling term ($K_2b - K_1a$) is zero, so that elastic coupling disappears if the ratio of dimensions a and b is as follows

$$\frac{a}{b} = \frac{K_2}{K_1} \quad (2.9)$$

Equation 2.9 shows that there is a unique point on this structure where a concentrated force, P , causes only a displacement while a moment, M , causes only rotation about that point. The first condition defines the shear center. The second condition defines the center of twist. For a linear elastic structure such as that shown in Figure 2.5, the position of the shear center and center of twist are identical.

The shear center concept

The shear center is formally defined as a point on a structural configuration where loading by a concentrated force will create only translational displacement but no rotation or twist about a specified axis. If $K_1 = K_2 = K$ for our example, from Eqn. 2.9 the center of the bar ($a = b$) fits our shear center description. If the springs have different stiffness, the shear center is located using Eqn. 2.9. We can solve for the shear center using its definition by first using Eqn. 2.8 to solve for h and θ when P and M are applied.

$$\begin{Bmatrix} h \\ \theta \end{Bmatrix} = \frac{1}{\Delta} \begin{bmatrix} (K_2b^2 + K_1a^2) & -(K_2b - K_1a) \\ -(K_2b - K_1a) & (K_1 + K_2) \end{bmatrix} \begin{Bmatrix} P \\ M \end{Bmatrix} \quad (2.10)$$

In Eqn. 2.10 $\Delta = K_1K_2(a^2 + b^2) + 2K_1K_2(ab)$ is the determinant of the stiffness matrix. To find the shear center we only apply the load P so that we set $M = 0$ and then find that

$$\begin{Bmatrix} h \\ \theta \end{Bmatrix} = \frac{P}{\Delta} \begin{Bmatrix} (K_2b^2 + K_1a^2) \\ -(K_2b - K_1a) \end{Bmatrix} \quad (2.11)$$

From Eqn. 2.11, we can verify that if $K_2b = K_1a$ then $\theta = 0$, no matter what the size of the load P . For a linear system, the shear center does not depend on the size of the load applied.

Static aerodynamic coefficients

The loads P and M are functions of the aerodynamic pressures acting on the airfoil surface. In subsonic flow, aerodynamic forces are created by moving air being deflected by a surface traveling with respect to the air, as shown in Figure 2.7. Because of this deflection, the momentum of the air is changed and forces result. The imparting of momentum change to the air to create lift with low drag creates a vortex motion around the lifting surface as it travels through the air. This vortex is created by the formation of a very thin viscous boundary layer next to the wing surface itself.

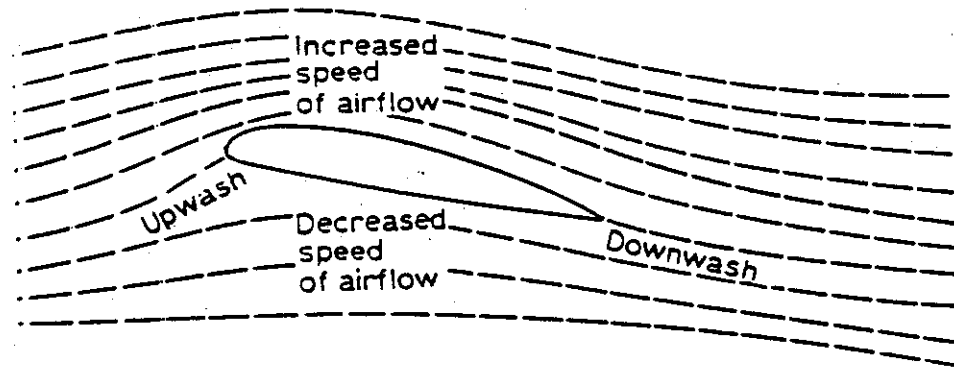


Figure 2.7 - Airflow around a wing section

Figure 2.7 shows that there is a slight flow upward (called upwash) before the air reaches the wing leading edge and there is a downward flow (called downwash) after the air passes the wing trailing edge. At a point slightly below the nose of the leading edge of the wing the flow stagnates and splits.

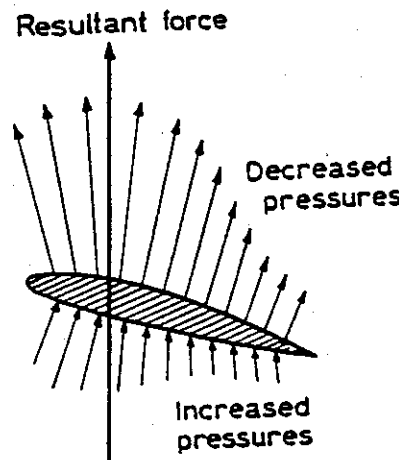


Figure 2.8 - Wing section (airfoil) pressure distribution in lifting flight

The velocity of the air over the top surface increases as we move upward from the stagnation point. From Bernoulli's law, the fluid static pressure must decrease, even if

(incompressible flow)

the fluid is incompressible. As a result of the pressure decrease or "suction" near the leading edge, the wing skin must be fastened tightly to the ribs or it would be pulled loose by this suction.

As shown in Figure 2.8, the pressures are lowest near the forward part of the wing section. The decreased pressure over the upper surface that is primarily responsible for the lift force on the wing, although, on the bottom surface, the air slows and the static pressure increases to help create even more lift.

We can replace the pressure distribution with a single force (with the moment computed to be zero) located near the leading edge of the wing section, as indicated in Figure 2.9. The position of the force is called the center of pressure. The lift resultant has a slight rearward angle because the pressure distribution and the viscous drag create drag as well as lift.

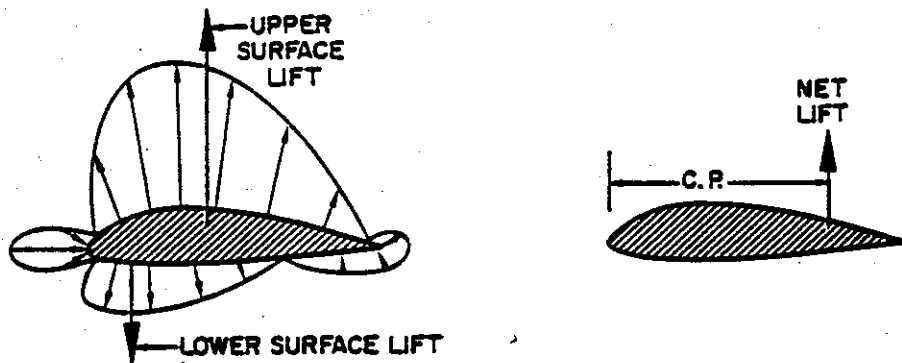


Figure 2.9 - Wing section center of pressure

When the wing or airfoil angle of attack is changed, the pressure distribution will change. Then the lift and the position of the center of pressure will change. At other locations on the chordline of the wing sections the pressure distributions will create the lift force and a pitching moment.

Experiments show that the lift and drag and pitching moment on a wing depend upon:

- wing cross-section shape
- wing planform shape
- air density
- dynamic pressure, $q = \frac{1}{2} \rho V^2$

The lift, drag, and pitching moment are denoted as L , D , and M , respectively, and defined with respect to surface planform area, S , dynamic pressure, q , and mean aerodynamic chord \bar{c} as:

$$L = C_L q S \quad (2.12a)$$

$$D = C_D q S \quad (2.12b)$$

$$M = C_m q S \bar{c} \quad (2.12c)$$

The local or two-dimensional lift, drag, and pitching moment coefficients, are written as l , d and m , respectively, so the force and moment per unit length and are defined by:

$$l = c_l q \bar{c} \quad (2.12d)$$

$$d = c_d q \bar{c} \quad (2.12e)$$

$$m = c_m q \bar{c}^2 \quad (2.12f)$$

Notice that l , d and m have units of force (or moment) per unit length (or unit span). These static aerodynamic coefficients change with the airfoil angle of attack, Reynolds number, and Mach number.

The lift force changes with angle of attack, α , as shown in Figure 2.10. Figure 2.10 indicates that this wing develops lift even when the incidence is at zero angle of attack. This is a characteristic of a cambered airfoil or wing. A symmetrical airfoil section will have no lift at zero angle of attack. At angles up to 12° the lift and lift coefficient are almost straight lines. At about 15° the lift coefficient reaches a maximum and then declines with further increases in angle of attack.

The loss of lift near 15° is called "stall" and is associated with the breakdown or detachment of the streamlines formed by the vortex flow from the wing. The shape of the cross-section makes little difference in the angle at which stall occurs, although it does affect the value of the maximum value of C_L achieved when stall occurs. At stall the suction seen near the leading edge decreases while the pressure distribution at other points remains approximately the same so that lift decreases.

The linear portion of the lift and pitching moment curves may be approximated by the expressions

$$c_l = c_{l_0} + \left(\frac{\partial c_l}{\partial \alpha} \right) \alpha = c_{l_0} + c_{l_\alpha} \alpha \quad (2.13a)$$

$$c_m = c_{m_0} + \left(\frac{\partial c_m}{\partial \alpha} \right) \alpha = c_{m_0} + c_{m_\alpha} \alpha \quad (2.13b)$$

The notation $()_\alpha$ indicates partial differentiation with respect to angle of attack, α . The equation for c_m versus α depends upon the reference point chosen for measurements of the pitching moment.

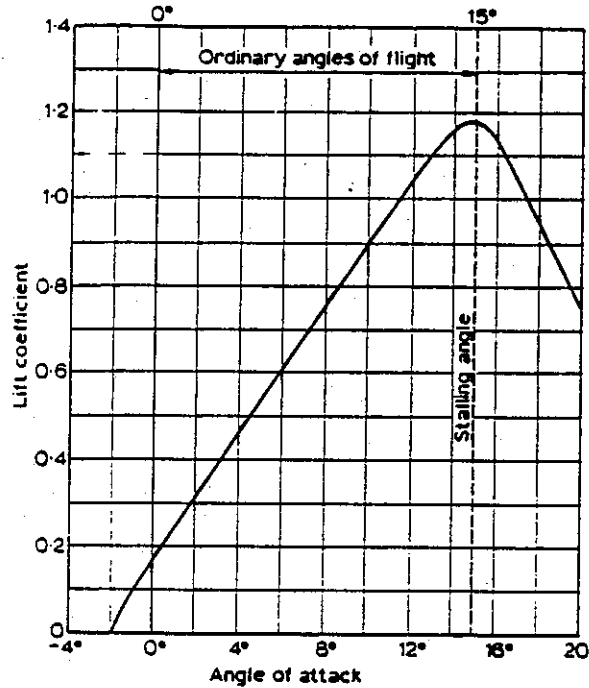


Figure 2.10 - Lift coefficient vs. wing angle of attack [2.2]

The drag on a wing depends on the angle of attack and also on the friction drag on the exposed or wetted area of the surface. The drag is plotted in Figure 2.11 against angle of attack. Note that the drag does not increase rapidly until we are near stall.

The analytical behavior of the drag coefficient is approximately quadratic for angles of attack within the linear region of the lift curve. This relationship is:

$$c_d = c_{d_0} + \left(\frac{\partial c_d}{\partial (\alpha^2)} \right) \alpha^2 \quad (2.14)$$

where α is measured from the position of zero lift. The term c_{d_0} is called the parasite or zero lift drag coefficient. Eqn. 2.14 can also be written as:

$$c_d = c_{d_0} + (k)c_l^2 \quad (2.15)$$

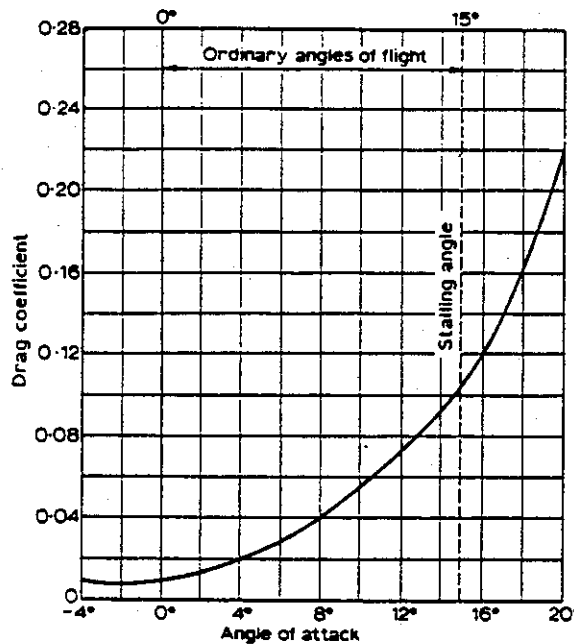


Figure 2.11 - Drag coefficient vs. angle of attack [2.2]

The second term in Eqns. 2.14 and 2.15 is the induced drag or drag due to lift. This induced drag only appears for wings with a finite aspect ratio (aspect ratio is defined as the span squared divided by the wing planform area) and becomes very small as the wings become more slender. If the aspect ratio is infinite, the induced drag is zero.

Center of pressure

The pitching moment on a wing or airfoil section depends on the angle of attack and upon the point at which we measure the pitching moment. By definition, the pitching moment is zero at the center of pressure. As angle of attack increases, the center of pressure position changes, as shown in Figure 2.12.

Figure 2.12 indicates that the center of pressure at negative angles of attack is far aft on the airfoil section. As the angle of attack increases, the center of pressure moves forward to near the 0.25 chord position (the quarter-chord) until near the stall condition. Near stall the center of pressure moves aft again as the angle of attack is increased.

The pitching moment coefficient at any point x aft of the wing leading edge is written as $C_M = C_L x + C_{M_{leading\ edge}}$. When $C_M(x)$ is zero, we are at the center of pressure.

Measured as a fraction of the airfoil chord aft of the leading edge, the center of pressure location is denoted as \bar{x}_{cp} and is given by the equation,

$$\bar{x}_{cp} = \frac{x_{cp}}{c} = \frac{-C_M}{C_L} \quad (2.16)$$

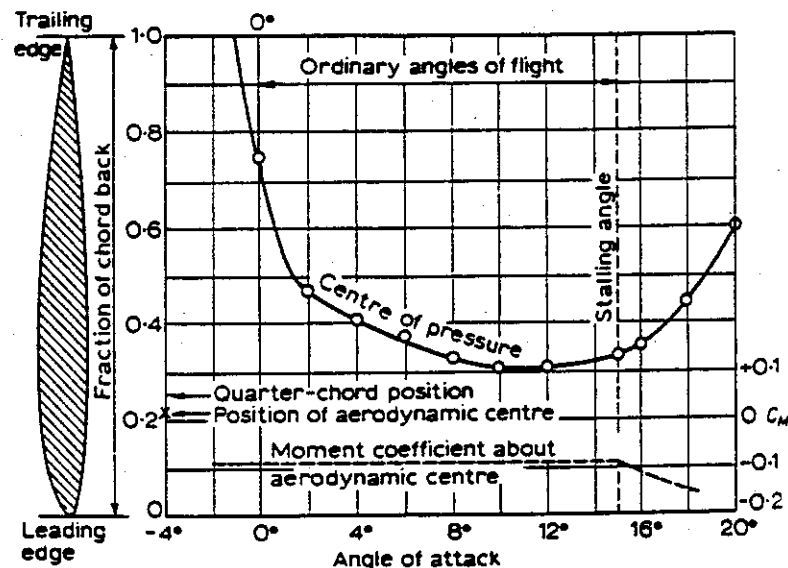


Figure 2.12 - Center of pressure & pitching moment coefficient at aerodynamic center [2.2]

Notice that the center of pressure location depends on the size of the lift coefficient.

Aerodynamic center

There is a point on the airfoil section and the wing where the pitching moment does not change with changes in angle of attack. This point is called the aerodynamic center. The pitching moment coefficient about the aerodynamic center for this airfoil is a small distance ahead of the quarter chord position.

To understand more about the concept of the aerodynamic center, consider Figure 2.13. In this figure the pitching moment coefficient is plotted at three points on the airfoil. At a point at the leading edge the pitching moment coefficient decreases as angle of attack increases. At a point near the trailing edge, the pitching moment coefficient increases as angle of attack increases.

There is an angle of attack (it occurs when the lift is zero) at which ~~both~~^{the} pitching moment coefficient at every point is the same. This special value of the pitching moment

coefficient is the pitching moment coefficient about the aerodynamic center. Notice that if the airfoil is a symmetrical section then the pitching moment is zero at zero angle of attack and the pitching moment coefficient at the AC is zero.

Since the aerodynamic center is defined as the point on the airfoil about which the pitching moment does not change with angle of attack (or changes in lift coefficient)

$$\frac{\partial C_M}{\partial \alpha} = C_{M_\alpha} = 0 = \frac{\partial C_L}{\partial \alpha} \frac{x_{AC}}{c} + \frac{\text{leading edge}}{\partial \alpha} \quad (2.17)$$

The aerodynamic center location behind the leading edge, as a fraction of the chord, is given by the relationship

$$\bar{x}_{ac} = -\frac{\frac{\partial C_M}{\partial \alpha} \text{leading edge}}{\frac{\partial C_L}{\partial \alpha}} = -\frac{C_{M_\alpha} \text{(leading edge)}}{C_{L_\alpha}} \quad (2.18)$$

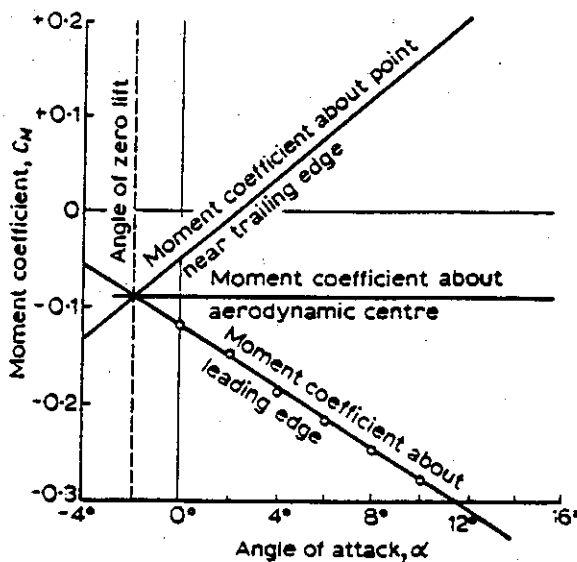


Figure 2.13 - Pitching moment coefficient about three reference points [2.2]

Both $C_{M_{\text{leading edge}}} = C_{M_0}$ and $\frac{\partial C_{M_0}}{\partial \alpha}$ are negative, so both \bar{x}_{ac} and \bar{x}_{cp} are positive. Note the

difference between Eqns. 2.16 and 2.18. Equation 2.16 uses the total lift and pitching moment about the leading edge while Eqn. 2.18 uses aerodynamic coefficient derivatives (or rates) with respect to the angle of attack, α .

Aeroelastic problems are concerned with the effect of changes in deflection and aerodynamic forces. As a result, the aerodynamic center is a more useful and convenient reference point than the center of pressure.

Compressibility and Mach number effects

Mach number is defined as the airspeed divided by the local speed of sound. It is convenient to define the importance of compressibility by defining four different Mach number regions. The subsonic regime is taken as $0 < M < 0.8$, the transonic regime as $0.8 < M < 1.2$, the supersonic regime as $1.2 < M < 4$, and the hypersonic regime as $M > 4$.

The dynamic pressure used to compute the aerodynamic forces and moments is the product of the air density at the operational altitude and the airspeed squared. Dynamic pressure is the energy of a unit volume of air when it is accelerated to an airspeed, V.

Although dynamic pressure, computed using the static air density, ρ_o , is a convenient reference quantity, it will not represent the actual density of the air if it is compressed at high speed. The effect of compressibility (and the ability of the flow to adjust to the presence of a wing speeding through it) is judged by computing the Mach number of the flow.

To understand why the aerodynamic coefficients change with Mach number we introduce the concept of a local pressure coefficient, called C_p and defined as

$$\Delta p = \frac{1}{2} \rho V_o^2 C_p = q C_p \quad (2.19)$$

Because of Bernoulli's equation, this relationship can be written as:

$$C_p = 1 - \left(\frac{V^2}{V_o^2} \right) \quad (2.20)$$

where V is the local velocity of the flow at any point on the wing outside the boundary layer and V_o is the freestream velocity.

At low speeds, less than $M=0.3$, the wing diverts the oncoming flow but does not compress it ahead of or on the wing itself (that's why we refer to it as incompressible flow). At higher speeds, the density will change because the fluid ahead of the wing is compressed. Because of this, the flow density ρ , used as the reference for dynamic pressure must be adjusted to account for compressibility.

When compressibility begins to become important, at a Mach number above 0.3 for instance, the pressure coefficient will change even if the wing angle of attack doesn't change. Prandtl and Glauert have suggested a correction factor for the pressure coefficient given by:

$$C_p = \frac{C_{p_{incomp}}}{\sqrt{1 - M^2}} \quad (2.21)$$

Since the aerodynamic coefficients (Eqns. 2.12 a-f) are integrals of the pressure coefficient, then the aerodynamic coefficients will themselves be modified by the same "rule" presented in Eqn. 2.21. The approximation in Eqn. 2.21 is accurate up to about $M=0.7$ or 0.8 .

An example of the use of this Prandtl-Glauret "transformation" to account for compressibility is modifying the lift curve slope for a two-dimensional airfoil section to give the subsonic value of $c_{l_a} = \frac{2\pi}{\sqrt{1 - M^2}}$. A similar analysis in the supersonic region results in a correction to the aerodynamic coefficients that is given by $c_{l_a} = \frac{4}{\sqrt{M^2 - 1}}$. Neither of these two approximations applies near Mach 1.

Effects of flexibility on two-dimensional airfoil lift generation

At low flight speeds the wing twists because the lift vector or line of action does not pass through the shear center. Figure 2.14 shows a symmetrical airfoil section with the lift acting at the aerodynamic center. The pitching moment about the aerodynamic center

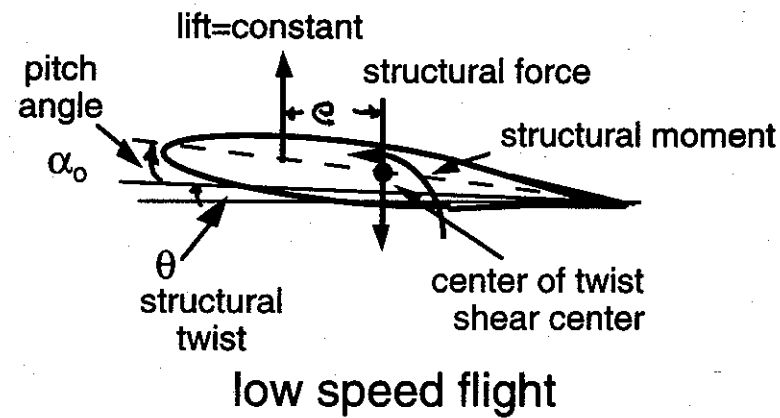


Figure 2.14 - Twist of a wing section in low speed flight

is zero because the section is symmetrical. The total airfoil incidence is the sum of the elastic twist angle and the pitch angle controlled by the pilot. The sum of these two angles is small, of the order of only a few degrees.

The wing lift is constant when the airplane weight or load factor is constant. As a result, the moment about the shear center or elastic axis is constant, no matter what the airspeed. If we go faster, the dynamic pressure increases and lift will increase if we do not reduce the angle of attack. The only way to keep lift constant, since the twist angle is constant, is to reduce the wing pitch angle, as indicated in Figure 2.15.

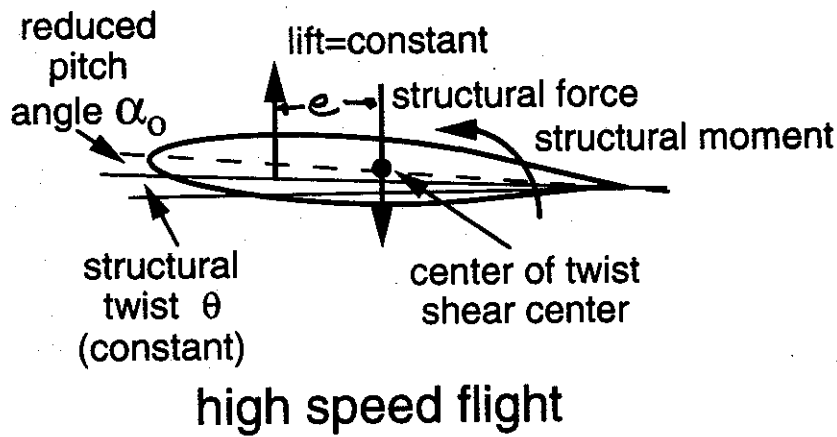


Figure 2.15 - Wing section in high speed flight showing reduced pitch angle

If we can make the airplane go fast enough, the pitch angle controlled by the pilot will be reduced to zero and all of the lift will be due to the twist angle of attack of the wing. A further increase in airspeed would require that the pilot put the airplane into a nose down attitude. We will show later that the airspeed at which the twist angle of attack is all that is required to generate lift to support the airplane is called the divergence speed. This airspeed results in an unstable flight condition.

As the "rigid body" pitch angle decreases relative to the wing twist angle, aeroelastic interaction increases. To analyze this situation, consider Figure 2.16 which shows an idealized airfoil model mounted on two springs that represent the reaction of the skin and spars to the lift.

The effect of these two springs is combined into a single spring, K_h , to resist translation and a single torsion spring, K_T , to resist twisting. Comparing Figure 2.16 with Figure 2.5, we have

$$K_h = K_1 + K_2 \text{ (plunge spring)} \quad (2.22)$$

$$K_T = \frac{K_1 + K_2(a+b)^2}{K_1 + K_2} \text{ (pitch spring)} \quad (2.23)$$

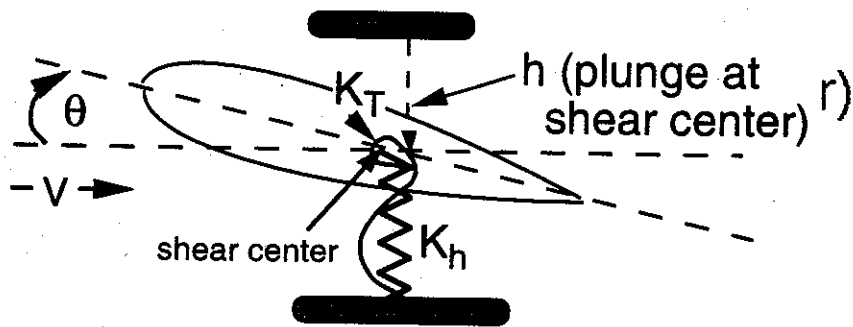


Figure 2.16 - Airfoil with pitch and plunge springs,

From Eqn. 2.8 we find that the relationship between the aerodynamic force and moment (L and M) and the shear center deflection; h , and the twist rotation, θ , is given, in the matrix form, as:

$$\begin{bmatrix} K_h & 0 \\ 0 & K_T \end{bmatrix} \begin{bmatrix} h \\ \theta \end{bmatrix} = \begin{bmatrix} -L \\ M \end{bmatrix} \quad (2.24)$$

If the airfoil is given an incremental angle of attack, α_0 , by the pilot's use of the tail surface to pitch the airplane, aerodynamic lift L and pitching moment M (about the shear center) will be generated. L and M are functions of both the known quantity α_0 and an unknown twist, θ .

The lift and moment at the shear center ~~are coefficient form as:~~

$$L = qSC_{L_a}(\alpha_0 + \theta) \quad (2.25)$$

$$M_{SC} = M_{AC} + Le \quad e = \text{distance between aero center and shear center}$$

or

$$M_{SC} = qcSC_{MAC} + qSeC_{L_a}(\alpha_0 + \theta) \quad (2.27)$$

Equations 2.25 and 2.27 are written in matrix form as:

$$\begin{Bmatrix} -L \\ M_{sc} \end{Bmatrix} = qSC_{L_a} \begin{bmatrix} 0 & -1 \\ 0 & e \end{bmatrix} \begin{Bmatrix} h \\ \theta \end{Bmatrix} + qSC_{L_a} \alpha_o \begin{Bmatrix} -1 \\ e \end{Bmatrix} + qScC_{MAC} \begin{Bmatrix} 0 \\ 1 \end{Bmatrix} \quad (2.28)$$

Equation 2.28 is substituted into the airfoil static equilibrium equation, Eqn. 2.24, to give:

$$\begin{bmatrix} K_h & 0 \\ 0 & K_T \end{bmatrix} \begin{Bmatrix} h \\ \theta \end{Bmatrix} = qSC_{L_a} \begin{bmatrix} 0 & -1 \\ 0 & e \end{bmatrix} \begin{Bmatrix} h \\ \theta \end{Bmatrix} + qSC_{L_a} \alpha_o \begin{Bmatrix} -1 \\ e \end{Bmatrix} + qScC_{MAC} \begin{Bmatrix} 0 \\ 1 \end{Bmatrix} \quad (2.29)$$

Gathering all of the deflection dependent terms on the left hand side of Eqn. 2.29, we have

$$\begin{bmatrix} K_h & 0 \\ 0 & K_T \end{bmatrix} \begin{Bmatrix} h \\ \theta \end{Bmatrix} - qSC_{L_a} \begin{bmatrix} 0 & -1 \\ 0 & e \end{bmatrix} \begin{Bmatrix} h \\ \theta \end{Bmatrix} = qSC_{L_a} \alpha_o \begin{Bmatrix} -1 \\ e \end{Bmatrix} + qScC_{MAC} \begin{Bmatrix} 0 \\ 1 \end{Bmatrix} \quad (2.30)$$

Because it appears with the structural stiffness matrix on the left hand side of Eqn. 2.30, the matrix proportional to aerodynamic pressure, q , is referred to as the aerodynamic stiffness matrix. Notice that this matrix couples together the equations for h and θ . On the other hand, the θ equilibrium equation, represented by the second row in Eqn. 2.30 does not contain the unknown displacement h and it can be solved for θ without first calculating h . Once θ is determined, then the value of h can be computed.

To solve for h and θ , first divide each term in Eqn. 2.30 by K_T .

$$\begin{bmatrix} K_h/K_T & qSC_{L_a}/K_T \\ 0 & 1 - qScC_{L_a}/K_T \end{bmatrix} \begin{Bmatrix} h \\ \theta \end{Bmatrix} = \frac{qSC_{L_a} \alpha_o}{K_T} \begin{Bmatrix} -1 \\ e \end{Bmatrix} + \frac{qScC_{MAC}}{K_T} \begin{Bmatrix} 0 \\ 1 \end{Bmatrix} \quad (2.31)$$

Solving for the plunge displacement and the elastic twist angle, we find

$$\begin{Bmatrix} h \\ \theta \end{Bmatrix} = \frac{qSC_{L_a} \alpha_o}{K_T} \begin{bmatrix} K_T/K_h & \frac{-qSC_{L_a}/K_h}{1 - qScC_{L_a}/K_T} \\ 0 & \frac{1}{1 - qScC_{L_a}/K_T} \end{bmatrix} \begin{Bmatrix} -1 \\ e \end{Bmatrix} + \frac{qScC_{MAC}}{K_T} \begin{bmatrix} K_T/K_h & \frac{-qSC_{L_a}/K_h}{1 - qScC_{L_a}/K_T} \\ 0 & \frac{1}{1 - qScC_{L_a}/K_T} \end{bmatrix} \begin{Bmatrix} 0 \\ 1 \end{Bmatrix}$$

or

$$\begin{Bmatrix} h \\ \theta \end{Bmatrix} = \frac{qSC_{L_a}\alpha_o}{K_T} \begin{Bmatrix} -K_T/K_h - \frac{qSeC_{L_a}/K_h}{1-qSeC_{L_a}/K_T} \\ \frac{e}{1-qSeC_{L_a}/K_T} \end{Bmatrix} + \frac{qScC_{MAC}}{K_T} \begin{Bmatrix} \frac{-qSC_{L_a}/K_h}{1-qSeC_{L_a}/K_T} \\ \frac{1}{1-qSeC_{L_a}/K_T} \end{Bmatrix}$$

This becomes

$$\begin{Bmatrix} h \\ \theta \end{Bmatrix} = \begin{Bmatrix} \frac{-qSC_{L_a}\alpha_o/K_h}{1-qSeC_{L_a}/K_T} \\ \frac{qSeC_{L_a}\alpha_o}{K_T} \end{Bmatrix} + \frac{qScC_{MAC}}{K_T} \begin{Bmatrix} \frac{-qSC_{L_a}/K_h}{1-qSeC_{L_a}/K_T} \\ \frac{1}{1-qSeC_{L_a}/K_T} \end{Bmatrix} \quad (2.32)$$

From Eqn. 2.32, the plunge displacement is

$$h = \frac{-qSC_{L_a}\alpha_o/K_h}{1-qSeC_{L_a}/K_T} - \frac{qScC_{MAC}}{K_T} \left(\frac{qSC_{L_a}/K_h}{1-qSeC_{L_a}/K_T} \right) \quad (2.33)$$

while the twist rotation is

$$\theta = \frac{\frac{qSeC_{L_a}\alpha_o}{K_T}}{1-qSeC_{L_a}/K_T} + \frac{qScC_{MAC}}{K_T} \left(\frac{1}{1-qSeC_{L_a}/K_T} \right) \quad (2.34)$$

Substituting the expression for elastic twist, Eqn. 2.34, into the expression for lift, Eqn. 2.25, we get the following expression for the lift on the wing section.

$$L = \frac{qSC_{L_a}}{1-qSeC_{L_a}/K_T} \alpha_o + \frac{qSC_{L_a}}{1-qSeC_{L_a}/K_T} \left(\frac{qScC_{MAC}}{K_T} \right) \quad (2.35)$$

Equation 2.35 shows two interesting features that relate to failure of early monoplanes. One of these features led to Langley's Aerodrome failure, while another led the British to "outlaw" monoplane designs in 1912.

Notice that the plunge stiffness of the airfoil, K_h , which comes from the combination of wing spar stiffness, bracing wires and skin bending stiffness, does not appear in the lift expression in Eqn. 2.35. In early airplane designs, the fabric skin contributed little or no bending stiffness. With low torsional stiffness K_T , the term in the denominator of Eqn. 2.35 can be large, even for small values of dynamic pressure, q . This occurs when the aerodynamic center and the shear center are far apart.

Early monoplane wings had very low torsional stiffness because they were thin and some allowed low torsional stiffness so that the wings could be warped for lateral control. The wing sections also had substantial camber, creating a large nose down (negative) pitching moment. The effect of the nose down pitching moment on wing twist is seen in the second term of Eqn. 2.35. This initial twist induced angle of attack is

$$\alpha_M = \left(\frac{qScC_{MAC}}{K_T} \right)$$

The term C_{MAC} decreases (from its value of zero for a symmetrical airfoil) with increasing camber. The twist due to camber becomes more negative as airspeed increases and its effect on lift is again amplified by aeroelastic interaction.

This interaction can explain why Langley's Aerodrome crashed on take-off from its houseboat platform. Since the camber on the Aerodrome wings was large, a large nose-down pitching moment was placed on the thin, torsionally flexible wings. Even though the shear center and aerodynamic center were close together so that e was nearly zero, the nose-down twist placed a downward load on the wing instead of the upward load the Langley expected. Thus structural flexibility, but not aeroelastic interaction, gave the first flight prize to the Wright Brothers.

The first term in Eqn. 2.35 is the lift due to an input angle of attack. The effect of the lift curve slope $C_{L\alpha}$ is amplified by the aeroelastic term

$$\frac{1}{1 - \frac{qSeC_{L\alpha}}{K_T}}$$

This amplification term increases with increasing airspeed when the aerodynamic center and the shear center are offset and the AC is ahead of the shear center, the normal case for subsonic aircraft.

The airfoil angle of attack α_o necessary to generate lift to sustain the airplane of weight W in level flight is computed from the following equation

$$L = \frac{W}{2} = qSC'_{L_a} \alpha_o + qSC'_{L_a} \alpha_M \quad (2.36)$$

where

$$L \text{ for each "wing"} \quad C'_{L_a} = \frac{C_{L_a}}{1 - qSeC_{L_a}/K_T} \quad (2.37)$$

Solving for the airfoil angle of attack α_o we have

$$\alpha_o = \frac{1}{2} \left(\frac{W}{S} \right) \left(\frac{1 - \bar{q}}{qC_{L_a}} \right) - \alpha_M \quad (2.38)$$

where

$$\bar{q} = \frac{qSeC_{L_a}}{K_T}$$

Equation 2.37 indicates that, for a wing with a symmetrical airfoil section ($\alpha_M = 0$), the pilot will have to reduce the wing attitude as dynamic pressure increases. If there is no aeroelastic interaction ($\bar{q} = 0$) then the angle of attack will have to be increased as airspeed increases.

These results approximate the effects of wing torsional flexibility on lift generation. An equally important facet of the influence of flexibility is how a slight change in angle of attack can change the load on a wing. To show this, we differentiate the expression for lift (Eqn. 2.36) with respect to the angle of attack α_o to obtain

$$\frac{\partial L}{\partial \alpha_o} = qSC'_{L_a} = \frac{qSC_{L_a}}{1 - \bar{q}} \quad (2.39)$$

The aircraft load factor, n, is defined as

$$n = \frac{L}{W}$$

When $n=1$ we have straight, level flight. We define the change in load factor with angle of attack as

$$\frac{\partial n}{\partial \alpha_o} = \frac{\partial L/W}{\partial \alpha_o} = \frac{qSC'_{L_a}}{W} = \frac{qC_{L_a}}{(W/S)(1 - \bar{q})} \quad (2.40)$$

Equation 2.40 shows that the increased load factor due to a change in aircraft attitude from a pilot input or encountering a gust will increase with increasing aeroelastic interaction. An airplane flying close to the divergence speed will be extremely sensitive to small changes in angle of attack.

A simplified single degree of freedom (torsion) aeroelastic model

We can focus on the aeroelastic interaction between the airstream and the wing torsional degree of freedom by developing a simpler model. Consider the modified idealized airfoil mounted on a torsional spring, as shown in Figure 2.17. The translation spring K_h and the plunge degree of freedom are removed and a frictionless pin is inserted at the shear center. A torsion spring is inserted at the shear center to resist the aerodynamic moment. The airfoil has an initial angle of attack, α_0 when the torsion spring is undeformed.

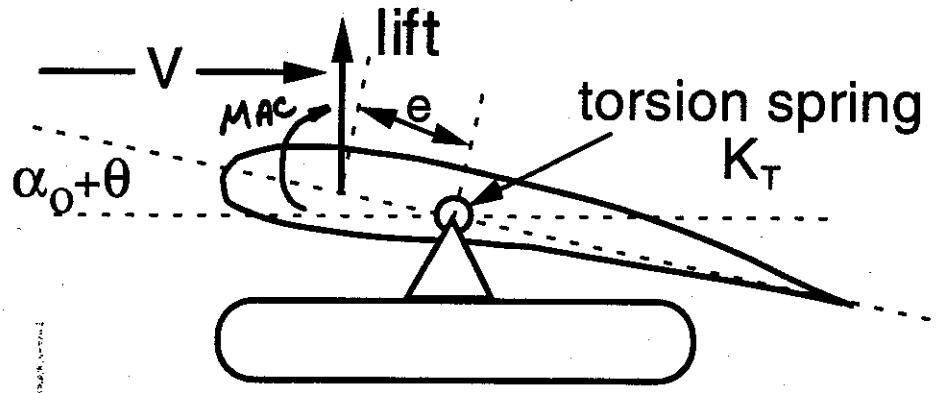


Figure 2.17 - Pin mounted airfoil with torsion spring restraint

As before, the aerodynamic moment about the shear center in Figure 2.17 is M_a , given as

$$M_a = Le + M_{AC}$$

with

$$M_{AC} = qcSC_{MAC}$$

The total lift, L , is

$$L = qSC_{L_a}(\alpha_0 + \theta)$$

The elastic restoring torque of the torsion spring is M_S , defined as

$$M_S = K_T\theta$$

in the counterclockwise direction.

The unknown elastic twist angle, θ , caused both by α_0 and the airfoil camber, is again found from the equation of torque static equilibrium written about the shear center. Summing moments at the pinned shear center gives

$$\sum M_{SC} = M_s - M_a = 0$$

or

$$K_T \theta - qSeC_{L_\alpha}(\alpha_0 + \theta) - qScC_{MAC} = 0$$

Solving for θ , we find

$$\theta = \frac{qSeC_{L_\alpha} \left(\alpha_0 + \left(\frac{c}{e} \right) \left(\frac{C_{MAC}}{C_{L_\alpha}} \right) \right)}{K_T - qSeC_{L_\alpha}} \quad (2.41)$$

aeroelastic torsional stiffness

Divide both the numerator and denominator by K_T to obtain an alternative expression for θ .

$$\theta = \frac{\left(\frac{qSeC_{L_\alpha}}{K_T} \right) \alpha_I}{\left(1 - \frac{qSeC_{L_\alpha}}{K_T} \right)} \quad (2.42)$$

where

$$\alpha_I = \alpha_0 + \left(\frac{c}{e} \right) \left(\frac{C_{MAC}}{C_{L_\alpha}} \right) \quad (2.43)$$

Once again, the size of the aeroelastic term $\bar{q} = qSeC_{L_\alpha} / K_T$ is very important because, as \bar{q} approaches unity, θ will approach infinity if the angle of attack is not changed. Aeroelastic divergence occurs when the dynamic pressure, q , equals q_D , where

$$q_D = \frac{K_T}{SeC_{L_\alpha}} \quad (2.44)$$

No matter how small α_I is, the theoretical twist angle θ tends to infinity as q approaches q_D .

The airfoil lift is

$$L = qSC_{L_\alpha} \left(\alpha_o + \frac{(\bar{q}/q_D)\alpha_I}{1 - \frac{q}{q_D}} \right)$$

or, with $\bar{q} = \frac{q}{q_D}$ we can write this as

$$L = \frac{qSC_{L_\alpha}}{1 - \bar{q}} \left(\alpha_o + \frac{q}{q_D} \left(\frac{cC_{MAC}}{eC_{L_\alpha}} \right) \right) \quad (2.45)$$

which matches the result in Eqn. 2.35.

Stiffness is defined as the change in the moment or force caused by a prescribed change in displacement (in this case twist). The aerodynamic stiffness is $\frac{\partial M_a}{\partial \theta} = -qSeC_{L_\alpha}$, while the structural stiffness is $\frac{\partial M_S}{\partial \theta} = K_T$. Aerodynamic stiffness resembles a negative torsion spring. While the mechanical spring stiffness is constant with airspeed and always greater than zero, if e is positive, the aerodynamic spring stiffness is negative and decreases with increasing flight dynamic pressure.

The term $(K_T - qSeC_{L_\alpha})$ (or $\bar{K} = K_T(1 - \frac{q}{q_D}) = K_T(1 - \bar{q})$) in Eqn. 2.41 is the aeroelastic torsional stiffness of this airfoil. The apparent torsional stiffness of the airfoil is the sum of the mechanical and aerodynamic stiffnesses. At dynamic pressures larger than the divergence dynamic pressure, the apparent torsional stiffness is negative, implying that any slight increase in angle of attack of the airfoil will cause it to twist without limit. As $q \rightarrow q_D$ the aeroelastic torsional stiffness declines to zero, as shown in Figure 2.18.

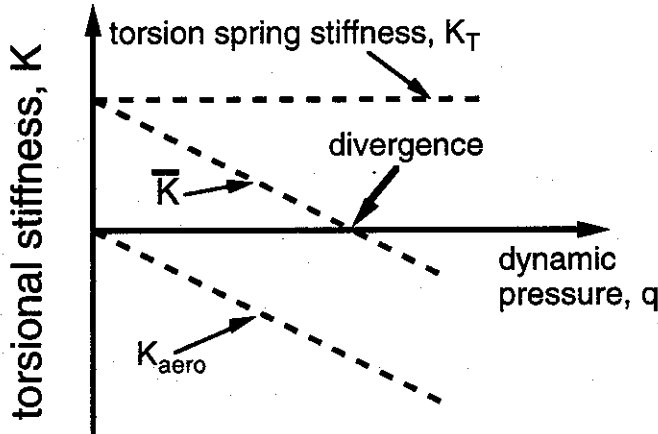


Figure 2.18 - Aeroelastic torsional stiffness vs. q

Unless the aeroelastic torsional stiffness is positive, there can be no solution to the static equilibrium equation for this airfoil. A negative stiffness gives a negative twist angle for a positive angle of attack input, clearly an impossible answer.

Twist angle amplification

Let's examine the importance of including aeroelastic interaction effects, characterized by the parameter \bar{q} . Equation 2.42 for the elastic twist can be written as follows.

$$\theta = \frac{\bar{q} \alpha_I}{1 - \bar{q}} = f \bar{q} \alpha_I$$

$$f = \frac{1}{1 - \bar{q}}$$
(2.46)

We can expand the amplification factor $f = \frac{1}{1 - \bar{q}}$ in Equation 2.46 as an infinite series that reads as follows.

$$f = \frac{1}{1 - \bar{q}} = 1 + \bar{q} + \bar{q}^2 + \bar{q}^3 + \dots = 1 + \sum_{n=1}^{\infty} \bar{q}^n$$
(2.47)

The infinite series in Eqn. 2.47 will converge or diverge depending on the size of the term \bar{q} compared to unity (1). We will have series convergence if $\bar{q} < 1$, but divergence if $\bar{q} \geq 1$. When $\bar{q} = 1$ we have a critical or cross-over condition. The size of the parameter \bar{q} provides a test for the static stability or convergence of the system when it is loaded.

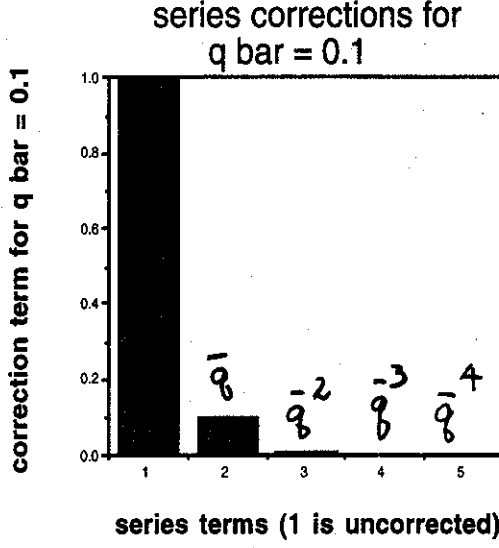


Figure 2.19 - Series terms for twist under load when $\bar{q} = 0.1$

Let's compare the size of the first 5 terms in the series in Eqn. 2.47 for different values of \bar{q} to see how quickly the series converges and thus estimate when aeroelastic effects are important and when they are not. The first term will always be equal to one while the second term will be equal to \bar{q} .

Figure 2.19 shows that terms beyond \bar{q} may be neglected with little inaccuracy. We conclude that aeroelastic interaction is contained in the \bar{q} term in Eqn. 2.47 and adds about 10% to the twist angle. When \bar{q} is larger, equal to 0.50, terms in the series out to \bar{q}^4 are important to the computation of the twist angle. Aeroelastic interaction adds a great deal to the size of the twist angle.

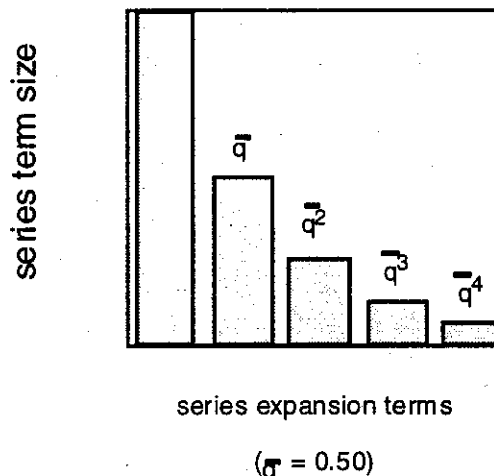


Figure 2.20 - Correction terms for twist when $\bar{q} = 0.50$

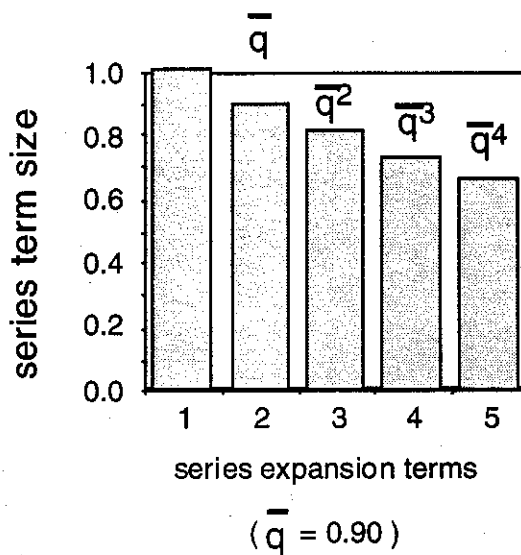


Figure 2.21 - Correction terms for twist when $\bar{q} = 0.90$

From Figure 2.20, we conclude that the aeroelastic effect adds nearly as much as the initial twist without including aeroelastic effects. Finally, as shown in Figure 2.21, the correction terms when $\bar{q} = 0.90$ are strong contributors to the infinite series well past the \bar{q}^4 term in the series.

Equations 2.46 and 2.47 can be combined to illustrate an aeroelastic feedback process in which an initial angle of attack α_I is input into the airfoil and a resulting twist is then fed back to generate a load that generates a twist... until convergence at some twist angle is reached. The series expression for elastic twist is written as

$$\theta = \frac{qSeC_{L\alpha}\alpha_I}{K_T} (1 + \bar{q} + \bar{q}^2 + \dots) \quad (2.48)$$

The first term in this series is written as

$$\theta_o = \frac{qSeC_{L\alpha}\alpha_I}{K_T} \quad (2.49)$$

The angle θ_o is twist angle when no aeroelastic interaction or feedback is included in the process.

The second term in the series is

$$\theta_1 = \bar{q}\theta_o = \frac{qSeC_{L\alpha}\theta_o}{K_T} \quad (2.50)$$

The term θ_1 is the airfoil twist in response to θ_o (not α_I). The third term in series is

$$\theta_2 = \bar{q}^2\theta_o = \bar{q}\theta_1 \quad (2.51)$$

This term is the system twist in response to θ_1 . Each term in the infinite series for twist is a corrector for the added moment due to the twist added by the previous term. As a result, the series for the twist including aeroelastic effects can be written as

$$\theta = \theta_o + \sum_{n=1}^{\infty} \theta_n \quad (2.52)$$

where $\theta_i = \bar{q}^i\theta_o = \bar{q}\theta_{i-1}$ so that when \bar{q} is near 1, the additional twist added to each term is nearly as large as the original input twist.

Static stability defined

When the airplane weight is fixed, the angle of attack controlled by the pilot was found to be

$$\alpha_o = \frac{1}{2} \left(\frac{W}{S} \right) \left(\frac{1 - \bar{q}}{qC_{L_a}} \right) - \left(\frac{qScC_{MAC}}{K_T} \right) \quad (2.53)$$

The twist angle at constant weight is

$$\theta = \frac{1}{K_T} \left(\frac{eW}{2} + qScC_{MAC} \right) \quad (2.54)$$

assuming $L = W/2$

For the normal case where the wing pitching moment coefficient is negative, the airplane angle of attack will decrease as the flight q approaches the divergence airspeed. At divergence, the airplane angle of attack will be $\alpha_o = -\left(\frac{qScC_{MAC}}{K_T}\right)$, but the twist angle will be as given in Eqn. 2.54. This number will not be infinite and it is worthwhile to explore the subject of static stability from a slightly different perspective.

Consider flying at a certain dynamic pressure so that the angle of attack is given by Eqn. 2.53 and the twist is given by Eqn. 2.54. We disturb (or to use stability jargon, "perturb") the airfoil twist slightly from the static equilibrium value θ (given in Eqn. 2.54) to $\theta + \Delta\theta$, using a disturbance moment of very short duration so that the airfoil is away from the equilibrium value in Eqn. 2.54. As shown in Figure 2.22, the aerodynamic and structural moments about the shear center change and are written as

$$\Delta M_a = qSeC_{L\alpha}(\Delta\theta)$$

and

$$\Delta M_s = K_T(\Delta\theta)$$

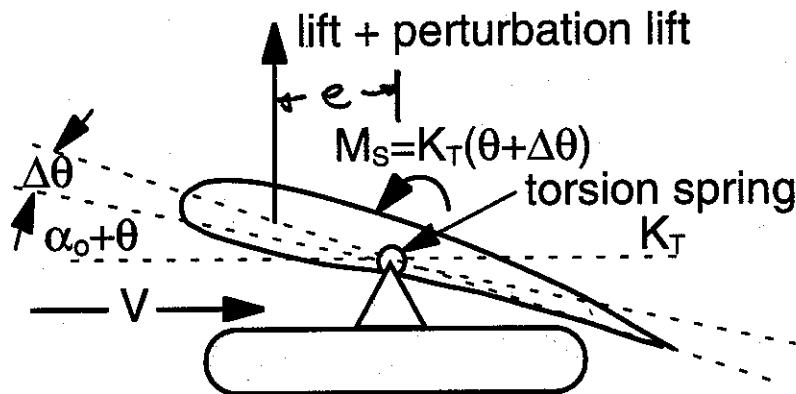


Figure 2.22 - Flexible airfoil perturbations in angle and load

The net restoring moment in the spring due to the moments that come from the unbalanced change in twist is

$$\Delta M_R = \Delta M_s - \Delta M_a = (K_T - qSeC_{L_\alpha})\Delta\theta \quad (2.55)$$

Stability analysis uses Eqn. 2.55 as a starting point and asks whether the perturbed airfoil tends to come back to the equilibrium value of twist in Eqn. 2.54 or whether it moves away. If it tends to come back we say that the equilibrium condition in Eqn. 2.54 is stable. If it tends to go away, we say that the system is unstable. There is a third possibility. If Eqn. 2.55 is zero when the perturbation is non-zero, then the system will be in static equilibrium in this perturbed state. This condition is called neutral stability.

If $\Delta M_s > \Delta M_a$, then static equilibrium at $\theta + \Delta\theta$ is not possible because the spring torsional moment will force the airfoil to return to its original equilibrium position at θ . On the other hand, if $\Delta M_s < \Delta M_a$, the airfoil will twist or diverge away from static equilibrium since the net moment due to $\Delta\theta$ will cause $\Delta\theta$ to increase and lead to more unbalanced moment and accelerated twisting motion away from the original equilibrium position.

Static stability is defined by what happens to a system that is in static equilibrium and then disturbed. If the system tends to come back to its undisturbed position, it is stable, if not, it is unstable.

Since $\Delta\theta$ can be factored out of the equation for the net moment the test for static stability is whether or not K_T is greater than or less than $qSeC_{L_\alpha}$. If K_T is greater than $qSeC_{L_\alpha}$ then static aeroelastic stability is assured. If K_T is less than $qSeC_{L_\alpha}$ then we will have torsional instability in which a small disturbance will start motion away from the initial equilibrium position. This equilibrium twist is ~~defined by~~ the weight of the airplane. *a function of*

The crossover between stability and instability occurs at the divergence dynamic pressure q_D , defined by setting the net moment to zero to get

$$K_T = q_D SeC_{L_\alpha}$$

so that

$$q_D = \frac{K_T}{SeC_{L_\alpha}} \quad (2.56)$$

This result checks with our previous results. Let's consider the following example to summarize the ideas that we have discussed in the previous sections.

Example - flexibility effects on an aircraft in steady turning flight

During a banked, constant altitude turn an airplane develops a load factor n . An item normally weighing 5 pounds will now weigh 5 times n pounds. The load factor n is defined as

$$n = \frac{\text{Total Lift}}{\text{Total Weight}}$$

where $\text{Total lift} = 2qSC_{L\alpha}(\alpha_0 + \theta)$ if the balancing tail load is ignored (this would not be a good idea in practice since the tail usually has a download on it equal to about 10% of the wing lift). The total aircraft weight is $W = (2m + M)g$, where

$m = \text{wing mass (per side)}$

$M = \text{fuselage mass}$

The idealized aircraft is shown at an angle α_0 in Figure 2.23 with its uncambered "wings" twisted an amount θ . With these definitions, the load factor is:

$$n = \frac{2qSC_{L\alpha}(\alpha_0 + \theta)}{(2m + M)g}$$

$S = \text{area of either left or right "wing."}$ (2.57)

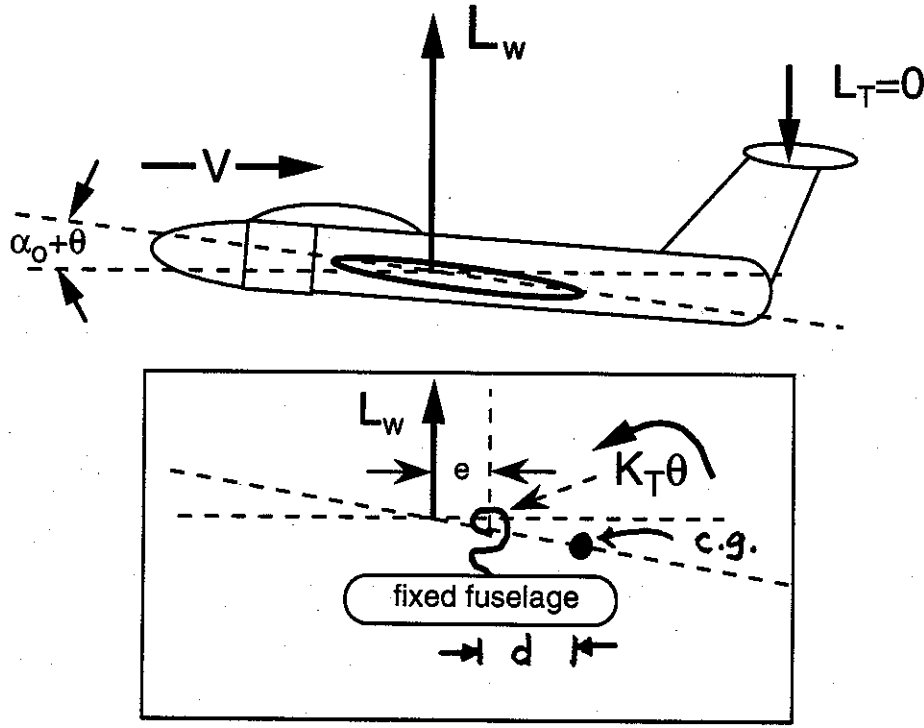


Figure 2.23 - Aircraft and wing free body diagram

Problem

Find α_o as a function of n (not θ) including flexibility effects. Solve for θ as a function of n , not α_o . Find the divergence dynamic pressure.

Solution

The wing lift for each idealized uncambered wing is $L_w = qSC_{L\alpha}(\alpha_o + \theta)$ where

$$\alpha_o = \text{wing initial angle of attack}$$

$$\theta = \text{wing elastic twist}$$

$$S = \text{wing area (per side)}$$

Equilibrium of forces requires:

$$L = nW = 2L_w \quad (2.58)$$

Either α_o or n can be the independent variable, but not both. If α_o is variable then n is determined by Eqn. 2.58. If n is variable, then α_o is determined from Eqn. 2.58.

The restoring torque, M_s , on each wing is $M_s = K_T\theta$ so that when we sum moments about the wing shear center we get the following

$$\sum M_{spring} = 0 = K_T\theta - L_w e - n mgd \quad (2.59)$$

$$K_T\theta = L_w e + nmgd \quad (2.60)$$

where $L_w = qSC_{L\alpha}(\alpha_o + \theta)$. Substituting for n (from Eqn. 2.58) into Eqn. 2.60, we get

$$K_T\theta = L_w \left(e + \frac{2mgd}{W} \right) \quad (2.61)$$

Now, we define

$$\mu = \frac{2mg}{W} < 1$$

so that

$$K_T\theta = (e + \mu d)[qSC_{L\alpha}(\alpha_o + \theta)] \quad (2.62)$$

and, finally we have the twist angle expressed as

$$\theta = \frac{qSC_{L\alpha}\alpha_o(e + \mu d)}{K_T - qSC_{L\alpha}(e + \mu d)} \quad (2.63)$$

dynamic pressure

Since the divergence speed for a restrained wing is $q_D = \frac{K_T}{SeC_{L\alpha}}$ we rewrite Eqn. 2.63 as

$$\theta = \frac{\frac{q}{q_D} \left(1 + \mu \frac{d}{e}\right) \alpha_o}{1 - \frac{q}{q_D} \left(1 + \mu \frac{d}{e}\right)} \quad (2.64)$$

The lift on each wing segment is then computed to be:

$$L_w = q S C_{L\alpha} (\alpha_o) \left\{ 1 + \frac{\frac{q}{q_D} \left(1 + \mu \frac{d}{e}\right)}{1 - \frac{q}{q_D} \left(1 + \mu \frac{d}{e}\right)} \right\} \quad (2.65)$$

We reduce Eqn. 2.65 to an expression with a common denominator to find

$$L_w = q S C_{L\alpha} \left\{ \frac{1}{1 - \frac{q}{q_D} \left(1 + \mu \frac{d}{e}\right)} \right\} \alpha_o \quad (2.66)$$

The angle of attack of the wings are found by realizing that $2L_w = nW$ so that $L_w = \frac{nW}{2}$ and solving for α_o using Eqn. 2.66 to get

$$\alpha_o = \frac{nW}{2} \left\{ \frac{1 - \frac{q}{q_D} \left(1 + \mu \frac{d}{e}\right)}{q S C_{L\alpha}} \right\} \quad (2.67)$$

Substitute Eqn. 2.67 into Eqn. 2.64. This gives an equation for θ in terms of n .

$$\theta = \frac{nW}{2} \frac{\left[1 - \frac{q}{q_D} \left(1 + \mu \frac{d}{e}\right) \right] \left[\frac{q}{q_D} \left(1 + \mu \frac{d}{e}\right) \right]}{q S C_{L\alpha} \left[1 - \frac{q}{q_D} \left(1 + \mu \frac{d}{e}\right) \right]} \quad (2.68)$$

Equation 2.68 reduces to

$$\theta = \left(\frac{nW}{2} \right) \left(\frac{e}{K_T} \right) \left(1 + \mu \frac{d}{e} \right) \quad (2.69)$$

Although the angle θ is a function of the load factor, the elastic twist θ given in Eqn. 2.69 is not a function of airspeed so it is impossible to determine anything about static

instability from this expression for θ . A separate stability analysis is necessary to find the divergence dynamic pressure.

In our previous discussions, we saw that the reason that θ does not become infinite as airspeed increases is that we are constantly reducing the angle of attack to keep the lift on the wing in balance with the weight. As we fly faster, we get more lift due to a reduced α_0 and a constant θ .

Let's examine the torsional stiffness of the wing as dynamic pressure increases to see if the divergence dynamic pressure of the freely flying wing will change for this model. Let us first return to the expression for θ in Eqn. 2.64

$$\theta = \frac{\frac{q}{q_D} \left(1 + \mu \frac{d}{e}\right) \alpha_0}{1 - \frac{q}{q_D} \left(1 + \mu \frac{d}{e}\right)} \quad (2.64)$$

From Eqn. 2.64, loss of torsional stiffness would seem to occur when the denominator approaches zero. This happens when

$$q = \frac{q_D}{1 + \mu \frac{d}{e}} \quad (2.70)$$

Since α_0 appears in Eqn. 2.64, we need to substitute the dynamic pressure given in Eqn. 2.70 into Eqn. 2.67, we get the following expression for α_0 (*this is Eqn. 2.67*)

$$\alpha_0 = \frac{nW}{2} \left\{ \frac{1 - \frac{q}{q_D} \left(1 + \mu \frac{d}{e}\right)}{q S C_{L\alpha}} \right\} \quad (2.71)$$

Substituting Eqn. 2.71 into Eqn. 2.64 we find that as $q \rightarrow \frac{q_D}{1 + \mu \frac{d}{e}}$ then $\alpha_0 \rightarrow 0$ and θ is

still finite and once again given by Eqn. 2.69. Obviously we must look elsewhere for stability information.

Divergence involves the reduction, and finally, the disappearance of torsional stiffness. To examine the effects of increased dynamic pressure on stiffness, we re-write the torsional equilibrium equation as

$$K_T \theta = q S e C_{L\alpha} (\alpha_0 + \theta) + n m g d \quad (2.72)$$

Combine like terms

$$(K_T - q S e C_{L\alpha}) \theta = q S e C_{L\alpha} \alpha_0 + n m g d \quad (2.73)$$

From Eqn. 2.73, we identify the familiar expression for the aeroelastic stiffness.

$$\bar{K} = K_T - qSeC_{L\alpha} \quad (2.74)$$

We also see that the load factor does not appear in Eqn. 2.74. When the aeroelastic stiffness is zero we have divergence, and Eqn. 2.74 indicates that the divergence q is still the same as found before. We conclude that inertia loads (or gravity) will not change the divergence speed, but will change the equilibrium twist angle.

Importance of Mach number and compressibility to divergence

The divergence condition at which the single degree of freedom airfoil loses its torsional stiffness occurs when

$$q_D = \left(\frac{1}{2}\right)\rho V_D^2 = \frac{K_T}{SeC_{L\alpha}}$$

The Prandtl-Glauert approximation for $C_{L\alpha}$ of an airfoil operating in compressible flow is $C_{L\alpha} = C_{L\alpha 0} / \sqrt{1 - M^2}$ where $C_{L\alpha 0}$ is the wing lift curve slope in incompressible flow conditions. The stiffness coefficient, K_T , does not change with Mach number and altitude, but might be affected if there is extreme aerodynamic heating, such as might occur in hypersonic flight. Note however, that Mach number changes the divergence dynamic pressure, but that we are not free to treat Mach number as an independent parameter.

We see that the divergence dynamic pressure depends on the flight Mach number as well as the usual parameters identified previously. The question is, if we operate at a certain altitude, at what airspeed or Mach number will we encounter divergence?

The airplane flight q is computed from the flight Mach number and atmospheric conditions at flight altitude to be

$$q = (\gamma / 2)pM^2 \quad (2.75)$$

where γ is the ratio of specific heats ($\gamma = 1.40$ for air) and p is the ambient or static pressure at the flight altitude. A different expression for flight dynamic pressure is

$$q = \frac{1}{2}\rho V^2 = \frac{1}{2}\rho a^2 M^2 \quad (2.76)$$

Equation 2.75 or 2.76 is sometimes called the "atmosphere line." The flight condition computed from either Eqn. 2.75 or 2.76 must match that computed from our divergence analysis. The divergence dynamic pressure including compressibility is

$$q_D = \frac{K_T \sqrt{1 - M^2}}{SeC_{L_{\alpha_0}}} = q_{D_0} \sqrt{1 - M^2} \quad (2.77)$$

where

$$q_{D_0} = \frac{K_T}{SeC_{L_{\alpha_0}}}$$

Equating Eqns. 2.76 and 2.77 we get the condition that matches flight conditions to computed divergence conditions.

$$\begin{aligned} q_{D_0} \sqrt{1 - M^2} &= \frac{1}{2} \rho a^2 M^2 = q_1 M^2 \\ (q_1 &= \frac{1}{2} \rho a^2) \end{aligned} \quad (2.78)$$

Now we square both sides of Eqn. 2.78 to get a quadratic in M_D^2 , the divergence Mach number.

$$M_D^4 + \left(\frac{q_{D_0}}{q_1} \right)^2 M_D^2 - \left(\frac{q_{D_0}}{q_1} \right)^2 = 0 \quad (2.79)$$

Finally, we have an expression for the divergence Mach number

$$M_D^2 = \frac{-\left(\frac{q_{D_0}}{q_1} \right)^2 + \sqrt{\left(\frac{q_{D_0}}{q_1} \right)^4 + 4 \left(\frac{q_{D_0}}{q_1} \right)^2}}{2} \quad (2.80)$$

The divergence Mach number is the intersection of two curves; Eqn. 2.76 plots flight dynamic pressure against Mach number while Eqn. 2.77 plots divergence dynamic pressure against Mach number and stiffness, incompressible lift curve slope and aerodynamic center shear center offset. This intersection point is called a "match point."

While the solution for the divergence Mach number is best done with Eqn. 2.80, it is helpful to see how the intersection point between the atmosphere line and the divergence line changes with altitude. An example of this change is plotted in Figure 2.24 for an airfoil which will diverge at 250 psf in incompressible flow.

Three different atmosphere lines are plotted in Figure 2.24, corresponding to three different altitudes. Figure 2.24 shows that divergence Mach number increases as altitude increases, all other things being the same. On the other hand, the dynamic pressure for divergence decreases with increasing altitude. Note that near Mach 1 the position of the aerodynamic center will begin to shift to a position near the mid-chord and the line marked "divergence q" will turn upward.

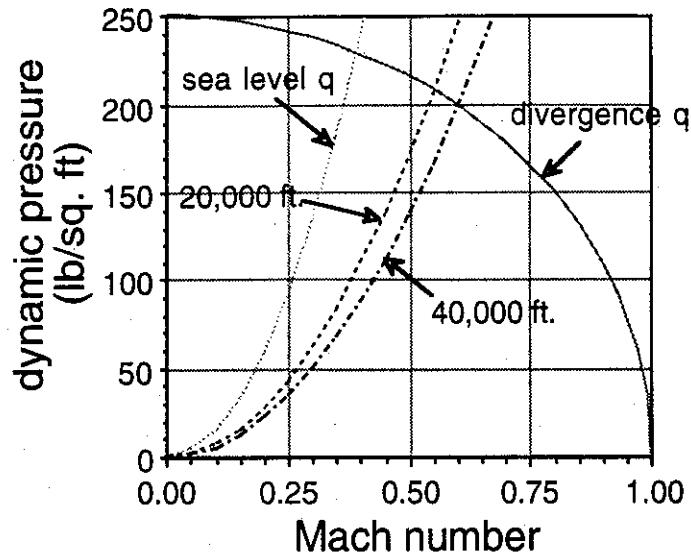


Figure 2.24 - Match point Mach number for divergence

An increase in the wing torsional stiffness will produce results such as those shown in Figure 2.25. In this figure, the divergence dynamic pressure in incompressible flow is increased by 50% from the value in Figure 2.24 and the results compared.

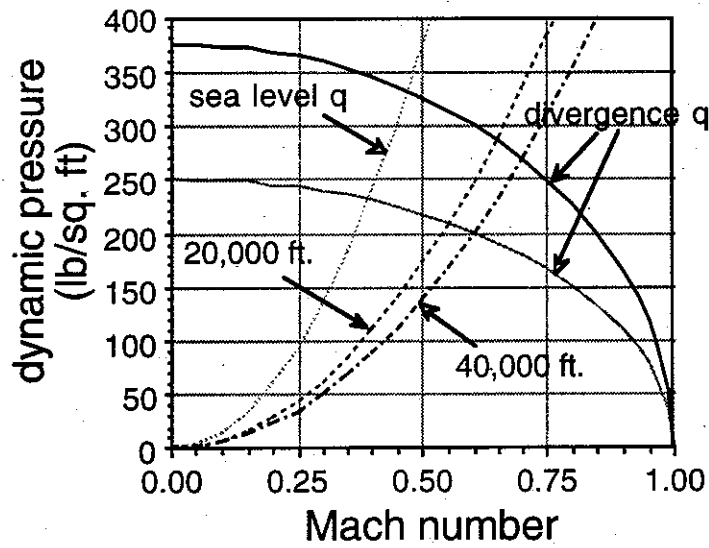


Figure 2.25 - Determination of divergence Mach number

The effect of increasing altitude and the change in speed of sound with altitude is indicated in Figure 2.26. In this figure, we see that divergence Mach number increases as altitude increases.

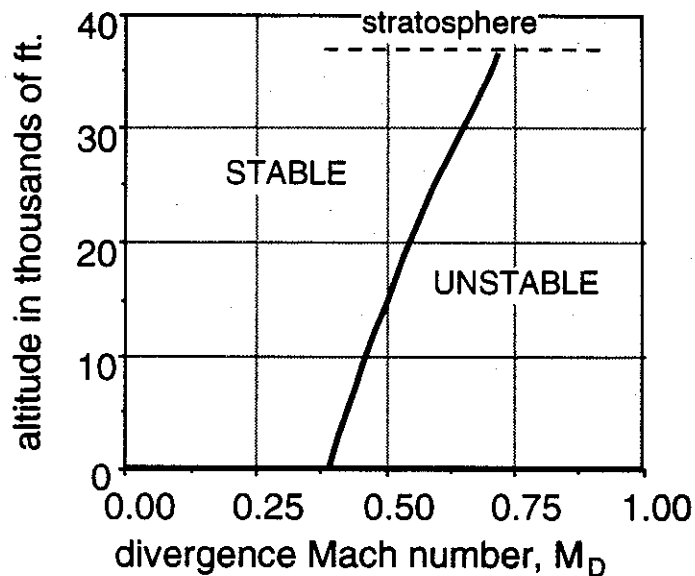


Figure 2.26 - Altitude vs. divergence Mach number ($q_{D_0} = 250 \text{ psf}$)

Figure 2.27 plots divergence speed as a function of altitude. Also shown is the result of the calculation of divergence speed when the effect of Mach number and compressibility on the lift curve slope are ignored. We see that the computed divergence speed is higher if compressibility effects are ignored.

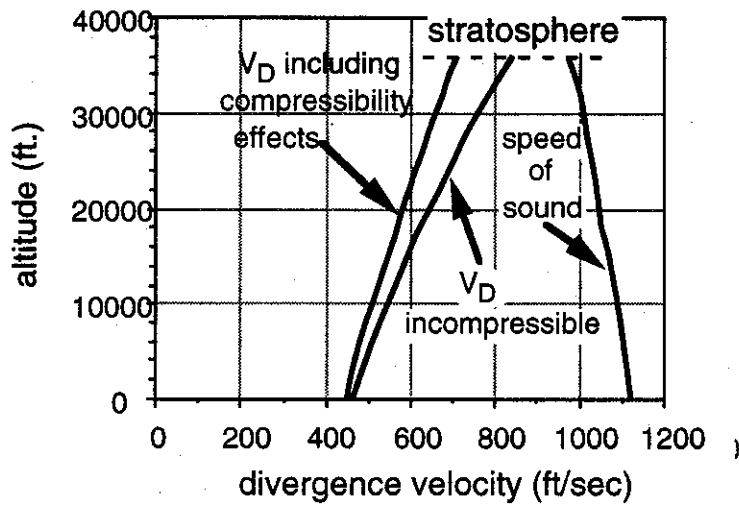


Figure 2.27 - Altitude vs. divergence speed showing compressibility effects
($q_{D_0} = 250 \text{ psf}$)

Summary - aeroelastic torsional divergence

- Aeroelastic divergence is an instability predicted by static stiffness analysis. Inertia effects (weight, weight distribution) are not important.
- Near the divergence dynamic pressure, small changes in wing incidence cause large changes in forces and moments and lead to even larger deformations. At the theoretical divergence speed, an infinitesimal change in angle of attack will cause an unbounded static twist and a similarly large increased load.
- Divergence dynamic pressure is a reference dynamic pressure indicating where in the flight envelope static flexibility is likely to have a significant effect upon lift computation.

Divergence of multi-degree of freedom systems

Static structural instability of the one degree of freedom airfoil occurs because the torsional stiffness is reduced to zero when a critical value of dynamic pressure is reached. The objective of this section is to associate stability analysis with an eigenvalue problem and the response of the airfoil to small perturbations away from an initial deformed static equilibrium position. We will choose a two-degree-of-freedom example to illustrate the general static stability problem and its solution.

Two airfoil sections shown in Figure 2.28 are mounted on a rigid shaft that excludes airfoil plunge but not rotation. Each section is uncambered and has the same initial angle of attack, α_o . Relative rotation of each section with respect to the other is restrained by a torsion spring that represents the action of the wing structure in resisting relative rotation between the sections. The rotation of the inboard section with respect to the wall is also restrained by a torsion spring. The locations and values of the torsion spring constants are shown on the figure, together with planform geometry.

The two airfoil twist angles are degrees of freedom. Both twist angles are measured with respect to the initial angle of attack α_o . The lift on each airfoil acts at its own aerodynamic center and is estimated to be

$$\begin{aligned} L_1 &= qSC_{L_\alpha}(\alpha_o + \theta_1) \\ L_2 &= qSC_{L_\alpha}(\alpha_o + \theta_2) \end{aligned} \quad (2.81 \text{ a,b})$$

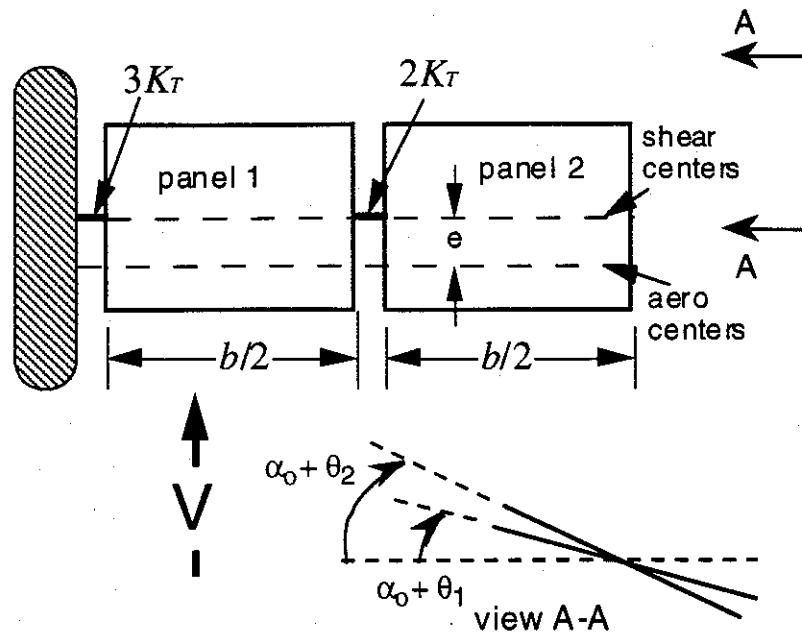


Figure 2.28 - Two degree of freedom wing.

We begin the analysis of this configuration by relating external aerodynamic forces and moments to internal (restoring) elastic forces and moments in the structural springs. In Figure 2.29, a free-body diagram of each of the two airfoil sections is shown, together with the external and internal forces and moments. These loads and reactions are shown for a typical deformed position of the system. Note that both θ_1 and θ_2 are positive as shown in the free body diagram. Summing forces does not provide useful aeroelastic information because these equations only relate the external forces to the shear reactions in the rod support.

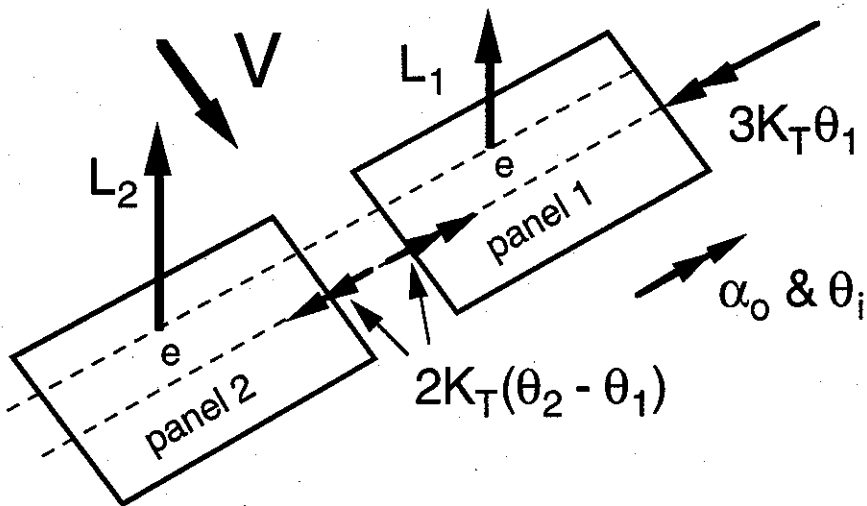


Figure 2.29 - Free body diagram of the airfoils.

Summing twisting moments about the rod support for each section in the positive, nose-up pitch, direction, we have:

$$\sum M_1 = 0 = 2K_T(\theta_2 - \theta_1) - 3K_T\theta_1 + L_1 e \quad (2.82)$$

$$\sum M_2 = 0 = -2K_T(\theta_2 - \theta_1) + L_2 e \quad (2.83)$$

Substituting for L_1 and L_2 in terms of α_o , θ_1 , and θ_2 , we have the following two equations.

$$5K_T\theta_1 - 2K_T\theta_2 = qSeC_{L_a}(\alpha_o + \theta_1) \quad (2.84)$$

$$-2K_T\theta_1 + 2K_T\theta_2 = qSeC_{L_a}(\alpha_o + \theta_2) \quad (2.85)$$

These equations are written in matrix form as:

$$K_T \begin{bmatrix} 5 & -2 \\ -2 & 2 \end{bmatrix} \begin{Bmatrix} \theta_1 \\ \theta_2 \end{Bmatrix} + qSeC_{L_a} \begin{bmatrix} -1 & 0 \\ 0 & -1 \end{bmatrix} \begin{Bmatrix} \theta_1 \\ \theta_2 \end{Bmatrix} = qSeC_{L_a} \alpha_o \begin{Bmatrix} 1 \\ 1 \end{Bmatrix} \quad (2.86)$$

In Eqn. 2.86 we have taken the portion of the aerodynamic loads proportional to deformations θ_1 and θ_2 from the right hand side and moved it to the left side of the equation with the structural stiffness matrix. As it is written in Eqn. 2.86, this matrix contribution from the aerodynamic load is referred to as the aerodynamic stiffness matrix. We divide Eqn. 2.86 by K_T and define a nondimensional parameter \bar{q} as

$$\bar{q} = \frac{qSeC_{L_a}}{K_T} \quad (2.87)$$

(note that this parameter is identical to that used for the single degree of freedom airfoil)
The equations of static equilibrium become:

$$\left[\begin{bmatrix} 5 & -2 \\ -2 & 2 \end{bmatrix} + \bar{q} \begin{bmatrix} -1 & 0 \\ 0 & -1 \end{bmatrix} \right] \begin{Bmatrix} \theta_1 \\ \theta_2 \end{Bmatrix} = \bar{q} \alpha_o \begin{Bmatrix} 1 \\ 1 \end{Bmatrix} \quad (2.88)$$

The solutions for the unknown static torsional deformations, θ_1 , and θ_2 , and the panel section lift forces with a fixed weight W are

$$\begin{Bmatrix} \theta_1 \\ \theta_2 \end{Bmatrix} = \bar{q} \frac{\alpha_o}{\Delta} \begin{Bmatrix} 4 - \bar{q} \\ 7 - \bar{q} \end{Bmatrix} \quad (2.89a)$$

$$\begin{Bmatrix} L_1 \\ L_2 \end{Bmatrix} = \frac{W}{2(4 - \bar{q})} \begin{Bmatrix} 2 - \bar{q} \\ 2 \end{Bmatrix} \quad (2.89b)$$

Note that the total lift on the two section wing is $\frac{W}{2}$. The lift on each section changes with dynamic pressure. On the other hand, if the angle of attack is constant, then the twist angles will become infinite if the denominator in Eqn. 2.89a is zero.

The term, Δ , is the determinant of the matrix on the left of Eqn. 2.88. This term is written as:

$$\Delta = \bar{q}^2 - 7\bar{q} + 6 = (\bar{q} - 1)(\bar{q} - 6) \quad (2.90)$$

The values for θ_1 and θ_2 (divided by α_o) are plotted as a function of the parameter \bar{q} and shown in Figure 2.30. This figure shows that both θ_1 and θ_2 approach infinity as $\bar{q} \rightarrow 1$, and $\Delta \rightarrow 0$. Above $\bar{q} = 1$, both θ_1 and θ_2 change signs. Near $\bar{q} = 6$, θ_1 and θ_2 again tend to infinity.

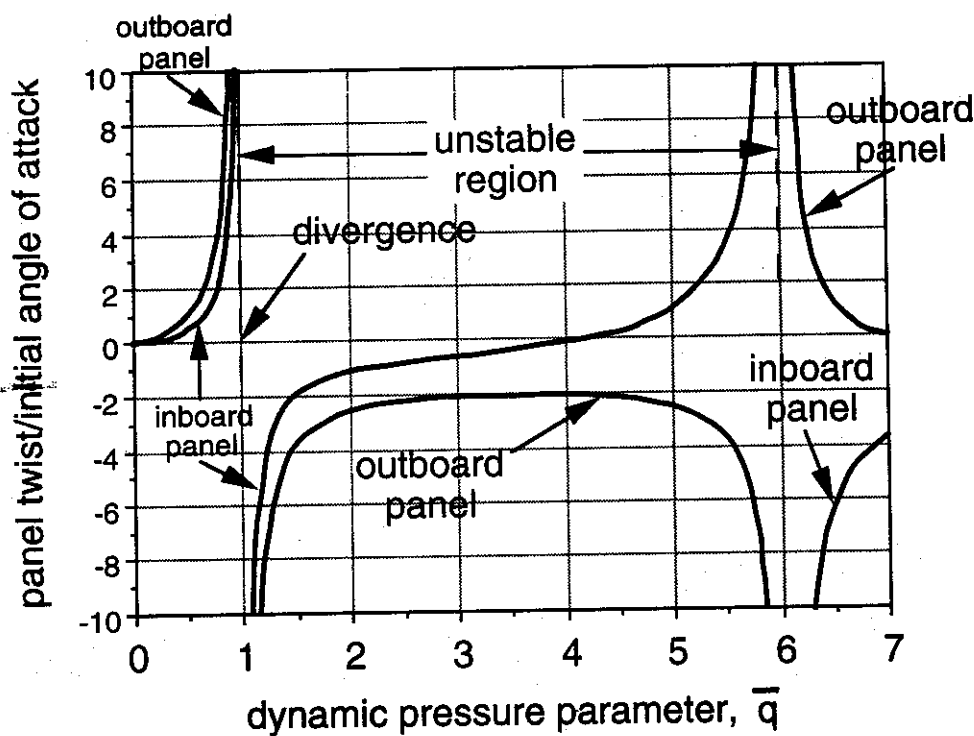


Figure 2.30 - Twist angles θ_1 and θ_2 vs. dynamic pressure.

It is apparent that two dynamic pressure conditions, $\bar{q} = 1$ and $\bar{q} = 6$, are associated with large torsional deformations and loss of stiffness in the two airfoil system. These values occur because the determinant of the total system stiffness matrix (structural plus aerodynamic) is zero. For the single-degree-of-freedom example, when the single aeroelastic torsional stiffness term became zero, divergence occurred. In the present case, the approach to zero of the determinant of the aeroelastic stiffness matrix signals to

approach of neutral stability and aeroelastic divergence. Thus the divergence condition for the two degree of freedom system is written as

$$\Delta = 0 \quad (2.91)$$

The determinant of the aeroelastic stiffness matrix is plotted in Figure 2.31. The determinant of the aeroelastic stiffness matrix is positive when the dynamic pressure is zero because the strain energy stored in the springs always must be positive. As the dynamic pressure increases, the determinant decreases because spring twist can still store energy in

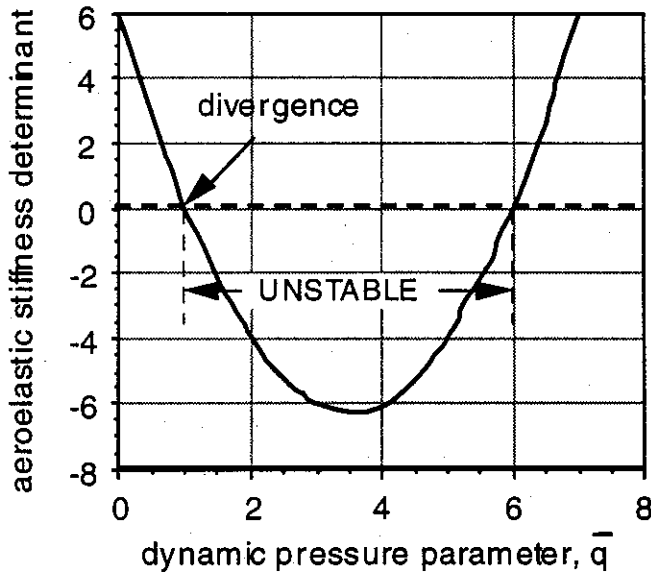


Figure 2.31- Aeroelastic stiffness matrix determinant vs. \bar{q}

the springs, but twisting allows the airstream to do work on the airfoil system. This work shows up as work done by springs with negative spring stiffness, the aerodynamic overturning moments.

At $\bar{q} = 1$ the total energy stored as the result of airfoil torsion is zero for some combinations of panel rotations. At this condition, we lose the ability to resist aerodynamic moments. Further increases in airspeed will cause the determinant to become negative, alerting us to the fact that static equilibrium is impossible and that any additional loads will cause motion. This motion is divergent motion that we will examine later.

At values of dynamic pressure above $\bar{q} = 6$ the determinant is again positive, indicating that the system appears to be able to store energy. While this may be so theoretically, the result is meaningless because divergence has already occurred and we have moved well beyond the initial equilibrium position.

All solutions to Eqn. 2.91 are associated with neutral static equilibrium. On the other hand, from Figure 2.31, some solutions to Eqn. 2.91 are associated with entry into an instability while others are associated with exit from the instability. The test of entry or

exit from static equilibrium is whether or not the determinant becomes positive or negative when the dynamic pressure is increased.

Static stability of multi-degree-of-freedom systems

The two-degree-of-freedom aeroelastic airfoil static equilibrium equations in Eqn. 2.86 are written in general as:

$$[[K_S] - q[K_A]] \begin{Bmatrix} \theta_1 \\ \theta_2 \end{Bmatrix} = \begin{Bmatrix} Q_1 \\ Q_2 \end{Bmatrix} \quad (2.92)$$

where Q_1 and Q_2 are initial, fixed loads. The vector $\begin{Bmatrix} \theta_1 \\ \theta_2 \end{Bmatrix}$ given in Eqn. 2.92 represents the equilibrium state for the deformed system.

A stable linear system has only one possible equilibrium state. When a system is in a state of neutral stability then more than one equilibrium state can exist, as we showed in our examination of the single degree of freedom airfoil. However, an unstable system has more than one possible equilibrium state since the original state and other nearby perturbed states are present. Let's see what special set of conditions must be present to obtain not one, but two solutions to Eqn. 2.92.

The twist on the wing if the twist angles are perturbed can be written as the sum of two vectors, as follows:

$$\begin{Bmatrix} \theta_1 \\ \theta_2 \end{Bmatrix} = \begin{Bmatrix} \theta_1^{(S)} \\ \theta_2^{(S)} \end{Bmatrix} + \begin{Bmatrix} \bar{\theta}_1 \\ \bar{\theta}_2 \end{Bmatrix} = \{\theta^{(S)}\} + \{\bar{\theta}\} \quad (2.93)$$

where, when the total load on the wing is fixed at $W/2$

$$\begin{Bmatrix} \theta_1^{(S)} \\ \theta_2^{(S)} \end{Bmatrix} = \frac{We}{6K_T} \begin{Bmatrix} 1 \\ \frac{7-\bar{q}}{4-\bar{q}} \end{Bmatrix} \quad (2.94)$$

Equation 2.94 shows the twist equilibrium state associated with straight and level flight when the airplane weight is W . Notice that the inboard section has a constant twist angle but the outer panel increases its angle as airspeed increases. Substituting Eqn. 2.93 into Eqn. 2.92, we have, using the notation $[\bar{K}] = [K_S] - q[K_A]$,

$$[\bar{K}]\{\theta^{(S)}\} + [\bar{K}]\{\bar{\theta}\} = \{Q\}$$

By definition $\{Q\} = [\bar{K}]\{\bar{\theta}^{(S)}\}$ so we have the following requirement if we want to have a nearby perturbed equilibrium state.

$$[\bar{K}]\{\bar{\theta}\} = \{Q\} + [\bar{K}]\{\theta^{(s)}\} = \{0\} \quad (2.95)$$

If such a state is to exist then we must find a solution to the following equation.

$$[\bar{K}]\{\bar{\theta}\} = \{0\} \quad (2.96)$$

Divergence eigenvalues

An obvious solution to Eqn. 2.96 is that $\{\bar{\theta}\} = 0$. This solution means that only the original equilibrium solution will satisfy the equilibrium equations and that any perturbation to the system would result in motion back to (or away from) the initial equilibrium state. If the perturbations $\bar{\theta}_1$ and $\bar{\theta}_2$ are nonzero, they must satisfy the homogeneous perturbation equilibrium equation, Eqn. 2.96.

If these perturbations are nonzero, then the system is, by definition, self-equilibrating and neutrally stable. The existence of this type of solution for neutral stability is known as Euler's criteria for neutral static stability. This condition is called a "self-equilibrating" condition since no other external inputs are supplied, such as a change in α_o , but the system is able to move from one state to another if it is disturbed slightly.

From linear algebra, we know that the perturbations $\bar{\theta}_1$ and $\bar{\theta}_2$ can be nonzero only if the determinant of the matrix $[\bar{K}]$ is zero. That is,

$$|\bar{K}| = \Delta = 0 \quad (2.97)$$

Equation 2.97 verifies the neutral stability condition we found in Eqn. 2.91; $|\bar{K}|$ is called the stability determinant or characteristic equation and it is a polynomial function of dynamic pressure or some non-dimensional counterpart, such as $\frac{qSeC_{L\alpha}}{K_T}$ which appears as an eigenvalue of the aeroelastic stiffness matrix. When q becomes equal to an eigenvalue a multiplicity of static equilibrium states appear. This is called a bifurcation point and Eqn. 2.97 is a formal mathematical condition for neutral stability.

For a system with n independent degrees of freedom (the present example has $n = 2$) there will be n eigenvalues. The eigenvalue that yields the lowest positive value of q usually has the most physical importance. (Note that there might be negative eigenvalues or even imaginary eigenvalues which would not make sense physically). For our present example, the eigenvalues \bar{q}_1 and \bar{q}_2 , for Eqn. 2.97 are given by

$$\bar{q}_1 = 1 \quad (2.98)$$

$$\bar{q}_2 = 6 \quad (2.99)$$

The plot of the stability determinant showed that the divergence dynamic pressure, the boundary between stable and unstable equilibrium is the lower of these two values. This means that

$$q_D = \bar{q}_1 \frac{K_T}{SeC_{L_\alpha}} = \frac{K_T}{SeC_{L_\alpha}} \quad (2.100)$$

While this result is mathematically identical to the previous single degree of freedom system result, we should note that if we change the value of one of the springs, say from $3K_T$ to $(1.8)K_T$ then the result in Eqn. 2.100 will be different. This will be illustrated in a later example problem.

Divergence eigenvectors

Let's now look at the airfoil system eigenvectors. These eigenvectors are found by substituting, one at a time, the two values of \bar{q}_i back into the equilibrium equations and then solving for $\bar{\theta}_1$ and $\bar{\theta}_2$. We will drop the over bars from the $\bar{\theta}_1$ and $\bar{\theta}_2$ notation in the discussion that follows to simplify the notation. When $\bar{q}_1 = 1$, the two homogeneous equilibrium equations in Eqn. 2.96 become

$$4\theta_1 - 2\theta_2 = 0 \quad (2.101)$$

$$-2\theta_1 + \theta_2 = 0 \quad (2.102)$$

Thus, for \bar{q}_1 , we find from either Eqn. 2.101 or 2.102 that

$$\theta_1 = \frac{\theta_2}{2} \quad (2.103)$$

Notice that any twist displacement vector with the ratio $\theta_2 / \theta_1 = 2$ satisfies Eqns. 2.101 and 2.102. We arbitrarily set $\theta_2 = 1$ and express the divergence "mode shape" associated with eigenvalue \bar{q}_1 as the vector

$$\begin{Bmatrix} \theta_1 \\ \theta_2 \end{Bmatrix}^{(1)} = \begin{Bmatrix} 0.5 \\ 1.0 \end{Bmatrix} \quad (2.104)$$

Equation 2.104 can be also expressed as

$$\begin{Bmatrix} \theta_1 \\ \theta_2 \end{Bmatrix}^{(1)} = C_1 \begin{Bmatrix} 0.5 \\ 1.0 \end{Bmatrix} \quad (2.105)$$

since any arbitrary constant C_1 , either positive or negative, can be used and still have the twists satisfy the perturbation equilibrium equations in Eqns. 2.101 and 2.102. Equation 2.104 is called a divergence mode shape.

When $\bar{q}_1 = 6$, the perturbed static equilibrium equations become

$$-\theta_1 - 2\theta_2 = 0 \quad (2.106)$$

$$-2\theta_1 - 4\theta_2 = 0 \quad (2.107)$$

Thus, we conclude that, when $\bar{q}_2 = 6$,

$$\theta_1 = -2\theta_2 \quad (2.108)$$

The mode shape for $\bar{q}_2 = 6$ is written as

$$\begin{Bmatrix} \theta_1 \\ \theta_2 \end{Bmatrix}^{(2)} = \begin{Bmatrix} -2 \\ 1 \end{Bmatrix} \quad (2.109)$$

Again we have arbitrarily taken $\theta_2 = 1$. As before, this result can be generalized to

$$\begin{Bmatrix} \theta_1 \\ \theta_2 \end{Bmatrix}^{(2)} = C_2 \begin{Bmatrix} -2 \\ 1 \end{Bmatrix} \quad (2.110)$$

towards

Look again at Figure 2.30, where we plotted the static response θ_1 / α_o and θ_2 / α_o as functions of \bar{q} . When $\bar{q} \rightarrow 1$, the ratio of θ_1 / θ_2 tends 0.5, the first eigenvector. Similarly, as $\bar{q} \rightarrow 6$, the ratio θ_1 / θ_2 is negative and approaches -2.0, the second eigenvector.

Let's compare the strain energy stored when we deform the system in each divergence mode shape. The strain energy, U , stored by torsion springs is, in general:

$$U = \frac{1}{2}(3K_T)(\theta_1)^2 + \frac{1}{2}(2K_T)(\theta_2 - \theta_1)^2 \quad (2.111)$$

With the first divergence eigenvector or "mode," the strain energy is computed to be:

$$U_1 = \left(\frac{3}{2}K_T\left(\frac{1}{4}\right) + K_T\left(\frac{1}{4}\right) \right) \theta_2^2 = \frac{5}{8}K_T\theta_2^2 \quad (2.112)$$

With the second divergence eigenvector or mode, the strain energy is found to be:

$$U_2 = \left(\frac{3}{2}K_T(4) + K_T(9) \right) \theta_2^2 = 15K_T\theta_2^2 \quad (2.113)$$

The strain energy stored in mode 2 is much higher than that in mode 1. Because of this, it takes more work by the external aerodynamic forces to deform the system into mode 2 and it is associated with larger dynamic pressures.

Summary - divergence of multi-degree of freedom systems

To construct the eigenvalue problem for static aeroelastic stability we first assume that the flexible structure is in a deformed state of static equilibrium. We then develop static equilibrium equations in terms of the system deformation. Then, all terms on the right hand side of the equation (for instance, α_o) are set to zero. This gives us the equilibrium equations for the neutrally stable perturbation states.

We can either directly expand the determinant of the resulting matrix equation in terms of q , K_T , etc. and solve for q_D , or, if we know the numerical values of K_T and the other problem parameters, we can let the computer find numerical values of q_D .

In general, the eigenvalue problem for static stability of an n^{th} order system is:

$$[K_S]\{\theta\} = q[K_A]\{\theta\} \quad (2.114)$$

This equation has the form

$$[A]\{x\} = \lambda[B]\{x\} \quad (2.115)$$

The eigenvalues, λ_i , correspond to values of dynamic pressure for which the system has neutral static stability. If the eigenvalues are negative or complex, divergence cannot occur.

Example - Shear center, center of twist and divergence

A wing surface for a wind tunnel test consists of a thin flexible shell surrounding and supported by three thin strips or leaf springs, as shown in Figure 2.32. The wing itself

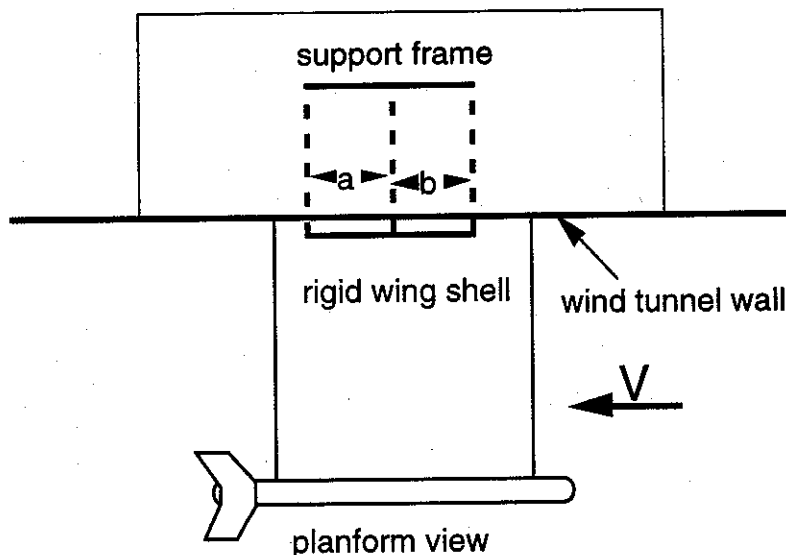


Figure 2.32 - Wind tunnel model with frame support

is rigid but can rotate and move upward. The structural stiffness effects of these strips are idealized to be three springs, K_1 , K_2 and K_3 as indicated in Figure 2.33. Because the strips are of equal size, the three spring constants are all equal to K (lb/in.).

The displacement of the idealized wing is represented by a downward displacement at the center strip. This displacement is h . The elastic twist of the wing section is θ , as shown in Figure 2.33. Figure 2.34 shows the free body diagram for this idealized system.

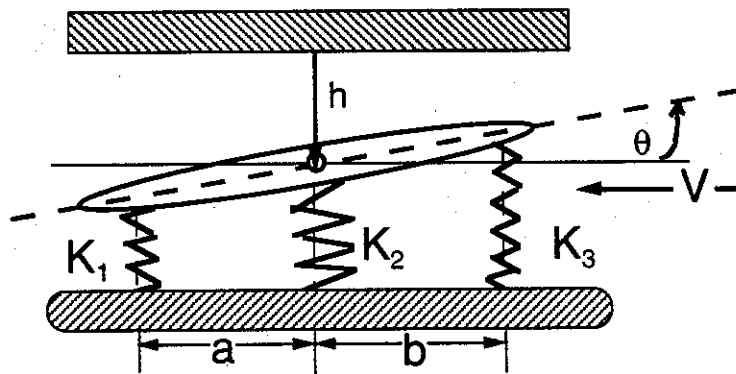


Figure 2.33 - Two-dimensional example idealization

When a downward force F and a nose-up torque T are applied to this idealized wing, the relationship between these loads and the rotation and the deflection at the center spring is represented as follows:

$$\begin{Bmatrix} F \\ T \end{Bmatrix} = \begin{bmatrix} 3K & Ka - Kb \\ Ka - Kb & Ka^2 + Kb^2 \end{bmatrix} \begin{Bmatrix} h \\ \theta \end{Bmatrix} = \begin{bmatrix} K_{11} & K_{12} \\ K_{12} & K_{22} \end{bmatrix} \begin{Bmatrix} h \\ \theta \end{Bmatrix} \quad (2.116)$$

Locating the model shear center

The wing sectional shear center is defined as a point on the wing section where a concentrated force may be applied without creating rotation. Solving Eqn. 2.116 for the two displacements,

$$\begin{Bmatrix} h \\ \theta \end{Bmatrix} = \frac{1}{\Delta} \begin{bmatrix} Ka^2 + Kb^2 & Kb - Ka \\ Kb - Ka & 3K \end{bmatrix} \begin{Bmatrix} F \\ T \end{Bmatrix} \quad (2.117)$$

$\Delta = |K| = 2K^2(a^2 + ab + b^2)$ is the determinant of the stiffness matrix. Suppose that the shear center is located at a distance \bar{x} to the left of the center spring as shown in Figure 2.34.

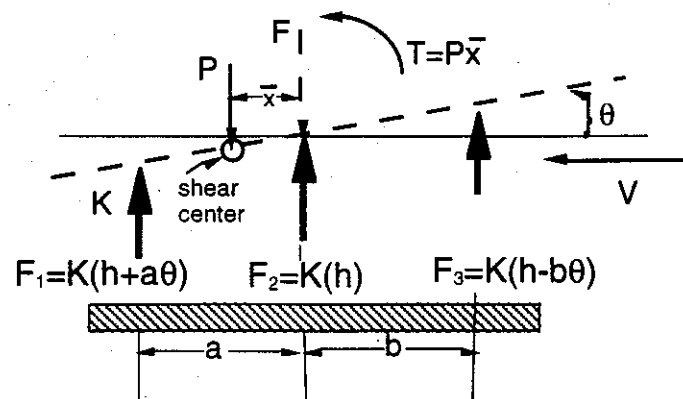


Figure 2.34 - Free body diagram with equivalent loads

When we apply a downward force P at the position \bar{x} to the left of the center spring in Figure 2.34 we create the following external loads on the airfoil:

$$F = P \quad \text{and} \quad T = P\bar{x}$$

so that Eqn. 2.117 becomes:

$$\begin{Bmatrix} h \\ \theta \end{Bmatrix} = \frac{1}{\Delta} \begin{bmatrix} K_{22} & -K_{12} \\ -K_{12} & K_{11} \end{bmatrix} \begin{Bmatrix} P \\ P\bar{x} \end{Bmatrix} \quad (2.118)$$

Depending on where we locate the force and how much force we apply, we can make the size of the deflections anything that we want them to be. If we want to have $\theta = 0$ then, by using Equation 2.118, we can find the following relationship between P , \bar{x} and the stiffness matrix elements:

$$\theta = \frac{P}{\Delta} [-K_{12} + K_{11}\bar{x}] = 0 \quad (2.119)$$

Notice that the value of the load P can be eliminated from Eqn. 2.119, so that its size does not matter when we locate the shear center. The unknown in Eqn. 2.119 is the value of \bar{x} given by:

$$\bar{x} = \frac{K_{12}}{K_{11}} = \frac{Ka - Kb}{3K} = \frac{a - b}{3} \quad (2.120)$$

Although the rotation is zero when the load P is applied at the shear center, the displacement of the section is not zero. It is given by the expression

$$h = \frac{P}{\Delta} (K_{22} - \bar{x}K_{12}) = \frac{2}{3} \left(\frac{PK}{\Delta} \right) (a^2 + ab + b^2) = \frac{P}{3K}$$

Example - center of twist

The center of twist is defined as a point about which the section appears to rotate when only a torque is applied. To find the center of twist, we apply a torque T at the position \bar{x} but do not apply a load F . (To say that we apply a torque at a point is not accurate since the torque is not actually applied at a point, it is due to two equal, opposite and parallel forces.) From Eqn. 2.117, the torque will cause both twist θ and deflection h given by the following expressions:

$$h = \frac{K(b-a)}{\Delta} T \quad (2.121)$$

and

$$\theta = \frac{3K}{\Delta} T \quad (2.122)$$

The downward deflection y a distance x from the center spring is given by

$$y = h + x\theta \quad (2.123)$$

Substituting Eqns. 2.121 and 2.122 into Eqn. 2.123 and setting $y=0$, we find that the downward displacement due to an applied torque is zero if we are at

$$x = \frac{-h}{\theta} = \frac{\frac{-K(b-a)T}{\Delta}}{\frac{3K}{\Delta} T} = \frac{-K(b-a)T}{3KT} = \frac{-(b-a)}{3} = \frac{a-b}{3}$$

or

$$x = \frac{a-b}{3} \quad (2.124)$$

Comparing Eqns 2.124 and 2.120, we see that the shear center and center of twist are located at the same point.

Example - wing divergence

To find the divergence dynamic pressure for this model, consider an aerodynamic force $F = -L$ located at the aerodynamic center. The aerodynamic center is located at a distance e to the right of the middle spring.

In this case, the force and moments are

$$F = -L \quad \text{and} \quad T = Le$$

From this we obtain the static equilibrium matrix equation.

$$\begin{Bmatrix} -L \\ Le \end{Bmatrix} = \begin{bmatrix} K_{11} & K_{12} \\ K_{12} & K_{22} \end{bmatrix} \begin{Bmatrix} h \\ \theta \end{Bmatrix}$$

The aerodynamic force is

$$L = qSC_{L\alpha}\alpha_o + qSC_{L\alpha}\theta$$

which yields

$$qSC_{L\alpha}\alpha_o \begin{Bmatrix} -1 \\ e \end{Bmatrix} = \begin{bmatrix} K_{11} & (K_{12} + qSC_{L\alpha}) \\ K_{12} & (K_{22} - qSC_{L\alpha}e) \end{bmatrix} \begin{Bmatrix} h \\ \theta \end{Bmatrix}$$

or

$$qSC_{L\alpha}\alpha_o \begin{Bmatrix} -1 \\ e \end{Bmatrix} = \begin{bmatrix} K_{11} & \bar{K}_{12} \\ K_{12} & \bar{K}_{22} \end{bmatrix} \begin{Bmatrix} h \\ \theta \end{Bmatrix}$$

Solving for the deflections, we have

$$\begin{Bmatrix} h \\ \theta \end{Bmatrix} = \frac{qSC_{L\alpha}\alpha_o}{\Delta} \begin{bmatrix} \bar{K}_{22} & -\bar{K}_{12} \\ -K_{12} & K_{11} \end{bmatrix} \begin{Bmatrix} -1 \\ e \end{Bmatrix}$$

$$\text{where } \Delta = K_{11}\bar{K}_{22} - K_{12}\bar{K}_{12}.$$

For a fixed value of α_o , the deflections will increase without bound if the determinant $\Delta = 0$, that is, when

$$K_{11}\bar{K}_{22} - K_{12}\bar{K}_{12} = 0$$

Expanding

$$K_{11}K_{22} - q_DSC_{L\alpha}K_{11}e - K_{12}^2 - q_DSC_{L\alpha}K_{12} = 0$$

Divide through by $-K_{11}$

$$-K_{22} + q_DSC_{L\alpha}e + \frac{K_{12}^2}{K_{11}} + q_DSC_{L\alpha}\frac{K_{12}}{K_{11}} = 0$$

The divergence dynamic pressure is then found to be

$$q_DSC_{L\alpha} \left(e + \frac{K_{12}}{K_{11}} \right) = K_{22} - \frac{K_{12}^2}{K_{11}}$$

$$q_DSC_{L\alpha} = \frac{K_{22} - \frac{K_{12}^2}{K_{11}}}{e + \frac{K_{12}}{K_{11}}}$$

The shear center is located at $\bar{x} = \frac{K_{12}}{K_{11}}$, so that

$$q_D = \left(\frac{K_{22} - K_{12}\bar{x}}{e + \bar{x}} \right) \cdot \frac{1}{SC_{L\alpha}} \quad (2.125)$$

Notice that when $e = -\bar{x}$ (aerodynamic center coincident with the shear center), divergence cannot occur. Substituting for \bar{x} , K_{22} and K_{12} , we have:

$$q_D SC_{L\alpha} = \frac{K_{11}K_{22} - K_{12}^2}{K_{11}e + K_{12}} = \frac{3K^2(a^2 + b^2) - K^2(a - b)^2}{3Ke + K(a - b)}$$

or

$$q_D SC_{L\alpha} = \frac{K[3a^2 + 3b^2 - a^2 - b^2 + 2ab]}{3e + a - b}$$

As noted earlier, e is the distance from the middle spring to the aerodynamic center. If e' is defined as the distance between the shear center and the aerodynamic center, then,

$$e' = e + \frac{a - b}{3}$$

Notice that this system has two degrees of freedom, but only one divergence eigenvalue. This occurs because the plunge degree of freedom does not cause aerodynamic forces. This is an exception to the general rule we discussed earlier. We may define as many degrees of freedom as we choose, but the divergence analysis will reveal only those that are important for aeroelastic feedback.

Feedback control for wing divergence artificial stabilization

Since aerodynamic forces and moments are fed back to create displacement dependent airloads that may create instabilities, we can use this same feedback process to control loads and create an artificial situation to change the divergence speed. In Chapter Three we will discuss this feedback process for time-dependent motion.

The purpose here is to see how the feedback process is changed by a small controllable device such as an aileron. The addition of a small trailing-edge control surface to the outboard panel 2 as indicated in Figure 2.35 requires a slight modification to our moment equilibrium equations for panel 2.

With the aileron deflected the lift is expressed as:

$$L_2 = qSC_{L\alpha}(\alpha_o + \theta_2) + qSC_{L\delta} \delta_o \quad (2.126)$$

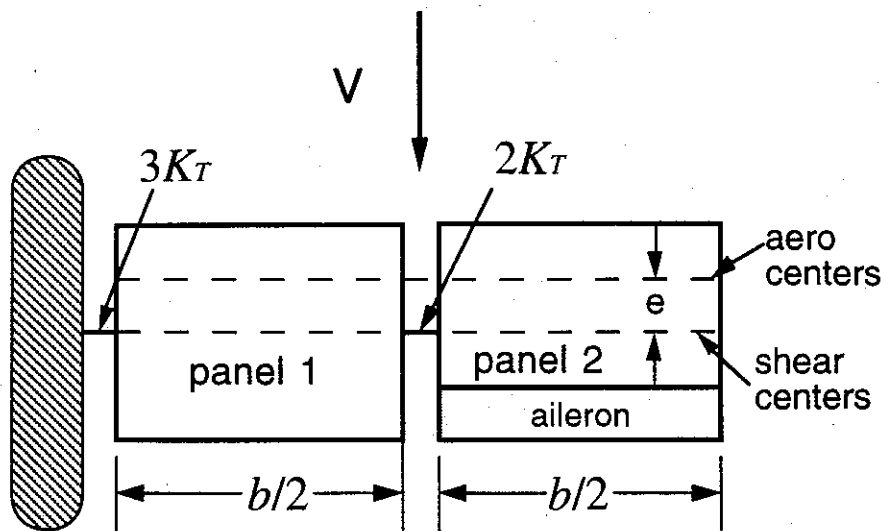


Figure 2.35 - Two degree of freedom wing with aileron.

Deflection of a control surface also changes the airfoil camber and causes a pitching moment about the axis of rotation. The moment is then written as:

$$M_2 = L_2 e + q S c C_{M_\delta} \delta_o \quad (2.127)$$

Expanding Eqn. 2.127, we have:

$$M_2 = q S e C_{L_\alpha} (\alpha_o + \theta_2) + q S e C_{L_\alpha} \left(\frac{C_{L_\delta}}{C_{L_\alpha}} + \left(\frac{c}{e} \right) \frac{C_{M_\delta}}{C_{L_\alpha}} \right) \delta_o \quad (2.128)$$

The matrix equation of static equilibrium, in terms of rotations θ_1 and θ_2 , now becomes

$$\begin{bmatrix} 5 & -2 \\ -2 & 2 \end{bmatrix} + \bar{q} \begin{bmatrix} -1 & 0 \\ 0 & -1 \end{bmatrix} \begin{Bmatrix} \theta_1 \\ \theta_2 \end{Bmatrix} = \bar{q} \alpha_o \begin{Bmatrix} 1 \\ 1 \end{Bmatrix} + \bar{q} \left(\frac{C_{L_\delta}}{C_{L_\alpha}} + \frac{c}{e} \frac{C_{M_\delta}}{C_{L_\alpha}} \right) \begin{Bmatrix} 0 \\ 1 \end{Bmatrix} \delta_o \quad (2.129)$$

Equation 2.129 indicates that the divergence eigenvalue problem is unchanged, because α_o and δ_o are inputs, independent of θ_1 and θ_2 . Let us suppose, however, that we include a feedback control system so that the control deflection, δ_o , responds to a sensor that measures the elastic deformation, θ_1 . The sensor, perhaps a strain gage, senses and sends signals to an aileron actuator to rotate the control surface an amount δ_o given by the relationship

$$\delta_o = [G \ 0] \begin{Bmatrix} \theta_1 \\ \theta_2 \end{Bmatrix} \quad (2.130)$$

The row matrix $[G \ 0]$ is the control gain matrix. The constant G is a gain and can be either positive or negative.

The second term on the right hand side of Eqn. 2.129 is now written as

$$\bar{q} \left(\frac{C_{L_\delta}}{C_{L_\alpha}} + \left(\frac{c}{e} \right) \frac{C_{M_\delta}}{C_{L_\alpha}} \right) \begin{Bmatrix} 0 \\ 1 \end{Bmatrix} [G \ 0] \begin{Bmatrix} \theta_1 \\ \theta_2 \end{Bmatrix} = \bar{q} \begin{Bmatrix} 0 & 0 \\ k & 0 \end{Bmatrix} \begin{Bmatrix} \theta_1 \\ \theta_2 \end{Bmatrix} \quad (2.131)$$

The matrix term in Eqn. 2.131 is now a function of the rotations θ_1 and θ_2 and belongs on left hand side of Eqn. 2.129. The divergence eigenvalue problem for the airfoil system with feedback control now is written as follows:

$$\begin{bmatrix} (5 - \bar{q}) & (-2) \\ (-2 - \bar{q}k) & (2 - \bar{q}) \end{bmatrix} \begin{Bmatrix} \theta_1 \\ \theta_2 \end{Bmatrix} = \begin{Bmatrix} 0 \\ 0 \end{Bmatrix} \quad (2.132)$$

The characteristic equation for the above stability matrix is:

$$\Delta = \bar{q}^2 - 7\bar{q} + 6 - 2\bar{q}k = 0 \quad (2.133)$$

In Figure 2.36, the determinant has been plotted for five different values of k , including the open loop case, $k=0$.

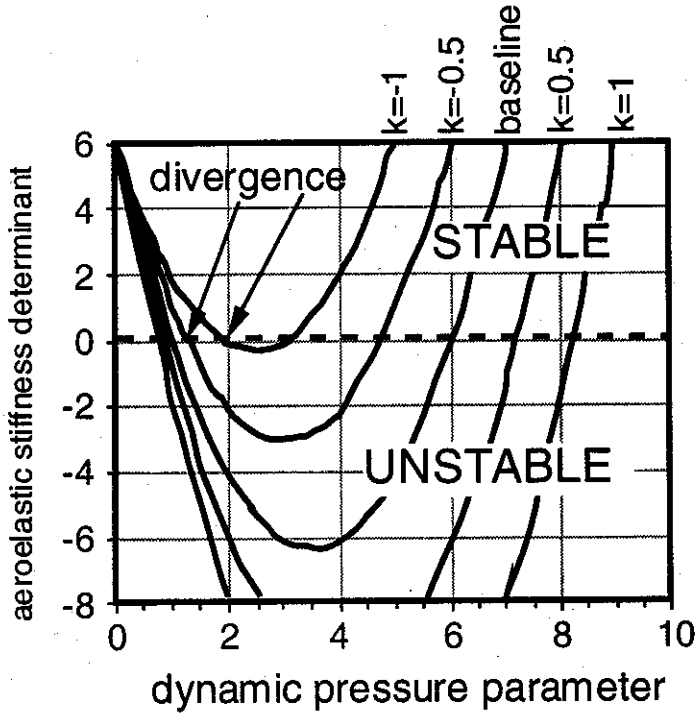


Figure 2.36 - Stability determinant vs \bar{q} ; five different values of k

When $k > 0$ the aileron rotates downward to increase lift outboard when $\theta_1 > 0$ and the open-loop system is destabilized by the addition of the feedback loop with $k > 0$. However, if $k < 0$, then the aeroelastic system is stabilized. Pitch up of the inboard panel is counteracted by the aileron "dumping" lift from the outboard panel. Notice that, as k becomes more negative, the value of the lowest eigenvalue (crossing points in Figure 2.36) increases while the second eigenvalue (originally at $\bar{q} = 6$) declines.

We can separate the effects of the active control from the original determinant by defining a term, Δ_o , as follows:

$$\Delta_o = \bar{q}^2 - 7\bar{q} + 6$$

This term Δ_o is the function associated with the uncontrolled or "open-loop" system (identified a "baseline" in Figure 2.36). This determinant is zero at $\bar{q} = 1$ and 6 and is plotted against \bar{q} in Figure 2.37 and labeled $k=0$. Eqn. 2.133 is written as

$$\Delta_o = 2\bar{q}k \quad (2.134)$$

The closed-loop eigenvalue problem has solutions if the function Δ_o is equal to $2\bar{q}k$. When $2\bar{q}k$ is plotted against \bar{q} , the result is a straight line with slope $2k$. Three lines corresponding to different values of k are shown in Figure 2.37, together with the baseline determinant and functions given in Eqn. 2.132. Intersection points between the Δ_o curve and the $2\bar{q}k$ lines correspond to eigenvalue solutions to the closed-loop problem and are indicated for the three values shown.

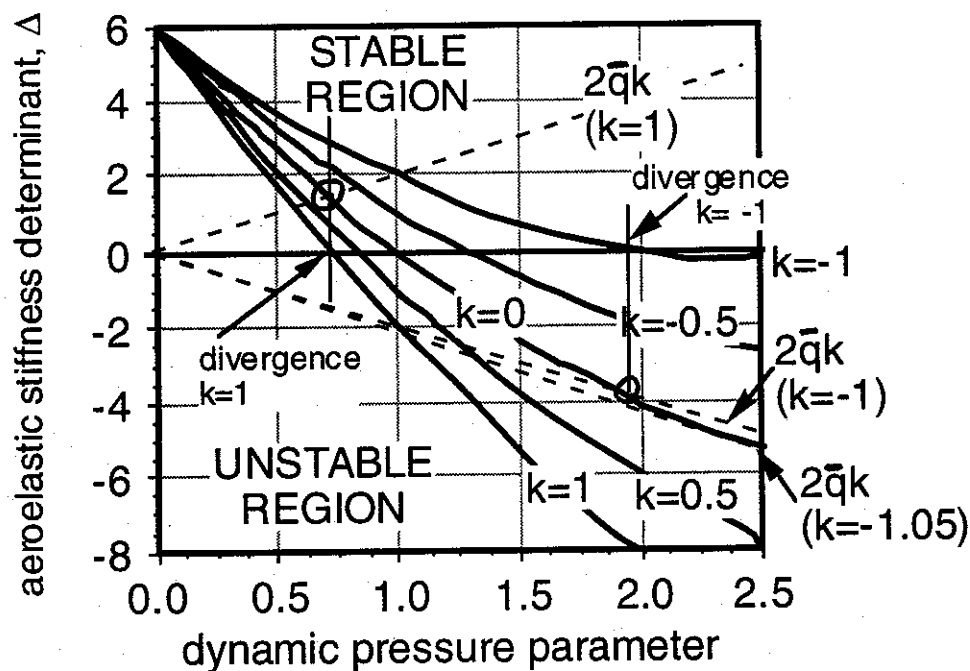


Figure 2.37 - Effect of control gain k on divergence stability determinant

Calculations show that when $k = -1.05$, the $2\bar{q}k$ line is tangent to the Δ_α curve. As a result there is a single intersection point and the two neutral stability eigenvalues merge together. If $k < -1.05$ then the line $2\bar{q}k$ never intersects the baseline determinant and divergence is impossible. Solution of Eqn. 2.132 will yield complex numbers for the eigenvalues, indicating that the dynamic pressure for divergence is complex. This means that divergence will not occur.

Example - divergence of a three-degree-of-freedom system

A shaft is attached to a wind tunnel wall as shown in Figure 2.38. Three airfoil sections are then attached to the shaft so that they are free to rotate about the shaft. Next, three torsion springs are added so that the relative motion of the airfoils with respect to each other and the wind tunnel wall is restrained. The spring connecting wing section 1 to the wind tunnel wall has spring constant $3K_T$ lb-in/radian. The other springs have spring constants $2K_T$ and K_T , respectively. Each wing section has equal aerodynamic and geometric parameters given as S , e and $C_{L\alpha}$.

The angles of incidence of the three airfoils are shown in Figure 2.38. This system is given an initial angle of attack α_0 at airspeed V . We will develop the equations of static equilibrium in matrix form using the parameter $\bar{q} = qSeC_{L\alpha}/2K$. We will then develop a polynomial relationship that defines the dynamic pressure at which aeroelastic divergence occurs and solve for the dynamic pressure at which divergence occurs.

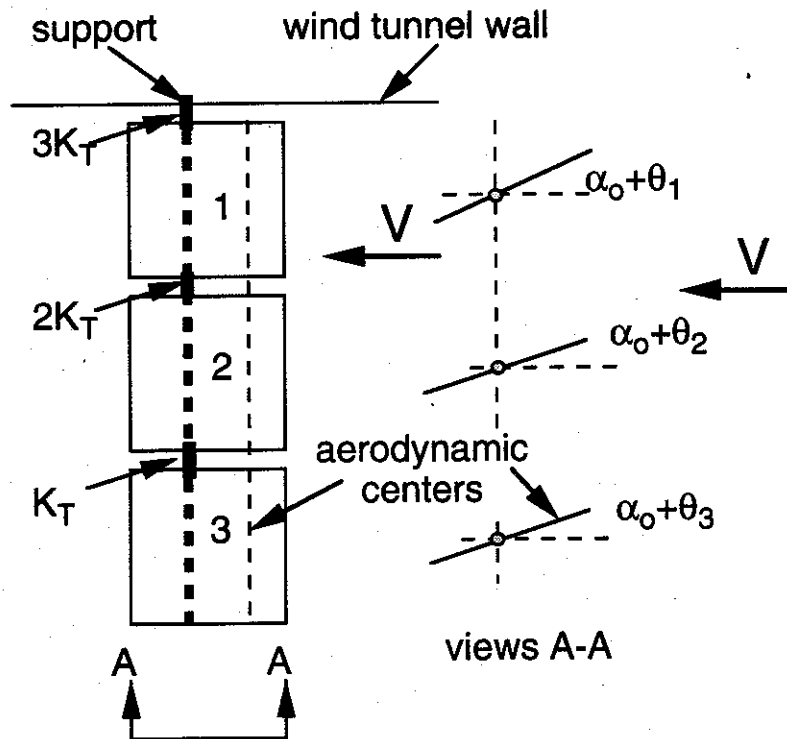


Figure 2.38 - Three degree of freedom wing planform and side view

If the wind tunnel is operating at a simulated altitude of 35,000 feet, at what Mach number will divergence occur? At what airspeed? If $V_o = \sqrt{\frac{2q_D}{\rho}}$ is the divergence airspeed for incompressible flow compute the ratio of V_c / V_o , where V_c represents the divergence airspeed accounting for compressibility. Let $\frac{K_T}{SeC_{L\alpha_0}} = 1500$ (where $C_{L\alpha_0}$ is the incompressible flow lift curve slope, uncorrected for Mach number). At divergence, solve for the eigenvector ratios $\frac{\theta_1}{\theta_3}$ and $\frac{\theta_2}{\theta_3}$.

Summing the moments for the three airfoil sections in the free-body diagram shown in Figure 2.39 produces the following equations.

$$\sum M_1 = 0 = L_1 e - 3K_T\theta_1 + 2K_T(\theta_2 - \theta_1)$$

$$\sum M_2 = 0 = L_2 e - 2K_T(\theta_2 - \theta_1) + K_T(\theta_3 - \theta_2)$$

$$\sum M_3 = 0 = L_3 e - K_T(\theta_3 - \theta_2)$$

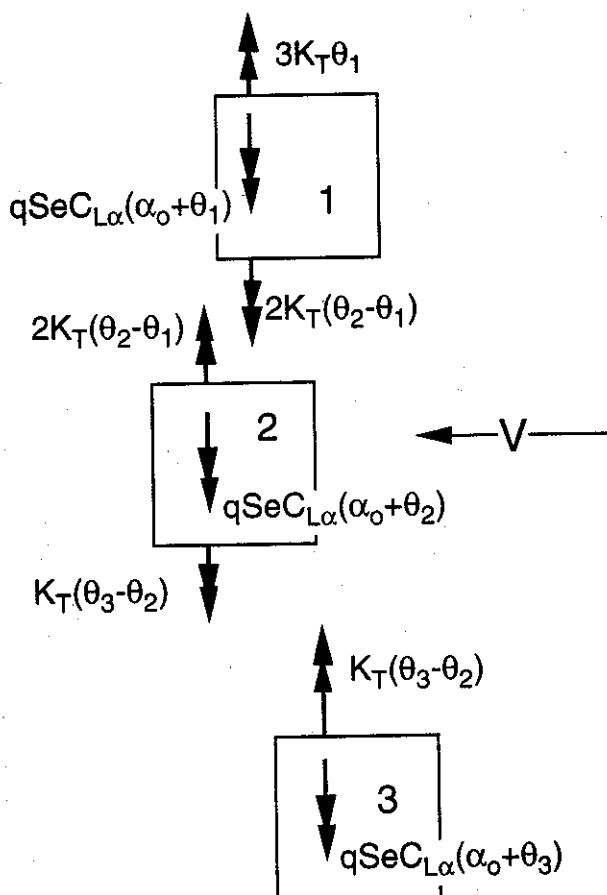


Figure 2.39 - Three degree of freedom free body diagram

In matrix form the moment equilibrium equations can be written as

$$\begin{bmatrix} (5K_T - qSeC_{L_a}) & -2K_T & 0 \\ -2K_T & (3K_T - qSeC_{L_a}) & -K_T \\ 0 & -K_T & (K_T - qSeC_{L_a}) \end{bmatrix} \begin{Bmatrix} \theta_1 \\ \theta_2 \\ \theta_3 \end{Bmatrix} = qSeC_{L_a} \alpha_o \begin{Bmatrix} 1 \\ 1 \\ 1 \end{Bmatrix} \quad (2.135)$$

Let $\bar{q} = \frac{q}{2K_T} = \frac{qSeC_{L_a}\alpha_o}{2K_T SeC_{L_a}}$ so that Eqn. 2.135 becomes

$$\begin{bmatrix} 5 - 2\bar{q} & -2 & 0 \\ -2 & 3 - 2\bar{q} & -1 \\ 0 & -1 & 1 - 2\bar{q} \end{bmatrix} \begin{Bmatrix} \theta_1 \\ \theta_2 \\ \theta_3 \end{Bmatrix} = 2\bar{q}\alpha_o \begin{Bmatrix} 1 \\ 1 \\ 1 \end{Bmatrix} \quad (2.136)$$

The divergence dynamic pressure is found by forming the determinant of the aeroelastic stiffness matrix in Eqn. 2.136 and setting it to zero. This gives the following equation.

$$\Delta = -8\bar{q}^3 + 36\bar{q}^2 - 36\bar{q} + 6 = 0$$

or

$$4\bar{q}^3 - 18\bar{q}^2 + 18\bar{q} - 3 = 0$$

The three roots to this polynomial are

$$\bar{q}_1 = 0.2079$$

$$\bar{q}_2 = 1.147$$

$$\bar{q}_3 = 3.145$$

Since the determinant is positive when the "wind" is off, divergence occurs at the lowest value of \bar{q} so the divergence dynamic pressure is

$$\bar{q}_D = 0.2079$$

or

$$q_D = 0.4158 \frac{K_T}{SeC_{L_a}}$$

Since the wind tunnel is operating at a simulated altitude of 35,000 feet the speed of sound and density are $a_\infty = 973 \frac{ft}{s}$ $\rho = 7.365 \times 10^{-4} \frac{lb - sec^2}{ft^4}$

The incompressible flow divergence speed V_o is

$$V_o^2 = \frac{2q_D}{\rho}$$

so that

$$V_o^2 = 2 \left(\frac{0.4158}{7.365 \times 10^{-4}} \right) \frac{K_T}{SeC_{L_a}}$$

$$V_o^2 = 1129 \frac{K_T}{SeC_{L_a}}$$

$$V_o = 33.6 \left(\frac{K_T}{SeC_{L_a}} \right)^{\frac{1}{2}} = 1301 \frac{ft}{s}$$

The divergence airspeed is greater than the speed of sound. The divergence Mach number is

$$M_o = \frac{V_o}{a_\infty}$$

or

$$M_{D_o} = 1.34$$

Let's include compressibility effects in our divergence analysis. The divergence dynamic pressure q_D is found by solving

$$q_D = \bar{q}_D \left(\frac{2K_T}{SeC_{L_{\alpha_o}}} \right) \sqrt{1 - M_D^2} = \frac{1}{2} \rho a_\infty^2 M_D^2$$

where $C_{L_{\alpha_o}}$ is the incompressible lift curve slope. Squaring both sides of this equation gives

$$\left(\frac{4\bar{q}_D}{\rho a_\infty^2} \frac{K_T}{SeC_{L_{\alpha_o}}} \right)^2 (1 - M_D^2) = M_D^4$$

This equation can be rewritten as the following,

$$M_D^4 + A^2 K^2 M_D^2 - A^2 K^2 = 0$$

$$A^2 = \left(\frac{4\bar{q}_D}{\rho a_\infty^2} \right)^2$$

where

$$K^2 = \left(\frac{K_T}{SeC_{L_{\alpha_o}}} \right)^2$$

Solving for M_D^2 , we have

$$M_D^2 = \frac{-A^2 K^2 \pm \sqrt{A^4 K^4 + 4 A^2 K^2}}{2}$$

Choosing the larger value of M_D^2

$$M_D^2 = \frac{-A^2 K^2 + \sqrt{A^4 K^4 + 4 A^2 K^2}}{2}$$

Taking the positive square root (Mach number should be positive) to find an expression for M_D results in the following equation.

$$M_D = AK \sqrt{\left[\frac{-1 + \sqrt{1 + \frac{4}{A^2 K^2}}}{2} \right]}$$

The values of \bar{q}_D , ρ , and a_∞ can be substituted into A^2 and K^2 to find M . This gives:

$$M = 0.84 \times 10^{-3} \left(\frac{K_T}{SeC_{L_{a_0}}} \right) \left[-1 + \sqrt{1 + 2.83 \times 10^6 \left(\frac{SeC_{L_{a_0}}}{K_T} \right)^2} \right]^{\frac{1}{2}}$$

The divergence velocity V_c is

$$V_c = a_\infty M_D$$

so that

$$V_c = 0.817 \left(\frac{K_T}{SeC_{L_{a_0}}} \right) \left[-1 + \sqrt{1 + 2.83 \times 10^6 \left(\frac{SeC_{L_{a_0}}}{K_T} \right)^2} \right]^{\frac{1}{2}}$$

When we divide V_c by V_o we get

$$\frac{V_c}{V_o} = 0.02439 \left(\frac{K_T}{SeC_{L_a}} \right)^{\frac{1}{2}} \left[-1 + \sqrt{1 + 2.83 \times 10^6 \left(\frac{SeC_{L_{a_0}}}{K_T} \right)^2} \right]^{\frac{1}{2}}$$

We were given that $\frac{SeC_{L_{a_0}}}{K_T} = \frac{1}{1500}$ so that $\frac{V_c}{V_o}$ is

$$\frac{V_c}{V_o} = 0.67$$

or

$$V_c = (0.67)(1301) = 871.7 \text{ fps.}$$

and

$$M_D = 0.898$$

The divergence mode shape at the two lower dynamic pressures of instability ($\bar{q} = 0.208$ and $\bar{q} = 1.147$) consist of the ratios of the elastic angles of attack. These ratios are defined as

$$\frac{\theta_1}{\theta_3} \quad \text{and} \quad \frac{\theta_2}{\theta_3}$$

These two ratios are found from the eigenvalue problem when $\bar{q} = 0.208$. At this value of dynamic pressure, the original equilibrium equations become:

$$\begin{bmatrix} 5 - 2\bar{q}_D & -2 & 0 \\ -2 & 3 - 2\bar{q}_D & -1 \\ 0 & -1 & 1 - 2\bar{q}_D \end{bmatrix} \begin{Bmatrix} \theta_1 \\ \theta_2 \\ \theta_3 \end{Bmatrix} = \begin{Bmatrix} 0 \\ 0 \\ 0 \end{Bmatrix}$$

or,

$$\begin{bmatrix} 4.584 & -2 & 0 \\ -2 & 2.584 & -1 \\ 0 & -1 & 0.584 \end{bmatrix} \begin{Bmatrix} \theta_1 \\ \theta_2 \\ \theta_3 \end{Bmatrix} = \begin{Bmatrix} 0 \\ 0 \\ 0 \end{Bmatrix}$$

If we let θ_3 equal one, then we can compute the ratios of the angles of attack to be:

$$\frac{\theta_1}{\theta_3} = 0.2549$$

$$\frac{\theta_2}{\theta_3} = 0.5842$$

Torsional divergence of an unswept flexible wing model

The interaction between aerodynamic loads and twisting deformation of slender wings can be idealized so that equilibrium conditions are represented with differential equations. The wing in Figure 2.40 is idealized as a uniform twisting element with constant mass per unit length and a constant distance between the line of aerodynamic centers and line of shear centers, called the elastic axis.

The wing is idealized to be a slender element with uniform stiffness per unit length. St. Venant's torsion theory, allowing warping of all sections, including those near the wing root, is allowed. Only torsional deformation is allowed, despite the fact that the wing will also bend under the distributed loads applied along the span. The idealized wing structure and a free body diagram of an infinitesimally small section of the wing structure (of length dx) are illustrated in Figure 2.41.

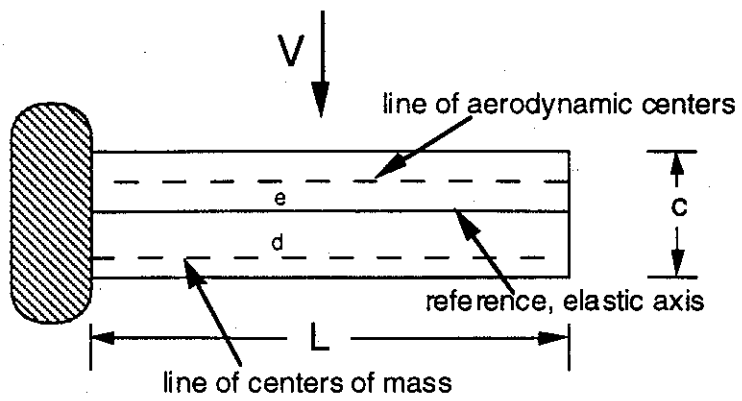


Figure 2.40 - Unswept wing planform

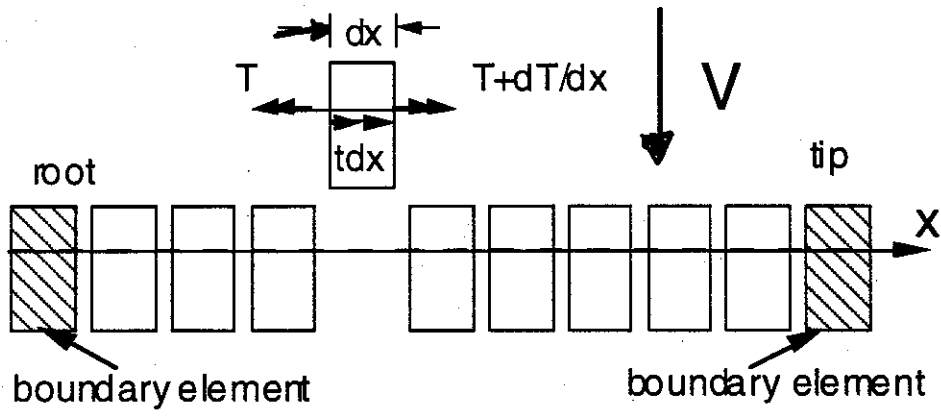


Figure 2.41 Unswept wing torsion idealization and torsion element

The relationship between the twist deformation along the length of this structure and an internal cross-sectional resultant torque, $T(x)$, shown in Figure 2.41, is given by the relationship:

$$T(x) = GJ \frac{d\theta}{dx} \quad (2.137)$$

GJ is the effective torsional stiffness of the cross-section, while $\theta(x)$ is the angle of twist.

Also shown in Figure 2.41 is a distributed external torque of intensity $t(x)$ in-lb/in. Its net value on this small element is $t(x)dx$ and is positive as shown. Equilibrium of internal and external torques about the x axis gives:

$$\sum M_x = 0 = T - tdx - \left(T + \frac{dT}{dx} dx \right) = \left(-t - \frac{dT}{dx} \right) dx \quad (2.138)$$

or

$$\frac{dT}{dx} = -t(x) \quad (2.139)$$

By using Eqn. 2.139, we can derive a relation between the torsional deformation θ and the applied external torque $t(x)$. This is

$$\frac{dT}{dx} = \frac{d}{dx} \left(GJ \frac{d\theta}{dx} \right) = -t(x) \quad (2.140)$$

Equation 2.140 can be used to predict the divergence conditions for an idealized, unswept, flexible wing as indicated in Figure 2.41. Lift forces $l(x)$ are distributed outward from the page along the line of aerodynamic centers and are computed as follows:

$$l(x) = qc c_{l_a} \alpha = qca_o (\alpha_o + \theta) \quad (\alpha_o = c_{l_a})$$

These lift forces produce a torque about the elastic axis. In addition, an aerodynamic pitching moment is distributed along the span at the AC and is equal to

$$M_{ac} = qc^2 c_{mac}$$

where c_{mac} is the sectional moment coefficient about the AC. The final part of the applied torque comes from the distributed wing weight. This contribution, t_w , is equal to:

$$t_w = nmgd$$

where n is the load factor normal to the wing surface ($n = 1$ for level flight) and mg is the weight per unit span.

Putting all these loads together, with an initial constant angle of attack for all sections equal to α_o , we find that the distributed torque is:

$$t(x) = qcea_o (\alpha_o + \theta) + qc^2 c_{mac} + nmgd$$

(note $a_o = c_{l_a}$)

The twist equilibrium equation, Eqn. 2.140, becomes:

$$\frac{d}{dx} \left(GJ \frac{d\theta}{dx} \right) + qcea_o \theta = -(qcea_o \alpha_o + qc^2 c_{mac} + nmgd) \quad (2.141)$$

Since our idealization restricts GJ to be constant along the wing, Eqn. 2.141 can be written as:

$$\frac{d^2\theta}{dx^2} + \left(\frac{qcea_o}{GJ} \right) \theta = -K \quad (2.142)$$

where

$$K = (qcea_o \alpha_o + qc^2 c_{mac} + nmgd) / GJ$$

Let us define an aeroelastic parameter, λ , as follows:

$$\lambda^2 = \frac{qcea_o}{GJ}$$

Then, Eqn. 2.147 can be written as: $\theta'' + \lambda^2\theta = -K$ (2.143)

The solution to Eqn. 2.143 is:

$$\theta(x) = A\sin\lambda x + B\cos\lambda x - K/\lambda^2 \quad (2.144)$$

where A and B are unknown constants. At $x = 0$,

$$\theta(0) = 0 = B - \frac{K}{\lambda^2}$$

This gives the value of B as: $B = \frac{K}{\lambda^2}$

The expression for $\theta(x)$ now becomes:

$$\theta(x) = A\sin\lambda x - \frac{K}{\lambda^2}(1 - \cos\lambda x)$$

At the wing tip, $x = L$, the torque $T(L)$ is zero because it is a free end. From Eqn. 2.137,

$$T(L) = GJ\theta'(L) = 0 = GJ\left[A\lambda\cos\lambda L - \frac{K}{\lambda}\sin\lambda L\right]$$

Solving for A and substituting it into Eqn. 2.144, we have:

$$\theta(x) = \frac{-K}{\lambda^2}[1 - \cos\lambda x - (\tan\lambda L)(\sin\lambda x)] \quad (2.145a,b)$$

$$\theta(x) = -\left(\alpha_o + \left[\frac{c}{e}\right]\left[\frac{c_{mac}}{a_o}\right] + \left[\frac{nmgd}{qcea_o}\right]\right)[1 - \cos\lambda x - (\tan\lambda L)(\sin\lambda x)]$$

Equation 2.145a or b provides the twist distribution along the wing from root to tip. We should not forget that the wing also undergoes bending deflections, but that these bending deflections are of no importance in the determination of airloads on unswept wings.

A close look at Eqn. 2.145a shows that the $\tan\lambda L$ term has a marked effect on twist displacement. A plot of $\tan\lambda L$ vs. λL , shown in Figure 2.42 illustrates this distortion. At $\lambda L = \frac{\pi}{2}$ the tangent function becomes infinite. If $\lambda = \frac{\pi}{2L}$, small initial wing loads produce (theoretically) infinite torsional deformations. Physically, this cannot happen because

structural and/or aerodynamic nonlinear effects would render our assumptions invalid. Still this theoretical result can be compared to the results obtained from the study of the typical section.

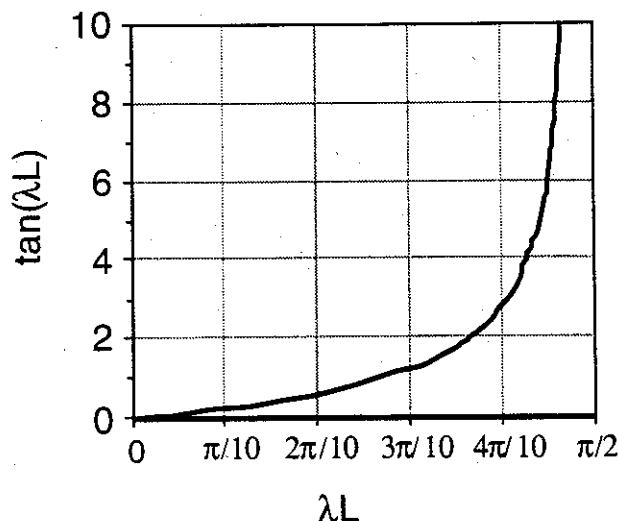


Figure 2.42- Twist amplification coefficient $\tan \lambda L$

Torsional divergence of the wing with constant GJ occurs when

$$\lambda^2 = \frac{qcea_o}{GJ} = \left(\frac{\pi}{2L} \right)^2 \quad (2.146)$$

or

$$q_D = \left(\frac{\pi}{2L} \right)^2 \left(\frac{GJ}{cea_o} \right) = \left(\frac{\pi}{2} \right)^2 \left(\frac{GJ}{L} \right) \left(\frac{1}{Sea_o} \right) \quad (2.147)$$

Equation 2.147 has been derived using aerodynamic strip theory and has limited applicability. More accurate analysis shows that the divergence q encountered by a similar wing is larger than that predicted by Equation 2.147. The typical section idealization predicted the divergence dynamic pressure to be $q_D = K_r / SeC_{L\alpha}$, the dynamic pressure at divergence is directly proportional to the stiffness parameter GJ/L and inversely proportional to wing area S ; the greater the wing semi-span, the lower the divergence q . Notice also that the sectional lift curve slope $c_{l\alpha} = a_o$ has replaced the wing lift curve slope in our equation $q_D = K_r / SeC_{L\alpha}$.

Formal solution for divergence dynamic pressure

The equation that must hold for perturbations away from any static equilibrium is simply Eqn. 2.142 with the right hand side set to zero. In this case, θ represents the

perturbation twist away from the static equilibrium position. The equation that must hold at neutral stability is

$$\frac{d^2\theta}{dx^2} + \left(\frac{qcea_o}{GJ} \right) \theta = 0 \quad (2.148)$$

The solution to this equation is

$$\theta(x) = A \sin \lambda x + B \cos \lambda x \quad (2.149)$$

The boundary conditions are

$$\theta(0) = 0 \quad (2.150)$$

and

$$T(L) = GJ\theta'(L) = 0 \quad (2.151)$$

Substituting Eqn. 2.149 into Eqn. 2.150, we have

$$\theta(0) = A \sin \lambda 0 + B \cos \lambda 0 = 0$$

or

$$A(0) + B(1) = 0$$

The end torque condition in Eqn. 2.151 becomes

or

$$\theta'(L) = A\lambda \cos \lambda L - B\lambda \sin \lambda L = 0 \quad (2.153)$$

$$A(\lambda \cos \lambda L) + B(-\lambda \sin \lambda L) = 0$$

Equations 2.152 and 2.153 can be written in matrix form as

$$\begin{bmatrix} 0 & 1 \\ (\lambda \cos \lambda L) & (-\lambda \sin \lambda L) \end{bmatrix} \begin{Bmatrix} A \\ B \end{Bmatrix} = \begin{Bmatrix} 0 \\ 0 \end{Bmatrix} \quad (2.154)$$

The determinant of the matrix in Eqn. 2.154 must be zero if A and B are to be nontrivial. This leads to the following condition for neutral stability at divergence to exist

$$\Delta = \lambda \cos \lambda L = 0 \quad (2.155)$$

This equation has the following solutions

$$\lambda L = \frac{\pi}{2}, \frac{3\pi}{2}, \dots \frac{(2n+1)\pi}{2} \quad (2.156)$$

The lowest value in Equation 2.156 is the divergence dynamic pressure. This leads to the divergence condition

$$\lambda^2 L^2 = \frac{\pi^2}{4} = \frac{q_D c e c_{la} L^2}{GJ} \quad (2.157)$$

Comparing the results in Eqns. 2.157 and 2.147 we see that the results are identical.

The influence of aeroelastic effects can be seen in Figure 2.43 which plots Eqn. 2.145b when K=1 and q equal to 10% of the divergence dynamic pressure. This twist distribution is very close to that found when aeroelastic effects are ignored. In this case, the twist distribution for the wing is

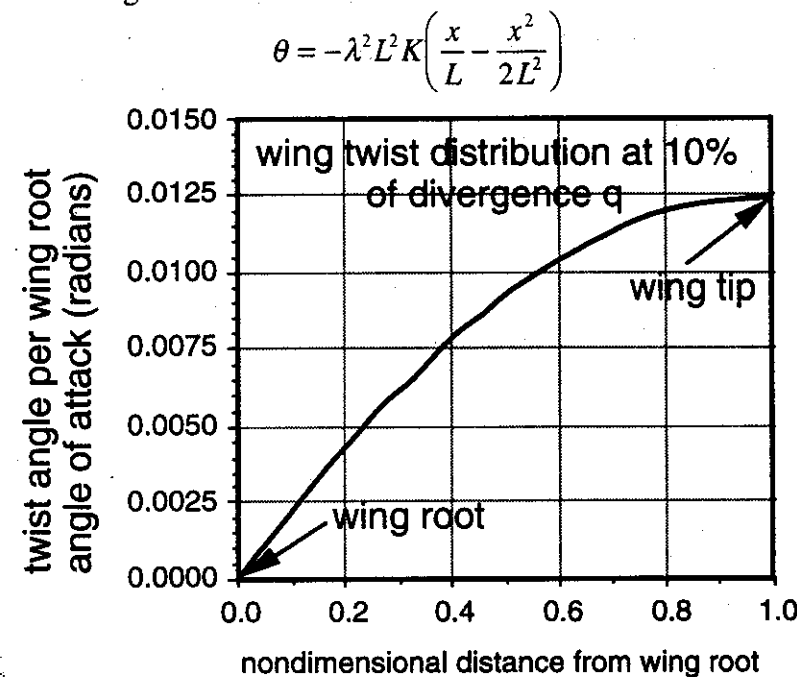


Figure 2.43 - Twist angle multiplier vs. distance from root at 10% divergence q

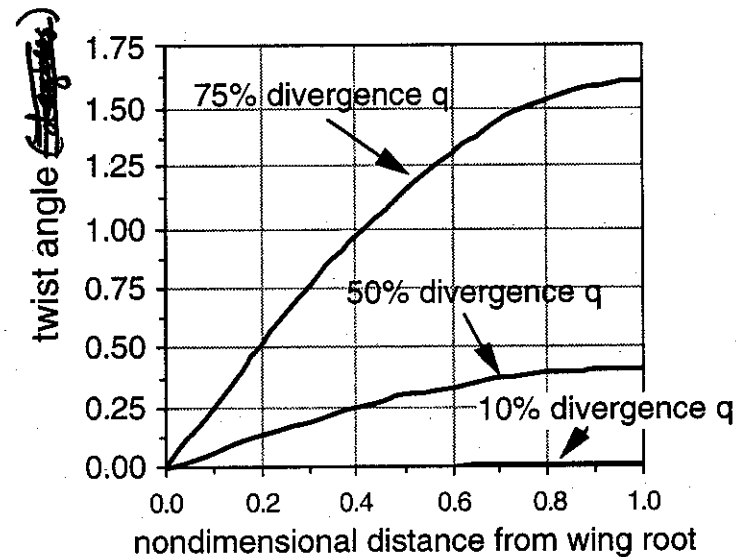


Figure 2.44 - Twist angle multiplier vs. distance from root for three different dynamic pressures

Figure 2.44 shows the effect of increasing the value of the nondimensional dynamic pressure to 75% of the divergence dynamic pressure. From this figure we see that an increase in dynamic pressure from 10% to 50% and 75% of the divergence dynamic pressure creates a substantial increase in twist if the angle of attack is not changed.

Control surface effectiveness

Control effectiveness is the ability of a control surface such as an elevator, aileron or rudder to produce a change in the airplane pitching moment, rolling moment, or yawing moment, respectively. Control effectiveness is essential to maneuvering performance and airplane stability. Horizontal tail, wing or vertical stabilizer torsional flexibility will reduce control effectiveness of most unswept lifting surfaces. Bending will reduce the control effectiveness of sweptback lifting surfaces.

The airfoil model used in our previous discussions is not entirely adequate for studying control surface effectiveness since it is a one dimensional surface for moments. We can compute twisting moments, but not rolling moment or yawing moment because there is no roll or yaw axis. However, an analysis of changes in lift on this airfoil model due to control surface input can still illustrate the concept of control effectiveness.

The airfoil idealization used to study control effectiveness has a symmetrical section whose "skeleton" is shown in Figure 2.45 (the actual airfoil section has thickness like all real airfoils). Control surface rotation changes the effective camber of the airfoil. Both the lift and the pitching moment are changed by δ_o . These changes will create lift and also twist the airfoil. The structural twist of the airfoil section is again represented by the angle θ .

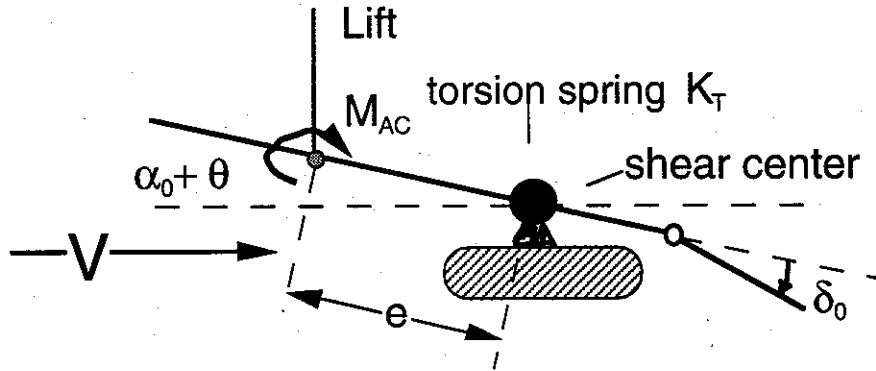


Figure 2.45 - Torsionally flexible airfoil with control surface.

The control surface is assumed to be connected to the airfoil section by a rigid hinge. The airfoil lift is given by

$$L = qSC_{L_\alpha}(\alpha_o + \theta) + qSC_{L_\delta}\delta_o \quad (2.158)$$

The term of C_{L_δ} in Eqn. 2.158 is shorthand notation for the derivative

$$\frac{\partial C_L}{\partial \delta} = C_{L_\delta} \quad (2.159)$$

The twisting moment about the airfoil aerodynamic center is:

$$M_{AC} = qScC_{MAC} + qScC_{M_\delta}\delta_o \quad (2.160)$$

The fact that a twisting moment is generated by control surface rotation is important to the control effectiveness phenomenon. Positive δ_o (downward as shown in Figure 2.45) causes a negative value of C_{M_δ} measured about the AC. This tends to twist the airfoil nose-down to decrease the airfoil angle of attack. Summing moments about the shear center, we find

$$Le + M_{AC} = M_s = K_T\theta \quad (2.161)$$

Substituting Eqns. 2.158 and 2.160 into 2.161 and solving for θ , we find

$$\theta = \frac{qSeC_{L_\alpha} \left[\alpha_o + \left(\frac{c}{e} \right) \frac{C_{MAC}}{C_{L_\alpha}} \right] + qSe \left[C_{L_\delta} + \left(\frac{c}{e} \right) C_{M_\delta} \right] \delta_o}{K_T - qSeC_{L_\alpha}} \quad (2.162)$$

Equation 2.162 reduces to our previous result when δ_o is zero. We also notice that the effects of α_o and δ_o on θ are additive and separable. Therefore, having studied the effect of α_o and C_{MAC} upon θ , we confine our attention solely to the second term in the numerator of Eqn. 2.162. This term may be written as:

$$\frac{\theta}{\delta_o} = \left(\frac{qSeC_{L_\delta}}{K_T} \right) \frac{\left(1 + \frac{c}{e} \frac{C_{M_\delta}}{C_{L_\delta}} \right)}{1 - q/q_D}$$

The lift due to δ_o ($\alpha_o = 0$) is computed from Eqns. 2.158 and 2.162 to be

$$L = qS \left(C_{L_\delta} + C_{L_\alpha} \frac{\theta}{\delta_o} \right) \delta_o$$

Further algebraic manipulation and reduction provides the following expression.

$$L = qsC_{L_\delta}\delta_o \left[\frac{1 - q \frac{Sc}{K_T} \left(\frac{C_{L_\alpha}}{C_{L_\delta}} \right) (-C_{M_\delta})}{1 - q/q_D} \right] \quad (2.163)$$

Since C_{M_δ} is negative ($-C_{M_\delta}$) is a positive number. The term in the numerator in Eqn. 2.163 can be simplified if we define a reference dynamic pressure, q_R , as:

$$q_R = \frac{-K_T}{ScC_{M_\delta}} \left(\frac{C_{L_\delta}}{C_{L_\alpha}} \right) \quad (2.164)$$

This reference dynamic pressure is called the reversal dynamic pressure and has a physical significance.

The ratio $C_{L_\delta} / C_{L_\alpha}$ in Eqn. 2.164 may be written as

$$\frac{C_{L_\delta}}{C_{L_\alpha}} = \frac{\partial C_L}{\partial \delta} \times \frac{\partial \alpha}{\partial C_L} = \frac{\partial \alpha}{\partial \delta}$$

This ratio of aerodynamic coefficients represents the apparent change in airfoil freestream angle of attack due to a unit (one radian or one degree) control deflection, δ_o . This term depends, upon among other things, the ratio of the control surface chord to wing chord ratio. Note that, for an all-movable control surface, where the control surface and the airfoil are one and the same, the ratio $C_{L_\delta} / C_{L_\alpha}$ is unity.

In the late 1920's Prandtl and Glauret developed equations to predict C_{L_δ} and C_{M_δ} as functions of the ratio of the flap chord to airfoil chord, expressed as $E = \frac{c_f}{c}$. This ratio is important because the theory to define the change in lift and the change in moment assumes that the camber of the airfoil section is changed discontinuously by the flap deflection. The estimators for lift and pitching moment are

$$C_{L_\delta} = \frac{C_{L_\alpha}}{\pi} \left(\cos^{-1}(1 - 2E) + 2\sqrt{E(1 - E)} \right)$$

$$C_{M_\delta} = -\frac{C_{L_\alpha}}{\pi} (1 - E) \sqrt{(1 - E)E}$$

The fact that we create a pitching moment when we deflect the flap can be understood if we examine the location of the center of pressure of the aerodynamic pressure created by the flap deflection.

(d)

Figure 2.46b shows the center of pressure location of the lift due to the flap. The center of pressure is located a distance d downstream (aft) of the airfoil quarter chord. If we move the reference point for the lift to the airfoil quarter chord we must add a twisting moment to compensate for the forward movement of the force. This situation is shown in Figure 2.46a.

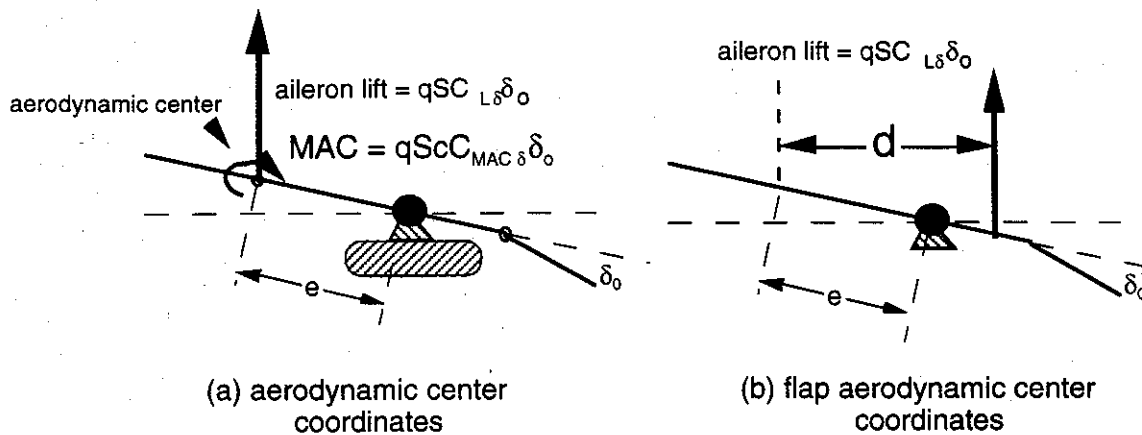


Figure 2.46 (a,b) - Force and moment equivalence for flap deflection

From moment equivalence, the moment about the airfoil 1/4 chord must be related to the lift as follows

$$-Ld = M_{AC\delta}$$

$$-C_{L\delta} d = c C_{MAC\delta}$$

L = lift due to aileron

The ratio d/c is computed to be

$$\frac{d}{c} = -\frac{C_{MAC\delta}}{C_{L\delta}}$$

and is plotted in Figure 2.47. This figure shows that when the flap is extremely small, the center of pressure is at the midchord and then travels forward when the flap size increases. This location can be either ahead of or behind the shear center.

Equation 2.163 can be written as:

$$L = L_r \left[\frac{1 - q_r / q_R}{1 - q_r / q_D} \right]$$

where

$$L_r = qSC_{L\delta}\delta_0$$

is the lift generated by control surface deflection δ_0 . The control effectiveness is defined as (for this idealization only since the primary purpose of the control is to produce a moment, not a force):

$$\frac{L}{L_r} = \left(\frac{1 - q/q_R}{1 - q/q_D} \right) \quad (2.165)$$

Assuming that the airfoil dynamic pressure is less than the divergence dynamic pressure, then, as dynamic pressure increases and approaches q_R , the ratio L/L_r decreases and becomes zero when $q = q_R$. At this point no net lift is produced by the control deflection, although the airfoil will twist and thus cancel the effects of control deflection lift.

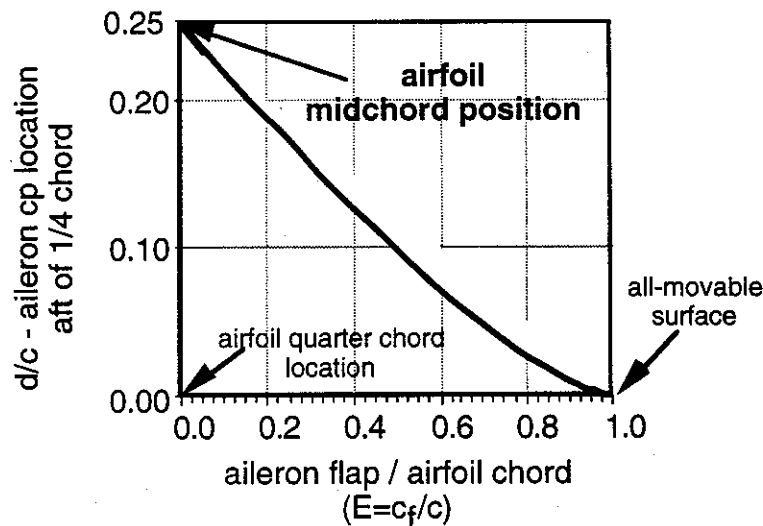


Figure 2.47 - Aileron center of pressure location vs. flap to chord ratio

When $q > q_R$, we say that the aileron is reversed because, from Eqn. 2.165 a positive δ_c decreases the lift instead of increasing it, because it causes the airfoil to twist nose downward so much that more lift is generated by negative twist than the camber due to control deflection.

Two different plots are necessary to examine lift effectiveness since q_R can be either greater than or less than q_D , depending on where the aileron center of pressure is (which in turn depends on how large the flap is). The divergence dynamic pressure appears in Eqn. 2.165 so we define a parameter, R , as

$$R = \frac{q_D}{q_R} = \frac{\frac{K_T}{ScC_{L\alpha}}}{\frac{-K_T}{ScC_{MAC\delta}} \left(\frac{C_{L\delta}}{C_{L\alpha}} \right)} \quad (2.166)$$

or

$$R = \frac{c}{e} \left(\frac{-C_{MAC\delta}}{C_{L\delta}} \right) = \frac{c}{e} \frac{d}{c} = \frac{d}{e}$$

With this definition of R , Eqn. 2.165 becomes

$$\frac{L}{L_r} = R \left[\frac{1 - q/q_R}{R - q/q_R} \right] \quad (2.167)$$

In Figure 2.48, the ratio L/L_r is plotted when $R > 1$. Note that there are two limiting conditions in Figure 2.48. When $q_R = q_D$, then $R = 1$ and rigid surface and flexible control effectiveness are identical. When $R = 1$ then $\%/\%_c = d/d_c = -C_{M_\delta}/C_{L_\delta}$. An additional limiting case in Figure 2.48 occurs when R is very large ($q_D \gg q_R$) so that

$$\lim_{R \rightarrow \infty} \frac{L}{L_r} = 1 - q/q_R \quad (2.168)$$

Notice that Eqn. 2.168 plots as a straight line in Figure 2.48. This control effectiveness behavior is typical of sweptback wings, as will be shown in a later section.

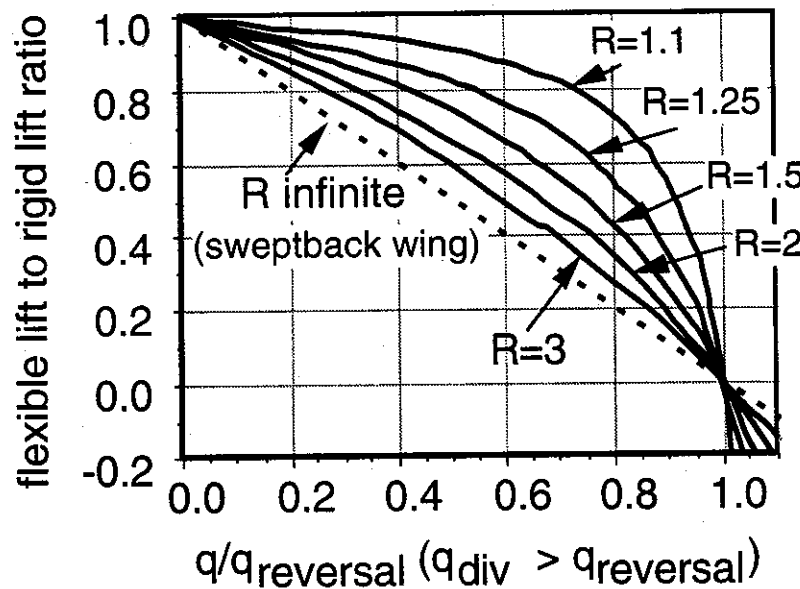


Figure 2.48 - Control effectiveness as a function of dynamic pressure ratio, q/q_R ($R > 1$).

Figure 2.49 plots control effectiveness vs. dynamic pressure when $q_D/q_R < 1$ ($R < 1$). In this case, control effectiveness always increases with increases in dynamic pressure. For instance, when $R = 0.5$ the control effectiveness is always greater than unity in the range of practical values of q/q_R . At $q/q_R = 0.5$, with $R = 0.5$, the effectiveness is computed to be infinite because divergence occurs in all cases when $q/q_R = R$.

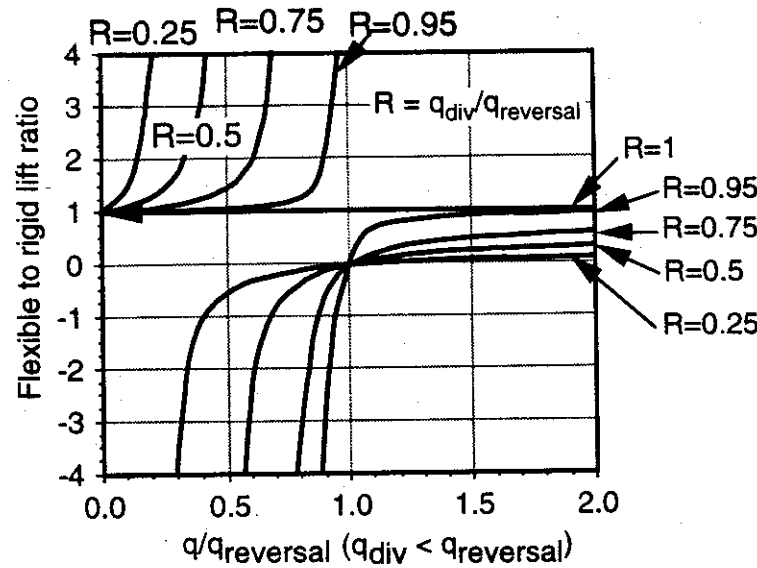


Figure 2.49 - Control (lift) effectiveness as a function of q / q_R ($R < 1$).

The reversal dynamic pressure defined in Eqn. 2.164 contains aerodynamic derivatives that are dependent upon Mach number, M . We can rewrite Eqn. 2.164 as

$$q_R = \frac{-K_T}{Sc C_{M\delta}} \left(\frac{C_{L\delta}}{C_{L_{\text{reversal}}}} \right) \sqrt{1 - M^2}$$

or

$$q_R = q_{R_0} \sqrt{1 - M^2}$$

where q_{R_0} is the reversal dynamic pressure computed assuming incompressible flow. As in the case of divergence, we must match the reversal dynamic pressure including Mach number with the atmospheric flight value $q = \frac{1}{2} \rho a^2 M^2$.

Control effectiveness - summary

Control reversal is not an instability like divergence. With divergence a small input, α_o , produces a large output, θ . For reversal a large input δ_o produces no output (L / L_r). The twist angle θ may be large at reversal or it may be small. Above the reversal speed, a control input δ_o produces lift or moment opposite to that intended. At pressures larger than the divergence speed, the wing is unstable and will diverge or twist off.

Example - aileron effectiveness for rolling motion

An airplane is rolling with a steady state (constant) rolling velocity p radians per second due to the differentially deflected ailerons shown in Figure 2.50. The airplane's forward

airspeed is V , while the rolling motion of the airplane produces another velocity component $v(y)$ along the wing, given by the relation $v(y) = py$, as shown in the figure. The aileron is small, so that the aileron rolling velocity $v(y)$ along the aileron surface is approximately $v = pb/2$.

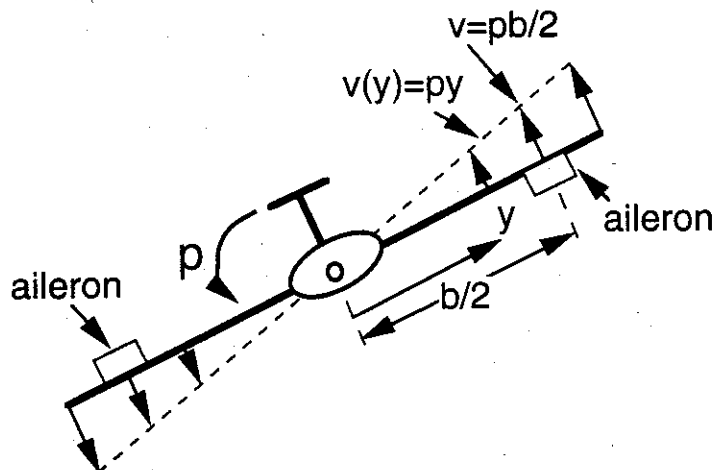


Figure 2.50 - Rolling airplane with small ailerons deflected.

We want to find the value of the steady state rolling velocity as a function of the aileron deflection angle δ_o , so we set up the following problem to simulate upward aileron motion at a constant speed. We will neglect all of the aerodynamic forces on the rest of the wing (not a good idea for a real airplane).

Figure 2.51 shows a small wing/aileron combination mounted on a frictionless vertical track that moves upward due to the action of lift. A torsion spring with a spring constant of K_T lb-in/radian restrains the ~~counterclockwise~~ clockwise twist, θ , of the airfoil. The upward velocity v is $v = pb/2$. The air appears to be coming downward with velocity v as the wing moves upward with velocity v .

Once the upward terminal velocity is reached, the lift at the airfoil aerodynamic center is given by the following expression:

$$L = qSC_{L_a} \left(\theta - \frac{v}{V} \right) + qSC_{L_\delta} \delta \quad (2.169)$$

$(v \ll V)$

The term $qSC_{L_a}(v/V)$ is called the aerodynamic damping force and acts downward, impeding upward motion. The aerodynamic pitching moment about the AC is $M_{AC} = qScC_{M_\delta} \delta_o$.

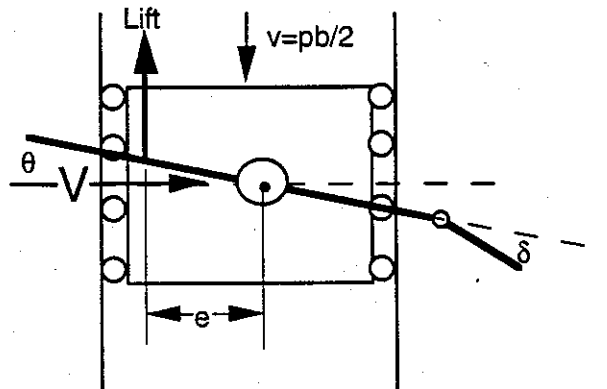


Figure 2.51 - Rolling effectiveness example

The free-body diagram for this example is shown in Figure 2.52. When the wing segment reaches its steady state-velocity, the net lift, L , is zero because the acceleration is zero.

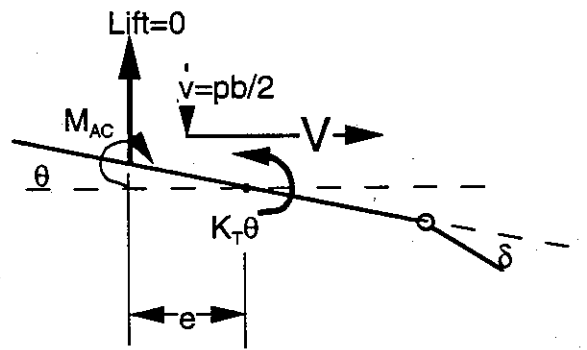


Figure 2.52 - Example problem geometry and free-body diagram

Although the lift is zero, there is a pitching moment, M_{AC} , that must be resisted by the torsion spring. Moment equilibrium requires that:

$$K_T\theta = M_{AC} = qScC_{M_\delta}\delta_o$$

Setting the lift expression in Eqn. 2.169 equal to zero provides an equation for v/V in terms of θ and δ_o .

$$\frac{v}{V} = \theta + \frac{C_{L_\delta}}{C_{L_a}}\delta_o \quad (2.170)$$

so that we can solve for θ .

$$\theta = qSc \frac{C_{M_\delta}}{K_T} \delta_o \quad (2.171)$$

Substituting Eqn. 2.171 into 2.170, we find the solution for the steady state roll velocity.

$$\frac{v}{V} = \frac{pb}{2V} = \left[qSc \frac{C_{M\delta}}{K_T} + \frac{C_{L\delta}}{C_{L\alpha}} \right] \delta_o$$

Then, using the definition of the reversal q_R , we have the following

$$\frac{v}{V} = \frac{pb}{2V} = \frac{C_{L\delta}}{C_{L\alpha}} [1 - q / q_R] \delta_o \quad (2.172)$$

Notice that, for this "maneuver", the divergence dynamic pressure does not appear in the expression for $v = pb/2V$. The term $pb/2V$ is a geometrical helix angle traced out in space by the aileron rolling at rate p and moving forward at velocity V .

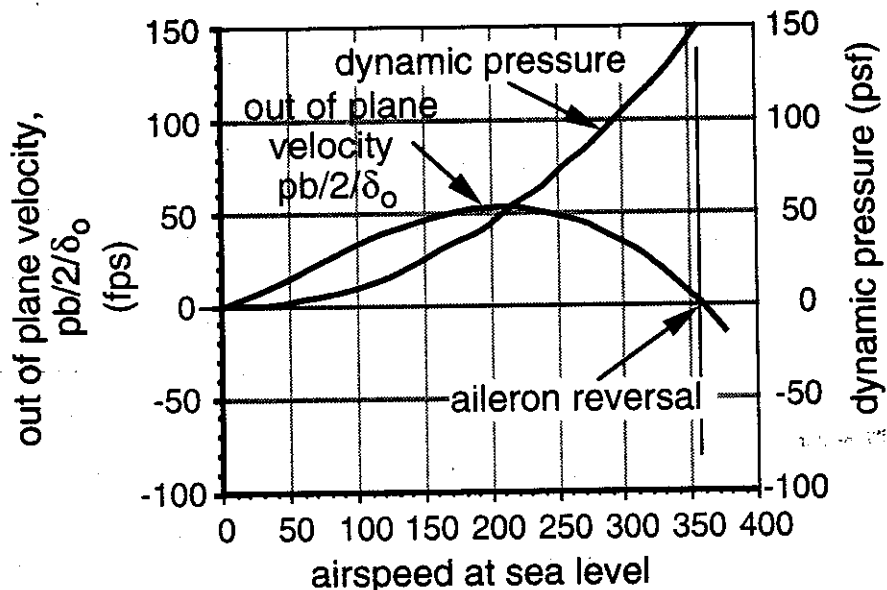


Figure 2.53 - Steady state "roll" effectiveness, $pb/2/\delta_o$ vs. airspeed, V

Figure 2.53 shows the results when Eqn. 2.172 is plotted for an airfoil with an aileron when $q_R = 150$ psf. As airspeed increases, steady-state roll rate (per unit aileron deflection) reaches a maximum and then declines, finally going to zero at the reversal airspeed. This occurs because this terminal roll rate depends on the ratio between rolling moment and damping in roll. Increased lift effectiveness due to a low divergence q also increases the damping in roll.

Swept wing static aeroelasticity

Sweeping a wing forward or backward changes its static aeroelastic characteristics, in particular the divergence speed and aileron reversal speed. When the wing is unswept, torsional deformation causes bending deformation, but the bending does not change the

aerodynamic loads and so it is uncoupled from the aeroelastic process. This is not the case when wing sweep is present, because bending and torsion displacement are aerodynamically coupled and aeroelastically interactive.

- There are three reasons for sweeping a wing forward or back.
- Trying to reduce the distance between the center of gravity and the aerodynamic center.
- Providing longitudinal and directional stability for tailless (flying) wings.
- Reducing high speed drag by delaying transonic drag rise (compressibility).

To understand why bending displacement produces aerodynamic forces, we will examine an aft swept wing planform shown in Figure 2.54. The chordwise lines labeled 1 (section CD) and 2 (section AB) are connected to each other (section BC) to form the letter "N" on the airfoil planform. Upward bending makes both lines move upward out of the plane of the paper. Line 1 will move upward less than line 2 since line 1 is located nearer the wing root. Line 2 has endpoints common to 1 and 2 so that line segment CB is inclined to the airstream because of bending.

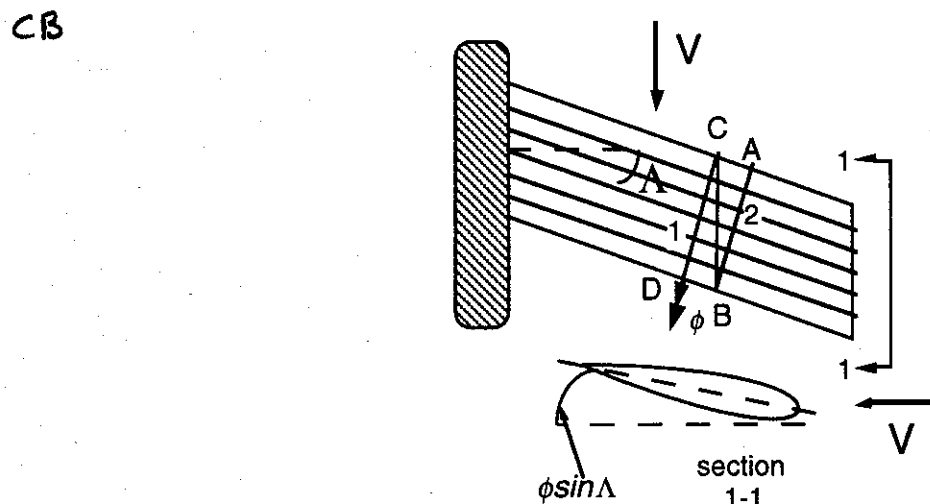


Figure 2.54 - Sweptback wing planform

Since point B lies on line 2, it will have a larger upward deformation than point C which lies on line 1. As a result, section BC has downward twist with respect to the airstream, as shown in the lower part of Figure 2.54. The slope of the wing bending along the swept axis is denoted as ϕ , positive in the direction shown in Figure 2.54.

We will later show that the streamwise inclination or angle of attack of line CB due to bending is $\alpha_{\text{streamwise}} = -\phi \sin \Lambda$, where the sweep angle is measured positive aft. As a

result, upward bending reduces the apparent angle of attack of a sweptback wing section, particularly those sections at the wing tip.

The opposite effect of wing bending occurs for a forward swept wing, as we can see from Figure 2.54 by simply reversing the velocity vector V . With upward bending of a swept forward wing, line BC has a nose-up incidence with respect to the flow. Remember, too, that twisting deformation along the swept axis must be added to these bending effects.

Swept wing strip theory aerodynamics

Two dimensional strip theory is an approximate method used to estimate the aerodynamic forces and moments distributed along a wing which has a moderate-to-high aspect ratio. This aerodynamic approximation assumes that the aerodynamic loads acting upon a spanwise section or wing strip with some chord dimension and an infinitesimal width are functions only of the angle of attack of that strip. Any interaction with aerodynamic loads on other parts of the surface is ignored. While this approximation becomes inaccurate if the wing aspect ratio is too small, it provides a convenient analytical tool for swept wing aeroelastic studies of the type we will consider.

Two different coordinate systems are used to develop expressions for the strip theory aerodynamic loads. The first coordinate system is a streamwise reference system with the x -axis parallel to the flow and the y -axis perpendicular to the airstream, as shown in Figure 2.55. The second system, also shown in Figure 2.55, is called the chordwise or "normal" axis system and is denoted by the axes \bar{x} , \bar{y} which are swept with respect to the flow and coincide with the wing structural layout.

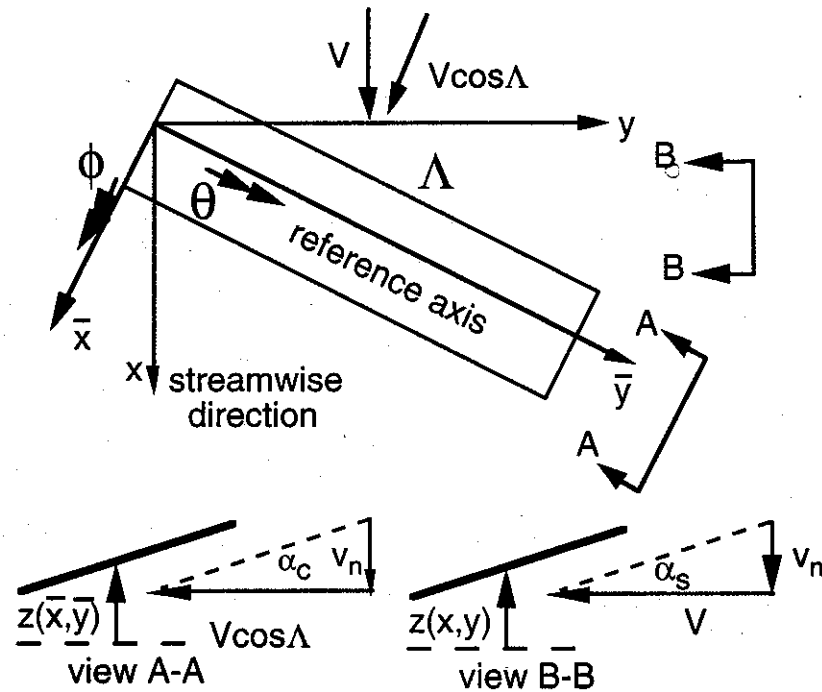


Figure 2.55 - Swept wing coordinate systems and downwash flow velocity

From an aerodynamic viewpoint, the streamwise reference system is more natural and, as a result, is used for modern aeroelastic analysis. However, since the structure is laid out along the swept or chordwise axis system, the chordwise reference system is more convenient for structural stiffness definition. The chordwise axis system is used for the discussion and illustrative examples in this text.

To understand the influence of bending on swept wing lift distribution look inboard along the y -axis in Figure 2.55 (view B-B). We see a local angle of attack, α_s , given by the expression

$$\alpha_s = -\left.\frac{\partial z}{\partial x}\right|_{EA} \quad (2.173)$$

where $z(x, y)$ represents the position of the deformed wing. This derivative is evaluated along the reference axis or "elastic axis."

The component of flow normal to the airfoil surface $z(x, y)$ is zero because the airstream must change direction and become tangent to the wing surface as it passes over the surface. From geometry in Figure 2.55 we see that, for the flow to be tangent to the wing, an airstream velocity component must appear. This local velocity component is called the downwash velocity and is defined as

$$v_n = V\alpha_s = -V\frac{\partial z}{\partial x} \quad (\text{small angle } \alpha)$$

The downwash velocity is unique and, no matter what coordinate system we use or what view we take, the downwash velocity v_n is invariant.

When the airfoil bends upward an amount $h(\bar{y})$ along the chordwise axis system reference axis and twists $\theta(\bar{y})$ about the same axis (positive nose-up) the wing surface deformation is approximated as follows

$$z = h(\bar{y}) - \bar{x}\theta(\bar{y}) \quad (2.174)$$

(this expression assumes that there is no camber bending of the wing section).

Equation 2.173 defines the angle of attack with respect to the flow direction, but Eqn. 2.174 defines the surface deflection with respect to the swept wing reference axis. To convert the angle of attack expression to flow in the swept reference axis system we must find the downwash velocity v_n in terms of the surface deflection $z(\bar{x}, \bar{y})$. To do this we transform coordinates from the swept system to the unswept system as follows.

$$\bar{y} = y\cos\Lambda + x\sin\Lambda \quad (2.175)$$

$$\bar{x} = -y\sin\Lambda + x\cos\Lambda \quad (2.176)$$

We use the chain rule for differentiation to find v_n as follows

$$v_n = -V \frac{\partial z}{\partial x} = -V \left[\frac{\partial \bar{y}}{\partial x} \frac{\partial z}{\partial \bar{y}} + \frac{\partial \bar{x}}{\partial x} \frac{\partial z}{\partial \bar{x}} \right] \quad (2.177)$$

From the coordinate transformation, Eqns. 2.175 and 2.176, we have

$$\frac{\partial \bar{y}}{\partial x} = \sin \Lambda \quad \text{and} \quad \frac{\partial \bar{x}}{\partial x} = \cos \Lambda$$

Differentiating the function $z(\bar{x}, \bar{y})$ we have

$$\frac{\partial z}{\partial \bar{y}} = \frac{\partial h}{\partial \bar{y}} - \bar{x} \frac{\partial \theta}{\partial \bar{y}} = h' - \bar{x} \theta' \quad (2.178)$$

and

$$\frac{\partial z}{\partial \bar{x}} = -\theta(y) \quad (2.179)$$

At any point on the reference axis (the line of shear centers or elastic axis) ($\bar{x} = 0$) the downwash velocity, v_n , is:

$$v_n = -V[h' \sin \Lambda - \theta \cos \Lambda] \quad (2.180)$$

As a result, we have

$$\alpha_s = \frac{v_n}{V} = \theta \cos \Lambda - h' \sin \Lambda \quad (2.181)$$

If we add the rigid angle of attack α_o input to the wing by the pilot to the angle of attack created by bending and twisting, we have

$$\alpha_s = \alpha_o + \theta \cos \Lambda - h' \sin \Lambda \quad (2.182)$$

The expression for the angle of attack, α_c , measured in the chordwise direction, is defined as:

$$\alpha_c = \frac{v_n}{V \cos \Lambda} = \theta - h' \tan \Lambda \quad (2.183)$$

and if we also add in the angle of attack α_o as before, we have

$$\alpha_c = \frac{v_n}{V \cos \Lambda} = \frac{\alpha_o}{\cos \Lambda} + \theta - h' \tan \Lambda \quad (2.184)$$

Notice that, while the downwash velocity v_n should not depend on the coordinate system, the reference velocity used to compute lift is changed from V to $V\cos\Lambda$ when we use a chordwise reference system to compute aerodynamic loads. This means that the effective dynamic pressure will have to be changed if we use the swept reference system.

Now that we have the effective angle of attack defined in the swept system so that we have the correct downwash velocity, we can develop an expression for the lift. Chordwise strip theory development assumes that the lift per unit span (sometimes called the "running lift") is given by the expression

$$l(\bar{y}) = \left(\frac{1}{2} \rho V_n^2 \right) c a_o \alpha_{eff} \quad (2.185)$$

where $V_n = V\cos\Lambda$ is the chordwise component of the airspeed, shown in Figure 2.55. The coefficient a_o is the sectional lift curve slope c_{l_a} while α_{eff} is the effective angle of attack of the section with respect to V_n , given in Eqn. 2.184.

The lift per unit span $l(\bar{y})$ along the swept elastic axis is then given by

$$l(\bar{y}) = (q \cos^2 \Lambda) (c a_o) \left(\frac{\alpha_o}{\cos \Lambda} + \theta - \frac{dh}{dy} \tan \Lambda \right) \quad (2.186)$$

The lift per unit length along the span is a function of twist angle and bending slope, as well as sweep angle. Notice also that, for sweepforward, Λ is negative so that wing bending deformation amplifies the aeroelastic angle of attack. These mathematical results are consistent with the previous discussion on the effect of wing bending and sweep on aerodynamic incidence.

One caution about the results in Eqn. 2.186 concerns their applicability to all sweep angles. At subsonic airspeeds, the lift is created by vortex development. Our recasting the problem in terms of downwash from a velocity component normal to the wing leading edge really assumes that the vortex created by the wing is shed parallel to the wing chord. This is only true if the sweep angle is zero and is approximately true for small sweep angles. It is very inaccurate for larger sweep angles, but still provides accurate trend information.

The semi-rigid swept wing model

To simplify our study of the static aeroelastic characteristics of swept wings, we will develop an idealization of a flexible swept lifting surface. This idealization is sometimes referred to as a semi-rigid swept wing because, although the airfoil surface is rigid from wing root to wing tip, it is elastically restrained at the wing root by two springs. This idealized section is shown in a planview in Figure 2.56.

The idealized swept wing is attached to a universal pin joint at the wing root that allows rotation about any axis, but is elastically restrained by two springs with constants K_1 and K_2 , as indicated in Figure 2.57. Because these springs are offset from the universal joint by distances f and d , respectively, they offer resistance to pitching rotation (θ) and bending rotation (ϕ). Views A-A and B-B in Figure 2.56 are shown in Figure 2.57 (a) and (b) to illustrate the chordwise (view A-A), spanwise (view B-B) views, respectively.

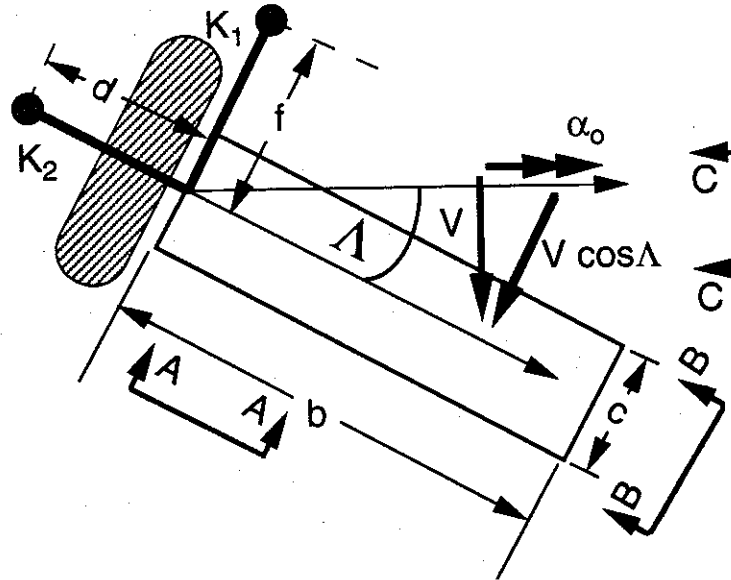


Figure 2.56 - Semi-rigid wing idealization.

The K_1 spring resists wing twist, θ , by developing a force $K_1 f \theta$ in the downward direction. This, in turn, causes a restoring twist of $(K_1 f \theta)f = K_1 f^2 \theta$. The product $K_1 f^2$ will be called K_θ in the development to follow, since it is associated with θ rotation. Similarly, ϕ rotation causes the K_2 spring to develop a force $K_2 d\phi$ in the upward direction. This force results in a restoring moment $(K_2 d\phi)d$ or $K_2 d^2 \phi$. The product $K_2 d^2$ is called K_ϕ in our development.

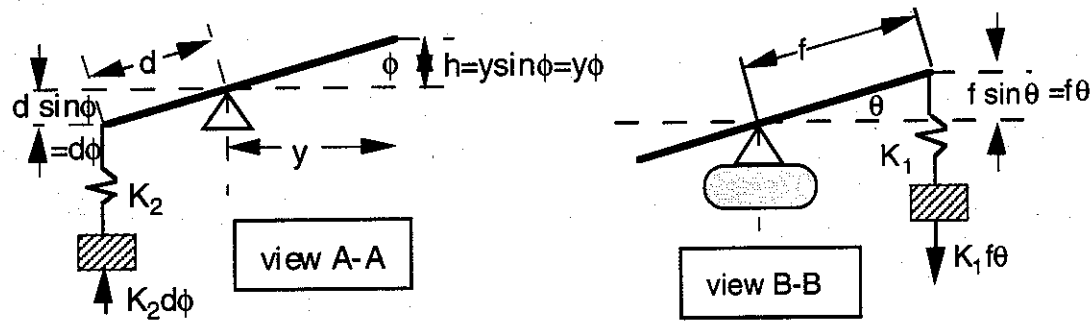


Figure 2.57 a,b - Spanwise and chordwise views of semi-rigid swept wing

The deflection of the swept \bar{y} -axis (representing the structural reference axis or elastic axis) is $h = \phi \bar{y}$ so that $\frac{dh}{d\bar{y}} = \phi$. The lift per unit length is defined in Equation 2.186. Since,

$h' = \phi$ then the lift distribution $l(\bar{y})$ is also constant along the swept wing span. Summing moments about the \bar{x} -axis (see view A-A in Figure 2.56), we find

$$K_\phi \phi = \int_0^b l \bar{y} d\bar{y} = q_n c a_o \frac{b^2}{2} \left(\frac{\alpha_o}{\cos \Lambda} + \theta - \phi \tan \Lambda \right) \quad (2.187)$$

Summing moments about the y -axis we find

$$K_\theta \theta = \int_0^b l e d\bar{y} = q_n c a_o e b \left(\frac{\alpha_o}{\cos \Lambda} + \theta - \phi \tan \Lambda \right) \quad (2.188)$$

where

$$q_n = \frac{1}{2} \rho V_n^2 = \frac{1}{2} \rho V^2 \cos^2 \Lambda = q \cos^2 \Lambda$$

We have two simultaneous equations with θ and ϕ as unknowns and α_o as the input. Before we can find the lift due to α_o we must first find ϕ , θ . Before proceeding, define the symbols Q , t and S as

$$Q = q_n c b a_o \quad t = \tan \Lambda \quad \text{and} \quad S = c b$$

We now introduce matrix notation to write the equilibrium equations given in Eqns. 2.187 and 2.188 as follows

$$\begin{bmatrix} K_\phi & 0 \\ 0 & K_\theta \end{bmatrix} \begin{Bmatrix} \phi \\ \theta \end{Bmatrix} = \frac{Q \alpha_o}{\cos \Lambda} \begin{Bmatrix} \frac{b}{2} \\ e \end{Bmatrix} + Q \begin{bmatrix} -tb & b/2 \\ 2 & e \end{bmatrix} \begin{Bmatrix} \phi \\ \theta \end{Bmatrix} \quad (2.189)$$

Notice that the structural stiffness matrix is uncoupled, i.e., it is diagonal. Re-writing Eqn. 2.189 we have

$$\left[\begin{bmatrix} K_\phi & 0 \\ 0 & K_\theta \end{bmatrix} - Q \begin{bmatrix} -tb & b \\ 2 & e \end{bmatrix} \right] \begin{Bmatrix} \phi \\ \theta \end{Bmatrix} = \frac{Q \alpha_o}{\cos \Lambda} \begin{Bmatrix} \frac{b}{2} \\ e \end{Bmatrix} \quad (2.190)$$

When the deflection dependent terms of the aerodynamic loads are taken from the right hand side of Eqn. 2.190 to the left side they become the aerodynamic stiffness matrix. Unlike the structural stiffness matrix, the aerodynamic stiffness matrix is not symmetric.

The system aeroelastic stiffness is the sum of structural and aerodynamic terms. Equation 2.190 is now written as:

$$\begin{bmatrix} (K_\phi + Qt\frac{b}{2}) & (-Q\frac{b}{2}) \\ (Qte) & (K_\theta - Qe) \end{bmatrix} \begin{Bmatrix} \phi \\ \theta \end{Bmatrix} = Q \frac{\alpha_o}{\cos \Lambda} \begin{Bmatrix} \frac{b}{2} \\ e \end{Bmatrix} \quad (2.191)$$

or

$$[\bar{K}] \begin{Bmatrix} \phi \\ \theta \end{Bmatrix} = \frac{Q\alpha_o}{\cos \Lambda} \begin{Bmatrix} \frac{b}{2} \\ e \end{Bmatrix} \quad (2.192)$$

The solution to Eqn. 2.192 ~~is~~ written as follows:

$$\begin{Bmatrix} \phi \\ \theta \end{Bmatrix} = \frac{Q\alpha_o}{\cos \Lambda} [\bar{K}]^{-1} \begin{Bmatrix} \frac{b}{2} \\ e \end{Bmatrix} = \frac{Q\alpha_o}{\cos \Lambda} \left(\frac{1}{\Delta} \begin{bmatrix} (K_\theta - Qe) & (Q\frac{b}{2}) \\ (-Qte) & (K_\phi + Qt\frac{b}{2}) \end{bmatrix} \right) \begin{Bmatrix} \frac{b}{2} \\ e \end{Bmatrix} \quad (2.193)$$

The solution for the bending slope and wing twist are found to be

$$\phi = \frac{Qb\alpha_o}{2\cos \Lambda} \left(\frac{K_\theta}{\Delta} \right) = \frac{Qb\alpha_o}{2\cos \Lambda} \left(\frac{1}{K_\theta + Q \left(\frac{b \tan \Lambda}{2} - \frac{K_\phi}{K_\theta} e \right)} \right) \quad (2.194)$$

and

$$\theta = \frac{Qe\alpha_o}{\cos \Lambda} \frac{K_\phi}{\Delta} = \frac{Qe\alpha_o}{\cos \Lambda} \left(\frac{1}{K_\theta + Q \left(\frac{K_\theta b \tan \Lambda}{2} - e \right)} \right) \quad (2.195)$$

When these expressions are substituted into the lift expression we have

$$L = qS\alpha_o \cos \Lambda \left(\frac{K_\theta K_\phi}{\Delta} \right) = qS\alpha_o \cos \Lambda \left(\frac{K_\theta K_\phi}{K_\theta K_\phi + Q \left(K_\theta \frac{b \tan \Lambda}{2} - K_\phi e \right)} \right) \quad (2.196)$$

From Eqns. 2.194-196 we see that the deformation and lift will grow without bound if we have the dynamic pressure such that

$$Q = \frac{K_\theta}{e - \left(\frac{K_\theta}{K_\phi} \right) \left(\frac{b}{2} \right) \tan \Lambda} \quad (2.197)$$

The determinant of $[\bar{K}]$ is computed to be

$$\Delta = |\bar{K}| = \left(K_\phi + \frac{Qbt}{2} \right) (K_\theta - Qe) + Q^2 \frac{bet}{2} \quad (2.198)$$

or

$$\Delta = K_\theta K_\phi + Q \left(K_\theta \frac{bt}{2} - K_\phi e \right) \quad (2.199)$$

When $\Delta = 0$ we will have the static aeroelastic divergence condition for the swept wing. Setting $\Delta = 0$ and solving for Q_D , we find that

$$Q_D = \frac{K_\phi K_\theta}{K_\phi e - K_\theta \frac{bt \tan \Lambda}{2}} = \frac{K_\theta}{e - \left(\frac{K_\theta}{K_\phi} \right) \left(\frac{b}{2} \right) \tan \Lambda} \quad (2.200)$$

Equation 2.200 is identical to Eqn. 2.197. The fact that the bending and twisting deformations will grow without bound if the angle of attack is not changed and that the system aeroelastic stiffness will disappear when this condition is reached is due to divergence of the wing. We can solve for the dynamic pressure to get

$$q_D = \frac{\frac{K_\theta}{Se a_o}}{\cos^2 \Lambda \left(1 - \left(\frac{b}{e} \right) \left(\frac{K_\theta}{K_\phi} \right) \frac{\tan \Lambda}{2} \right)} \quad (2.201)$$

As a check of this expression, we note that when $\Lambda = 0$ Eqn. 2.201 becomes $q_D = \frac{K_\theta}{Se a_o}$, which is identical to our previously derived unswept airfoil result if we set $a_o = C_{L_a}$.

If the parameters e and Λ are greater than zero, Eqn. 2.201 indicates that the divergence dynamic pressure will increase if the wing is swept backwards. If the denominator in Eqn. 2.201 is equal to zero, then q_D will be infinite.

If we set the denominator in Eqn. 2.201 to zero, we define a critical cross-over point at which the divergence dynamic pressure becomes infinite and then becomes negative, indicating that the wing will not diverge. Setting the denominator equal to zero gives us the following equation for the critical sweep angle, Λ_{crit} , at which the wing divergence dynamic pressure is infinite.

$$1 - \left(\frac{b}{e} \right) \left(\frac{K_\theta}{K_\phi} \right) \frac{\tan \Lambda_{crit}}{2} = 0 \quad (2.202)$$

We find that the wing sweep angle, Λ_{crit} , to cause q_D to be infinite is

$$\tan \Lambda_{crit} = 2 \left(\frac{e}{c} \right) \left(\frac{c}{b} \right) \left(\frac{K_\phi}{K_\theta} \right) \quad (2.203)$$

If we have a wing for which the sweep angle Λ is greater than Λ_{crit} , then $q_D < 0$ (V_D is imaginary).

Consider an example with the parameters

$$\frac{e}{c} = 0.1 \quad \frac{b}{c} = 6 \quad \frac{e}{b} = \frac{0.1}{6} \quad \frac{K_\phi}{K_\theta} = 3.$$

The solution to Eqn. 2.203 is

$$\tan \Lambda_{cr} = 0.1$$

so that

$$\Lambda_{cr} = 5.71^\circ$$

This means that, if this wing is swept back more than 5.71° aeroelastic divergence will not occur.

Equation 2.203 for the critical sweep angle depends on wing structural aspect ratio b/c and bending stiffness to torsional stiffness ratio K_ϕ/K_θ . Figure 2.58 shows the critical sweep angle plotted against stiffness ratio K_ϕ/K_θ for three different values of structural aspect ratio b/c .

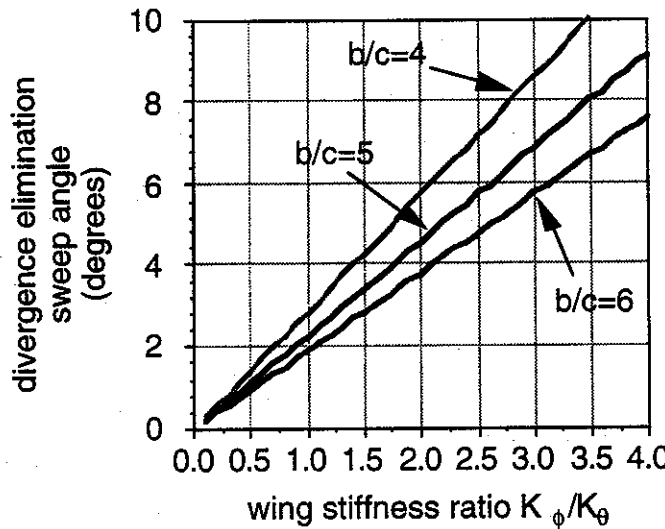


Figure 2.58 - Critical sweep angle for divergence vs. wing bending to torsion stiffness ratio

Figure 2.58 indicates that it is very unlikely that a wing with even a small amount of sweepback will diverge. While this is good news as far as stability is concerned, it creates other problems. The main difficulty with a very stable wing surface is that the lift effectiveness declines as static aeroelastic stability increases.

Lift effectiveness is defined as the lift produced by a flexible wing at an fixed angle of attack α_o divided by the lift produced by an identical, but rigid, wing at the same angle of attack. From Eqn. 2.196 we see that when there are no aeroelastic effects the lift is given by

$$L_{rigid} = qSa_o\alpha_o \cos \Lambda \quad (2.204)$$

As a result, the lift effectiveness is defined as

$$\text{lift effectiveness} \frac{L}{L_{rigid}} = \left(\frac{1}{1 + \frac{Q}{K_\theta K_\phi} \left(K_\theta \frac{b \tan \Lambda}{2} - K_\phi e \right)} \right) \quad (2.205)$$

The value of Q at divergence has been found previously to be $Q_D = \frac{K_\phi K_\theta}{K_\phi e - \frac{K_\theta b \tan \Lambda}{2}}$

so that the lift is now written as $L_{flex} = \frac{qSa_o\alpha_o \cos \Lambda}{1 - \frac{Q}{Q_D}}$. The lift effectiveness is

$$\text{lift effectiveness} = \frac{L_{flex}}{qSa_o\alpha_o \cos \Lambda} = \frac{1}{1 - \frac{q}{q_D}} \quad (2.206)$$

where

$$q_D = \frac{q_0}{\cos^2 \Lambda \left(1 - \left(\frac{b}{c} \right) \left(\frac{c}{e} \right) \left(\frac{K_\theta}{K_\phi} \right) \frac{\tan \Lambda}{2} \right)} \quad (2.207)$$

$$\text{and } q_o = \frac{K_\theta}{Sea_o}$$

To illustrate the effect of wing sweep on lift effectiveness, consider two swept back wings ($\Lambda = 15^\circ, 30^\circ$) with $\frac{b}{c} = 6, \frac{e}{c} = 0.1, \frac{K_\phi}{K_\theta} = 3$ and $q_o = 250 \text{ lb / ft}^2$. These results

are shown in Figure 2.59. From this figure we see that the lift from a flexible swept wing decreases as the wing is swept and as dynamic pressure increases. At half the divergence dynamic pressure of the unswept wing, the 30° swept wing is only about 30% that of the unswept wing. This means that the swept wing angle of attack must be larger than the unswept wing angle of attack if they generate the same amount of lift.

lift effectiveness of the

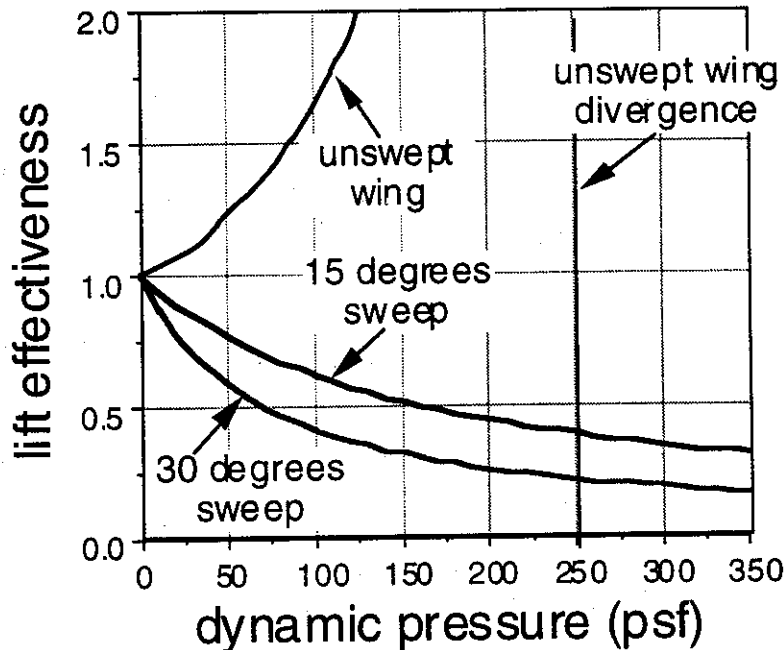


Figure 2.59 - The effect of wing sweep on lift effectiveness

Since only the denominator in Eqn. 2.207 is a function of Λ , if we minimize (or maximize) this denominator with respect to Λ we maximize (or minimize) the divergence dynamic pressure q_D . Define this denominator as D , written as

$$D = \cos^2 \Lambda - \left(\frac{b}{e} \right) \left(\frac{K_\theta}{K_\phi} \right) \frac{\tan \Lambda \cos^2 \Lambda}{2}$$

or

$$D = \cos^2 \Lambda - (b/e) \left(\frac{K_\theta}{K_\phi} \right) \frac{\sin \Lambda \cos \Lambda}{2} \quad (2.208)$$

Differentiating D with respect to the sweep angle, Λ , and setting the result to zero,

$$0 = \frac{\partial D}{\partial \Lambda} = -2 \sin \Lambda \cos \Lambda - (b/c)(c/e) \left(\frac{K_\theta}{K_\phi} \right) \left(\frac{\cos \Lambda \cos \Lambda - \sin \Lambda \sin \Lambda}{2} \right)$$

Re-arranging terms,

$$\frac{\partial D}{\partial \Lambda} = 0 = -\sin 2\Lambda - \left(\frac{b}{c} \right) \left(\frac{c}{e} \right) \left(\frac{K_\theta}{K_\phi} \right) \frac{\cos 2\Lambda}{2} \quad (2.209)$$

Finally, solving for Λ from Eqn. 2.209, we find that:

$$\frac{\sin 2\Lambda}{\cos 2\Lambda} = \tan 2\Lambda_{\max}^{\min} = -\frac{1}{2} \left(\frac{b}{c} \right) \left(\frac{c}{e} \right) \left(\frac{K_\theta}{K_\phi} \right) \quad (2.210)$$

Substituting the parameter values from our previous example ($b/e = 60$ $\frac{K_\phi}{K_\theta} = 3$) we have

$$\tan 2\Lambda_{\max}^{\min} = -10$$

This means that $2\Lambda_{\max}^{\min} = -84.3^\circ$ or 95.7° so that

$$\Lambda_{\max}^{\min} = -42.1^\circ \text{ and } 47.9^\circ$$

Note that if $\frac{K_\theta}{K_\phi} = \infty$ (total rigidity in bending), then $2\Lambda_{\max}^{\min} = -90^\circ$ or $+90^\circ$ and

$$\Lambda_{\max}^{\min} = \pm 45^\circ$$

From this example we see that decreasing the torsional flexibility causes Λ_{\min} to increase (become less negative) from -45° to some value close to zero. To understand how sweep changes the divergence dynamic pressure, the term \bar{q}_D is first defined as:

$$\bar{q}_D = \frac{q_D}{K_\theta / \text{Sea}_o} = \frac{q_D}{q_o} = \frac{1}{\cos^2 \Lambda - \left(\frac{b}{e} \right) \left(\frac{K_\theta}{K_\phi} \right) \frac{\sin \Lambda \cos \Lambda}{2}} \quad (2.211)$$

Substituting the example problem parameters into Eqn. 2.211, we have:

$$\bar{q}_D = \frac{1}{\cos^2 \Lambda - 5 \sin 2\Lambda} \quad (2.212)$$

A plot of \bar{q}_D versus Λ is shown in Figure 2.60. Notice the relatively low values of \bar{q}_D in the sweptforward region and the negative values of \bar{q}_D in most of the sweptback region. These negative values mean that the wing will not diverge.

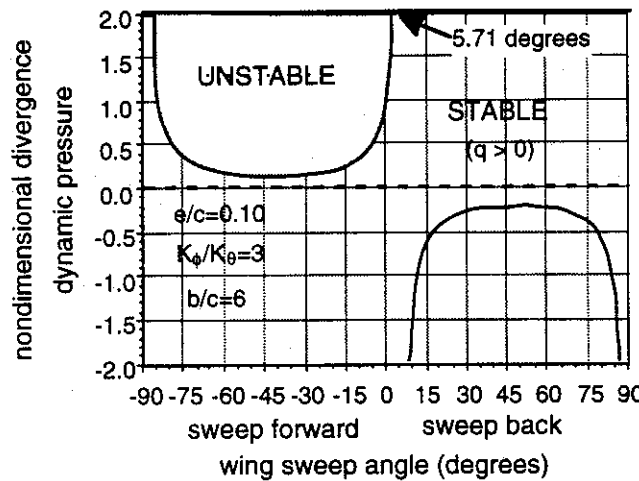


Figure 2.60 - Nondimensional divergence parameter \bar{q}_D , plotted against sweep angle Λ for semi-rigid wing example

Swept wing control effectiveness

Swept wing bending reduces aileron lift generation effectiveness. This section will show the reasons for this loss of effectiveness by using the semi-rigid swept wing model with a full span control surface as sketched in Figure 2.61. Without bending and twisting, the lift per unit length along the line of aerodynamic centers due to control surface deflection, δ_o , is

$$l(y) = (q \cos^2 \Lambda) c c_{l_\delta} \delta_o$$

and the pitching moment per unit length (positive nose-up) about the line of aerodynamic centers is

$$m_{ac} = (q \cos^2 \Lambda) c^2 c_{m_\delta} \delta_o$$

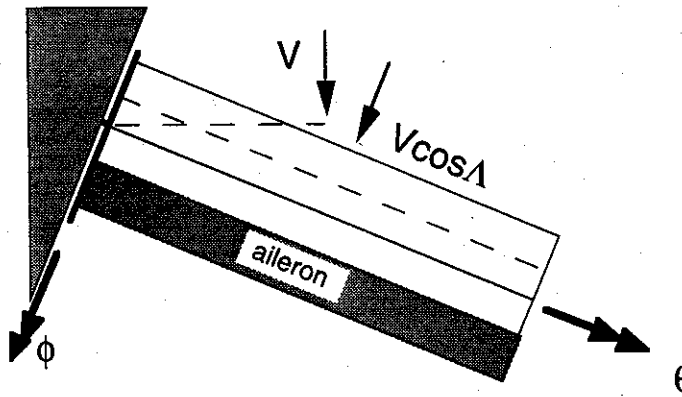


Figure 2.61 - Swept semi-rigid wing with full-span aileron

With bending and twisting deformation included, the lift per unit length, constant along the span, is

$$l(y) = (qc \cos^2 \Lambda) [c_{l\delta} \delta_o + a_o (\theta - \phi \tan \Lambda)] \quad (2.213a)$$

where $a_o = c_{l\alpha}$. The twisting moment per unit length along the wing span reference axis is

$$m_{y-axis} = (qecc \cos^2 \Lambda) [c_{l\delta} \delta_o + a_o (\theta - \phi \tan \Lambda)] + (q \cos^2 \Lambda) c^2 c_{m\delta} \delta_o \quad (2.213b)$$

Integrating Eqn. 2.213a along the wing span, the total wing lift due to the aileron deflection is given by the expression

$$L = q_n S a_o (\theta - \phi \tan \Lambda) + q_n S a_o \delta_o \quad (2.214)$$

When we sum moments about the wing root and the reference axis by integrating Eqns. 2.213a and b along the wing span, we obtain the following matrix equation of static equilibrium.

$$\begin{bmatrix} \bar{K}_{11} & \bar{K}_{12} \\ \bar{K}_{21} & \bar{K}_{22} \end{bmatrix} \begin{Bmatrix} \phi \\ \theta \end{Bmatrix} = q_n S e a_o \delta_o \begin{Bmatrix} \frac{c_{l\delta}}{a_o} \frac{b}{2e} \\ \frac{c_{l\delta}}{a_o} \left(1 + \frac{c c_{m\delta}}{e c_{l\delta}} \right) \end{Bmatrix} \quad (2.215)$$

where

$$\bar{K}_{11} = K_\phi + Q \frac{b \tan \Lambda}{2} \quad \bar{K}_{12} = -Q \frac{b}{2}$$

$$\bar{K}_{21} = Q e \tan \Lambda \quad \bar{K}_{22} = K_\theta - Q e$$

and

$$Q = q_n S a_o$$

We define the aerodynamic coefficient combinations in Eqn. 2.215 as

$$c_1 = \frac{c_{l\delta}}{a_o} \frac{b}{2e} \quad \text{and} \quad c_2 = \frac{c_{l\delta}}{a_o} \left(1 + \frac{c c_{m\delta}}{e c_{l\delta}} \right) \quad (2.216)$$

Inverting $[\bar{K}_{ij}]$ and pre-multiplying Eqn. 2.215 by $[\bar{K}_{ij}]^{-1}$ we find the bending and twisting deformations of the semi-rigid model to be

$$\phi = \frac{Q e \delta_o}{\Delta} (\bar{K}_{22} c_1 - \bar{K}_{12} c_2) \quad (2.217)$$

$$\theta = \frac{Q e \delta_o}{\Delta} (-\bar{K}_{21} c_1 + \bar{K}_{11} c_2) \quad (2.218)$$

where Δ is the determinant of the aeroelastic stiffness matrix, given previously in Eqn. 2.199. Combining Eqns. 2.214, 2.217 and 2.218 we find the lift due to the aileron to be

$$L = Q\delta_o \left(\frac{K_\phi Q e c_2 - K_\theta Q e c_1 \tan \Lambda + \frac{c_{l\delta}}{a_o} \Delta}{\Delta} \right) \quad (2.219)$$

Substitute the definition of Q into Eqn. 2.219 to get

$$L = \frac{q_n S c_{l\delta} \delta_o}{\Delta} K_\phi K_\theta \left(1 + q_n \frac{S a_o c c_{m\delta}}{K_\theta c_{l\delta}} \right)$$

δ_o measured with respect to swept axis.

and then substitute the expression for the determinant to get the following expression

$$L = \frac{q \cos^2 \Lambda S c_{l\delta} \delta_o}{1 + \frac{Q}{K_\theta K_\phi} \left(K_\theta \frac{b \tan \Lambda}{2} - K_\phi e \right)} \left(1 + \frac{q \cos^2 \Lambda S a_o c c_{m\delta}}{K_\theta c_{l\delta}} \right) \quad (2.220)$$

From Eqn. 2.200, $Q_D = \frac{K_\theta K_\phi}{K_\phi e - K_\theta \frac{b \tan \Lambda}{2}}$ so we can write Eqn. 2.220 as

$$L = \frac{q (\cos^2 \Lambda) S c_{l\delta} \delta_o}{1 - \frac{Q}{Q_D}} \left(1 + q \cos^2 \Lambda \frac{S a_o c c_{m\delta}}{K_\theta c_{l\delta}} \right) \quad (2.221)$$

If the wing were rigid, then the lift generated by the control input would be

$$L_{rigid} = (q S c_{l\delta} \cos^2 \Lambda) \delta_o \quad (2.222)$$

We define the aileron effectiveness for this swept wing model as the ratio L_{flex}/L_{rigid} .

Combining Eqns. 2.221 and 2.222, and recognizing that $\%/\!Q_D = q/q_D$ we find this measure of swept wing aileron effectiveness to be

$$\frac{L_{flex}}{L_{rigid}} = \frac{\left(1 + q \frac{S a_o c c_{m\delta}}{K_\theta c_{l\delta}} \cos^2 \Lambda \right)}{1 - \frac{q}{q_D}} \quad (2.223)$$

where q_D is given in Eqn. 2.201.

Aileron effectiveness will be zero when the numerator in Eqn. 2.223 is zero. This is the reversal condition and provides the equation for the swept wing reversal dynamic pressure, q_R .

$$q_R = -\frac{K_\theta C_{l\delta}}{S c a_o c_{m\delta} \cos^2 \Lambda} \quad (2.224)$$

The swept wing reversal expression in Eqn. 2.224 reduces to the unswept wing reversal result (Eqn. 2.164) when the sweep is zero and the sectional aerodynamic coefficients are replaced by their ~~wing~~ coefficient counterparts.

wing

If we define the reversal dynamic pressure at sweep angle zero as $q_{R_0} = -\frac{K_\theta C_{l\delta}}{S c a_o c_{m\delta}}$ then Eqn. 2.224 is written as

$$q_R = \frac{q_{R_0}}{\cos^2 \Lambda}$$

The semi-rigid swept wing model predicts that the reversal speed is the same for sweptforward and sweptback wings and that the bending stiffness K_ϕ does not affect the reversal dynamic pressure. On the other hand, since bending stiffness K_ϕ appears in q_D , the effectiveness of the aileron (as given in Eqn. 2.223) at speeds other than the reversal speed is a function of bending stiffness.

Equation 2.223 can also be written as

$$\frac{L_{flex}}{L_{rigid}} = \frac{1 - q_R}{1 - q_D} \quad (2.225)$$

with q_R given in Eqn. 2.224 and q_D given in Eqn. 2.201. We can write Eqn. 2.225 as

$$\frac{L_{flex}}{L_{rigid}} = \frac{1 - \left(\frac{q_R}{q_{R_0}}\right) \cos^2 \Lambda}{1 - \left(\frac{q_D}{q_{D_0}}\right) \left(1 - \frac{b}{c} \frac{e}{e} \frac{K_\theta}{K_\phi} \frac{\tan \Lambda}{2}\right) \cos^2 \Lambda} \quad (2.226)$$

$$q_{D_0} = \frac{K_\phi}{S c a_o}$$

Consider our example configuration with $b/c = 6$, $e/c = 0.1$ and $\frac{K_\phi}{K_\theta} = 3$. Additionally, we let $q_{R_0} = 150 \text{ lb / ft}^2$ and $q_{D_0} = 250 \text{ lb / ft}^2$. In this case, Eqn. 2.226 becomes

$$\frac{L_{flex}}{L_{rigid}} = \frac{1 - (q/150) \cos^2 \Lambda}{1 - (q/250)(\cos^2 \Lambda - 5 \sin 2\Lambda)} \quad (2.227)$$

Figure 2.62 shows the plot of aileron effectiveness for this example configuration and the sweep angles 0° , 15° , 30° , 45° . Mindful of the limitations of our model, we can conclude from this figure that sweepback reduces this measure of aileron effectiveness, but that the actual reversal speed is increased with increasing wing sweep angle.

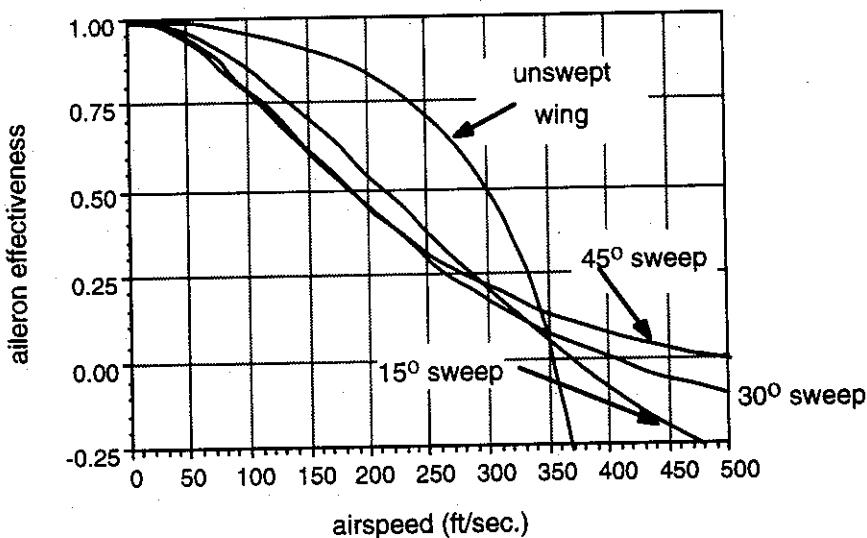


Figure 2.62 - Aileron (lift) effectiveness vs. airspeed for three sweep angles.

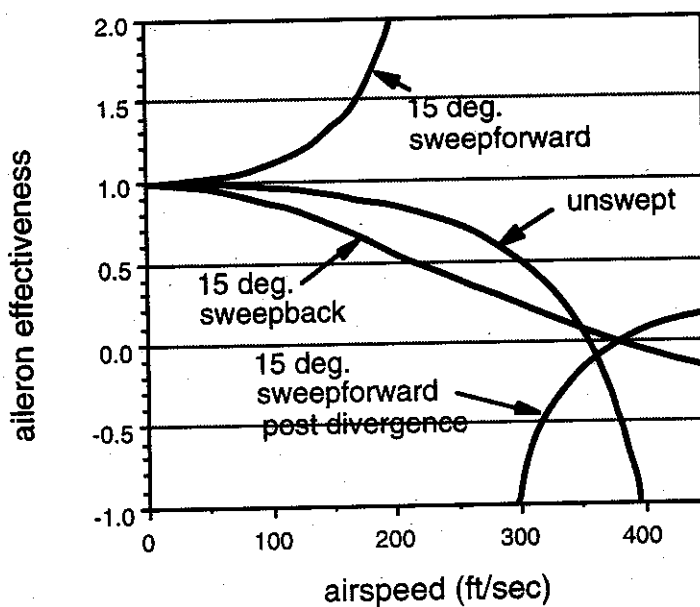


Figure 2.63 - The effect of forward sweep on aileron effectiveness

Figure 2.63 shows the lift effectiveness of a 15° forward swept wing vs. airspeed for our example configuration. This figure shows that the 15° forward swept wing and the 15° sweptback wing have the same reversal speed, but the reversal speed for the forward swept wing occurs in the unstable region.

Stiffness axis tailoring for static aeroelastic performance

Aeroelastic tailoring uses the strong directional stiffness features of advanced composites to couple together wing bending and twisting deformation. Because the laminates in the skin can be re-oriented or "tailored" to satisfy design stiffness requirements, we need to understand the interactions between bending stiffness, torsional stiffness and the orientation of major stiffness axes. The purpose of this section is to illustrate how this directional stiffness affects the divergence dynamic pressure of a swept wing with bending and torsional freedom.

The semi-rigid, swept wing model, similar to that drawn in Figure 2.56, is shown in Figure 2.64. The wing is mounted on a pivot to permit bending and torsion rotation, but the spring attachments are rotated at an angle γ with respect to the spanwise axis. This alignment is intended to simulate the off-axis orientation of a bi-directional laminate or off-axis orientation of internal stiffeners in the wing. This off-axis arrangement will couple together the elastic deformations ϕ and θ .

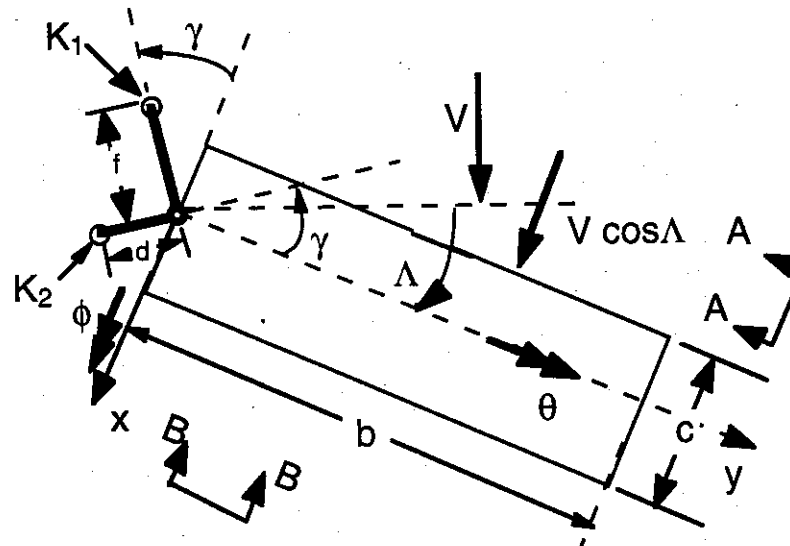


Figure 2.64 - Swept wing model with offset structural stiffness axis.

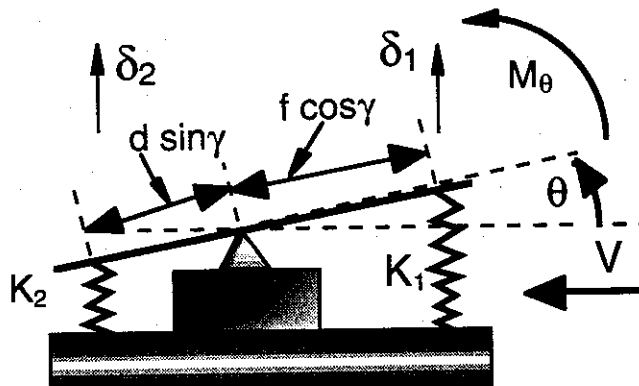
Deforming the wing about the x -axis an amount ϕ will cause compression of the two springs that restrain the wing root. This deformation is shown in Figures 2.65 a,b. Twisting the wing about the y -axis an amount θ will extend spring 1 and compress spring

2. From Figure 2.65 a,b we can conclude that the ϕ and θ rotations cause deformation of the springs that are computed to be

$$\delta_1 = +(f \cos \gamma) \theta - (f \sin \gamma) \phi \quad (2.228)$$

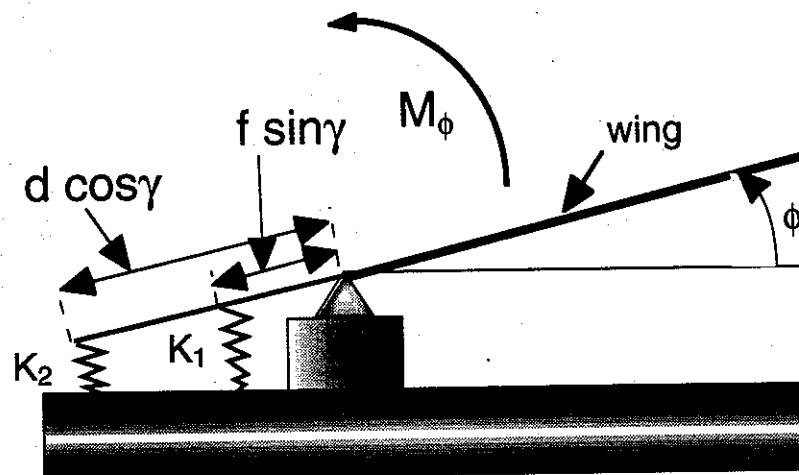
$$\delta_2 = -(d \sin \gamma) \theta - (d \cos \gamma) \phi \quad (2.229)$$

where δ_1 and δ_2 are deflections of the springs K_1 and K_2 respectively. These deflections are positive when the springs are stretched.



view A-A (looking inboard toward root)

Figure 2.65a - Chordwise view of spring deflections



view B-B (looking upstream, chordwise)

Figure 2.65b - Semi-rigid swept wing deflections, looking upstream

Deformations δ_1 and δ_2 create spring reaction forces. These forces create moments about the wing root x-y axes that resist applied aerodynamic moments. When external moments M_θ and M_ϕ are applied in the positive directions shown in Figure 2.65a,b, the

equations for static moment equilibrium about the chordwise axes at the root read as follows

$$\begin{aligned}\Sigma M_x = 0 &= M_\phi - [K_2 d^2 - K_1 f^2](\sin \gamma \cos \gamma) \theta \\ &\quad - [K_2 d^2 \cos^2 \gamma + K_1 f^2 \sin^2 \gamma] \phi\end{aligned}\quad (2.230)$$

$$\begin{aligned}\Sigma M_y = 0 &= M_\theta - [K_1 f^2 \cos^2 \gamma + K_2 d^2 \sin^2 \gamma] \theta \\ &\quad - [K_2 d^2 - K_1 f^2](\sin \gamma \cos \gamma) \phi\end{aligned}\quad (2.231)$$

We use the notation, $K_2 d^2 = K_\phi$ and $K_1 f^2 = K_\theta$ and write the matrix equilibrium equation as

$$[K_{ij}] \begin{Bmatrix} \phi \\ \theta \end{Bmatrix} = \begin{bmatrix} K_\phi \cos^2 \gamma + K_\theta \sin^2 \gamma & (K_\phi - K_\theta) \sin \gamma \cos \gamma \\ (K_\phi - K_\theta) \sin \gamma \cos \gamma & K_\phi \sin^2 \gamma + K_\theta \cos^2 \gamma \end{bmatrix} \begin{Bmatrix} \phi \\ \theta \end{Bmatrix} = \begin{Bmatrix} M_\phi \\ M_\theta \end{Bmatrix} \quad (2.232)$$

When $\gamma = 0$ this expression reduces to previous results and the stiffness matrix is uncoupled.

Swept wing flexural axis

Rotating the principal stiffness axis will change the divergence speed. The reason for this is that the position of a reference axis called the "flexural axis" is changed. The swept wing effective angle of attack $\theta_E = \theta - \phi \tan \Lambda$ determines the chordwise airloads in Eqn. 2.183. The flexural axis is the locus of points on the wing where we can apply an external load without increasing the local airload at the section where the load is applied.

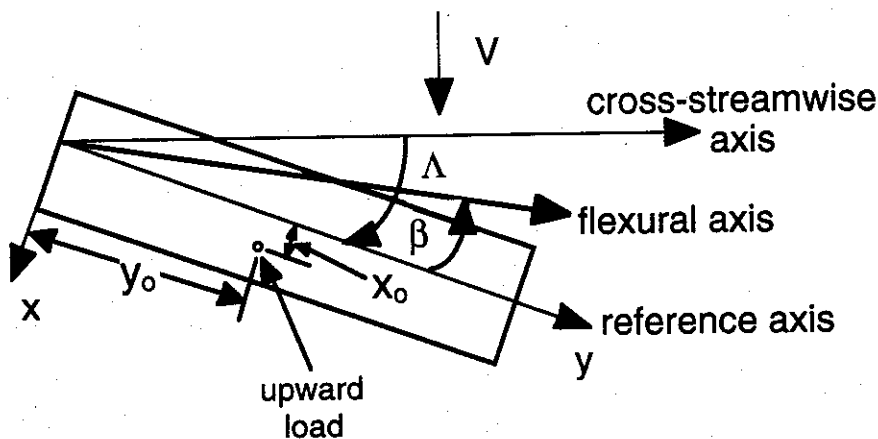


Figure 2.66 - Semi-rigid wing model with flexural axis geometry

The flexural axis for the semi-rigid wing is shown in Figure 2.66 as a line inclined at an angle β to the y -axis, the reference axis for the wing. The location of the flexural axis is important because if the airloads are applied downstream of the flexural axis they will tend to rotate the wing nose-down. In this case, called wash-out, divergence does not occur, but

the wing is ineffective in generating lift. If the flexural axis is downstream of the airloads application point the wing will rotate nose up (a situation called wash-in) and divergence can occur.

Consider the semi-rigid wing shown in Figure 2.66 with no airloads, but with an upward force P at point (x_o, y_o) in Figure 2.66. This upward force will create the following external moments.

$$\begin{aligned} M_\phi &= Py_o \\ M_\theta &= -Px_o \end{aligned} \quad (2.233)$$

The moment equilibrium relationship, Eqn. 2.232 is then written as

$$\begin{bmatrix} K_\phi \cos^2 \gamma + K_\theta \sin^2 \gamma & (K_\phi - K_\theta) \sin \gamma \cos \gamma \\ (K_\phi - K_\theta) \sin \gamma \cos \gamma & K_\theta \cos^2 \gamma + K_\phi \sin^2 \gamma \end{bmatrix} \begin{Bmatrix} \phi \\ \theta \end{Bmatrix} = \begin{Bmatrix} Py_o \\ -Px_o \end{Bmatrix} \quad (2.234)$$

The next step in locating the flexural axis coordinates is to find the displacements. We solve Eqn. 2.234 to find

$$\begin{Bmatrix} \phi \\ \theta \end{Bmatrix} = \frac{1}{\Delta} \begin{bmatrix} K_\theta \cos^2 \gamma + K_\phi \sin^2 \gamma & -(K_\phi - K_\theta) \sin \gamma \cos \gamma \\ -(K_\phi - K_\theta) \sin \gamma \cos \gamma & K_\phi \cos^2 \gamma + K_\theta \sin^2 \gamma \end{bmatrix} \begin{Bmatrix} Py_o \\ -Px_o \end{Bmatrix} \quad (2.235)$$

The stiffness matrix determinant Δ is computed to be

$$\begin{aligned} \Delta &= K_\phi K_\theta (\cos^4 \gamma + \sin^4 \gamma) + K_\theta^2 \cos^2 \gamma \sin^2 \gamma + K_\phi^2 \sin^2 \gamma \cos^2 \gamma \\ &\quad - (K_\phi^2 - 2K_\theta K_\phi + K_\theta^2) \sin^2 \gamma \cos^2 \gamma \end{aligned}$$

or

$$\Delta = K_\phi K_\theta \quad (2.236)$$

The determinant of the stiffness matrix is independent of the principal axis orientation.

The expressions for ϕ and θ reduce to the following:

$$\phi = \frac{P}{K_\phi K_\theta} [(K_\theta \cos^2 \gamma + K_\phi \sin^2 \gamma) y_o + (K_\phi - K_\theta) \sin \gamma \cos \gamma x_o] \quad (2.237a)$$

$$\theta = \frac{-P}{K_\phi K_\theta} [(K_\phi - K_\theta) \sin \gamma \cos \gamma y_o + (K_\phi \cos^2 \gamma + K_\theta \sin^2 \gamma) x_o] \quad (2.237b)$$

To find the flexural axis, set $\theta_E = \theta - \phi \tan \Lambda = 0$ and solve the resulting equation for x_o and y_o . This approach results in only one equation, written as

$$-y_o(K_\phi - K_\theta)\sin\gamma\cos\gamma - x_o(K_\phi \cos^2\gamma + K_\theta \sin^2\gamma) - (K_\theta \cos^2\gamma + K_\phi \sin^2\gamma)y_o \tan\Lambda - (K_\phi - K_\theta)\sin\gamma\cos\gamma x_o \tan\Lambda = 0 \quad (2.238)$$

Collecting terms common to x_o and y_o , we have

$$x_o[K_\phi \cos^2\gamma + K_\theta \sin^2\gamma + (K_\phi - K_\theta)\sin\gamma\cos\gamma \tan\Lambda]$$

$$+y_o[(K_\phi - K_\theta)\sin\gamma\cos\gamma + K_\theta \cos^2\gamma \tan\Lambda + K_\phi \sin^2\gamma \tan\Lambda] = 0$$

Since we have only one equation, we can solve only for the ratio $\frac{x_o}{y_o}$. Recalling that this ratio determines the flexural axis angle β in Figure 2.66 because $\tan\beta = -\frac{x_o}{y_o}$, we have

$$\frac{-x_o}{y_o} = \tan\beta = \frac{(K_\phi - K_\theta)\sin\gamma\cos\gamma + (K_\theta \cos^2\gamma + K_\phi \sin^2\gamma)\tan\Lambda}{K_\phi \cos^2\gamma + K_\theta \sin^2\gamma + (K_\phi - K_\theta)\sin\gamma\cos\gamma \tan\Lambda}$$

Now, define the parameter $R = \frac{K_\theta}{K_\phi}$ so that $\tan\beta$ is given as

$$\tan\beta = \frac{(1-R)\sin\gamma\cos\gamma + [1-(1-R)\cos^2\gamma]\tan\Lambda}{1-(1-R)\sin^2\gamma + (1-R)\sin\gamma\cos\gamma \tan\Lambda} \quad (2.239)$$

This equation reduces to the relationship $\tan\beta = R\tan\Lambda = \frac{K_\theta}{K_\phi}\tan\Lambda$ when $\gamma=0$.

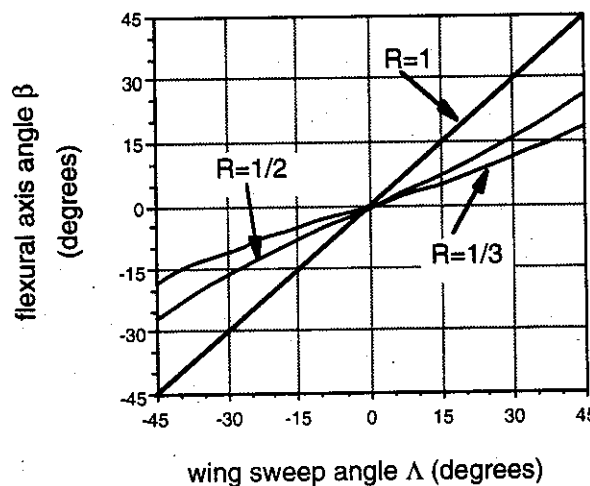


Figure 2.67 - Flexural axis angle β vs. wing sweep angle Λ for three values of relative stiffness R ($\gamma=0$).

As shown in Figure 2.67, when the stiffness axis orientation is $\gamma = 0$ and the ratio $R=1$, then $\beta = \Lambda$ and the flexural axis lies coincident with the unswept, cross-streamwise axis. When $R>1$ the flexural axis angle β is larger than the wing sweep angle Λ and the flexural axis angle lies ahead of the cross-streamwise axis. When $R<1$, which is the usual case, the flexural axis is less than Λ and the flexural axis lies behind the cross-streamwise axis.

The flexural axis position can be controlled by tailoring the position of the principal stiffness axis. A plot of β versus γ when the wing sweep is $\Lambda = -30^\circ, -15^\circ, 0^\circ, 15^\circ$, and 30° with $R = 1/3$ is shown in Figure 2.68.

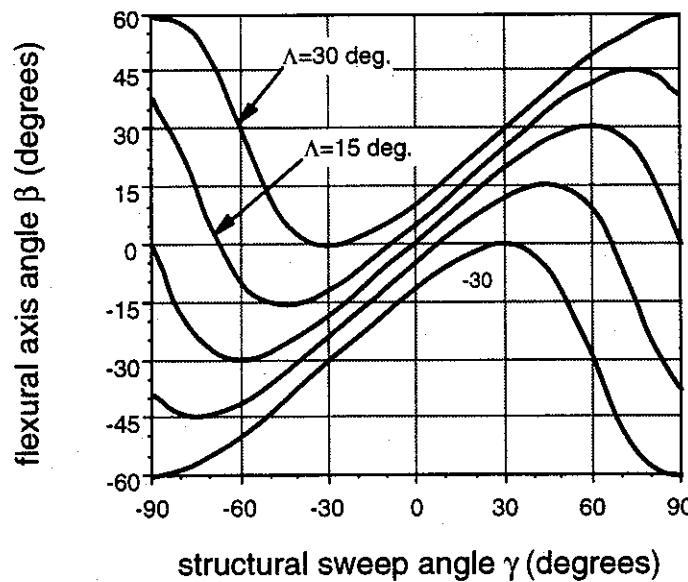


Figure 2.68 - Flexural axis orientation β vs. stiffness axis angle γ

Effect of structural axis orientation on wing divergence

To study how the structural axis orientation changes the wing divergence dynamic pressure, we must add aerodynamic loads to the wing aerodynamic stiffness matrix. The rotation of the principal structural axes in the wing does not affect the aerodynamic stiffness matrix elements that we developed previously. The aerodynamic matrix $[K_A]$ from Eqn. 2.190 is written as

$$[K_A] = \begin{bmatrix} -\frac{b}{2} \tan \Lambda & \frac{b}{2} \\ -e \tan \Lambda & e \end{bmatrix} q Sa_o \cos^2 \Lambda \quad (2.240)$$

Using this result, combining it with the structural stiffness matrix and defining $Q = q Sa_o \cos^2 \Lambda$ we can write the expression for the aeroelastic stiffness matrix $[\bar{K}_{ij}]$ as

$$[\bar{K}_{ij}] = \begin{bmatrix} K_\phi \cos^2 \gamma + K_\theta \sin^2 \gamma + \frac{b}{2} Q \tan \Lambda & (K_\phi - K_\theta) \sin \gamma \cos \gamma - Q \frac{b}{2} \\ (K_\phi - K_\theta) \sin \gamma \cos \gamma + Q e \tan \Lambda & K_\theta \cos^2 \gamma + K_\phi \sin^2 \gamma - Q e \end{bmatrix} \quad (2.241)$$

so that the static equilibrium equation becomes

$$[\bar{K}_{ij}] \begin{Bmatrix} \phi \\ \theta \end{Bmatrix} = \frac{Q \alpha_o}{\cos \Lambda} \begin{Bmatrix} b/2 \\ e \end{Bmatrix} \quad (2.242)$$

The divergence dynamic pressure is found by setting the determinant of $[\bar{K}_{ij}]$ equal to zero. This gives the following lengthy equation.

$$\begin{aligned} \Delta = |\bar{K}| &= (K_\phi \cos^2 \gamma + K_\theta \sin^2 \gamma)(K_\theta \cos^2 \gamma + K_\phi \sin^2 \gamma) - (K_\phi - K_\theta)^2 \sin^2 \gamma \cos^2 \gamma \\ &\quad - (K_\phi \cos^2 \gamma + K_\theta \sin^2 \gamma) Q e + (K_\theta \cos^2 \gamma + K_\phi \sin^2 \gamma) \left(\frac{b}{2} \right) Q \tan \Lambda \\ &\quad - \frac{b}{2} e Q^2 \tan \Lambda + (K_\phi - K_\theta) \sin \gamma \cos \gamma \left(Q \frac{b}{2} - Q e \tan \Lambda \right) + \frac{b}{2} e Q^2 \tan \Lambda = 0 \end{aligned}$$

Simplifying this equation, we get the following

$$K_\theta = Q e \left[\frac{(1-R)}{2} \sin 2\gamma \left(\tan \Lambda - \frac{b}{2e} \right) + \left(1 - \frac{Rb}{2e} \tan \Lambda \right) + (R-1) \left(1 + \frac{b}{2e} \tan \Lambda \right) \sin^2 \gamma \right] \quad (2.243)$$

Solving for Q and recalling that it is defined as $Q = q_n c b a_o = q S a_o \cos^2 \Lambda$ we find q_D to be

$$q_D = \frac{\frac{K_\theta}{S a_o}}{\cos^2 \Lambda \left[\frac{(1-R)}{2} \left(\tan \Lambda - \frac{b}{2e} \right) \sin 2\gamma + \left(1 - \frac{Rb}{2e} \tan \Lambda \right) + (R-1) \left(1 + \frac{b}{2e} \tan \Lambda \right) \sin^2 \gamma \right]} \quad (2.244)$$

To prevent divergence, we require that $q_D \leq 0$. This occurs when the denominator in Eqn. 2.244 is less than or equal to zero. If we treat sweep angle Λ as a design parameter and solve for the sweep angle Λ_{CR} necessary to make the denominator zero we find the following equation.

$$\frac{(1-R)}{2} \left(\tan \Lambda_{CR} - \frac{b}{2e} \right) \sin 2\gamma + \left(1 - \frac{Rb}{2e} \tan \Lambda_{CR} \right) + (R-1) \left(1 + \frac{b}{2e} \tan \Lambda_{CR} \right) \sin^2 \gamma = 0 \quad (2.245)$$

Solving for Λ_{CR} , the sweep angle above which we will not diverge, we have

$$\Lambda_{CR} = \tan^{-1} \left(\frac{\frac{1}{4e}(R-1)\sin 2\gamma + (R-1)\sin^2 \gamma}{\frac{Rb}{2e} + \frac{(R-1)}{2}\sin 2\gamma + \frac{b}{2e}(1-R)\sin^2 \gamma} \right) \quad (2.246)$$

A plot of Λ_{CR} as a function of γ with $\frac{b}{c} = 6$ with $e/c = 0.1$ and $e/c = 0.3$ is shown in Figure 2.69. This figure indicates that stiffness axes rotation will be able to eliminate wing divergence, even at fairly large forward sweep angles. The figure also shows that it is more difficult to prevent divergence when the offset between the reference axis and the aerodynamic centers (e) is large.

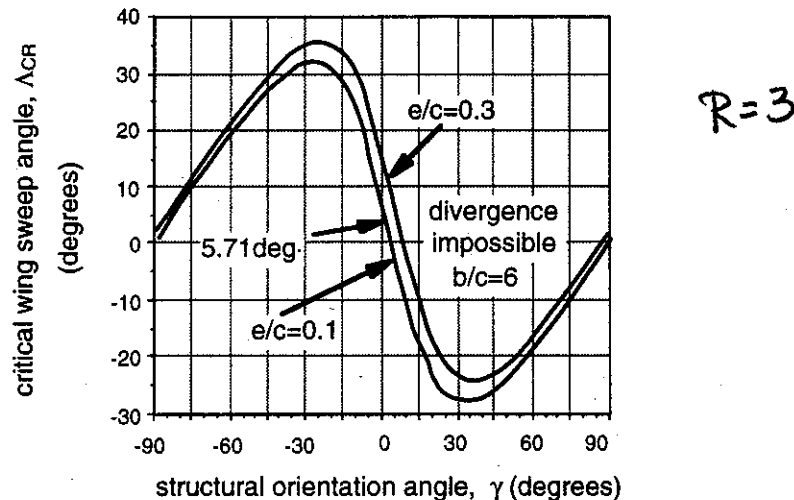
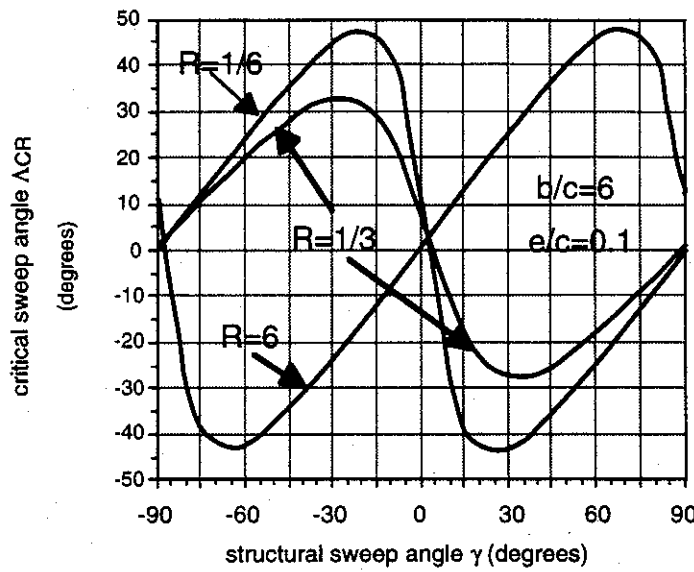


Figure 2.69 - Critical wing sweep angle for divergence vs. structural axis orientation

The effect of changing stiffness ratio, R , is shown in Figure 2.70 with $e/c=0.10$ and $b/c=6$. As wing principal bending stiffness is increased, the stiffness ratio R decreases, but the swept divergence speed should increase because of bending stiffening. This effect is seen as an increase in the critical sweep angle when the structural orientation angle is zero and R changes from $1/3$ to $1/6$.

On the other hand, when the bending stiffness is reduced, we find that the critical sweep angle is much larger because we ~~can't~~ use bending flexibility to reduce the airloads on the swept wing. When we ~~can't~~ change bending and torsional stiffness so that $R=6$, the maximum and minimum values of critical sweep angle are reversed. Reduced bending stiffness allows the wing to become less lift effective and to "dump" lift, thereby increasing the divergence dynamic pressure, all else being equal.

Figure 2.70 - Critical sweep angle Λ_{cr} vs. spring stiffness axis angle γ

To understand why there is a critical sweep angle for preventing divergence look at Figure 2.71. The spanwise center of pressure for this mathematical model is located as shown in the figure. The angle made by a line drawn from the origin of the x-y system to this center of pressure is shown as ψ in the figure. The angle ψ is given by the equation $\tan \psi = 2e/b$.

If the angle made by the flexural axis is greater than ψ then the aerodynamic load in the model will be aft of the flexural axis, meaning that aeroelastic loads will tend to rotate the wing nose down or wash-out the wing. This means that divergence cannot occur. If the flexural axis lies behind the center of pressure, the reverse is true and the wing will have a finite divergence speed. Thus, it is the control of the flexural axis position that controls divergence and it is the flexural axis control provided by stiffness tailoring that gives a designer control over divergence.

To see this, return to the simpler expression for the orthotropic wing flexural axis position. From Eqn. 2.239, when $\gamma = 0$, we have the simplified relation for the angle β

$$\tan \beta = R \tan \Lambda = \frac{K_\theta}{K_\phi} \tan \Lambda$$

When $\beta = \psi$ then

$$\tan \beta = \frac{K_\theta}{K_\phi} \tan \Lambda_{CR} = \tan \psi = \frac{2e}{b}$$

As a result, we can solve for Λ_{CR} without first solving for the divergence dynamic pressure. The same type of result will be apparent if we use the expression for $\tan \beta$ given in Eqn. 2.239.

For a real wing with additional degrees of freedom, the flexural axis will not be a straight line. However, the approach to controlling the divergence dynamic pressure will be the same. The key to this control is the ability to change the flexural axis position. If this control is not present, then aeroelastic tailoring will not be an option available to the designer.

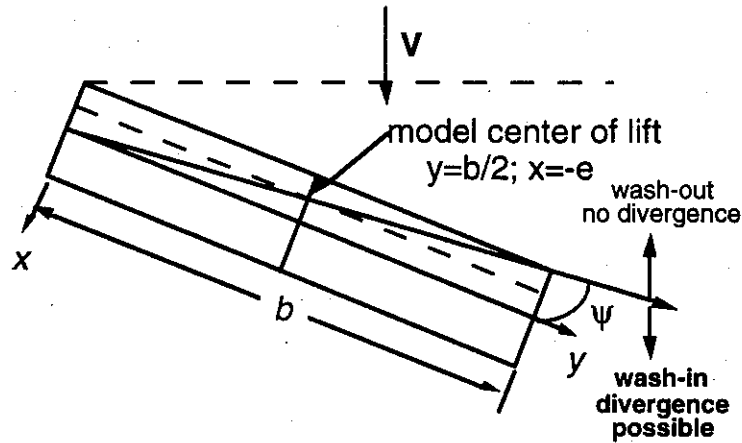


Figure 2.71 - Critical flexural axis angle to prevent wing divergence

Summary

This chapter has discussed the consequences of lifting surface flexibility. These consequences all stem from the fact that there will be an interaction between the loads and the deflection of the lifting surface. In the case of unswept wings, this interaction is confined to interaction between torsional deformation and the lift. For swept wings, this interaction is more complicated because bending introduces additional loads.

In both swept and unswept wings, the interaction is better understood by examining the concept of the flexural axis and the relationship in space between the wing center of lift and the flexural axis. If the center of lift is upstream of the flexural axis, then the aerodynamic loads will be amplified and divergence will occur at some airspeed, although this airspeed may be high. If the center of lift is downstream, then the aerodynamic loads will be attenuated and divergence will never be a problem.

The introduction of more representative aerodynamic loads and more representative structural models with additional degrees of freedom will change some of our results slightly. However, the basic conclusions about the effects of flexibility on the performance of swept and unswept wings will not change. We can consider the effects demonstrated in this chapter as "zeroth order" effects of static aeroelasticity to be modified in specific cases where we must include other effects such as wing taper, the variable distribution of bending and torsional stiffness and the effects of finite span aerodynamic load distributions at subsonic, compressible flight speeds and supersonic or even hypersonic speeds.

CHAPTER THREE

Vibration and Flutter

Structural deformation of an aircraft may occur as the result of steady, time-dependent loads or random loads - such as gusts. In every aircraft company there is an organization or group with a title such as Loads and Aeroelasticity or Dynamics and Loads. The purpose of such an organization is to define and predict the loads on the airplane structure - these loads and the stresses they cause must take structural flexibility into account.

Our purpose in this chapter is to investigate the consequences of time-dependent aeroelastic loads. These objectives will be accomplished in two steps. First of all, the subject of the dynamic response of idealized, multi-degree of freedom mechanical systems will be reviewed. Secondly, we will build upon this material by developing illustrative examples of dynamic aeroelastic response, in particular, flutter.

Vibration of Multi-degree of Freedom Systems

Chapter Two focused upon analytical idealizations with a finite number of degrees-of-freedom, as discussed in Chapter 2, the structural idealization of a real aircraft is usually done with a sophisticated finite-element model such as that shown in Figure 3.1, assembled by a sophisticated program such as NASTRAN. The mathematical form of the algebraic equations of motion is written as:

$$[M]\{\ddot{X}\} + [K]\{X\} = \{F(t)\} \quad (3.1)$$

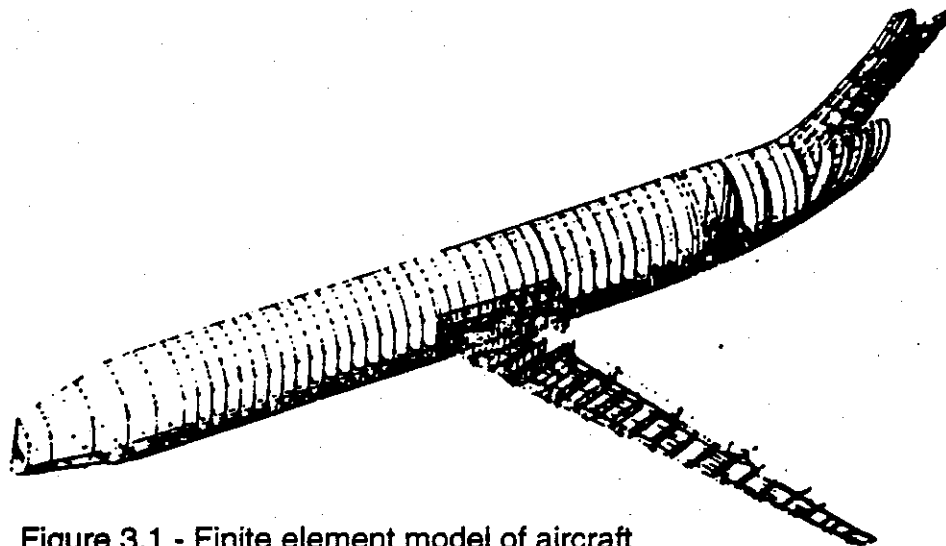


Figure 3.1 - Finite element model of aircraft

Equation 3.1 expresses a linearized relationship between the deformation variables - the system degrees of freedom - $X_i(t)$ and their time derivatives. The matrix $[M]$ is the mass or inertia matrix. The values of the elements M_{ij} are functions of the reference system one chooses to describe the state of the mechanical system.

If the matrix $[M]$ is diagonal, that is, $M_{ij} = 0$ when $i \neq j$, then the system equations are said to be inertially (or dynamically) uncoupled. If, on the other hand, the equations are dynamically coupled, then $M_{ij} \neq 0$. Dynamic coupling indicates that acceleration in one of the degrees of freedom will be accompanied by simultaneous motion in one or more additional freedoms.

The structural stiffness matrix, $[K]$ in Eqn. 3.1 contains elements whose values depend upon the arrangement of stiffness elements and the coordinate system used to describe deformation, including its origin. When the off-diagonal elements, $K_{ij}(i \neq j)$ are nonzero then the system is said to be statically (or elastically) coupled.

Steady and unsteady external loads will create a load vector $\{F(t)\}$. These loads include diverse sets of loads that occur during landing and take-off, towing the aircraft from the gate, climb and descent, maneuvering and penetration of gusts due to turbulence. An important special case of structural dynamic response is free vibration, when the external loads are zero and the vector $\{F(t)\}$ is a null vector, that is $\{F(t)\} = \{0\}$. In this case (called *in vacuo* vibration, or vibration in a vacuum) the only loads are internal, those created by structural deflection and inertial acceleration.

The mathematical development of the free vibration problem will introduce us to the concept of eigenvalues and eigenvectors that are, in reality, natural frequencies and mode shapes. An excellent discussion of these concepts is presented by Meirovitch in Chapter Four of *Elements of Vibration Analysis* (McGraw-Hill, 1975). What follows is a summary of ideas necessary to begin our aeroelastic analysis.

Example - A flexible model with two degrees of freedom .

The model shown in Figure 3.2 was considered at the beginning of Chapter 2 and has two degrees of freedom. The translation $h(t)$ measures the displacement of a reference

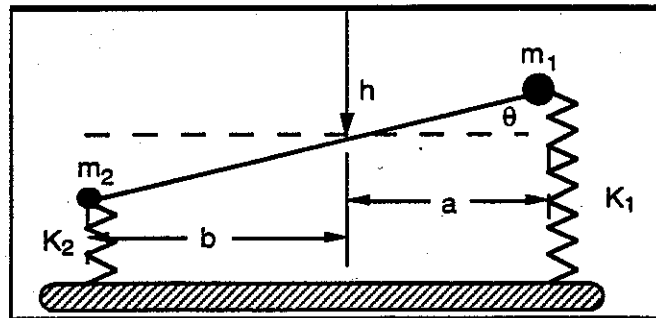


Figure 3.2 - Example configuration

point located on a massless bar with two lumped masses at either end. The second coordinate or degree of freedom, $\theta(t)$, measures the inclination of the massless bar with

respect to the horizontal. The bar is in static equilibrium when both coordinates are zero. The differential equations of motion for free vibration of the bar are written as follows:

$$(m_1 + m_2)\ddot{h} + (m_2 b - m_1 a)\ddot{\theta} + K_1(h - a\theta) + K_2(h + b\theta) = 0 \quad (3.2)$$

$$(m_2 b - m_1 a)\ddot{h} + (m_1 a^2 + m_2 b^2)\ddot{\theta} - K_1 a(h - a\theta) + K_2 b(h + b\theta) = 0 \quad (3.3)$$

These equations are written in matrix form as

$$[M_{ij}]\{\ddot{x}\} + [K_{ij}]\{x_j\} = \{0\}$$

where

$$\{x_j\} = \begin{Bmatrix} h \\ \theta \end{Bmatrix} \quad (3.4)$$

and

$$[M_{ij}] = \begin{bmatrix} (m_1 + m_2) & (-m_1 a + m_2 b) \\ (-m_1 a + m_2 b) & (m_1 a^2 + m_2 b^2) \end{bmatrix} \quad (3.5)$$

$$[K_{ij}] = \begin{bmatrix} (K_1 + K_2) & (-K_1 a + K_2 b) \\ (-K_1 a + K_2 b) & (K_1 a^2 + K_2 b^2) \end{bmatrix} \quad (3.6)$$

The mass matrix is symmetrical, as is the stiffness matrix. If $a = b$, $m_1 = m_2$ and $K_1 = K_2$, then the off-diagonal elements in the mass and stiffness matrices will be reduced to zero. This illustrates how the elements of the mass and stiffness matrix depend upon where the origin of the coordinates is chosen.

Free vibration is caused by initial deformation and initial velocity at an initial instant of time $t = 0$. The analysis problem then becomes one of solving for $\{x(t)\}$ given initial conditions $\{x(0)\}$ and $\{\dot{x}(0)\}$ and the matrices $[M]$ and $[K]$.

Consider the case where $m_1 = m_2 = m$, $b = a$, $K_1 = 2K$ and $K_2 = K$. In this case, the deflection coordinate $h(t)$ measures the displacement of the center of mass of the bar. The matrix equations for $[M]$ and $[K]$ are

$$[M_{ij}] = \begin{bmatrix} 2m & 0 \\ 0 & 2ma^2 \end{bmatrix}$$

and

$$[K_{ij}] = \begin{bmatrix} 3K & -Ka \\ -Ka & 3Ka^2 \end{bmatrix}$$

We will restrain the free motion of this system so that $h(t) = \theta(t)a$. We can do this by inputting the proper set of initial conditions, as will be shown later. We substitute this constraint relationship into the equations of motion. Equation 3.2 becomes

$$2m\ddot{h} + K(2h) = 0$$

while Eqn. 3.3 becomes

$$2ma^2\ddot{\theta} + 2Ka^2\theta = 0$$

Dividing by $2m$ and $2ma^2$, respectively, the two equations of motion become

$$\ddot{h} + \frac{K}{m}h = 0$$

and

$$\ddot{\theta} + \frac{K}{m}\theta = 0$$

These two simultaneous equations have the identical form, even though one is for translation and the other is for rotation. They both are equations for a single degree of freedom harmonic oscillator with natural frequency $\omega = \sqrt{K/m}$.

If we were to give the system an initial displacement of θ radians and an h displacement of $h = \theta a$ (this would be an downward displacement in our coordinate system) then the system would oscillate at the frequency $\omega = \sqrt{K/m}$ and the "shape" of the oscillation would always be the same.

The shape $h = \theta a$ is called a natural mode of vibration for the system that will occur naturally under the proper set of initial conditions, and the frequency $\omega = \sqrt{K/m}$ is a natural frequency of the system. There is a second natural frequency, $\omega = \sqrt{2K/m}$ that occurs if we restrain the system to vibrate with the shape $h = -\theta a$.

Synchronous motion

When all external loads are removed the general form of Eqn. 3.1 is

$$[M]\{\ddot{x}\} + [K]\{x\} = \{0\} \quad (3.7)$$

Equation 3.7 represents a set of n simultaneous, coupled, differential equations. These equations are homogeneous (the right-hand side of Eqn. 3.7 is zero). If there are n degrees of freedom, then the vector $\{x\}$ is composed of n elements. $[M]$ and $[K]$ are $n \times n$ square matrices.

Synchronous motion occurs when each of the n degrees of freedom $x_i(t)$ has the same time dependence but can have a different amplitude. Motion for which $x_1(t) = 60t$ and $x_2(t) = 2t^2$ is, for example, is not synchronous. Free vibration is a type of synchronous motion where the ratio between any two displacement coordinates is a constant. This means that the time-dependent displacement can be written as:

$$\{x(t)\} = \{u_i\}f(t) \quad (3.8)$$

where u_i represents a constant (non-time-dependent) amplitude coefficient, associated with degree of freedom $x_i(t)$, while $f(t)$ is a function of time. This function must be determined when we analyze free vibration.

Our objective is to determine $f(t)$. Let us now substitute the expression in Eqn. 3.8 into Eqn. 3.7. The result is

$$\ddot{f}[M]\{u\} + f[K]\{u\} = 0 \quad (3.9)$$

where the notation (\cdot) refers to differentiation with respect to time, t . Let us now arbitrarily multiply Eqn. 3.9 by the same vector $\{u\}^T$ that appears in Eqn. 3.8 so that a scalar equation is created. The result becomes:

$$\ddot{f}\{u_i\}^T[M_{ij}]\{u_j\} + f\{u_i\}^T[K_{ij}]\{u_j\} = 0 \quad (3.10)$$

When $[M]$ and $[K]$ are composed only of real numbers the relationship in Eqn. 3.10 can be written as:

$$\ddot{f}a + fb = 0 \quad (3.11)$$

Where a and b are real numbers that represent the two triple matrix products that appear in Eqn. 3.10.

From Eqn. 3.11,

$$\frac{\ddot{f}}{f} = \frac{-b}{a} \quad (3.12)$$

The right-hand side of Eqn. 3.12 does not depend upon time so the ratio on the left-hand side cannot be a function of time either. Let us write the ratio b/a as a constant, $\lambda^2 = b/a$ so that Eqn. 3.12 is written as

$$\ddot{f} + \lambda^2 f = 0 \quad (3.13)$$

Equation 3.13 is a second-order, ordinary differential equation with constant coefficients; the solution to this equation is

$$f(t) = Ae^{st} \quad (3.14)$$

Substituting Eqn. 3.14 into Eqn. 3.13 we get:

$$(s^2 + \lambda^2)Ae^{st} = 0 \quad (3.15)$$

From the characteristic equation in Eqn. 3.15, we find the solution for s to be

$$s = \pm\sqrt{-\lambda^2} \quad (3.16)$$

Since a and b in Eqn. 3.11 are real, λ^2 is a real number, but we have not determined if it is positive or negative. If λ^2 is negative, the two solutions for s are real numbers, equal in magnitude, but opposite in sign. In this case,

$$f(t) = A_1 e^{ct} + A_2 e^{-ct} \quad (3.17)$$

where $c = +\sqrt{|\lambda^2|}$.

From Eqn. 3.17 we see that the time response of our system to an initial disturbance consists of two parts. One part decays exponentially with time while the other grows exponentially.

Our primary interest is vibration of mechanical systems for which the $[K_{ij}]$ matrix is due to structural restoring forces that are conservative. By conservative we mean that, when we load such a system, it moves and we store energy; when we unload the system, an equal amount of energy is released. As a result, a solution such as Eqn. 3.17 is not acceptable since a small disturbance would grow as time increased and would need energy to feed it. No such energy source is present here. The existence of a solution such as Eqn. 3.17 would also indicate that the system is unstable.

The only other possibility left for the solution to Eqn. 3.15 is that the ratio λ^2 is real and positive. This is the case if $[M]$ and $[K]$ are both positive definite matrices. In this case,

$$s = \pm i\lambda \quad (i = \sqrt{-1}) \quad (3.18)$$

so that

$$f(t) = A_1 e^{i\lambda t} + A_2 e^{-i\lambda t} \quad (3.19)$$

Since $f(t)$ must be a real function of time, A_1 and A_2 must be complex so that Eqn. 3.19 can be written either as :

$$f(t) = C_1 \sin \lambda t + C_2 \cos \lambda t \quad (3.20)$$

or in an alternative form,

$$f(t) = C \cos(\lambda t - \beta) \quad (3.21)$$

In Eqn. 3.21 the arbitrary constants C and β have replaced the constants C_1 and C_2 appearing in Eqn. 3.20.

Let's examine Eqns. 3.20 and 3.21. This solution is harmonic (composed of sine and cosine functions) with frequency λ (radians per unit time), although the magnitude of λ is not yet known. The amplitude of $f(t)$ is

$$C = \sqrt{C_1^2 + C_2^2} \quad (3.22)$$

Two initial conditions (boundary conditions at $t = 0$ are necessary to determine C_1 and C_2 (or C and β). Thus, we conclude that, if motion of the freely vibrating energy conservative system is synchronous, it must be harmonic. The frequency at which the motion occurs and the elements of the vector $\{u_i\}$ are still unknown.

Characteristic equation for free vibration

Let's change our notation for oscillation frequency (in radians/sec) from λ to the more usual notation, ω , so that

$$\omega = \lambda$$

Remembering that $\ddot{f} = -\omega^2 f$ (from Eqn. 3.12) we write Eqn. 3.9 as

$$f[-\omega^2[M] + [K]]\{u\} = \{0\} \quad (3.23)$$

Since $f(t)$ cannot be zero at all instants of time, the following condition must be true when synchronous motion occurs for a conservative system.

$$[-\omega^2[M] + [K]]\{u\} = \{0\} \quad (3.24)$$

Eqn. 3.24 is the eigenvalue problem associated with the matrices $[M]$ and $[K]$.

Since the right-hand side of Eqn. 3.24 is zero (the equation is homogeneous), one obvious solution to this equation is to make $\{u\}$ identically zero. The problem with this choice is that if the elements of $\{u_i\}$ were all zero then there would be no motion. Certainly one or more of the elements of $\{u_i\}$ must be nonzero. To guarantee such a situation (a nontrivial solution for $\{u_i\}$) linear algebra theory requires vanishing of the determinant

$$\Delta = |-\omega^2[M] + [K]| = 0 \quad (3.25)$$

The elements of $[M]$ and $[K]$ are known while ω^2 is unknown. The determinant Δ is called the characteristic equation or frequency equation for $[M_{ij}]$ and $[K_{ij}]$.

Expansion of the characteristic equation given in Eqn. 3.25 yields an n th order polynomial (the $[M]$ and $[K]$ matrices are $n \times n$) with ω^2 as the independent variable. The roots ω^2 of this n th order polynomial are called characteristic values or eigenvalues. There are n values of ω^2 and n values of ω ; both ω^2 and ω are positive (we ignore the negative square roots $-\omega$ because they are already accounted for in the solution).

Example - Natural frequencies

The matrix equilibrium equations (Eqns. 3.5 and 3.6 with $m_1 = m_2 = m$, $b = a$, $K_1 = 2K$ and $K_2 = K$) of the example system is

$$\left[-\omega^2 \begin{bmatrix} 2m & 0 \\ 0 & 2ma^2 \end{bmatrix} + \begin{bmatrix} 3K & -Ka \\ -Ka & 3Ka^2 \end{bmatrix} \right] \begin{Bmatrix} h \\ \theta \end{Bmatrix} = \begin{Bmatrix} 0 \\ 0 \end{Bmatrix}$$

The determinant of this matrix is

$$\Delta = m^2 \left[\left(-2\omega^2 + 3\frac{K}{m} \right) \left(-2a^2\omega^2 + 3\frac{K}{m}a^2 \right) - a^2 \left(\frac{K}{m} \right)^2 \right]$$

Expanding terms, the frequency equation becomes,

$$\omega^4 - 3\frac{K}{m}\omega^2 + 2\left(\frac{K}{m}\right)^2 = 0$$

This equation has two solutions, the two natural frequencies of the system. These frequencies are:

$$\omega_1 = \sqrt{\frac{K}{m}} \quad \text{and} \quad \omega_2 = \sqrt{\frac{2K}{m}}$$

These two frequencies are identical to those found before when the motion was restrained.

Free vibration mode shapes

The free vibration of a stable conservative mechanical system is synchronous. The time response is harmonic (sinusoidally periodic) with frequency ω . The frequency ω is computed from the characteristic equation constructed from Eqn. 3.25. For a conservative system all values of ω will be greater than zero.

Once the natural frequencies, ω_i , are known, only the elements of $\{u_i\}$ remain to be determined. Let us take one of the known frequencies, ω_j , and insert it into Eqn. 3.24. The result is

$$[-\omega_j^2[M] + [K]]\{u_i\} = \{0\} \quad (3.26)$$

In Eqn. 3.26, there are n equations in n unknowns (the n elements of $\{u_i\}$). Unfortunately one of the n equations defined in Eqn. 3.26 is not independent of the remaining $n-1$ equations.

The determinant of a matrix is zero only if one or more rows (or columns) are linear combinations of other rows (or columns). When we forced Δ to be zero when $\omega = \omega_j$ we eliminated the independence of one of the equations in Eqn. 3.26. This means that Eqn. 3.26 actually represents $n - 1$ independent equations for n unknowns, so we are one equation short.

We can solve for $n - 1$ values of the vector $\{u_i\}$ in terms of, for instance, the value of the element such as u_2 . Thus, the relative amplitudes of the motion can be determined, but the absolute amplitude of the motion cannot be determined from the eigenvalue/eigenvector equations until initial conditions are considered. The shape (or ratio of values u_i / u_j ($i \neq j$)) of the eigenvector is unique, but the amplitude (the actual value of u_i) is not, since if $\{u_i\}$ is a solution to Eqn. 3.26, then any multiple of $\{u_i\}$ (for instance, 10 $\{u_i\}$ or $-52.6 \{u_i\}$) is also a solution.

Since there are n values of frequencies ω_i , there also will be n corresponding values of the displacement vector (eigenvector or characteristic vector). These eigenvectors are referred to as "natural modes" and are also called normal modes or simply mode shapes..

Example - Mode shapes

When $\omega = \omega_1 = \sqrt{\frac{K}{m}}$ then the matrix equations of equilibrium for our example discussed previously become

$$\left[-\frac{K}{m} \begin{bmatrix} 2m & 0 \\ 0 & 2ma^2 \end{bmatrix} + \begin{bmatrix} 3K & -Ka \\ -Ka & 3Ka^2 \end{bmatrix} \right] \begin{Bmatrix} h \\ \theta \end{Bmatrix} = \begin{Bmatrix} 0 \\ 0 \end{Bmatrix}$$

or

$$\begin{bmatrix} K & -Ka \\ -Ka & Ka^2 \end{bmatrix} \begin{Bmatrix} h \\ \theta \end{Bmatrix} = \begin{Bmatrix} 0 \\ 0 \end{Bmatrix}$$

Both rows of this matrix equation are identical (row 2 is $-a$ times row 1), as predicted by linear algebra. Using the first row, we have

$$Kh - Ka\theta = 0$$

If we arbitrarily let $h = 1$ then we have $\theta = \frac{h}{a} = \frac{1}{a}$ so that the mode shape becomes

$$\{u^{(1)}\} = C_1 \begin{Bmatrix} 1 \\ 1/a \end{Bmatrix}$$

When we repeat this process for the second frequency ($\omega = \omega_2 = \sqrt{\frac{2K}{m}}$) we get the second mode shape

$$\{u^{(2)}\} = C_2 \begin{Bmatrix} 1 \\ -1/a \end{Bmatrix}$$

Note that C_1 and C_2 are amplitude constants whose value is arbitrary unless we know the initial conditions.

Mode Shape Orthogonality

The computed mode shapes have a valuable feature known as modal orthogonality. Consider two different mode shapes; call one of these mode shapes $\{u^{(j)}\}$ and the other $\{u^{(k)}\}$. Equation 3.24 can be written, for $\{u^{(j)}\}$ and ω_j , as

$$[-\omega_j^2[M] + [K]]\{u^{(j)}\} = \{0\} \quad (3.27)$$

Pre-multiply Eqn. 3.27 by $\{u^{(k)}\}^T$ (not $\{u^{(j)}\}$). The result is a scalar equation:

$$-\omega_j^2\{u^{(k)}\}^T[M]\{u^{(j)}\} + \{u^{(k)}\}^T[K]\{u^{(j)}\} = 0 \quad (3.28)$$

Now, repeat the procedure, but interchange the vectors $\{u^{(j)}\}$ and $\{u^{(k)}\}$ and frequencies ω_j and ω_k . This second operation yields:

$$-\omega_k^2\{u^{(j)}\}^T[M]\{u^{(k)}\} + \{u^{(j)}\}^T[K]\{u^{(k)}\} = 0 \quad (3.29)$$

If, as is the usual case, $[M]$ and $[K]$ are symmetric, $[M]^T = [M]$ and $[K]^T = [K]$. Take the transpose of Eqn. 3.29 so that:

$$-\omega_k^2\{u^{(k)}\}^T[M]\{u^{(j)}\} + \{u^{(k)}\}^T[K]\{u^{(j)}\} = 0 \quad (3.30)$$

Now, subtract Eqn. 3.30 from Eqn. 3.28 to obtain the result:

$$(\omega_k^2 - \omega_j^2)\{u^{(k)}\}^T[M]\{u^{(j)}\} = 0 \quad (j \neq k) \quad (3.31)$$

If $\omega_j^2 \neq \omega_k^2$ then the following must be true.

$$\{u^{(k)}\}^T[M]\{u^{(j)}\} = 0 \quad (j \neq k) \quad (3.32)$$

Because of the relationship in Eqn. 3.32, the eigenvectors $\{u^{(j)}\}$ and $\{u^{(k)}\}$ are said to be orthogonal with respect to the mass matrix $[M]$.

Using Eqn. 3.30 and Eqn. 3.28 we can also show that the eigenvectors or mode shapes are also orthogonal with respect to the stiffness matrix, $[K]$. This condition is written as follows.

$$\{u^{(k)}\}^T [K] \{u^{(j)}\} = 0 \quad k \neq j \quad (3.33)$$

Eqns. 3.32 and 3.33 are valid only if $[M]$ and $[K]$ are symmetric matrices.

Modal mass and modal stiffness

When $k = j$ Eqns. 3.32 and 3.33 are written as

$$\{u^{(k)}\}^T [M] \{u^{(k)}\} = M_{kk} \quad (3.34)$$

$$\{u^{(k)}\}^T [K] \{u^{(k)}\} = K_{kk} \quad (3.35)$$

The scalar quantities M_{kk} and K_{kk} are positive constants whose magnitudes depend upon the arbitrary value selected to compute the $n-1$ elements of $\{u^{(k)}\}$. The constant M_{kk} is called the modal mass for mode (k) while K_{kk} is the modal stiffness.

With $k = j$, Eqn. 3.30 becomes

$$-\omega_k^2 M_{kk} + K_{kk} = 0 \quad (3.36)$$

from which we find that:

$$K_{kk} = \omega_k^2 M_{kk} \quad (3.37)$$

In other words, the modal stiffness K_{kk} is proportional to the square of the modal frequency. If we now define a new vector $\{\eta\}$ as

$$\{\eta^{(k)}\} = \frac{1}{\sqrt{M_{kk}}} \{u^{(k)}\} \quad (3.38)$$

then

$$\{\eta^{(k)}\}^T [M] \{\eta^{(k)}\} = 1 \quad (3.39)$$

and

$$\{\eta^{(k)}\}^T [K] \{\eta^{(k)}\} = \omega_k^2 \quad (3.40)$$

The modes $\{\eta^{(k)}\}$, computed using the relationship in Eqn. 3.38, are not only orthogonal but also have unit length with respect to the mass matrix. They are called orthonormal modes.

Example: Mode shape orthogonality

Let's use the mode shapes found previously and test the orthogonality relations that we just developed.

$$C_3 = \{u^{(1)}\}^T [M_{ij}] \{u^{(2)}\} = C_1 C_2 \begin{Bmatrix} 1 \\ 1/a \end{Bmatrix}^T \begin{bmatrix} 2m & 0 \\ 0 & 2ma^2 \end{bmatrix} \begin{Bmatrix} 1 \\ -1/a \end{Bmatrix}$$

then

$$C_3 = C_1 C_2 \begin{Bmatrix} 1 \\ 1/a \end{Bmatrix}^T \begin{Bmatrix} 2m \\ -2ma \end{Bmatrix} = 0$$

so that orthogonality is satisfied.

When we compute the matrix product $\{u^{(1)}\}^T [M] \{u^{(1)}\}$ we find it is

$$\{u^{(1)}\}^T [M] \{u^{(1)}\} = 4mC_1^2.$$

If we want to use orthonormal modes, then we require that $4mC_1^2 = 1$ or

$$C_1 = \frac{1}{2\sqrt{m}}$$

Performing the same operations with mode 2, we have

$$C_2 = \frac{1}{2\sqrt{m}}$$

The fact that C_1 and C_2 are identical is unusual, but, as shown here, not impossible.

Inserting the values of C_1 and C_2 into the mode shapes, the orthonormal mode shapes of our example system are:

$$\{u^{(1)}\} = \frac{0.5}{\sqrt{m}} \begin{Bmatrix} 1 \\ 1/a \end{Bmatrix} \quad \{u^{(2)}\} = \frac{0.5}{\sqrt{m}} \begin{Bmatrix} 1 \\ -1/a \end{Bmatrix}$$

While the magnitude of individual elements of the matrices $[M]$ and $[K]$ depend on the coordinate system used to describe the structure, the mode shapes and frequencies of the actual structure are unique to that structure. The mode shape/frequency combinations represent a unique structural dynamic signature used to provide information necessary for response calculations.

Modal transformation matrix

The n mode shape vectors can be arranged to form a square matrix of order $n \times n$ (n column vectors, each having n elements). This matrix is called the modal transformation matrix and is used to transform our dynamic response calculations from those involving structural deflections to those involving mode shapes. The modal transformation matrix is constructed by using the mode shape or eigenvectors from the free vibration analysis and is as follows

$$[u] = [[u^{(1)}] [u^{(2)}] [u^{(3)}] \dots [u^{(n)}]] \quad (3.41)$$

Because of orthogonality, the triple matrix products of the modal transformation matrix and the mass and stiffness matrices yield diagonal matrices.

$$[u]^T [M] [u] = [M_{ii}] \quad (3.42)$$

$$[u]^T [K] [u] = [\omega_i^2 M_{ii}] \quad (3.43)$$

The matrix on the right-hand side of Eqn. 3.42 is a diagonal matrix composed of the modal masses (note that $M_{11} \neq M_{22} \neq M_{33}$, but all elements will be equal to unity if orthonormal modes are used). Similarly, the matrix on the right-hand side of Eqn. 3.43 is also diagonal. If $[u]$ is constructed exclusively with orthonormal modes, then

$$[u]^T [M] [u] = [I] \quad (3.44)$$

$$[u]^T [K] [u] = [\omega_i^2] \quad (3.45)$$

where $[I]$ is the identity matrix, composed of a diagonal of "ones." The elements of Eqns. 3.42 or 3.44 are modal masses while the elements of Eqns. 3.43 or 3.45 are modal stiffnesses.

Free vibration - response to initial conditions

Consider a structural dynamic model with n -degrees of freedom, and whose equation of motion is

$$[M]\{\ddot{x}\} + [K]\{x\} = \{0\} \quad (3.46)$$

At $t = 0$ the initial values of displacement and velocity are given.

$$\{x(0)\} = \{x_o\}$$

$$\{\dot{x}(0)\} = \{v_o\}$$

To find the motion of the system after $t = 0$, we assume that all n free vibration (normal) modes of the system are known. The response $x(t)$ can be expressed as a linear combination of these modes, written as

$$\{x(t)\} = \sum_{i=1}^n q_i \{u^{(i)}\}$$

or

$$\{x(t)\} = [u]\{q(t)\}$$

these are generalized displacements, not dynamic pressure.

(3.47)

where $[u]$ is the square, $n \times n$ modal matrix defined in Eqn. 3.41.

Equation 3.47 is a transformation relationship between the n unknown values of $q_i(t)$ (called "normal coordinates") that represent the amplitude of free vibration modes. They are the unknown functions of time.

We differentiate Eqn. 3.47 twice with respect to time and use that result and Eqn. 3.47 itself to write the free vibration equations in Eqns. 3.46 as

$$[M][u]\{\ddot{q}\} + [K][u]\{q\} = \{0\} \quad (3.48)$$

Once symmetric matrices $[M]$ and $[K]$ are multiplied by $[u]$, Equation 3.48 no longer contains symmetrical matrices. Symmetry can be restored to Eqn. 3.48 by pre-multiplying by $[u]^T$.

$$[u]^T[M][u]\{\ddot{q}\} + [u]^T[K][u]\{q\} = \{0\} \quad (3.49)$$

There are two reasons for pre-multiplication by $[u]^T$. First of all, displacements on the structure x_i were transformed to modal coordinates q_i in Eqn. 3.47. This suggests that we should also, in the interests of consistency, transform external forces into the same modal system. The pre-multiplication operation in Eqn. 3.49 accomplishes that transformation, even though no external forces are present here.

Premultiplication by $[u]^T$ also decouples the equations of motion. Recalling Eqns. 3.42 and 3.43, Eqn. 3.49 now becomes:

$$[M_{ii}]\{\ddot{q}_i\} + [\omega_i^2 M_{ii}]\{q_i\} = \{0\} \quad (3.50)$$

or

$$\{\ddot{q}_i\} + [\omega_i^2]\{q_i\} = \{0\} \quad (3.51)$$

Equation 3.51 is composed of a set on n uncoupled equations of the form:

$$q_i(t) = A_i \sin \omega_i t + B_i \cos \omega_i t \quad (i = 1, 2, \dots, n) \quad (3.52)$$

where A_i and B_i are constants to be determined from initial conditions.

To determine the constants A_i and B_i in Eqn. 3.52, we use Eqn. 3.47, together with the initial conditions. From Eqn. 3.47,

$$\{x(0)\} = [u]\{q(0)\} = \{x_o\} \quad (3.53)$$

$$\{\dot{x}(0)\} = [u]\{\dot{q}(0)\} = \{v_o\} \quad (3.54)$$

Pre-multiplying Eqns. 3.53 and 3.54 by $[u]^T[M]$, we have

$$[u]^T[M][u]\{q(0)\} = [M_{ii}]\{q(0)\} = [u]^T[M]\{x_o\}$$

$$[u]^T[M][u]\{\dot{q}(0)\} = [M_{ii}]\{\dot{q}(0)\} = [u]^T[M]\{v_o\}$$

Solving for $\{q(0)\}$ and $\{\dot{q}(0)\}$, we have

$$\begin{aligned}\{q_i(0)\} &= \left[\frac{1}{M_{ii}} \right] [u]^T[M]\{x_o\} \\ \{\dot{q}_i(0)\} &= \left[\frac{1}{M_{ii}} \right] [u]^T[M]\{v_o\}\end{aligned}$$

where the matrix $\left[\frac{1}{M_{ii}} \right]$ is a diagonal matrix with elements $\frac{1}{M_{ii}}$.

The individual values for each mode are

$$q_i(0) = \frac{1}{M_{ii}} \{u^{(i)}\}^T [M] \{x_o\} = B_i$$

$$\dot{q}_i(0) = \frac{1}{M_{ii}} \{u^{(i)}\}^T [M] \{v_o\} = A_i \omega_i$$

Notice that the more nearly the initial condition vectors $\{x_o\}$ and $\{v_o\}$ resemble a particular mode shape $\{u^{(i)}\}$, the larger will be the value $q_i(0)$ or $\dot{q}_i(0)$. If, for instance, $\{v_o\}$ is zero and shape of the initial displacement vector $\{x_o\}$ is identical to the shape of the fifth mode, only the fifth mode will be excited and the system will vibrate only at frequency ω_5 since the other modes of vibration are undisturbed.

Finally, the response of the system to the initial displacements $\{x_o\}$ and velocities $\{v_o\}$ is written as:

$$\{x(t)\} = \sum_{i=1}^n \left(\frac{1}{M_{ii}} \{u^{(i)}\}^T [M] \{v_o\} \frac{1}{\omega_i} \sin \omega_i t + \frac{1}{M_{ii}} \{u^{(i)}\}^T [M] \{x_o\} \cos \omega_i t \right) \quad (3.55)$$

The amplitude and time-dependency of the response $\{x(t)\}$ are uniquely determined.

Motion dependent forces

When elements of the load vector $\{F(t)\}$ in Eqn. 3.1 are deformation dependent (for example, lift due to twist) or depend upon velocity and acceleration, we indicate this dependence by using the following notation:

$$\{F(t)\} = \{F(X, \dot{X}, \ddot{X})\} \quad (3.56)$$

The forces in Eqn. 3.56 are different from inertial or internal structural forces because they are usually (but not always) external to the structural components. One type of motion dependent forces represented by Eqn. 3.56 is viscous damping, for example, $F_d = -C\dot{x}(t)$ where F_d is the force due to velocity \dot{x} and C is the damping constant.

Assume that the motion dependent forces in Eqn. 3.56 are written as follows:

$$\{F(t)\} = [\bar{M}]\{\ddot{x}\} + [\bar{B}]\{\dot{x}\} + [\bar{K}]\{x\} \quad (3.57)$$

The negative value of the first term ($-[\bar{M}]$) is commonly called apparent mass. The negative value of the second term is called the damping while the negative of the third term is the effective stiffness. The form (e.g. diagonal or nondiagonal, symmetric or unsymmetric) of the matrices $[\bar{M}]$, $[\bar{B}]$, $[\bar{K}]$ depends upon the source of the forces.

The equation of motion becomes, upon substitution of Eqn. 3.57 into the equations of motion

$$[[M] - [\bar{M}]]\{\ddot{x}\} - [\bar{B}]\{\dot{x}\} + [[K] - [\bar{K}]]\{x\} = \{0\} \quad (3.58)$$

A more complicated situation occurs if the force is due to the history of previous values of the deformation state. This means that the force at some time, t , is a function of the cumulative effect of what happened at previous times in the displacement time history. Such a dependence may be written as follows

$$\{F(t)\} = \left\{ \int_0^t Q(t-\tau) d\tau \right\} \quad (3.59)$$

where τ is a dummy variable of integration that takes on values between the initial time $t = 0$ and the time, t . The type of force described by Eqn. 3.59 makes solution of Eqn. 3.1 more complicated and is the type of force most often encountered in dynamic aeroelastic work.

Response to External Loads - Modal Analysis

Consider an undamped physical system that is acted upon by time-dependent external loads that are not displacement dependent. We idealize this system by a set of n degrees-of-freedom with n discrete forces applied to the structure. We represent the structural response $\{x(t)\}$ as a linear combination of modal responses, whose amplitudes are unknown.

$$\{x(t)\} = [u]\{q_i(t)\} \quad (3.60)$$

Once again, substituting Eqn. 3.60 into Eqn. 3.1 and multiplying the result by $[u]^T$, gives the following equation of motion:

$$[M_{ii}]\{\ddot{q}\} + [\omega_i^2 M_{ii}]\{q\} = [u]^T\{F_i(t)\} = \{Q_i(t)\} \quad (3.61)$$

so that Eqn. 3.61 also can be written as

$$\ddot{q}_i(t) + \omega_i^2 q_i(t) = \frac{1}{M_{ii}} Q_i(t) \quad (i = 1, 2, \dots, n) \quad (3.62)$$

The n elements of the vector $\{Q_i(t)\}$ represent modal forces or generalized forces associated with normal coordinates $q_i(t)$. Note that initial modal displacement and modal velocity conditions are necessary to complete the problem statement.

When $Q_i(t)$ is not motion dependent, the n equations represented by Eqn. 3.62 are uncoupled and may be solved rather easily. The use of normal modes allows us to reduce a large problem with n degrees of freedom, all coupled together, down to a set of n uncoupled, single degree-of-freedom, linear oscillator problems. After Eqn. 3.62 is solved for each normal coordinate value, Eqn. 3.60 is used to provide the response of individual degrees of freedom.

Stability of Motion

Let's consider the linear system whose equations of motion are described by the matrix equation

$$[M]\{\ddot{x}\} + [B]\{\dot{x}\} + [K]\{x\} = \{F(t)\} \quad (3.63)$$

To examine stability (in response to small disturbances), we set $\{F\} = \{0\}$ and consider the homogeneous equation set. In this case, as with divergence, $\{x\}$ represents a set of perturbation displacements measured from the steady-state solution generated with the functions $F(t)$ non-zero.

The elements of $[B]$ in Eqn. 3.63 are coefficients of rate-dependent terms. Viscous damping produces such terms, but there are other kinds of forces in nature that may cause

such terms to appear. The matrix $[K]$ contains coefficients of deformation dependent terms. Spring stiffnesses create such terms, but we have observed that aerodynamic forces also produce equivalent stiffness terms. As a result, $[B]$ and $[K]$ need not be symmetric matrices.

Assume that the solution to Eqn. 3.63 is separable and of the form

$$\{x(t)\} = \{u\}e^{st} \quad (3.64)$$

Then, Eqn. 3.63 becomes

$$s^2[M]\{u\} + s[B]\{u\} + [K]\{u\} = \{0\} \quad (3.65)$$

Equation 3.65 is an eigenvalue problem with s being the eigenvalue and $\{u\}$ the eigenvector. We cannot count on $[B]$ being a null (zero) matrix and $[K]$ being positive definite and symmetric. As a result, the eigenvalues s may be positive or negative real numbers or complex numbers.

Equation 3.65 is not in a convenient form for computer solution. We return to Eqn. 3.63, and solve for $\{\ddot{x}\}$ to get

$$\{\ddot{x}\} = -[M]^{-1}[B]\{\dot{x}\} - [M]^{-1}[K]\{x\} \quad (3.66)$$

Equation 3.66 then may be written as

$$\{\ddot{x}\} = [[-M^{-1}K][-M^{-1}B]]\{y\} \quad (3.67)$$

where

$$\{y\} = \begin{Bmatrix} x \\ \dot{x} \end{Bmatrix} \quad (3.68)$$

The vector $\{y\}$ is the state vector and its elements are called state variables (displacements and velocities). Equation 3.67 provides the acceleration of the system in terms of the system states. Because of the way we form the state vector by combining the displacement and velocity elements, the $\{y\}$ vector is a $2n$ element vector where the displacement vector $\{x\}$ has n elements.

Now, differentiate Eqn. 3.68 to get

$$\{\dot{y}\} = \begin{Bmatrix} \dot{x} \\ \ddot{x} \end{Bmatrix} \quad (3.69a)$$

and

$$\{\dot{x}\} = [[0][I]]\{y\} \quad (3.69b)$$

Combining Eqns. 3.67 and 3.69a,b, we have the following result:

$$\{\ddot{y}\} = \begin{bmatrix} 0 & I \\ -M^{-1}K & -M^{-1}B \end{bmatrix} \{y\} = [A]\{y\} \quad (3.70)$$

Although Eqns. 3.70 and 3.65 are written in different forms, they describe the same problem. Equation 3.70 has a standard form for an eigenvalue problem in which the eigenvalue appears linearly (as opposed to nonlinearly as in Eqn. 3.65).

Notice that all the matrices that appear in Eqn. 3.70 are real. However, the eigenvalues may be real or complex. Let us assume that

$$\{y\} = \{u\}e^{st}$$

where $\{u\}$ is now a modal state vector consisting of both amplitudes of velocities and displacements. Equation 3.70 then becomes:

$$s\{u\} = [A]\{u\} \quad (3.71)$$

Eigenvalues or roots of the characteristic equation for Eqn. 3.71 are found from constructing the following determinant.

$$\Delta = |A - sI| = 0 \quad (3.72)$$

In general, the eigenvalues s can be written as

$$s = \sigma + j\omega$$

where $j = \sqrt{-1}$ so that

$$\{y\} = \{u\}e^{\sigma t}e^{j\omega t}$$

In this case, σ represents exponential damping while ω gives the response an oscillatory feature. The eigenvector $\{u\}$ is, in general, a vector of complex numbers. Thus

$$\{y\} = \{u\}e^{\sigma t}e^{j\omega t} = e^{\sigma t}\{u\}(\cos \omega t + j \sin \omega t)$$

If a root s is complex, its complex conjugate is also a root so that

$$s_{1,2} = \sigma \pm j\omega$$

and s_1 times s_2 is $\sigma^2 + \omega^2$, a real number. In other cases, s may be purely real ($j\omega = 0$) or purely imaginary ($\sigma = 0$). One convenient way to display the eigenvalue information is in s -plane format, as shown in Figure 3.3. One axis measures the magnitude of the exponential part of the eigenvalue while the other represents the imaginary or frequency portion.

Roots lying to the left of the $j\omega$ axis (the left half plane) are associated with stable response to a small disturbance or perturbation to the system.

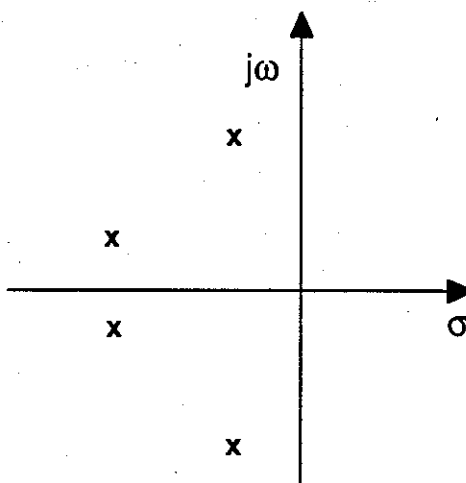


Figure 3.3 - Eigenvalues displayed in root locus format.

If $\sigma < 0$ then the response to an initial disturbance decays exponentially with time. Roots (eigenvalues) to the right of the $j\omega$ axis are associated with unstable modes of motion. Notice that complex roots in the upper one-half of this s-plane have counterparts symmetrically located in the lower half because of the complex conjugate feature of these complex eigenvalues ($s_1 = \sigma + j\omega$ in the upper half and $s_2 = \sigma - j\omega$ in the lower half).

The eigenvalues of the $[A]$ matrix are unique. However, if a system parameter such as airspeed is changed then some elements of $[A]$ will change. As a result, the eigenvalues then change their positions in the s-plane. Changes in velocity will result in a so-called velocity root-locus curve of the type illustrated in Figure 3.4

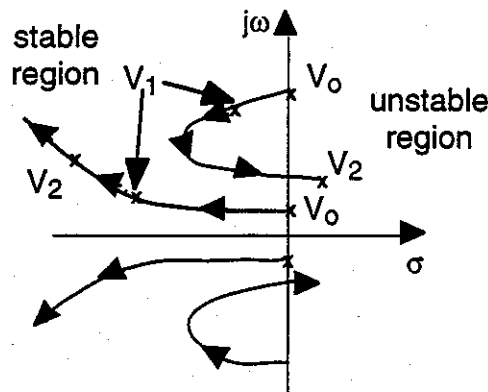


Figure 3.4 - Velocity root-locus representation.

In Figure 3.4, eigenvalues at two different airspeeds are shown. With no airspeed and no internal damping, the roots of this flexible system lie on the $j\omega$ axis, indicating undamped simple harmonic motion. At velocity V_1 the roots move left, indicating damping due to aerodynamic loads. At velocity V_2 , however an eigenvalue root associated with a certain mode of motion has become unstable. Both roots are oscillatory since $j\omega$ is not zero. The complex conjugate roots are shown as roots in the lower half plane but do not furnish additional information about stability.

An alternative type of root-locus is shown in Figure 3.5. In this figure one complex conjugate pair of roots that are initially oscillatory (but damped and stable) intersect the real (σ) axis at a certain airspeed and then split as airspeed increases. Roots along the real axis are associated with nonoscillatory motion and are referred to as aperiodic. Further increases in airspeed cause one root along the σ -axis to move left (become more stable) while the other real root moves right and intersects the $j\omega - \sigma$ axis origin. A further increase in airspeed will push this latter root further to the right, at which point instability occurs.

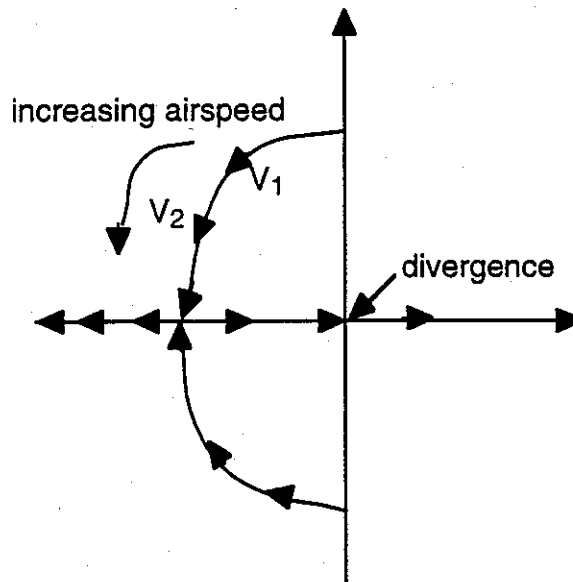


Figure 3.5 - Velocity root locus associated with divergence

When an eigenvalue moves to the right half plane through the origin, this is divergence. If, on the other hand, the root enters the right half-plane at a point along the $j\omega$ axis, this type of oscillatory instability is called flutter.

Free vibration of a typical section

Consider the typical section shown in Figure 3.6. This model consists of distributed mass along the x -axis, with its origin centered at the shear center, and two springs representing the stiffness of the wing structure and its resistance to deformation. We will develop free vibration equations of motion when no external loads are applied.

A translational spring with stiffness K_h restrains up-and-down or plunge motion of the airfoil. This spring is attached to the airfoil at the shear center. A torsion spring, with stiffness K_T restrains pitch or twist deformation θ due to structural flexibility. The airfoil has a planform area S .

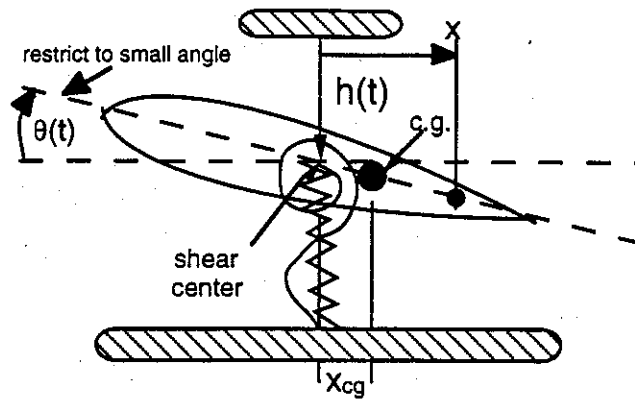


Figure 3.6 - Two-degree of freedom typical section

The pitch coordinate θ measures inclination with respect to the static equilibrium position that we found in Chapter 2. The downward displacement $h(t)$ measures the position of a point on the airfoil, again with respect to the static equilibrium position. In Figure 3.6, this reference position is located at the shear center.

On the other hand, the downward displacement of any other point on the airfoil, located at a distance x from the shear center, is given by $z(t)$, defined in terms of h and θ as

$$z(t) = h + x\theta \quad (3.73)$$

The strain energy stored in the linear elastic springs is a function of the spring stiffnesses K_h and K_T and displacements θ and h . The spring strain energy is denoted by the symbol U and given by the relationship

$$U = \frac{1}{2} K_T \theta^2 + \frac{1}{2} K_h h^2 \quad (3.74)$$

Let ρ be the mass per unit length of the airfoil, measured along a streamwise axis, x , shown in Figure 3.6. The kinetic energy is denoted by the symbol T and is written in terms of $\dot{z} = dz / dt$ as

$$T = \frac{1}{2} \int_{x_L}^{x_T} \rho \dot{z}^2 dx \quad (3.75)$$

where x_L is the location of the leading edge with respect to the shear center coordinate system and x_T is the coordinate of the trailing edge. The expression for kinetic energy can be expanded in terms of h and $\dot{\theta}$ to give

$$T = \frac{1}{2} \left(h^2 \int \rho dx + 2h\dot{\theta} \int \rho x dx + \dot{\theta}^2 \int \rho x^2 dx \right) \quad (3.76)$$

The first integral in Eqn. 3.76 is the total mass of the airfoil, defined as:

$$m = \int \rho dx$$

The second integral measures a quantity called the static unbalance of the airfoil with respect to the shear center. The term static unbalance refers to the fact that, in a downward acting gravitational field, airfoil twist is present if x_θ is not zero. If the origin of the x -axis were at the airfoil chordwise center of mass, this integral would be zero. The static unbalance is represented by the symbol, S_θ

$$S_\theta = \int \rho x dx$$

S_θ may be positive, negative or zero.

An equivalent method of computing S_θ is to recognize that the total mass m can be lumped at the center of mass, a distance x_θ aft of the coordinate system origin. In this case, equivalence requires that

$$\int \rho x dx = S_\theta = mx_\theta$$

The third integral in Eqn. 3.76 is the mass moment of inertia, measured (or computed) about the origin of the x -axis. This integral is defined as:

$$I_\theta = \int \rho x^2 dx$$

The kinetic energy is written as follows:

$$T = \frac{1}{2} m h^2 + mx_\theta h \dot{\theta} + \frac{1}{2} I_\theta \dot{\theta}^2$$

Lagrange's equations provide the equations of motion for the shear center displacement. The first of these two equations is the plunge equation with the plunge coordinate h used as the independent parameter.

$$\frac{d}{dt} \left(\frac{\partial(T-U)}{\partial h} \right) - \frac{\partial(T-U)}{\partial h} = 0$$

The twist equilibrium equation is

$$\frac{d}{dt} \left(\frac{\partial(T-U)}{\partial \theta} \right) - \frac{\partial(T-U)}{\partial \theta} = 0$$

From Lagrange's equations, the elements of the mass matrix and stiffness matrix are determined by differentiation of T and U with respect to the displacements and their first derivatives. Let h be coordinate u_1 , and θ be u_2 , then, by definition we have

$$\frac{\partial^2 T}{\partial u_i \partial u_j} = m_{ij} \quad \text{and} \quad \frac{\partial^2 U}{\partial u_i \partial u_j} = k_{ij}$$

so that

$$[m_{ij}] = \begin{bmatrix} m & mx_\theta \\ mx_\theta & I_\theta \end{bmatrix} \quad (3.77)$$

and

$$[k_{ij}] = \begin{bmatrix} K_h & 0 \\ 0 & K_T \end{bmatrix} \quad (3.78)$$

With the co-ordinate system origin located at the shear center, the equations of motion in matrix form are

$$\begin{bmatrix} m & mx_\theta \\ mx_\theta & I_\theta \end{bmatrix} \begin{Bmatrix} \ddot{h} \\ \ddot{\theta} \end{Bmatrix} + \begin{bmatrix} K_h & 0 \\ 0 & K_T \end{bmatrix} \begin{Bmatrix} h \\ \theta \end{Bmatrix} = \begin{Bmatrix} 0 \\ 0 \end{Bmatrix} \quad (3.79)$$

To understand the significance of the terms appearing in Eqn. 3.79 we will use Newton's law to derive the same equation. Figure 3.7 shows the free body diagram with forces and moments at the shear center and accelerations at the center of gravity. Summation of forces gives:

$$\Sigma F = m\ddot{z}_{c,g} = m(\ddot{h} + x_\theta \ddot{\theta}) = -K_h h \quad (3.80)$$

or

$$m\ddot{h} + mx_\theta \ddot{\theta} + K_h h = 0 \quad (3.81)$$

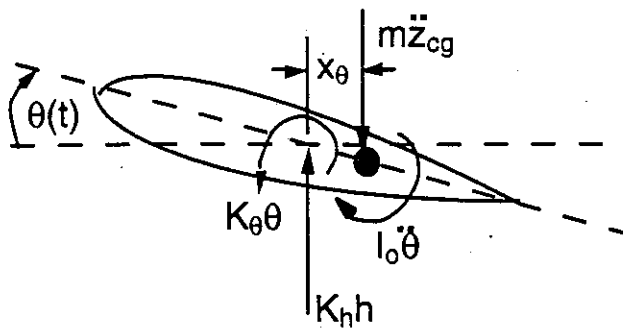


Figure 3.7 - Free body diagram for equations of motion

When we sum moments about the center of gravity we get:

$$I_\theta \ddot{\theta} = -K_T \theta + (K_h h)x_\theta \quad (3.82)$$

or

$$I_\theta \ddot{\theta} - K_h h x_\theta + K_T \theta = 0 \quad (3.83)$$

Equation 3.83 appears to give a result different than its counterpart in Eqn. 3.79 since I_θ is not equal to I_θ . Equation 3.81 can be used to convert Eqn. 3.83 to the results given in Eqns. 3.79. First, multiply Eqn. 3.81 by x_θ to get the following:

$$-K_h h x_\theta = m x_\theta \ddot{h} + m x_\theta^2 \ddot{\theta} \quad (3.84)$$

Substitute Eqn. 3.84 into Eqn. 3.83 to get:

$$(I_\theta + m x_\theta^2) \ddot{\theta} + m x_\theta \ddot{h} + K_T \theta = 0 \quad (3.85)$$

The parallel axis theorem transfers moments of inertia from the c.g. to the shear center, i.e. $I_\theta = I_\theta + m x_\theta^2$, we find that Eqn. 3.85 is identical to that given in Eqn. 3.79.

We first assume that motion is synchronous and harmonic so that

$$\begin{Bmatrix} h(t) \\ \theta(t) \end{Bmatrix} = \begin{Bmatrix} \bar{h} \\ \bar{\theta} \end{Bmatrix} e^{i\omega t}$$

The eigenvalue problem for free vibration in Eqn. 3.79 is

$$\left[-\omega^2 \begin{bmatrix} m & m x_\theta \\ m x_\theta & I_\theta \end{bmatrix} + \begin{bmatrix} K_h & 0 \\ 0 & K_T \end{bmatrix} \right] \begin{Bmatrix} \bar{h} \\ \bar{\theta} \end{Bmatrix} = \begin{Bmatrix} 0 \\ 0 \end{Bmatrix} \quad (3.86)$$

It is convenient to nondimensionalize these equations. First, divide all terms by m . This gives

$$\left[-\omega^2 \begin{bmatrix} 1 & x_\theta \\ x_\theta & \frac{I_\theta}{m} \end{bmatrix} + \begin{bmatrix} K_h/m & 0 \\ 0 & K_T/m \end{bmatrix} \right] \begin{Bmatrix} \bar{h} \\ \bar{\theta} \end{Bmatrix} = \begin{Bmatrix} 0 \\ 0 \end{Bmatrix} \quad (3.87)$$

Define the radius of gyration, r_θ , from the relationship:

$$r_\theta^2 = \frac{I_\theta}{m} \quad (3.88)$$

Furthermore, define the reference frequency ω_h by:

$$\omega_h^2 = \frac{K_h}{m} \quad (3.89)$$

and the reference frequency ω_θ from

$$\omega_\theta^2 = \frac{K_T}{I_\theta} = \frac{K_T}{mr_\theta^2} \quad (3.90)$$

Using these definitions and dividing the two equations of motion by ω_θ^2 yields

$$\left[-\left(\frac{\omega}{\omega_\theta} \right)^2 \begin{bmatrix} 1 & x_\theta \\ x_\theta & r_\theta^2 \end{bmatrix} + \begin{bmatrix} (\omega_h^2 / \omega_\theta^2) & 0 \\ 0 & r_\theta^2 \end{bmatrix} \right] \begin{Bmatrix} \bar{h} \\ \bar{\theta} \end{Bmatrix} = \begin{Bmatrix} 0 \\ 0 \end{Bmatrix} \quad (3.91)$$

Now, define nondimensional frequency ratios as

$$\Omega = \left(\frac{\omega}{\omega_\theta} \right) \quad \text{and} \quad R = \frac{\omega_h}{\omega_\theta} \quad (3.92)$$

Finally we have the final form of the eigenvalue problem for the equations of motion.

$$\begin{bmatrix} (-\Omega^2 + R^2) & -\Omega^2 x_\theta \\ -\Omega^2 x_\theta & (-\Omega^2 + 1)r_\theta^2 \end{bmatrix} \begin{Bmatrix} \bar{h} \\ \bar{\theta} \end{Bmatrix} = \begin{Bmatrix} 0 \\ 0 \end{Bmatrix} \quad (3.93)$$

The characteristic equation is

$$\Delta = \Omega^4 \left(1 - \left(\frac{x_\theta}{r_\theta} \right)^2 \right) - (1 + R^2)\Omega^2 + R^2 = 0 \quad (3.94)$$

Using the parallel axis theorem

$$r_\theta^2 = r_o^2 + x_\theta^2 \quad (3.95)$$

where r_o is the radius of gyration of the airfoil, measured with respect to the c.g. Therefore

$$1 - \left(\frac{x_\theta}{r_\theta} \right)^2 = \left(\frac{r_o}{r_\theta} \right)^2 > 0 \quad (3.96)$$

The quadratic formula is applied to Eqn. 3.94 to provide (after some algebraic manipulation) the following expression for the two nondimensional natural frequencies, Ω_1 , and Ω_2 .

$$\Omega_{1,2}^2 = \frac{1 + R^2 \pm \sqrt{(1 - R^2)^2 + 4R^2 \left(\frac{x_\theta}{r_\theta} \right)^2}}{2 \left(\frac{r_o}{r_\theta} \right)^2} \quad (3.97)$$

Neither Ω_1^2 nor Ω_2^2 can be negative or zero. In addition, for fixed values of R and r_o , increased static unbalance ($\pm x_\theta$) causes Ω_1 and Ω_2 to separate, as indicated in Figure 3.8. The first row of Eqn. 3.93 is the plunge equation for force balance in the h direction. This equation provides the modal relationship

$$\frac{\bar{h}}{\bar{\theta}} = \frac{\Omega^2 x_\theta}{R^2 - \Omega^2} \quad (3.98)$$

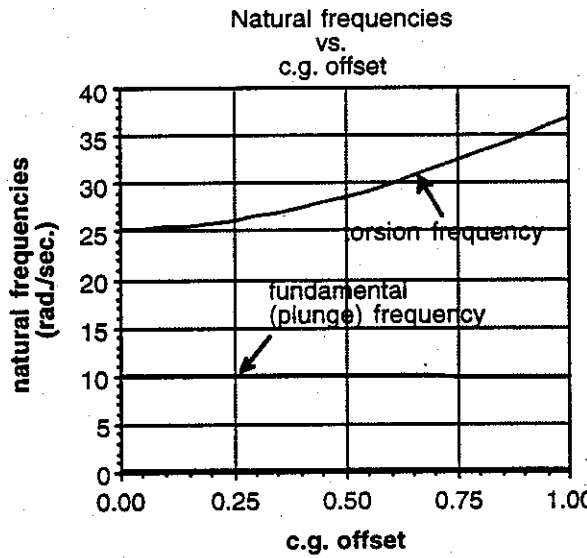


Figure 3.8 - The dependence of Ω_1 and Ω_2 on x_θ

From the torsional motion equation (the second row) we find:

$$\frac{\bar{h}}{\bar{\theta}} = \frac{(1-\Omega^2)r_\theta^2}{x_\theta\Omega^2} \quad (3.99)$$

or

$$\frac{\bar{\theta}}{\bar{h}} = \frac{\Omega^2 r_\theta^2}{\Omega^2 x_\theta} \quad (3.100)$$

Equation 3.98 provides an expression for the amount of plunge motion present (per unit of twist, θ) when x_θ is non-zero and Ω^2 is close to unity. In this case, since the natural frequency is close to the reference value ω_θ , this value of Ω^2 is referred to as a torsion frequency. So, the plunge equation is used to compute the coupled plunge/twist displacement ratio when the system oscillates at or near the original uncoupled torsion frequency. Similarly, the pitch equation is used to compute the amount of twist (per unit of plunge, h) when the system is oscillating at or near the uncoupled plunge frequency, ω_h . This value of Ω is close to R .

Although we have two expressions for the mode shape, we must be careful to use the correct relationship in limiting cases. As x_θ tends to zero, Ω^2 tends to the values $\Omega^2 = 1$ and $\Omega^2 = R^2$. The mode shape in Eqn. 3.100 tends to zero if the values near $\Omega^2 = 1$ are inserted, indicating that the free vibration is purely torsional. If x_θ is zero and $\Omega^2 = R^2$ the expression in Eqn. 3.98 is infinite. This is so, not because \bar{h} is infinite, but because θ is zero and the vibration when $\Omega^2 = R^2$ is purely translational in plunge. Similarly, if Eqn. 3.100 is written as

$$\frac{\bar{\theta}}{\bar{h}} = \frac{\Omega^2 x_\theta}{(1-\Omega^2)r_\theta^2} \quad (3.101)$$

then with $x_\theta = 0$ and $\Omega^2 = R^2$, θ/h is zero. If $x_\theta = 0$ and $\Omega^2 = 1$, then Eqn. 3.101 cannot be evaluated because the motion is purely torsional.

The value h/θ is small when $\Omega^2 = 1$ while the value θ/h is small when $\Omega^2 = R^2$. As a result we call values of ω near ω_θ the torsion roots and associated values of h/θ are called torsion modes even though plunge and pitch motion are coupled and occur simultaneously. Similarly, a value of ω near ω_h and its associated mode shape are plunge roots or plunge modes.

Let's examine a mode shape for our example airfoil. Data for this example is

$$x_\theta = 0.10 b \quad r_\theta^2 = 0.25 b^2$$

$$\omega_h = 10 \text{ rad/sec.} \quad \omega_\theta = 25 \text{ rad/sec.}$$

where the semi-chord is defined as $b = c/2$ and c is the airfoil chord dimension. With static unbalance x_θ , and with $R = 10/25 = 0.40$, Eqn. 3.97 gives the following two values of natural frequency.

$$\omega_1 = \Omega_1 \omega_\theta = 9.9625 \text{ rad/sec.}$$

$$\omega_2 = \Omega_2 \omega_\theta = 25.612 \text{ rad/sec.}$$

Notice that, as predicted, the inclusion of x_θ has increased the separation between the frequencies, compared to their uncoupled values of 10 rad/sec. and 25 rad/sec.

When $x_\theta = 0.10b$, we have $\Omega_1 = 0.3985$ which is near to the value $\omega_h / \omega_\theta = 0.40$. This value is the plunge root. We find $\bar{\theta} / h$ to be

$$\frac{\bar{\theta}}{h} = \frac{(0.10b)(0.3985)^2}{(0.25b^2)(1 - 0.1588)} = \frac{1}{b}(0.07551)$$

or

$$\bar{\theta} = \left(\frac{h}{b}\right)(0.07551)$$

In this mode of vibration, a downward movement a distance of one semi-chord (b) (so that $\bar{h}/b = 1$) is accompanied by a nose-up rotation of 0.07551 radians (4.326 degrees). (This would be an extremely large plunge displacement, but it is used as an example length to indicate that the amount of rotation accompanying it is rather small.) Thus the vibratory motion is a coupled plunging and twisting occurring simultaneously at $\omega_1 = \Omega_1 \omega_\theta = 9.9625 \text{ rad/sec.}$

From Eqn. 3.73, the deflection of the points lying along the x-axis is

$$z(t) = h(t) + x\bar{\theta}(t) \quad (3.102)$$

or

$$z(t) = h(t)\left(1 + x\frac{\bar{\theta}}{h}\right)$$

We can solve for a position x so that the quantity within the brackets in Eqn. 3.102 is zero. Then, as the system oscillates, at a single frequency one point on the airfoil (or its extension) is always stationary. This point is called a node point. The equation for the node point is, from Eqn. 3.102

$$1 + x_n\left(\frac{\bar{\theta}}{h}\right) = 0$$

or

$$x_n = \frac{-1}{\bar{\theta} / h}$$

or

$$\frac{x_n}{b} = \frac{-1}{\bar{\theta} / \bar{h} / b} \quad (3.103)$$

When $\Omega = 0.3985$ we have $\frac{\bar{\theta}}{\bar{h}/b} = 0.07551$. Substituting this value into Eqn. 3.103, we

have, for this mode

$$\frac{x_n}{b} = -13.243 \quad (3.104)$$

The result in Eqn. 3.104 indicates that the node point or apparent center of rotation of the airfoil cross-section, when oscillating in this predominantly plunge mode at $\omega_1 = \Omega_1 \omega_0 = 9.9625$ rad/sec., is 13.243 semi-chord lengths to the left (towards the leading edge) of the shear center. This position is well off the airfoil section in Figure 3.6.

If coupling between plunge and pitch is reduced by decreasing static unbalance, the absolute value of x_n/b would become quite large. This remote position of the node point from the shear center is a characteristic of a mode of vibration with plunge predominating.

To complete the discussion, let us examine the other mode of oscillation. With $\omega_2 = 25.612$ rad/sec. rad/sec. or $\Omega_2 = 1.0245$, we have

$$\frac{\bar{h}/b}{\bar{\theta}} = -0.11799 \quad (3.105)$$

The relationship in Eqn. 3.105 can be interpreted as having the airfoil shear center move up an amount 0.11799 semi-chords as θ rotates one radian. The node point on the cross-section is located at

$$\frac{x_n}{b} = 0.11799$$

or approximately 0.12 semi-chords aft (towards the trailing edge) of the shear center. This position of the node line aft of the shear center is caused by aft placement of the c.g. ($x_g > 0$).

An Aerodynamic Load Idealization

To study the time-dependent response of the 2-D typical section when it is subjected to external aerodynamic forces and moments we need to develop expressions for the unsteady

fluid mechanic pressures that develop because of motion ($h(t)$ and $\theta(t)$) of the airfoil as the airstream moves past. These aerodynamic forces and moments are due to vortex action in subsonic flow and the airfoil motion creates flow unsteadiness. A complete discussion of the effects of flow unsteadiness on time-dependent aerodynamic forces will be left until we have a better understanding of the source of the dynamic instability problem.

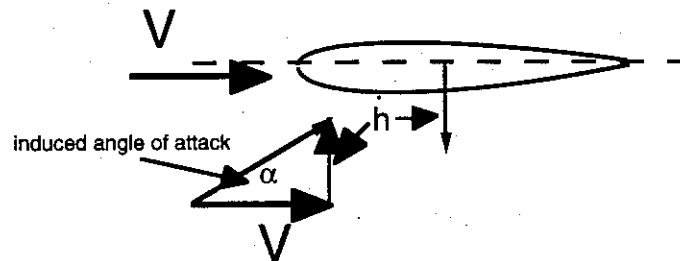


Figure 3.9- Induced angle of attack due to plunge

As a first approximation to motion dependent airloads, we assume that the aerodynamic forces and moments are the result of quasi-steady motion. By quasi-steady, we mean that lift and pitching moment measured at the aerodynamic center are functions of an apparent angle of attack θ_T , given as

$$\theta_T = \theta + \frac{h}{V} \quad (3.106)$$

If the motion is extremely slow, in terms of some time scale related to the flow velocity, then this approximation will approach reality.

As indicated in Figure 3.9, the apparent angle θ_T is composed of the usual steady-state angle-of-attack θ , to which the apparent angle h/V is added. This latter component arises because the apparent flow direction is rotated due to plunge of the airfoil. For small angles, this apparent angle is h/V as indicated in the figure.

The lift, assumed to act at the static aerodynamic center, can be written as

$$L = qSC_{L_a} \theta_T \quad (3.107)$$

The pitching moment due to motion is also measured about the aerodynamic center and is still zero, because of the definition of the aerodynamic center.

$$M(t)_{AC} = 0 \quad (3.108)$$

The motion-dependent aerodynamic force and moment requires the addition of two terms to the original equations of motion in Eqn. 3.79. In matrix form, these equations become

$$\begin{bmatrix} M_{ij} \\ \ddot{\theta} \end{bmatrix} \begin{Bmatrix} \ddot{h} \\ \ddot{\theta} \end{Bmatrix} + \begin{bmatrix} K_{ij} \\ \theta \end{bmatrix} \begin{Bmatrix} h \\ \theta \end{Bmatrix} = \begin{Bmatrix} -L \\ Le \end{Bmatrix} \quad (3.109)$$

The $-L$ term in Eqn. 3.109 occurs because positive lift acts upward while $+h$ is downward. The term Le is the pitching moment (positive nose-up) about the shear center. Substituting the expressions for L and Le into Eqn. 3.109 and dividing each term by m , we obtain the following relationship

$$\begin{bmatrix} 1 & x_\theta \\ x_\theta & r_\theta^2 \end{bmatrix} \begin{Bmatrix} \ddot{h} \\ \ddot{\theta} \end{Bmatrix} + \frac{qSC_{L\alpha}}{m} \begin{bmatrix} 1/V & 0 \\ -e/V & 0 \end{bmatrix} \begin{Bmatrix} \dot{h} \\ \dot{\theta} \end{Bmatrix} + \begin{bmatrix} K_h/m & 0 \\ 0 & K_T/m \end{bmatrix} \begin{Bmatrix} h \\ \theta \end{Bmatrix} + \frac{qSC_{L\alpha}}{m} \begin{bmatrix} 0 & 1 \\ 0 & -e \end{bmatrix} \begin{Bmatrix} h \\ \theta \end{Bmatrix} = \begin{Bmatrix} 0 \\ 0 \end{Bmatrix}$$

or

$$\begin{bmatrix} M_{ij} \\ \theta \end{bmatrix} \begin{Bmatrix} h \\ \theta \end{Bmatrix} + \begin{bmatrix} D_{ij} \\ \theta \end{bmatrix} \begin{Bmatrix} \dot{h} \\ \dot{\theta} \end{Bmatrix} + \begin{bmatrix} K_{ij} \\ \theta \end{bmatrix} \begin{Bmatrix} h \\ \theta \end{Bmatrix} + \begin{bmatrix} A_{ij} \\ \theta \end{bmatrix} \begin{Bmatrix} h \\ \theta \end{Bmatrix} = \begin{Bmatrix} 0 \\ 0 \end{Bmatrix} \quad (3.110)$$

This is the equation of motion for free vibration of the airfoil in the airstream. If h and θ are not time dependent, Eqn. 3.110 reduces to the equations used for divergence analysis in Chapter 2.

To find the motion of the airfoil when it is subjected to an arbitrary initial displacement and velocity we again assume synchronous motion.

$$\begin{Bmatrix} h(t) \\ \theta(t) \end{Bmatrix} = \begin{Bmatrix} \bar{h}/b \\ \bar{\theta} \end{Bmatrix} f(t) = \begin{Bmatrix} u_1 \\ u_2 \end{Bmatrix} f(t) \quad (3.111)$$

where the terms \bar{h} and $\bar{\theta}$ are amplitudes. After substitution of Eqn. 3.111 into Eqn. 3.110 and premultiplication by $\{u\}^T$ we obtain a relationship involving $f(t)$ and its derivatives written as

$$\ddot{f} M_i + \dot{f} D_i + f(K_i + A_i) = 0 \quad (3.112)$$

where

$$\{u\}^T [M] \{u\} = M_i$$

$$\{u\}^T [K] \{u\} = K_i$$

$$\{u\}^T [D] \{u\} = D_i$$

$$\{u\}^T [A] \{u\} = A_i$$

The subscript i refers to the results of computations using a particular mode shape $\{u^{(i)}\}$ although this mode shape is unknown until we solve the vibration problem for frequencies. D_i arises from the aerodynamic damping effect, while A_i appears due to the aerodynamic stiffness. Next, we assume that

$$f(t) = ae^{st} \quad (3.113)$$

so that substitution of Eqn. 3.113 into Eqn. 3.112 gives:

$$ae^{st} [s^2 M_i + s D_i + (K_i + A_i)] = 0 \quad (3.114)$$

With the D_i term included, motion cannot be harmonic, that is, $s \neq i\omega$. Without aerodynamic damping motion may be harmonic ($s = i\omega; s^2 < 0$) if the sum $K_i + A_i$ is greater than zero. When we exclude the $\frac{h}{V}$ term in our lift approximation then we can assume that the airfoil oscillation is harmonic motion with the form

$$f(t) = ae^{i\omega t}$$

Let us nondimensionalize the equations of motion without the damping terms by dividing the first row of Eqn. 3.109 (the plunge equation) by the airfoil semi-chord dimension, b , and then dividing the second row by b^2 . Then we will divide all terms by the reference frequency ω_0^2 . The result is

$$\frac{1}{\omega_0^2} \begin{bmatrix} 1 & \bar{x}_\theta \\ \bar{x}_\theta & \bar{r}_\theta^2 \end{bmatrix} \begin{Bmatrix} \dot{\bar{h}}/b \\ \ddot{\theta} \end{Bmatrix} + \begin{bmatrix} R^2 & 0 \\ 0 & \bar{r}_\theta^2 \end{bmatrix} \begin{Bmatrix} h/b \\ \theta \end{Bmatrix} + \frac{q S C_{L_a}}{m \omega_0^2 b} \begin{bmatrix} 0 & 1 \\ 0 & -\bar{e} \end{bmatrix} \begin{Bmatrix} h/b \\ \theta \end{Bmatrix} = \begin{Bmatrix} 0 \\ 0 \end{Bmatrix} \quad (3.115)$$

In Eqn. 3.115 the barred quantities such as \bar{x}_θ , represent nondimensionalized parameters with respect to b . Let us assume synchronous motion of the form

$$\begin{Bmatrix} h/b \\ \theta \end{Bmatrix} = \begin{Bmatrix} \bar{h} \\ \bar{\theta} \end{Bmatrix} e^{i\omega t} = \begin{Bmatrix} u_1 \\ u_2 \end{Bmatrix} e^{i\omega t}$$

Let $\Omega = \omega/\omega_0$ so that Eqn. 3.115 is written as

$$-\Omega^2 \begin{bmatrix} 1 & \bar{x}_\theta \\ \bar{x}_\theta & \bar{r}_\theta^2 \end{bmatrix} \{u_i\} + \begin{bmatrix} R^2 & 0 \\ 0 & \bar{r}_\theta^2 \end{bmatrix} \{u_i\} + \frac{1}{2} \frac{\rho V^2 C_{L_a} S}{mb\omega_0^2} \begin{bmatrix} 0 & 1 \\ 0 & -\bar{e} \end{bmatrix} \{u_i\} = \begin{Bmatrix} 0 \\ 0 \end{Bmatrix} \quad (3.116)$$

The coefficient multiplying the aerodynamic stiffness matrix in Eqn. 3.116 is a combination of nondimensional parameters. We define a parameter called the mass ratio, μ , as:

$$\mu = \frac{m}{\pi \rho b^2 l} \quad (3.117)$$

where m represents the total mass of the airfoil with planform dimensions of $2b$ by l , the airfoil span. The term $\pi \rho b^2 l$ represents the mass of a cylinder of air with length l and radius b , filled with fluid of density ρ . As a result, the term that multiplies the aerodynamic stiffness matrix in Eqn. 3.116 becomes

$$\frac{1}{2} \frac{\rho V^2 S C_{L\alpha}}{mb\omega_\theta^2} = \left(\frac{V}{b\omega_\theta} \right)^2 \frac{C_{L\alpha}}{\pi\mu} \quad (3.118)$$

Next we define the nondimensional or "reduced" velocity $\frac{V}{b\omega_\theta} = \bar{V}$ and introduce these parameters into Eqn. 3.116. We then multiply every term by (-1) to obtain

$$\begin{bmatrix} (\Omega^2 - R^2) & (\Omega^2 \bar{x}_\theta - \bar{V}^2 \frac{C_{L\alpha}}{\pi\mu}) \\ (\Omega^2 \bar{x}_\theta) & (\Omega^2 \bar{r}_\theta^2 - \bar{r}_\theta^2 + \bar{V}^2 \frac{C_{L\alpha}}{\pi\mu}) \end{bmatrix} \begin{Bmatrix} u_1 \\ u_2 \end{Bmatrix} = \begin{Bmatrix} 0 \\ 0 \end{Bmatrix} \quad (3.119)$$

When the airfoil geometry, inertial and stiffness characteristics and the flow velocity are known, then Ω^2 and $\{u\}$ become the only unknowns. To solve for these unknowns, Ω^2 we form the frequency determinant of Eqn. 3.119. The resulting frequency equation becomes:

$$(\bar{r}_\theta^2 - \bar{x}_\theta^2)\Omega^4 - \left(\bar{r}_\theta^2 [1 + R^2] - \frac{(\bar{e} + \bar{x}_\theta)C_{L\alpha}\bar{V}^2}{\pi\mu} \right) \Omega^2 + R^2 \left(\bar{r}_\theta^2 - \frac{\bar{V}^2 \bar{e} C_{L\alpha}}{\pi\mu} \right) = 0 \quad (3.120)$$

Equation 3.120 can be written in the form

$$A\Omega^4 - B\Omega^2 + C = 0 \quad (3.121)$$

where the coefficients A , B and C are

$$A = \bar{r}_\theta^2 - \bar{x}_\theta^2 = \bar{r}_o^2 > 0 \quad (3.122)$$

$$B = \bar{r}_\theta^2(1+R^2) - [\frac{\bar{d}C_{L\alpha}}{\pi\mu}] \bar{V}^2 \quad (3.123)$$

$$C = R^2 \left(\bar{r}_\theta^2 - [\frac{C_{L\alpha}\bar{e}}{\pi\mu}] \bar{V}^2 \right) \quad (3.124)$$

The dimension $\bar{d} = \bar{e} + \bar{x}_\theta$ in Eqn. 3.123 is the nondimensional distance between the airfoil aerodynamic center and center of mass. The coefficients B and C are velocity dependent and have the form $B = b_1 - b_2 \bar{V}^2$ and $C = c_1 - c_2 \bar{V}^2$, where b_1, b_2, c_1 and c_2 are defined by inspection of the terms in Eqns. 3.121-124. The parameter $b_1 = \bar{r}_\theta^2(1+R^2)$ always will be positive.

Equation 3.120 yields two values of Ω^2 , given conceptually as follows

$$\Omega_{1,2}^2 = \frac{B \pm \sqrt{B^2 - 4AC}}{2A} \quad (3.125)$$

Since $b_1 > 0$ then our initial assumption of harmonic motion appears to be satisfied. When \bar{V}^2 is zero, because the frequency determinant gives values of $\Omega_{1,2}^2$ identical to the system natural frequencies.

Changes in airspeed cause the term under the radical in Eqn. 3.125 to change. The term $B^2 - 4AC$ is positive when $\bar{V}^2 = 0$ and decreases as \bar{V} increases. This is an important effect of increased aerodynamic coupling.

Figure 3.10 shows behavior of the term $B^2 - 4AC$ as a function of reduced airspeed \bar{V} .

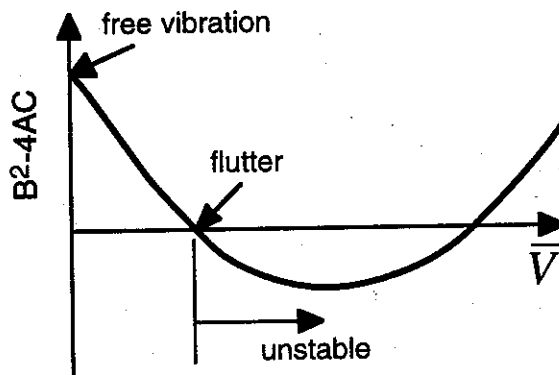


Figure 3.10 - Frequency term $B^2 - 4AC$ vs. \bar{V}

As $B^2 - 4AC$ becomes smaller with increasing airspeed, it may become zero and then negative above a critical value of \bar{V} . This critical point is the flutter speed, as indicated in Figure 3.10. If $B^2 - 4AC$ becomes negative, then Eqn. 3.125 will produce a pair of complex conjugate roots, written as

$$\omega = \omega_o \pm i\sigma \quad (\sigma > 0) \quad (3.126)$$

This means that the synchronous time response has the form

$$f(t) = a \begin{cases} e^{i\omega_o t} e^{\sigma t} \\ e^{i\omega_o t} e^{-\sigma t} \end{cases} \quad (3.127)$$

Both roots indicate oscillatory airfoil motion, but the root with the factor $e^{\sigma t}$ indicates that the amplitude of its motion has an exponentially increasing amplitude. This type of root is associated with the dynamic instability called flutter.

The flutter condition for this mathematical model occurs when $B^2 - 4AC = 0$ and can be written as

$$B^2 = 4AC \quad (3.128)$$

In terms of the definitions of A , B and C in Eqns. 3.122-124, Eqn. 3.128 may be written as:

$$(b_1 - b_2 \bar{V}_{CR}^2)^2 = 4\bar{r}_o^2(c_1 - c_2 \bar{V}_{CR}^2) \quad (3.129)$$

or

$$b_2^2 \bar{V}_{CR}^4 + (4\bar{r}_o^2 c_2 - 2b_1 b_2) \bar{V}_{CR}^2 + (b_1^2 - 4\bar{r}_o^2 c_1) = 0 \quad (3.130)$$

Equation 3.130 is a quadratic in \bar{V}_{CR}^2 and is written symbolically as follows:

$$\bar{A} \bar{V}_{CR}^4 + \bar{B} \bar{V}_{CR}^2 + \bar{C} = 0 \quad (3.131)$$

from which

$$\bar{V}_{CR}^2 = \frac{-\bar{B} \pm \sqrt{\bar{B}^2 - 4\bar{A}\bar{C}}}{2\bar{A}} \quad (3.132)$$

This type of airfoil vibration behavior can be represented by plotting the real part of the airfoil frequency as indicated in Figure 3.11.

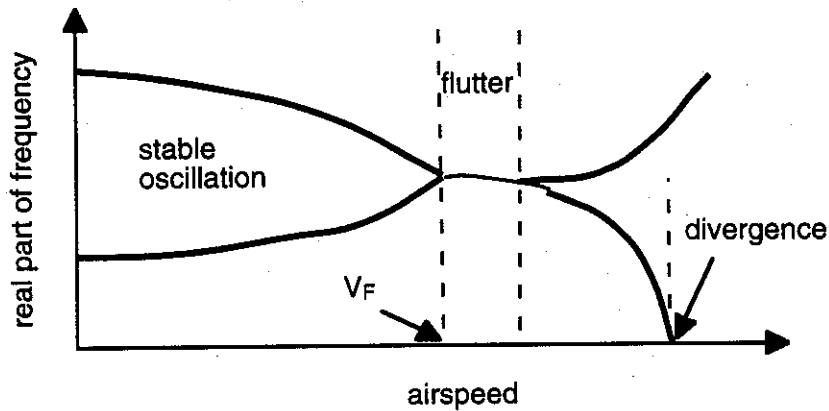


Figure 3.11 - Real part of frequency roots vs. airspeed

The lower of the two values of \bar{V}_{CR} is the flutter speed. This flutter condition occurs here at frequency coalescence where the natural frequencies have been forced together by the aerodynamic coupling. For values of \bar{V} greater than the upper value of \bar{V}_{CR} the quasi-steady airfoil model predicts that stability is restored since Ω_1 and Ω_2 become real and distinct.

The instability speed range is given by the magnitude of the radical $\sqrt{\bar{B}^2 - 4\bar{A}\bar{C}}$. If, by changing airfoil characteristics or the flow conditions, we can reduce this term to zero or, better yet, make it negative, the airfoil will be stable at all airspeeds.

The airfoil stability airspeed range is summarized as follows

$$\bar{V}^2 < \bar{V}_{CR1}^2 \quad \text{Stability}$$

$$\bar{V}_{CR1}^2 \leq \bar{V}^2 \leq \bar{V}_{CR2} \quad \text{Instability}$$

$$\bar{V}^2 > \bar{V}_{CR2} \quad \text{Stability}$$

As indicated in Figure 3.11, divergence is a special case in the flutter analysis. Since the frequency equation is written as

$$A\Omega^4 - B\Omega^2 + C = 0$$

then, if C is zero, this frequency equation reduces to

$$\Omega^2(A\Omega^2 - B) = 0 \quad (3.133)$$

One solution to Eqn. 3.133 is $\Omega_1^2 = 0$ while the other is $\Omega_2^2 = B/A$. This is shown conceptually in Figure 3.11.

When \bar{V}^2 increases a negative real value of Ω_1^2 results so that Ω_1 is an imaginary number, i.e. $\Omega_1 = \pm i\sigma$. As a result, the time dependence of the motion is

$$e^{i\omega_0 t} = \begin{cases} e^{-\sigma\omega_0 t} \\ e^{\sigma\omega_0 t} \end{cases}$$

Both of these roots indicate that the synchronous motion is nonoscillatory. One form of motion decreases exponentially while the other increases exponentially, hence the use of the term divergence.

Since the onset of divergence instability occurs when Ω (or ω) is equal to zero, the inertial properties of the airfoil (\bar{x}_θ for instance) should not be involved. The onset of divergence occurs when

$$C = c_1 - c_2 \bar{V}_D^2 = 0$$

so that

$$\bar{V}_D^2 = c_1 / c_2 \quad (3.134)$$

or

$$\bar{V}_D^2 = \frac{\bar{r}_\theta^2 R^2}{R^2 C_{L_\alpha} \bar{e}} \quad (3.135)$$

Using the definitions of \bar{r}_θ^2 and mass ratio, μ , Eqn. 3.135 is written as

$$\bar{V}_D^2 = \frac{V_D^2}{b^2 \omega_\theta^2} = \frac{m \bar{r}_\theta^2}{C_{L_\alpha} \bar{e} \rho b} \frac{S}{2} \quad (3.136)$$

or

$$V_D^2 = \frac{2 K_T}{\rho e C_{L_\alpha} S} \quad (3.137)$$

This result is identical to that found in Chapter 2.

Example - Quasi-steady flutter predictions

Let us apply what we have learned to the flutter and divergence analysis of an example airfoil. The example airfoil has the following characteristics.

$$\bar{e} + \bar{x}_\theta = 0.30 + 0.10 = 0.40 \quad \bar{x}_\theta = 0.10$$

$$\omega_h = 10 \text{ rad / sec.}$$

$$\omega_\theta = 25 \text{ rad / sec.}$$

$$\bar{r}_\theta = 0.50$$

$$\mu = 20$$

$$C_{L_\alpha} = 2\pi$$

$$b = 3 \text{ ft.}$$

Using these data, Eqn. 3.120 provides the following frequency equation

$$A\Omega^4 - B\Omega^2 + C = 0$$

with

$$A = 0.2400$$

$$B = 0.2900 - 0.04\bar{V}^2$$

$$C = 0.0400 - 0.0048\bar{V}^2$$

From Eqns. 3.131 and 3.132 the lowest value of \bar{V}_{CR} is $\bar{V}_F = \bar{V}_{CR} = \frac{V_F}{b\omega_\theta} = 1.8791$, or

$$V_F = 140.93 \text{ ft / sec.}$$

The divergence speed is computed to be $\bar{V}_D^2 = c_1 / c_2 = 8.33$ so that $\bar{V}_D = 2.89$ or $V_D = 216.5 \text{ ft / sec.}$ A graph of the real part of ω versus V is shown in Figure 3.12.

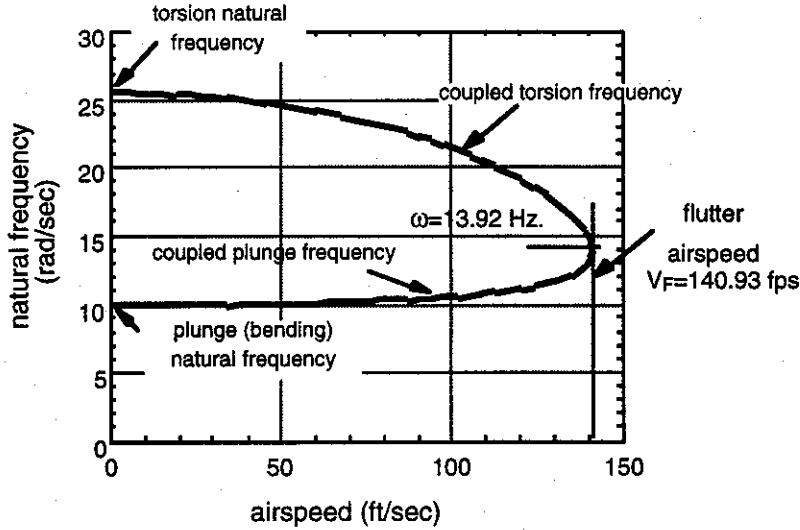


Figure 3.12 - Natural frequency vs. airspeed,

The effect of changing the mass ratio is shown in Figure 3.13. This change from $\mu = 20$ to $\mu = 30$ reflects an increase in altitude.

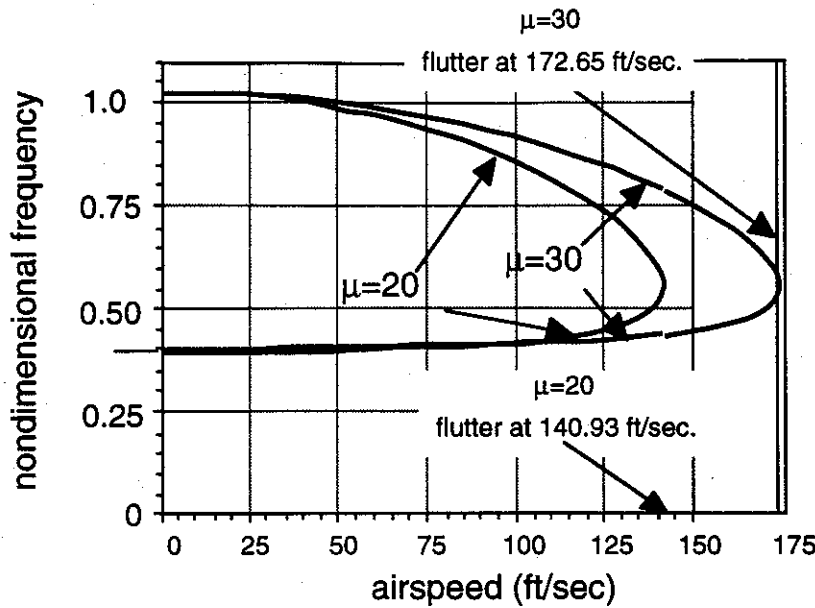


Figure 3.13 - Effect of mass ratio on flutter speed

Necessary conditions for flutter

The necessary condition for the onset of classical flutter requires that two or more modes interact. This requirement can be found from the equations of motion of a two-degree-of-freedom system oscillating harmonically at frequency ω . These equations are written as follows:

$$[-\omega^2[m_{ij}] + [k_{ij}] + q[a_{ij}]]\{u\} = \{0\} \quad (3.138)$$

The matrices m_{ij} , k_{ij} , and a_{ij} are, in general, fully populated. If we use orthogonal modal coordinates such that the system vibration is expressed in terms of normal vibration modes.

$$\begin{Bmatrix} u_1 \\ u_2 \end{Bmatrix} = \begin{Bmatrix} h \\ \theta \end{Bmatrix} = [\Phi] \begin{Bmatrix} \eta_1(t) \\ \eta_2(t) \end{Bmatrix} \quad (3.139)$$

The mass and stiffness matrices can be diagonalized as follows.

$$\begin{bmatrix} M_1 & 0 \\ 0 & M_2 \end{bmatrix} = [\Phi]^T [m_{ij}] [\Phi] \quad (3.140)$$

$$\begin{bmatrix} K_1 & 0 \\ 0 & K_2 \end{bmatrix} = [\Phi]^T [k_{ij}] [\Phi] \quad (3.141)$$

The transformed aerodynamic stiffness matrix is still fully populated and given by

$$\begin{bmatrix} A_{11} & A_{12} \\ A_{21} & A_{22} \end{bmatrix} = [\Phi]^T [a_{ij}] [\Phi] \quad (3.142)$$

The harmonic equations of motion are now written as

$$[-\omega^2[M] + [K] + q[A]]\{\eta\} = \{0\} \quad (3.143)$$

We define two reference frequencies as

$$\frac{K_1 + qA_{11}}{M_1} = \omega_1^2 \quad \text{and} \quad \frac{K_2 + qA_{22}}{M_2} = \omega_2^2$$

and will show that flutter occurs when $(\omega_1^2 - \omega_2^2)^2 = -\frac{4q^2 A_{12} A_{21}}{M_1 M_2}$. We will use this result to explain why flutter cannot if the coefficients A_{12} and A_{21} have the same sign. This means that the aeroelastic stiffness matrix must have a non-symmetrical component.

Flutter involves predicting the behavior of the airfoil natural frequencies when dynamic pressure increases. We first solve for ω^2 by computing the frequency equation for the system in Eqn. 3.143. This relationship is

$$(-\omega^2 M_1 + K_1 + qA_{11})(-\omega^2 M_2 + K_2 + qA_{22}) - q^2 A_{12} A_{21} = \Delta = 0 \quad (3.144)$$

Equation 3.144 can be expanded to give

$$\begin{aligned} \omega^4 M_1 M_2 - \omega^2 (M_1 K_2 + qA_{22} M_1 + M_2 K_1 + qA_{11} M_2) \\ + K_1 K_2 + qK_1 A_{22} + qA_{11} K_2 + q^2 A_{11} A_{22} - q^2 A_{12} A_{21} = 0 \end{aligned} \quad (3.145)$$

Divide each term in Eqn. 3.145 by the product $M_1 M_2$ to obtain

$$\begin{aligned} \omega^4 - \omega^2 \left(\frac{K_2}{M_2} + q \frac{A_{22}}{M_2} + \frac{K_1}{M_1} + q \frac{A_{11}}{M_1} \right) + \left(\frac{K_1}{M_1} \frac{K_2}{M_2} \right) \\ + q \left(\frac{K_1}{M_1} \frac{A_{22}}{M_2} + \frac{A_{11}}{M_1} \frac{K_2}{M_2} \right) + q^2 \left(\frac{A_{11} A_{22}}{M_1 M_2} - \frac{A_{12} A_{21}}{M_1 M_2} \right) = 0 \end{aligned} \quad (3.146)$$

We can solve for the square of the frequency by using the bi-quadratic equation formula

$$\omega^2 = \frac{-b \pm \sqrt{b^2 - 4ac}}{2a} \quad (3.147)$$

and defining a, b and c as follows.

$$a = 1$$

$$b = -\left(\frac{K_2}{M_2} + \frac{K_1}{M_1} + q \frac{A_{22}}{M_2} + q \frac{A_{11}}{M_1}\right)$$

Using our previous definitions of the reference frequencies ω_1^2 and ω_2^2 we find that the coefficient b in the frequency equation is

$$b = -(\omega_1^2 + \omega_2^2)$$

Finally, we can rearrange terms in Eqn. 3.146 to give

$$c = \frac{K_1}{M_1} \left(\frac{K_2}{M_2} + q \frac{A_{22}}{M_2} \right) + q \frac{K_2}{M_2} \frac{A_{11}}{M_1} + q^2 \left(\frac{A_{11}A_{22}}{M_1 M_2} - \frac{A_{12}A_{21}}{M_1 M_2} \right) \quad (3.148)$$

The first term of Eqn. 3.148 has the reference frequency ω_2^2 present so that we can write Eqn. 3.148 as:

$$c = \frac{K_1}{M_1} \omega_2^2 + q \frac{K_2}{M_2} \frac{A_{11}}{M_1} + q^2 \left(\frac{A_{11}A_{22}}{M_1 M_2} - \frac{A_{12}A_{21}}{M_1 M_2} \right) \quad (3.149)$$

The onset of flutter occurs when $b^2 = 4ac$ so that we have the following relationship at the onset of flutter

$$(\omega_1^2 + \omega_2^2)^2 = 4 \left(\frac{K_1}{M_1} \omega_2^2 + q \frac{K_2}{M_2} \frac{A_{11}}{M_1} + q^2 \left(\frac{A_{11}A_{22}}{M_1 M_2} - \frac{A_{12}A_{21}}{M_1 M_2} \right) \right) \quad (3.150)$$

Equation 3.150 can be simplified if we use the identities.

$$\frac{K_1}{M_1} = \omega_1^2 - q \frac{A_{11}}{M_1} \quad \frac{K_2}{M_2} = \omega_2^2 - q \frac{A_{22}}{M_2}$$

Then, Eqn. 3.150 becomes

$$(\omega_1^2 + \omega_2^2)^2 = 4 \left[\omega_2^2 \left(\omega_1^2 - q \frac{A_{11}}{M_1} \right) + q \frac{A_{11}}{M_1} \left(\omega_2^2 - q \frac{A_{22}}{M_2} \right) + q^2 \frac{A_{11}A_{22}}{M_1 M_2} \right] - 4 \frac{A_{12}A_{21}}{M_1 M_2} q^2 \quad (3.151)$$

Equation 3.151 can be simplified further to

$$(\omega_1^2 + \omega_2^2)^2 = 4\omega_1^2\omega_2^2 - 4\frac{q^2 A_{12}A_{21}}{M_1 M_2} \quad (3.152)$$

Expanding Eqn. 3.152, we find that at the onset of flutter the relationship between aerodynamic coefficients and stiffness and dynamic coefficients must be

$$(\omega_1^2 - \omega_2^2)^2 = -4\frac{q^2 A_{12}A_{21}}{M_1 M_2} \quad (3.153)$$

Because $(\omega_1^2 - \omega_2^2)^2$ is always a positive number, Eqn. 3.153 requires that the product $A_{12}A_{21}$ must be negative. This means that these coefficients must have opposite signs. This also means that the aeroelastic stiffness matrix must have a nonsymmetrical component. Since the elastic stiffness matrix is symmetrical, the aerodynamic stiffness must be nonsymmetrical.

Any nonsymmetric matrix can be subdivided into the sum of a symmetrical and an anti-symmetrical matrix. We can show this by separating the off-diagonal elements into two parts; a symmetrical part \bar{A}_{ij} and an anti-symmetrical part \tilde{A}_{ij} as follows

$$A_{ij} = \bar{A}_{ij} + \tilde{A}_{ij} \quad (3.154)$$

$$A_{ji} = \bar{A}_{ij} - \tilde{A}_{ij} \quad (3.155)$$

From Eqns. 3.154 and 3.155 we solve for \bar{A}_{ij} and \tilde{A}_{ij}

$$\tilde{A}_{ij} = \frac{A_{ij} - A_{ji}}{2} \quad (3.156a)$$

$$\bar{A}_{ij} = \frac{A_{ji} + A_{ij}}{2} \quad (3.156b)$$

Thus, any nonsymmetrical load dependent matrix can lead to flutter if the load is large enough.

Divergence will occur when the load is large enough to cause system motion to become nonoscillatory. This condition can be written as $\omega^2 = 0$. Setting the frequency equal to zero and then requiring that the determinant of the remaining aeroelastic stiffness matrix be zero gives:

$$\begin{vmatrix} (K_1 + qA_{11}) & (qA_{12}) \\ (qA_{21}) & (K_2 + qA_{22}) \end{vmatrix} = 0 \quad (3.157)$$

Expanding the determinant, we have

$$(K_1 + qA_{11})(K_2 + qA_{22}) - q^2 A_{12} A_{21} = 0$$

which expands to

$$q^2(A_{11}A_{22} - A_{12}A_{21}) + q(K_1A_{22} + A_{11}K_2) + K_1K_2 = 0 \quad (3.158)$$

Applying the quadratic formula to Eqn. 3.158 gives the following formula for divergence dynamic pressure.

$$q_D = \frac{-(K_1A_{22} + A_{11}K_2) \pm \sqrt{(K_1A_{22} + A_{11}K_2)^2 - 4K_1K_2(A_{11}A_{22} - A_{12}A_{21})}}{2(A_{11}A_{22} - A_{12}A_{21})} \quad (3.159)$$

The source of flutter

Flutter cannot occur unless we have two different types of motion that interact in a certain way. In particular, these modes of motion must be slightly different in their time response. To understand this, let us assume that the plunge motion harmonic with amplitude h_o and is given by

$$h(t) = h_o \cos \omega t \quad (3.160)$$

while the torsional motion is also harmonic, with amplitude θ_o but with a different phase. This can be written as

$$\theta(t) = \theta_o \cos(\omega t + \phi) \quad (3.161)$$

The term "phase" represented by the arbitrary angle ϕ refers to the fact that the torsional motion reaches its maximum amplitude at a different time than does the plunging motion. This difference in phase is essential for flutter.

We will assume that we are able to force the motion so that the plunging and pitching motions have constant amplitude and constant phase angle ϕ . We will compute the work done by the lift force acting at the aerodynamic center when the airfoil goes through one complete cycle of motion. The time to complete one cycle is T_p , and the relation between this time or "period" of motion and the frequency of oscillation is $\omega T_p = 2\pi$ so that

$$T_p = 2\pi/\omega \quad (3.162)$$

The work done by the airstream through the lift is written as

$$W_{air} = work = - \int_0^{T_p} L \bullet dz = - \int_0^{T_p} L \bullet \frac{dz}{dt} dt \quad (3.163)$$

where the displacement $z(t) = h - e\theta$ is the downward displacement of the aerodynamic center. The minus sign in Eqn. 3.163 is due to the lift force being positive in the upward direction and the aerodynamic center displacement being positive in the downward direction.

The lift force (we neglect our damping due to plunge) is expressed as

$$L = qSC_{L\alpha}\theta = qSC_{L\alpha}\theta_o \cos(\omega t + \phi) \quad (3.164)$$

so that

$$W_{air} = - \int_0^{T_p} qSC_{L\alpha}\theta_o \cos(\omega t + \phi) \cdot (h - e\theta) dt \quad (3.165)$$

Substituting our expressions for pitch and plunge velocities into Eqn. 3.165 we have

$$W_{air} = qSC_{L\alpha}\theta_o \int_0^{T_p} \cos(\omega t + \phi) \cdot \omega(h_o \sin \omega t - e\theta_o \sin(\omega t + \phi)) dt \quad (3.166)$$

Expanding this expression we have

$$\begin{aligned} W_{air} &= qSC_{L\alpha}h_o\theta_o \int_0^{T_p} \cos(\omega t + \phi)(\sin \omega t)d(\omega t) \\ &\quad - qSC_{L\alpha}e\theta_o^2 \int_0^{T_p} (\cos(\omega t + \phi))(\sin(\omega t + \phi))d(\omega t) \end{aligned} \quad (3.167)$$

Integrating this expression, we have, because of orthogonality,

$$W_{air} = -qSC_{L\alpha}\pi h_o\theta_o \sin \phi \quad (3.168)$$

Equation 3.168 is an important result because it shows that unless the phase angle between plunging and pitching is greater than π (or 180°) we cannot absorb energy from the airstream. We conclude that the airstream will do negative work (the airfoil will transfer kinetic and strain energy into the airstream and the amplitude of the motion will tend to decay) when $0^\circ < \phi < 180^\circ$ and neutrally stable at $\phi = 0$ and $\phi = 180^\circ$ where the work done is exactly zero. On the other hand, when $-180^\circ < \phi < 0^\circ$ the airstream will transfer energy into the airfoil and the motion will tend to increase in amplitude unless we somehow restrain it.

The question that has not been answered here is how we create conditions in which the phasing is right for flutter. The phasing is created by the aerodynamic stiffness in our model. As long as the frequencies are real, the motion is neutrally stable and oscillatory. An examination of the mode shapes in this case will show that the only possibility for motion in a subcritical case is that the motion is either in-phase ($\phi = 0$) or out-of-phase ($\phi = 180$). In neither of these cases can the airstream input energy into the system.

If the pitching motion is out-of-phase so that it "lags" the plunge then flutter will occur because $\phi < 0$. To provide the motion for this lag, the mode shapes must be complex. It is

not obvious why the condition of complex mode shapes creates a lag motion, but we will discuss this in the next section when we discuss complex numbers.

For now we will simply consider a schematic of the type of motion that will occur when the mode shapes are complex. This motion, shown in Figure 3.14, is such that the pitch angle of the airfoil is zero when the plunge amplitude is most negative. As the plunge velocity increases, the pitch angle of the airfoil decreases and the lift acts in the direction of increasing plunge.

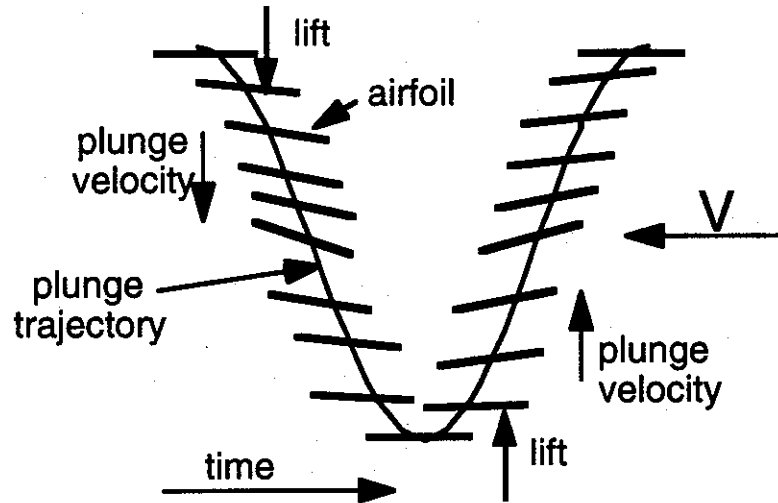


Figure 3.14 - Airfoil trajectory during one cycle of oscillation - energy absorbed from the airstream

When the plunge displacement is zero, the pitch angle is its most negative. As plunge increases, the pitch angle decreases, but is still negative so that lift acts downward. As the plunge velocity goes to zero and the airfoil reaches its largest positive value, the pitch of the airfoil is again zero. When the airfoil moves upward, the lift acts upward. The result is that work is done by the airstream during the entire cycle.